

Characterisation of T Cells Induced by Candidate Conserved Region HIV-1 Vaccines in Healthy HIV-1/2 Negative Volunteers

Thesis submitted for the degree of Doctor of Philosophy

Trinity Term 2014

Tina M Ahmed

Green Templeton College

Department of Clinical Medicine

University of Oxford

Word count: ~45,000

Abstract

HIV-1 has claimed the lives of millions of people globally and continues to spread despite development of highly active antiretroviral therapy. In 2013, 2.1 million new infections occurred and over 35 million people were living with HIV-1 infection. A prophylactic HIV-1 vaccine that can prevent infection or reduce viremia and subsequent transmission will always be an important part of the solution to bring this epidemic under control.

In this thesis, the first HIV-1 vaccine candidate to focus on conserved regions of the virus (HIVconsv) was assessed in a phase I clinical trial conducted in healthy HIV-1/2 negative volunteers in Oxford. The HIVconsv T-cell immunogen was delivered using three leading vaccine modalities (DNA (D), modified vaccinia virus Ankara (M) and chimpanzee adenovirus serotype 63 (C)), in several novel heterologous prime-boost regimens.

The frequency of T cells elicited through HIVconsv vaccination in the CM and DDDCM regimens surpassed that of previous HIV-1 cell-mediated vaccines. A large proportion of these T cells produced multiple cytokines and proliferated in response to recall peptides. The breadth of T-cell responses were also greater than the non-efficacious STEP study vaccine, with an average of 10 T-cell epitopes per vaccine recipient recognised across CM and DDDCM regimens. *In vitro* HIV-1 control mediated by $CD8^+$ T cells was demonstrated for all vaccinees receiving the CM regimen, mainly against clade A (U455) and clade B (IIIB) isolates. Two vaccinees, demonstrated superior control of 6/8 and 7/8 viruses from the panel. The CM regimen induced significantly higher magnitudes of viral inhibition compared to the DDDCM or DDDMC regimens, with this regimen showing potential to overcome the disadvantage for subjects of carrying non-protective HLA alleles.

Investigation of T-cell specificities revealed that the frequencies of T cells specific for conserved Gag but more so Pol regions significantly correlated with *in vitro* virus control. Direct examination of peptide expanded T-cell lines showed that all Pol pool- and limited Gag

pool-specific cell lines reduced HIV-1 replication *in vitro*. In most individuals, targeting multiple HIV-1 epitopes concomitantly resulted in higher levels of virus inhibition than targeting a single viral epitope and two T-cell specificities showed enhanced control of HIV-1; the first within Pol (TAFTIPSI) and second from Gag (TERQANFL). These data support further development of the conserved region strategy for T-cell vaccines against HIV-1.

Acknowledgements

I would like to acknowledge all of those who have directly supported this project; firstly, my supervisor Professor Tomáš Hanke for his guidance and support throughout my D.Phil studies. Secondly, I would like to thank Dr Jill Gilmour and Dr Peter Hayes from the IAVI Human Immunology Laboratory at the Chelsea and Westminster Hospital, for allowing me to use their facilities and for their training and support whilst I stayed in London. Whilst at Oxford I have benefited from the vast knowledge and advice available from principal investigators, post-doctoral scientists, college advisors as well as research support staff and fellow students, which has helped to enrich my work.

I would especially like to thank Dr Nicola Borthwick, the post-doctoral scientist responsible for organising the laboratory clinical research, for her time, support and friendship. During my research at the Jenner Institute and the WIMM there have been many friends that have made even the hard times enjoyable.

This research would not have been possible without generous funding from the Medical Research Council and I would not have been able to disseminate and discuss ideas without receiving travel scholarships from the Boston and Barcelona AIDS vaccine conferences and the British Society for Immunology.

I would also like to thank my family, who have always pushed me to do my best, my close friends, who have never doubted that I would get there and lastly my husband Richard who has shared in my triumphs and failures during my studies and never fails to provide encouragement in all that I do.

Table of Contents

Abstract 2

Acknowledgements 4

Table of Contents 5

List of Figures 11

List of Tables 15

Abbreviations 16

Publications arising from this thesis 18

1 Introduction 19

1.1 The origins of HIV-1 19

1.2 HIV-1 virology and pathogenesis 20

1.3 The global epidemic 31

1.4 Harnessing the host immune response to HIV-1 34

1.5 Vaccines against disease 41

1.6 Tackling HIV-1 diversity with the HIVconsv T-cell vaccine 47

1.7 How do we prioritise HIV-1 vaccine candidates? 50

1.8 Aims of this thesis 51

2 Materials and Methods 52

2.1 Isolation and Freezing of PBMC 52

2.2 *Ex vivo* IFN-γ ELISpot Assay 52

2.3 Growth of HIV-1 Virus Stocks 54

2.4 Harvesting Virus Stock 55

2.5 Titration of HIV-1 Virus Stock 56

2.6 *Ex vivo* Virus Inhibition Assay 56

2.7 Set-up of *Ex vivo* Virus Inhibition Co-cultures 58

2.8 Quantification of HIV-1 Infection by Flow Cytometry 58

2.9 Cultured Virus Inhibition Assay 59

2.10 Expanded $CD8^+$ T Cell ELISpot Assay 60

2.11 HIV-1 Quantitative p24 ELISA 61

2.12 Luminex Analysis 62

2.13 Peptide and Epitope Mapping 63

2.14 Generation of Gag- and Pol-Specific Cell Lines 64

2.15 *In vitro* Cell Killing Assay 66

2.16 ICS of Antiviral Factors 67

3 HIV-CORE 002: Investigating the safety and immunogenicity of candidate HIV-1 vaccines in HIV-1/2 negative volunteers 68

3.1 Introduction 68

3.2 Aims of chapter 3 72

3.3 The low dose ChAdV63.HIVconsv vaccine was immunogenic 73

3.4 HIVconsv vaccines induced high frequencies of HIV-1 specific T cells 74

3.5 A breadth of T-cell specificities were induced by HIVconsv vaccination 77

3.6 The HIVconsv vaccine elicited $CD8^+$ and $CD4^+$ T cells were polyfunctional 85

3.7 Vaccine induced $CD8^+$ and $CD4^+$ T cells proliferated in response to recall antigen. 90

3.8 Chapter 3 Discussion 91

3.9 Summary of key findings from Chapter 3 95

4 Optimisation of an *ex vivo* virus inhibition assay for the assessment of vaccine induced $CD8^+$ T cells 96

4.1 Introduction 96

4.2 Aims of Chapter 4 99

4.3 Growth of HIV-1 clade A, B and C virus stocks 100

4.4 Determining the titre of HIV-1 stocks 104

4.5 HIV-1 infection kinetics and cell viability in $CD4^+$ T cells 107

4.6 The optimal MOI for HIV-1 Bal isolate is 0.005 108

4.7 Comparable cell purity by negative and positive selection of $CD8^+$ T-cell effectors 110

4.8 Negatively selected $CD8^+$ T cells show reduced non-specific virus inhibition 111

4.9 Establishing the level of non-specific *ex vivo* virus inhibition in healthy controls 112

4.10 Chronically infected HIV+ patients weakly control HIV-1 Bal when assessed in an *ex vivo* VIA 115

4.11 Vaccinees show low to undetectable levels of HIV-1 Bal virus control when assessed by an *ex vivo* VIA 118

4.12 Chapter 4 Discussion 120

4.13 Summary of key findings from Chapter 4 125

5 Assessment of HIVconsv vaccine-elicited $CD8^+$ T cells using an *in vitro* cultured virus inhibition assay 126

5.1 Introduction 126

5.2 Aims of Chapter 5 128

5.3 The HIVconsv vaccine induced $CD8^+$ T cells are capable of controlling HIV-1 clade A and B isolates. 129

5.4 Virus replication capacity does not account for differential virus control 142

5.5 The influence of HLA on virus control 145

5.6 Pol- and Gag-specific $CD8^+$ T cells induced by HIVconsv vaccination correlate with virus control 149

5.7 Total frequencies of *ex vivo* PBMC specific for conserved regions of HIV-1 correlate with virus control 154

5.8 Investigating the role of soluble factors on virus inhibition 154

5.9 Discussion 157

5.10 Summary of key findings from Chapter 5 164

6 Characterising vaccine-elicited conserved region Gag- and Pol-specific T cells 165

6.1 Introduction 165

6.2 Aims of Chapter 6 167

6.3 Vaccine-elicited Gag- and Pol-specific T cells can control in vitro HIV-1 replication 168

6.4 Gag- and Pol-specific T cells from broad virus controllers are cytotoxic and produce soluble antiviral factors 173

6.5 Multiple T-cell specificities can contribute to control of *in vitro* HIV-1 replication 184

6.6 Identification of T-cell epitopes contributing to control of *in vitro* HIV-1 infection 193

6.7 Pol-specific T cells recognise multiple escape variants of YQYMDDLYV 196

6.8 Chapter 6 Discussion 197

6.9 Summary of key findings from Chapter 6 203

7 Conclusions and recommendations for future work 204

7.1 Summary of research objectives 204

7.2 Future work based on this thesis 207

7.3 The future of HIV-1 vaccines 210

8 References 214

9 Appendix 239

List of Figures

Figure 1 Evolution tree showing envelope protein sequence homology between the HIV-1 and the SIVcpz lineage 20

Figure 2 A schematic representation of the HIV-1 genome 21

Figure 3 An overview of the HIV-1 life cycle 27

Figure 4 The window of opportunity following HIV-1 infection 30

Figure 5 Global clade distribution of HIV-1 33

Figure 6 The dynamics of $CD8^+$ and $CD4^+$ T cell counts and viral load during HIV-1 infection 38

Figure 7 The 14 conserved regions of HIV-1 included in the HIVconsv immunogen 48

Figure 8 The HIVconsv immunogen and trial design 70

Figure 9 Magnitude and breadth of vaccine-elicited T cells induced by low dose ChAdV63.HIVconsv 73

Figure 10 Frequencies of vaccine-elicited T cells recognising conserved regions of HIV-1 76

Figure 11 Comparison of vaccination regimens based on summed *ex vivo* IFN-γ ELISpot assay responses 77

Figure 12 Breadth of T-cell responses induced by the CM, DDDCM and DDDMC regimens 79

Figure 13 Comparison of magnitude and breadth of T-cell responses induced by CM, DDDCM and DDDMC to individual peptide pools 82

Figure 14 T-cell specificities induced through vaccination with CM and DDDCM regimens 84

Figure 15 Polychromatic flow cytometry analysis of vaccine-elicited T cells 85

Figure 16 Vaccine-induced cytokine profiles for the CM and DDDCM regimens 87

Figure 17 Comparison of vaccine regimen on cytokine induction from peptide stimulated PBMC 89
Figure 18 $CD8^+$ and $CD4^+$ T proliferation data for the CM, DDDCM and DDDMC vaccine regimens 90
Figure 19 An overview of an *ex vivo* VIA protocol 97
Figure 20 *Ex vivo* VIA gating strategy for the p24 intracellular staining protocol 101
Figure 21 Growth kinetics of HIV-1 virus stocks and $CD4^+$ T cell counts 102
Figure 22 Calculation of $TCID_{50}$ and percentage infection for HIV-1 clade A (92UG029), B (Bal) and C (HIV-1 ES x-1936) viral stocks 104
Figure 23 HIV-1 infection kinetics and effect on $CD4^+$ T cell viability 107
Figure 24 Optimising the MOI for HIV-1 Bal in healthy donors 108
Figure 25 Purity and recovery of $CD8^+$ and $CD4^+$ T cells isolated by negative and positive selection methods 110
Figure 26 Background HIV-1 Bal inhibition in a healthy donor at three effector to target (E:T) ratios 111
Figure 27 Establishing HIV-1-specific virus inhibition within healthy controls 113
Figure 28 Evaluation of chronic HIV+ patient by ex vivo VIA 116
Figure 29 Comparison of HIV-1 Bal stocks in a chronic HIV-1+ patient 117
Figure 30 Determining the inhibitory capacity of elite controllers and HIV-CORE 002 vaccinees by an *ex vivo* VIA 119
Figure 31 An overview of a cultured viral inhibition assay 131
Figure 32 CVIA data for the CM, DDDCM and DDDMC groups, respectively 134
Figure 33 IIIB and U455 CVIA data for each vaccine regimen 139
Figure 34 Comparison of vaccine regimens on the induction of viral inhibition 140
Figure 35 Replicative capacity of HIV-1 viral isolates in vaccinee $CD4^+$ T cells 144

Figure 36 The influence of HLA on virus inhibition 147
Figure 37 $CD8^+$ T cell specificity assessed by IFN-γ-ELISpot assay 152
Figure 38 Correlation of frequencies of Gag- and Pol-specific $CD8^+$ T cells with virus inhibition 153
Figure 39 Correlation of total *ex vivo* frequencies of HIVconsv-specific PBMC with virus inhibition 154
Figure 40 Correlation of p24 concentration with chemokine secretion from virally infected $CD4^+$ target cells on day 13 post infection 156
Figure 41 Example flow cytometry gating used to sort a Pol-specific T cell line 171
Figure 42 Inhibition of HIV-1 isolates by HIVconsv vaccine-elicited Gag pool- and Pol pool-specific T cells 172
Figure 43 Example flow cytometry gating for the in vitro cell killing assay 174
Figure 44 Determining the specificities of vaccine-elicited T cells with cytotoxic effector function 175
Figure 45 Example flow cytometry gating of mono- and poly-functional antiviral T-cells 177
Figure 46 Frequencies of Gag- and Pol-specific T cells with antiviral effector functions 178
Figure 47 Frequencies of polyfunctional peptide pool expanded Gag- and Pol-specific T cells 179
Figure 48 Correlation between the magnitude of peptide pool expanded HIV-1-specific T cells and the magnitude of the polyfunctional T-cell response 183
Figure 49 HIV-1 virus inhibition mediated by single peptide-expanded T-cell lines from vaccinee 411 185
Figure 50 HIV-1 inhibition mediated by single peptide-expanded T-cell lines for vaccinee 418 186

Figure 51 HIV-1 inhibition mediated by single peptide-specific T-cell lines for vaccinee 421 189
Figure 52 Intracellular cytokine staining of single peptide-expanded T-cell lines from vaccinees 411, 418 and 421 190
Figure 53 Cell phenotype analyses of peptide expanded T-cell lines for vaccinee 418 192
Figure 54 Identification of $CD8^+$ T cell epitopes contributing to in vitro control of HIV-1 infection 194
Figure 55 Recognition of multiple variants of YQYMDDLYV by Pol-specific T cells 197

List of Tables

Table 1 NK cell main receptor families 36

Table 2 Potency and neutralisation breadth of isolated bNAbs 40

Table 3 Summary of HIV-1 vaccine candidates reaching phase IIb and III clinical trials 43

Table 4 Calculation of the *ex vivo* VIA HIV-1 specific cut-off on day 13 by p24 ELISA 114

Table 5 HIV-1 viral isolates selected for CVIA 129

Table 6 CVIA assay positivity values based on 99.9th percentile 132

Table 7 The HLA Genotype of HIV-CORE 002 vaccinees 146

Table 8 Mapped peptides used for the generation of $CD8^+$ T-cell lines 170

Table 9 Mapped $CD8^+$ T cell epitopes for vaccinees 411, 418 and 421 195

Abbreviations

A3G	Apolipoprotein B mRNA Editing Enzyme, Catalytic Polypeptide-like 3G
AIDS	Acquired Immune Deficiency Syndrome
ADCC	Antibody Dependant Cell Cytotoxicity
AZT	Azidothymidine
bNAb	Broadly Neutralising Antibody
BSA	Bovine Serum Albumin
C	ChAdV63.HIVconsv
CAF	$CD8^+$ Antiviral Factor
CFSE	Carboxyfluorescein Succinimidyl Ester
CRF	Circulating Recombinant Form
CCR5	C-C Chemokine Receptor Type 5
ChAdV-63	Chimpanzee Adenovirus Serotype 63
CMTMR	(5-(and-6)-(((4-Chloromethyl)Benzoyl)Amino)Tetramethylrhodamine)
CMV	Cytomegalovirus
CTL	Cytotoxic T Lymphocyte
CVIA	Cultured Virus Inhibition Assay
CXCR4	C-X-C Chemokine Receptor Type 4
CyTOF	Cytometry by Time-of-Flight
D	pSG2.HIVconsv
DCs	Dendritic Cells
DC-SIGN	DC-Specific ICAM3-Grabbing Non-Integrin
DMSO	Dimethyl Sulphoxide
DNA	Deoxyribonucleic Acid
ELISpot	Enzyme Linked Immuno Spot
ELISA	Enzyme Linked Immunosorbant Assay
Env	Envelope
FBS	Foetal Bovine Serum
CEF	Flu, Epstein-Barr virus and Cytomegalovirus
Gag	Group-Specific Antigen
GALT	Gut-Associated Lymphoid Tissue
HAART	Highly Active Antiretroviral Therapy
HAdV	Human Adenovirus
HESN	HIV-1 Exposed Persistently Seronegative
HIV-1	Human Immunodeficiency Virus Type 1
HIV-1+	HIV-1 Infected Patients
HLA	Human Leukocyte Antigen
HVTN	HIV Vaccine Trials Network
IAVI	International AIDS Vaccine Initiative
ICS	Intracellular Cytokine Staining
IDU	Injection Drug Users
IEDB	Immune Epitope Database and Analysis Resource
IFN-α	Interferon Alpha
IFN- γ	Interferon Gamma
IL-2	Interleukin-2
i.m.	Intra-Muscular
IMC	Infectious Molecular Clone
IP-10	Interferon-γ Inducible Protein 10
KIR	Killer-Immunoglobulin-Like-Receptor
LANL	Los Alamos National Laboratory

LTNP	Long-Term Non-Progressor
LTR	Long Terminal Repeat
M	MVA.HIVconsv
mAb	Monoclonal Antibody
MACS	Magnetic Affinity Cell Sorting
MHC	Major Histocompatibility Complex
MIG	Monokine Induced by Interferon Gamma
MIP-1α	Macrophage Inflammatory Protein 1 Alpha
MIP-1β	Macrophage Inflammatory Protein 1 Beta
MOI	Multiplicity of Infection
MSM	Men who have Sex with Men
MVA	Modified Vaccinia Virus Ankara
NAbs	Neutralising Antibodies
NCR	Natural Cytotoxicity Receptors
NK	Natural Killer Cell
NKG2D	Natural Killer Group-2 member D
NKT	Natural Killer T Cell
NNRTI	Non-Nucleoside Reverse Transcriptase Inhibitor
NRTI	Nucleoside Reverse Transcriptase Inhibitor
NtRTI	Nucleotide Reverse Transcriptase Inhibitor
PBMCs	Peripheral Blood Mononuclear Cells
pDC	Plasmacytoid Dendritic Cells
pDNA	Plasmid DNA
pfu	Plaque Forming Unit
PHA	Phytohemagglutinin
PMA	Phorbol 12-Myristate 13 Acetate
Pol	Polymerase
PreP	Pre-Exposure Prophylaxis
RANTES	Regulated upon Activation, Normal T-Cell Expressed and Secreted
rhCMV	Rhesus Cytomegalovirus
RLU	Relative Light Units
RNA	Ribonucleic Acid
RNAse H	Ribonuclease H
RRE	Rev Response Element
RT	Reverse Transcriptase
SDF-1α	Stromal Cell-Derived Factor 1 Alpha
SFU	Spot-Forming Unit
SHIV	Simian-Human Immunodeficiency Virus
SIV	Simian Immunodeficiency Virus
SIVcpz	Chimpanzee Simian Immunodeficiency Virus
STCL	Short-Term Cell-Line
$TCID_{50}$	Tissue Culture Infectious Dose Infecting 50% of Cultures
TCR	T-Cell Receptor
T_{CM}	Central Memory T cell
T_{EM}	Effector Memory T cell
T_{TEM}	Terminal Effector Memory T cell
TNF-α	Tumor Necrosis Factor-Alpha
URF	Unique Recombinant Form
UNG	Uracil DNA Glycosylase
VIA	Virus Inhibition Assay
vp	Virus Particle

Publications arising from this thesis

1. Borthwick N, Ahmed T, Ondondo B, Hayes P, Rose A, Ibrahimsa U, Hayton E, Black A, Bridgeman A, Rosario M, Hill A, Berrie E, Moyle S, Frahm N, Cox J, Colloca S, Nicosia A, Gilmour J, McMichael A, Dorrell L, Hanke T. Vaccine-elicited human T cells recognizing conserved protein regions inhibit HIV-1. Molecular Therapy. 2014, **22** (2): p. 464-475.

2. Naarding M, Fernandez N, Kappes JC, Hayes P, Ahmed T, Lcyuz M, Edmonds TG, Bergin P, Anzala O, Hanke T, Clark L, Cox JH, Cormier E, Ochsenbauer C, Gilmour J. Development of a luciferase based viral inhibition assay to evaluate vaccine induced CD8 T-cell responses. J Immunol Methods. 2014 Jul, **409**: p.161-173.

1 Introduction

1.1 The origins of HIV-1

1.1.1 Crossing species

The first clinical presentation of acquired immune deficiency syndrome (AIDS), later shown to be caused by the human immunodeficiency virus type 1 (HIV-1), was reported in homosexual men from California in 1981 [1]. The group of individuals examined presented with a rare form of cancer, Kaposi's sarcoma, in addition to increased susceptibility to opportunistic infection by Pneumocystis pneumonia [1]. Subsequently, more cases of AIDS were described; in intravenous drug users [2], recipients of blood transfusion products [3, 4], heterosexual partners [5] and children of those infected. However, it was not until 1983, that Luc Montagnier and colleagues hypothesised that a retrovirus was the causative agent of HIV-1 [6] and this was then confirmed by Robert Gallo's laboratory in 1984 [7, 8].

The elucidation of a relationship between simian immunodeficiency virus (SIV) and HIV-1 arose in 1985 when rhesus macaques were shown to bear symptoms similar to those reported for patients infected with HIV-1 [9]. Since then many SIVs have been isolated from multiple subspecies of African monkeys [10]. Chimpanzee SIV (SIVcpz) sequences obtained from animals captured in the wild, in areas of the initial HIV-1 endemic, revealed viruses that were genetically similar to HIV-1 (Figure 1) [11-14]. Chimpanzees infected with variants of SIVcpz most closely related to HIV-1 were found to be from the *Pan troglodites troglodites* subspecies [15]. Moreover, the highly significant phenotypic clustering suggested that HIV-1 was likely to have arisen as a result of a zoonotic transfer from chimpanzees to humans [15].

HIV-1 has been classified into three groups; main (M), outlier (O) and non-outlier/main (N), with the M group being responsible for the global epidemic. Due to the phylogenetic distance between the three groups of HIV-1, it is suggested that three separate transmission events are likely to have occurred [15]. HIV-2 discovered in 1986, is distantly related to

HIV-1 and is less pathogenic [16, 17]. Its emergence in West Africa is thought to have originated from SIV transmission from sooty mangabeys [18, 19] which were often kept as pets.

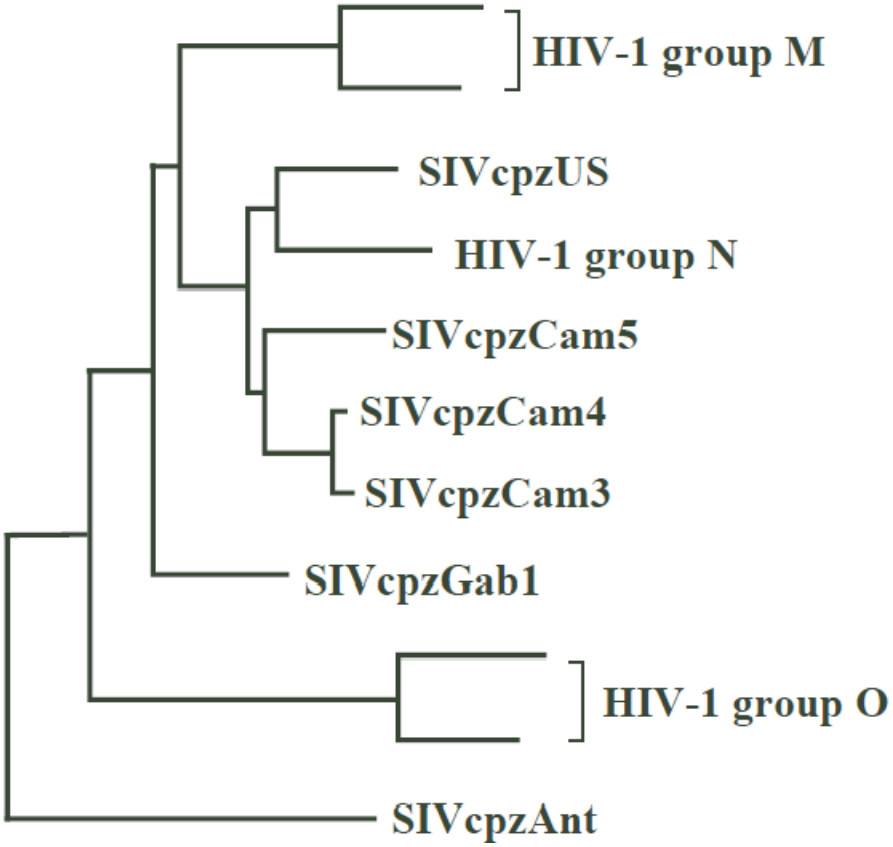


Figure 1 Evolution tree showing envelope protein sequence homology between the HIV-1 and the SIVcpz lineage, taken from Beer et al. 1999 [10].

1.2 HIV-1 virology and pathogenesis

1.2.1 HIV-1 is a retrovirus

HIV-1 is a member of the retrovirus family, *Retroviridae*. Retroviruses are defined by their ability to reverse transcribe positive sense RNA genome into negative sense DNA using the reverse transcriptase enzyme. This DNA template is subsequently stably integrated into the host genome as a 'provirus'. Retroviruses are subdivided into 5 genera; Alpha, Beta, Gamma, Delta, Epsilon, Spuma and Lentiviruses. The first three genera include 'simple

viruses' which only encode structural genes, whereas viruses from the remaining genera also encode accessory genes and are therefore more complex. HIV-1 is classified as a Lentivirus, meaning 'slow virus', due to the significant length of time between infection and clinical presentation. Despite this, it is now known that the virus has a rapid dissemination rate and establishes a latent reservoir in mucosal and lymphoid tissues soon after infection [20].

1.2.2 Genomic structure and function of the HIV-1 proteome

1.2.2.1 Essential proteins and viral enzymes

The HIV-1 genome is comprised of 9 genes encoded by a double stranded RNA genome of 9.7 kbp (Figure 2). The majority of viral genes are conserved between HIV-1 and HIV-2, with the exception of the accessory genes Vpu which is found in HIV-1 and Vpx present in HIV-2. The three main genes encoded by HIV-1 are the group-specific antigen (Gag), polymerase (Pol) and envelope (Env).

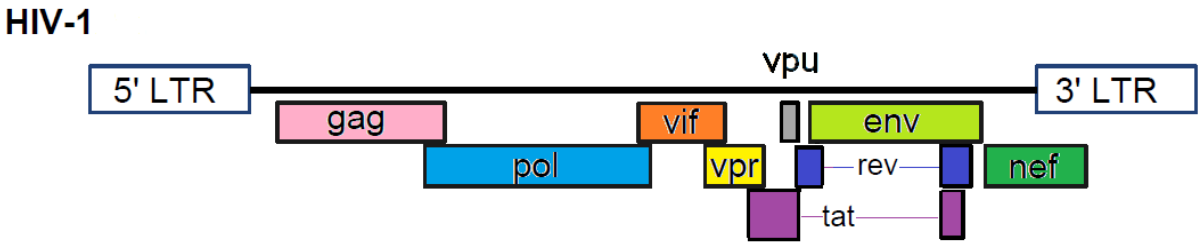


Figure 2 A schematic representation of the HIV-1 genome. Adapted from Beer et al. 1999 [10]. The HIV-1 viral RNA genome encodes 3 essential genes (Gag, Pol and Env) as well as six accessory genes (Vif, Vpr, Vpu, Rev, Tat and Nef). Each end of the genome is flanked by a long terminal repeat (LTR) which allows binding of the host transcription factors and trans-activation by Tat.

Gag contains four proteins essential for the virion structure; the matrix protein (p17) found on the internal face of the virion, the capsid protein (p24) which generates the conical core, the nucleocapsid (p7) which aids in stabilising the viral genomic RNA dimers and p6 which allows budding of the virus and incorporation of the Vpr protein into the virion, as reviewed in Freed et al. 1998 [21].

The enzymes required at multiple stages of the virus life cycle, described in section 1.2.3, are encoded by the Pol gene. The Pol protein is produced as a Gag-Pol precursor of 160 kDa by a -1 frameshift during translation [22]. This occurs relatively infrequently, thus leading to a Gag to Pol ratio of ~20:1. The Gag-Pol precursor encodes a viral Protease (p10), which is first auto-processed to release free Protease molecules [23]. During virion maturation both Gag and Gag-Pol precursors are cleaved by Protease into mature structural proteins and the active enzymes required for the following round of infection [24], failure to do so results in HIV-1 virions which are non-infectious [25]. Inside the cell the first viral enzyme required is Reverse Transcriptase (RT), which has two major subunits p66 & p51 [26]. The p66 subunit includes both the catalytic sites for reverse transcription (Asp110, Asp 185 and Asp186) [27] and a ribonuclease H (RNase H) domain [26]. RNase H is an endonuclease essential for the degradation of RNA strands of newly transcribed RNA/DNA templates [28]. Once the viral genome has been converted to double stranded DNA by RT, it is actively cleaved and stably inserted in to the host genome by viral Integrase (p32) [29].

The Env gene encodes the pre-cursor protein gp160, which is cleaved into gp120 and gp41 sub-units to form the mature envelope within the host cell membrane [30, 31]. As these sub-units are non-covalently bound, gp120 can be released from new virions [32]. This can stimulate and recruit resting $CD4^+$ cells which then become available as targets for further infection [33]. The complete structure exists on the cell surface as a trimer anchored by gp41 [34]. The gp120 molecule is heavily glycosylated at 24 asparagine sites [35], providing a shield of complex and variable oligosaccharides that prevent neutralising antibodies from reaching more conserved residues [36]. The inner constant region forms the core of gp120 and contains the sites relevant for CD4 binding [37, 38] and the more variable V3 loop contains co-receptor binding sites [39]. High sequence plasticity in the variable regions of gp120 contributes to the diversity found between viral clades [40]. Furthermore, changes in

the number of envelope molecules incorporated into infectious virions may also play a role in the efficiency of initial infection and later evasion of host humoral responses during chronic infection [41].

1.2.2.2 HIV-1 accessory proteins

HIV-1 has evolved to evade several intrinsic cellular mechanisms of virus inhibition through the acquisition of its accessory/regulatory genes Nef, Vif, Vpr and Vpu. The encoded proteins also aid in the efficient infection and productivity of a virally infected cell.

The Nef protein plays a key role in evasion of both cytotoxic T lymphocyte (CTL) and natural killer (NK) cell lysis. CTL recognise and kill virally infected target cells through the cell surface presentation of endogenous viral epitopes bound by human leukocyte antigen (HLA) [42]. Nef selectively down-regulates the primary HLA class I A and B alleles that present antigen to CTL, whilst leaving HLA C alleles on the cell surface [43]. NK cells have inhibitory receptors specific for HLA C [44] and E [45] and therefore do not kill HIV-1 infected cells that continue to express these alleles [43]. Nef also disrupts B cell maturation as in its soluble form [46] it has been shown to prohibit the class-switch from IgM to IgG and IgA [47], thus directly contributing to the early impaired antibody response towards HIV-1. Nef is also capable of inducing macrophages to secrete chemoattractants that activate and recruit $CD4^+$ T cells to the site of viral infection [48]. Sustained viral production is also achieved as Nef prevents apoptosis of infected cells [49] and efficient release of virions from the cell surface is aided by the ability of Nef to down-regulate CD4 and target it for lysosomal degradation [50].

The host cell protein APOBEC3G (A3G) is an intrinsic antiviral DNA editing enzyme incorporated into new virions to prevent reverse transcription in the new target cell [51]. The enzyme binds to reverse transcriptase and catalyses the deamination of a cytosine residue into

a uracil, resulting in viral cDNA transcripts that cannot be used as effective templates for the second DNA strand [52]. It has also been reported to reduce the levels of viral cDNA within the cell by binding to the cDNA templates and preventing reverse transcriptase from producing full length proviral genomes [53, 54]. To counter this activity Vif reduces the translation of A3G mRNA [55] and prevents the A3G protein from being packaged into new virions by targeting the protein for degradation by the cellular proteasome [56, 57].

Vpr is a pleiotropic viral protein involved in many stages of the virus lifecycle and is packaged into new virions via its interaction with the p6 protein in Gag [58]. It can also recruit the DNA repair enzyme uracil DNA glycosylase (UNG) into nacent virions [59]. UNG removes misincorporated uracil thus reducing reverse transcription errors and limiting the effect of the host A3G enzyme [60]. The Vpr protein is also found as a part of the pre-integration complex; the group of host and viral proteins responsible for shuttling viral DNA into the host cell nucleus [61]. Of these Vpr in particular is believed to be important in docking with the nuclear envelope [62] and also plays a key role in maintaining the cell cycle in G2 (growth 2) phase [63, 64], which is when the virus is optimally transcribed [65]. It has been hypothesised that Vpr does this by preventing activation of the cyclin dependant kinase 2 which would normally allow the cell to enter mitosis [64, 66]. Overall, this is likely to increase viral production by preventing apoptosis of the HIV-1 infected cells.

The final stages of viral budding are inhibited by the interferon-inducible host cell protein tetherin. This protein acts as an anchor between the virus and host cell membranes, preventing virion release [67]. The bound virions are then endocytosed [68] and degraded in host endosomes [67]. Vpu antagonises tetherin by countering its actions and thus effectively releasing new viruses from the cell surface [69]. Vpu also mediates the degradation of CD4 molecules bound to gp160 in the endoplasmic reticulum [70]; release of gp160 allows for

envelope maturation [71] and also prevents CD4 levels increasing at the cell surface which could impair virion release.

1.2.3 HIV-1 Life cycle

Mathematical models have shown that HIV-1 takes 1.2 days to replicate and that infected cells survive for an average of 2.2 days [72]. Despite this short survival time, total virion production is high, with approximately 0.68×10^9 virions released per day [73]. HIV-1 infection therefore results in rapid cell turnover and is sustained by continuous virion production and propagation.

The life cycle of HIV-1 begins with the gp120 envelope binding to the host cell surface receptor CD4 [74] and a specific chemokine co-receptor which dictates its tropism [75]. *In vivo*, viruses commonly utilise the chemokine co-receptors CCR5 [76], CXCR4 [76, 77] or both CCR5 and CXCR4 [75] and as a result are classified as R5, X4 or dual tropic respectively. Once bound, the envelope undergoes conformational changes which expose the coiled coils of gp41 [78], allowing membrane fusion and delivery of the viral core into the cytoplasm of the target cell [79].

Within the cell, the viral capsid is removed and the RNA genome is reverse transcribed into double stranded DNA using the reverse transcriptase enzyme [80]. This step yields many genetic variants of the parent virus due to the lack of fidelity of the RT enzyme [81] and its ability to switch between RNA templates [82]. The variants generated contribute to the viral 'quasispecies' or 'swarm' present within an infected individual [83]. The pre-integration complex is then transferred into the nucleus of the target cell, aided by Vpr [62]. Viral Integrase facilitates 3' cleavage and strand transfer of the viral DNA into the host genomic DNA [29] and this often occurs at 'hot spots' of increased transcriptional activity [84]. Once integrated, the viral genome is transcribed at a low level by the host RNA polymerase II [85],

aided by host transcription factors [86] akin to a ‘self’ gene. This process requires activation of the cell [87], otherwise the virus can enter a state of latency [88]. Translation occurs within the cytoplasm resulting in the production of viral Tat, Rev and Nef at low levels. In order to increase the low level transcription of the viral proteins, Tat migrates to the nucleus [89] where it increases the production of full length mRNA transcripts [90]. These viral transcripts are then rescued from the nucleus by Rev, which binds specifically to Rev-responsive elements (RRE) in un-spliced and single-spliced transcripts and then transports them to the cytoplasm [91]. Here they are translated into the Gag, Gag-Pol and Env gp160 pre-cursor proteins. The mature envelope together with the Gag, Gag-Pol precursors and viral RNA genome are then incorporated into new virions at the plasma cell membrane [21].

The virion is not mature until it buds from the host cell membrane, activating the viral Protease enzyme to cleave the precursor Gag and Gag-Pol proteins. Cleavage results in formation of the mature conical capsid core [92] and releases the viral enzymes Integrase and RT [21]. These new infectious virions are estimated to be viable for less than 8 hours [72] and therefore must find a new permissive host cell to guarantee survival.

Understanding these processes has been critical for the effective design of antiretroviral therapeutics which actively target multiple stages of the virus life cycle. These are discussed further in section 1.3.3 and are highlighted in the schematic diagram of the virus life cycle (Figure 3).

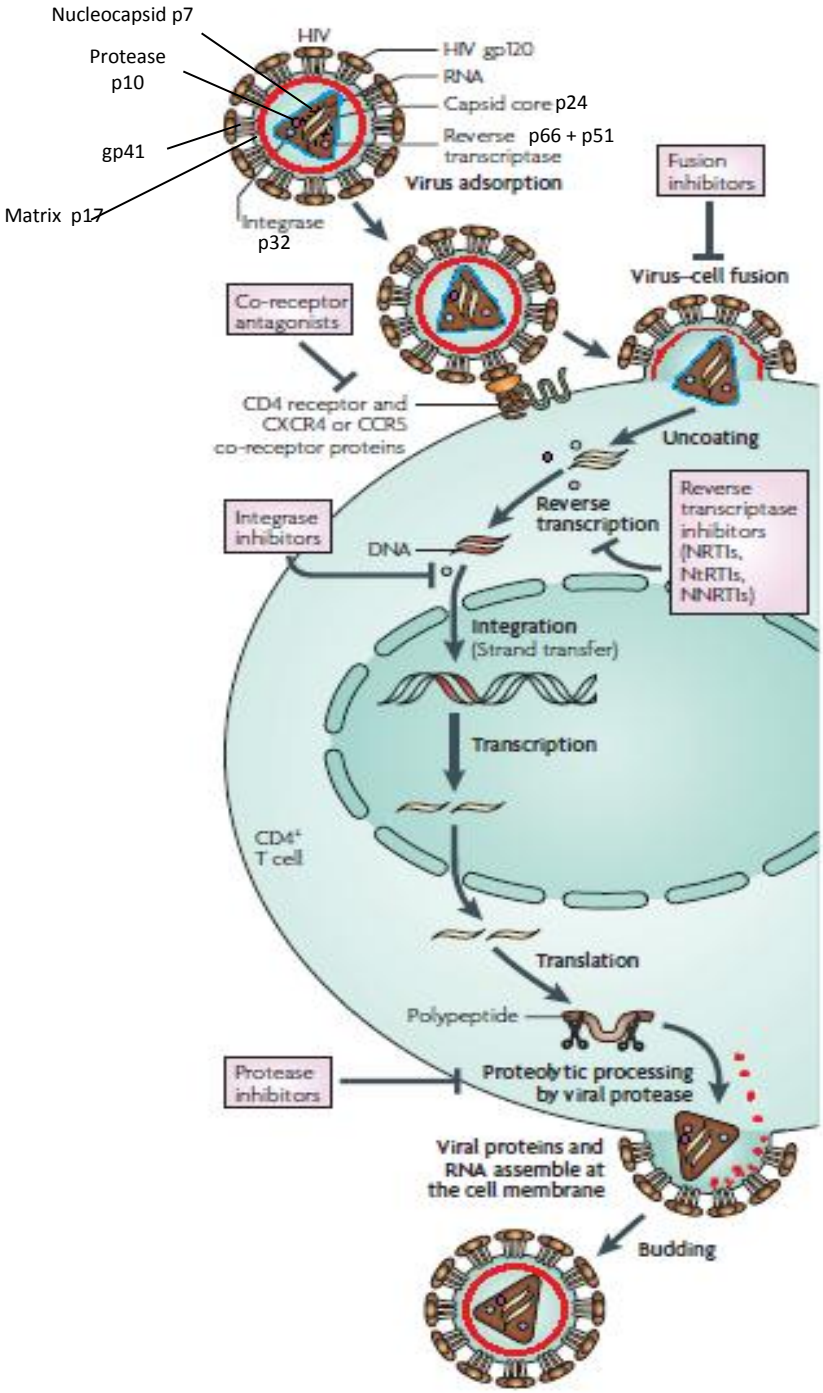


Figure 3 An overview of the HIV-1 life cycle. Adapted from De Clercq 2007 [93]. The key steps of HIV-1 infection and replication discussed in section 1.2.3 are depicted in Figure 3. Antiretroviral drugs have been developed to target multiple stages of the replicative cycle. These are binding of the HIV-1 co-receptors (CCR5 and CXCR4) by gp120, gp41 mediated cell fusion, reverse transcription by nucleoside, nucleotide and non-nucleoside reverse transcriptase inhibitors - NRTI, NtRTIs and NNRTIs respectively, as well as viral DNA integration and proteolytic cleavage of the viral polyprotein precursors [93].

1.2.4 The pathogenesis of HIV-1

HIV-1 is able to infect multiple cell types including T helper cells, macrophages, monocytes, microglia and dendritic cells (DCs). These cells are permissive to HIV-1 infection due to the expression of relevant cell membrane receptors, in particular CCR5 [94-96] which is used preferentially during acute infection [97]. Memory $CD4^+$ T cells are the prominent targets of HIV-1 infection [98] with HIV-1-specific memory cells infected at a higher frequency than other cell specificities, such as CMV [99]. Over time this preferential targeting could contribute to the weakened anamnestic responses observed in chronically infected individuals [100]. Furthermore, as disease progresses the virus can alter its tropism to utilise CXCR4 [77] which is expressed to a higher level on naïve T cells [94]. The emergence of this tropism is associated with a decline in $CD4^+$ T cell populations [101] and is a probable contributor to the heightened vulnerability of the immune system to new opportunistic infections.

Dendritic cells (DCs) also express the DC-specific ICAM3-grabbing non-integrin (DC-SIGN), a C-type lectin, which is the primary receptor used by HIV-1 to bind immature DCs prevalent within mucosal tissues [102]. These cells are capable of internalising [103] and transmitting the virus to $CD4^+$ T cells within secondary lymphoid tissues, with SIV infected DCs having been shown to be detected in the draining lymph node of rhesus macaques within 18 hours of intra-vaginal exposure [104]. Once the virus reaches distal sites, controlling infection becomes more challenging as the number of productively infected cells increases and is replenished with each round of viral replication [72].

One of the most severely affected areas is the gut-associated lymphoid tissue (GALT), here the greatest depletion of memory $CD4^+$ T cells is observed [105, 106]. GALT $CD4^+$ T cells are shown to be actively proliferating, therefore, significant reductions are likely to be as a direct result of HIV-1 infection as well as activation-induced cell death and potentially cell

lysis by cytotoxic T lymphocytes [106, 107]. Importantly, these cells fail to be fully reconstituted following therapeutic treatment [108], but early initiation of therapy may help to reduce these pathogenic effects [106]. A further impact of HIV-1 infection of the GALT is the disruption of the intestinal epithelial cell layer, resulting in microbial translocation and chronic activation of the innate and adaptive immune response [109]. On-going HIV-1 infection also damages the lymphoid tissues and lymph node architecture due to increased collagen deposition in the T cell zones. This significantly reduces naïve T cell numbers, leading to detrimental effects on the development of adaptive T and B cell responses [110]. Destruction of the germinal centres essential for B cell development is also observed early after HIV-1 infection and may contribute to the delayed emergence of an HIV-1-specific humoral response [111]. In addition, polyclonal B cell activation can be detected [111], suggesting a loss of regulation of B cell function.

In addition to the chronic disruption of the immune system by HIV-1 replication described above, the virus is also able to establish a latent reservoir of infected but resting T cells that do not produce infectious virions and are therefore invisible to the immune system [112]. The latent pool of $CD4^+$ T cells is suggested to be established early, by day 3 post infection, in mucosal and lymphoid tissues [20]. Latently infected cells are capable of persisting despite effective antiretroviral treatment with an average half-life of 43.9 months, meaning it may take 60 years to clear this reservoir using standard therapeutic regimens alone [113].

However, studies into mucosal transmission, currently the most common route of infection [114], have revealed hope for vaccine intervention in this cascade of events. Firstly, there is only a small founder population of infected cells present in the endocervix of rhesus macaques following intra-vaginal inoculation [115]. Secondly, viral sequence analysis of acutely infected HIV-1+ patients suggests that in 76% of cases a single founder virus

establishes infection [97] and the rhesus macaque model is in agreement [116]. Therefore, the mucosa, if not disrupted by damage or infection, acts as formidable barrier to HIV-1 transmission [117].

For mucosal transmission the window of opportunity for a prophylactic vaccine to stop the virus founder while this replicates locally at the site of entry is ~5-10 days [118] before it spreads throughout the body and establishes a self-propagating systemic infection. Therefore, a prophylactic vaccine would need to induce a cellular response that acts rapidly in response to viral infection and targets functionally conserved protein regions that HIV-1 cannot easily change.

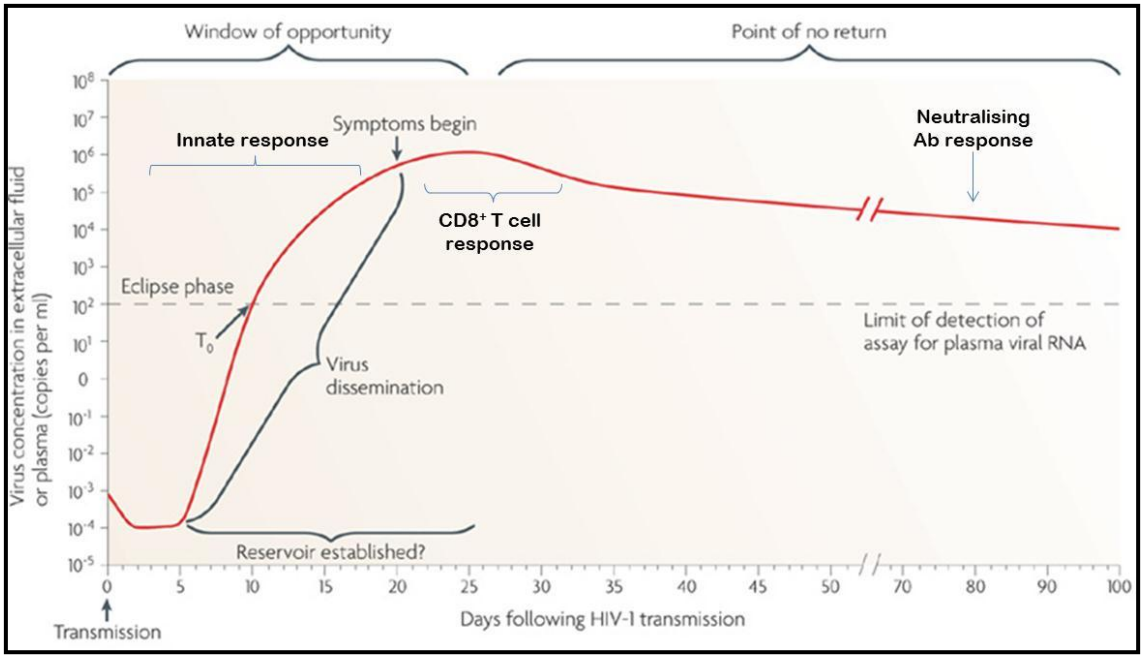


Figure 4 The window of opportunity following HIV-1 infection. Adapted from McMichael et al. 2010 [119]. The window of opportunity for a prophylactic vaccine is believed to be ~5-10 days before the virus disseminates to distal lymphoid sites. Innate immune responses to HIV-1 appear during this time but have little effect on the progression of infection. $CD8^+$ T cells begin to arise as peak viremia is reached, but do not significantly impact the viral sequence until after peak viremia and target mainly early variable proteins (Nef, Tat and Env). Autologous neutralising antibodies emerge much later post infection from approximately day 80 onwards. It is therefore believed that the natural response to HIV-1 infection is 'too little too late' [120] and that a vaccine must train the immune system to respond faster and target more vulnerable regions of HIV-1.

1.3 The global epidemic

1.3.1 Global burden of HIV-1 infection

Since HIV-1 was first isolated in 1983 [6, 121], it has claimed the lives of millions of adults and children. In 2013, an estimated 35.3 million people were living with HIV-1 and 2.1 million new infections occurred. Up to 70% of these new infections were within Sub-Saharan Africa [114], where there is insufficient medical infrastructure and limited access to antiretroviral therapy. There are several groups that are particularly vulnerable to HIV-1 infection, including young women who represent up to 60% of new infections [114], commercial sex workers, injection drug users (IDU) and men who have sex with men (MSM). Stigmatisation of these high risk groups and those individuals infected with HIV-1 often causes difficulties in monitoring and therefore also the provision of appropriate preventative or therapeutic measures [122].

1.3.2 Therapeutic strategies for control of HIV-1

Highly-active antiretroviral therapy (HAART) is currently the primary global therapeutic strategy employed to manage HIV-1 infection, which has also more recently been offered as a preventative measure (PreP) for HIV-1 negative individuals at high risk of infection [123]. Initially, a single antiretroviral agent, Zidovudine (AZT), was shown to increase patient survival and reduce the occurrence of opportunistic infections in HIV-1 infected (HIV-1+) patients suffering from AIDS [124]. The rapid emergence of drug resistance mutations [125], however, led to the development of new antiretrovirals and the implementation of combination or HAART therapy [126].

During the search for new therapeutic products a pioneering study conducted by Connor et al. demonstrated that AZT administered to pregnant women before birth, during delivery and to the newborn infant for up to 6 weeks, reduced transmission by 67.5% [127]. The WHO guidelines now advise that all pregnant women should begin HAART immediately and

that this should be continued throughout breastfeeding [123]. These potent triple regimens delivered to HIV+ patients result in dramatic reductions in viral load which significantly decreases the risk of viral transmission to partners [128-130] and between mother to child [131].

The introduction of PreP was proposed as a result of a study conducted in MSM which demonstrated a 44% reduction in HIV-1 incidence, though this was strongly associated with adherence to the regimen [132]. In addition to this there is growing evidence supporting early antiretroviral treatment (immediately after diagnosis) of HIV-1 infection, as in sero-discordant couples this was shown to reduce the rate of transmission by 96% [133].

1.3.3 Antiretroviral drugs approved for HIV-1 treatment

HAART typically utilises a combination of three classes of antiretrovirals; a nucleoside reverse transcriptase inhibitor (NRTI) such as Lamivudine (3TC), a nucleotide reverse transcriptase (NtRTI) inhibitor such as Tenofovir disoproxil fumarate (TDF) and a non-nucleoside reverse transcriptase (NNRTI) inhibitor such as Efavirenz (EFV) [123], which are all designed to inhibit proviral DNA production. NRTIs and NtRTIs are designed to cause early DNA chain termination by acting as a competitive dNTP substrate, whereas NNRTIs bind to a side pocket of RT which prevents the ATP-mediated excision of the NRTI and reversion of blocked DNA chains [134]. EVF, a member of the NNRTI class, has also been shown to increase RNase H mediated cleavage events, resulting in shorter DNA/RNA transcripts that RT is also unable to rescue [135]. Currently, more than 30 different antiretroviral drugs have been developed and approved [136]; these target various stages of the viral life cycle and include protease inhibitors, co-receptor entry inhibitors, membrane fusion inhibitors and strand transfer inhibitors targeting viral Integrase.

Despite the significant impact that antiretroviral therapy has had, there are several drawbacks to its widespread use. The high cost of production and provision continues to be a challenge [137, 138], side effects and toxicity in patients [139, 140] adds additional complexity to the effective management of treatment and the increasing emergence of drug resistance [125, 141] means that novel therapeutic compounds will need to be found which can tackle these divergent strains whilst still maintaining suitable safety profiles.

Alternative measures such as providing HIV-1 education programmes for young adolescence, voluntary circumcision, which can reduce the risk of infection by up to 60% in areas of high endemicity [142], and provision of condoms and clean needles have all helped to reduce the growing infection rates in areas such as Zambia, Tanzania and Kenya but many other countries have struggled to implement these programs and as a result show increased incidences of infection [114] (Figure 5). Thus, the development of an effective prophylactic HIV-1 vaccine still remains paramount for controlling the continuing epidemic [143].

1.3.4 The genetic diversity of HIV-1

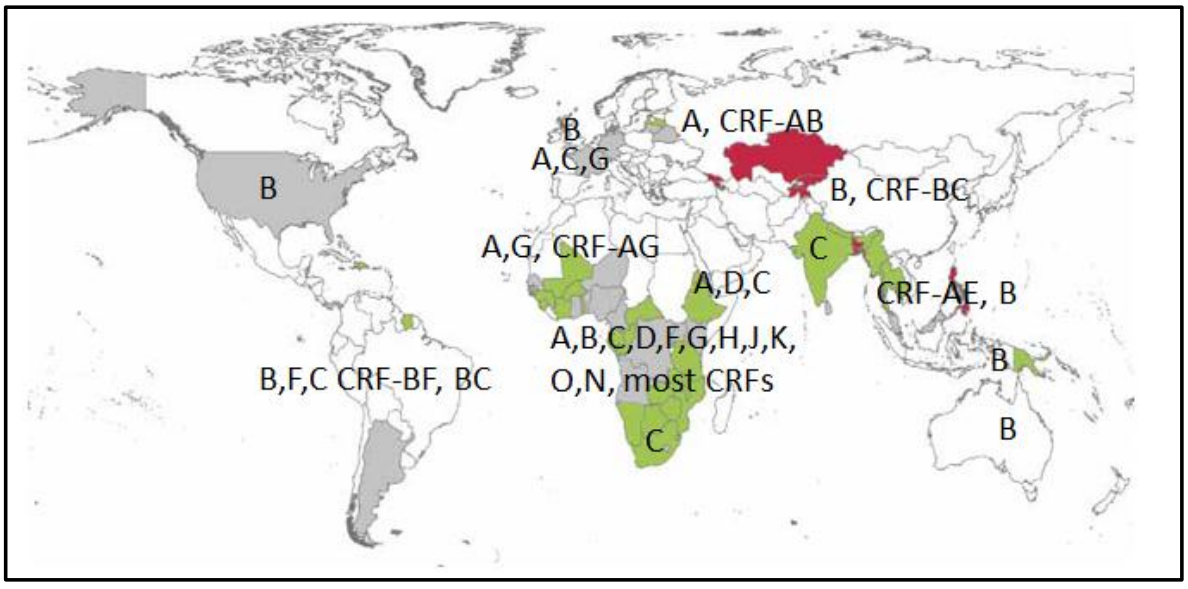


Figure 5 Global clade distribution of HIV-1. Grey, green and red colour-coding represents areas with stable, decreasing, or increasing HIV-1 infection rates respectively. Adapted from UNAIDS global report 2010 [144] and Korber et al. 2001 [145].

One of the greatest hurdles facing HIV-1 vaccine design is the tremendous genetic diversity demonstrated by HIV-1. The main group comprises nine genetic subtypes of HIV-1 (A-K excluding E and I) and there are an increasing number of circulating recombinant forms (CRFs) [146] and unique recombinant forms (URF) [147] being reported. These recombinant forms are believed to arise as a result of co-infection of a single cell with two different subtypes of HIV-1 that subsequently recombine during virus replication [145]. Clade distribution varies between continents and countries (Figure 5), but the most predominant clades globally are A-C [148]. In some regions, however, CRFs have become the prominent subtype. For example, CRF01-AE, which originated in Thailand [149, 150], is responsible for greater than 75% of new infections across Asia [148]. Similarly, in western Africa, CRF02-AG has become a dominant subtype, responsible for up to 50% of new infections [148]. Currently, the reason for the differing prevalence of particular HIV-1 clades in select regions is unknown.

Genetic variation between the clades is substantial with 15 - 20% sequence diversity reported for more conserved regions of the genome such as Gag, but this increases markedly, up to 35%, for the variable Env protein [145]. Furthermore, immune pressures within an infected individual enhance the complexity of the viral 'quasispecies' that are subsequently transmitted [151]. A successful vaccine will have to deal with the multiple circulating viruses in the population and with the escape mutants generated within infected individuals.

1.4 Harnessing the host immune response to HIV-1

Although HIV-1 infection results in the induction of innate, cell-mediated and humoral responses most individuals fail to control HIV-1 infection without therapeutic intervention and will subsequently develop AIDS. There are a select number of individuals (5 - 15%) who do not progress rapidly to AIDS but instead are able to control viral replication for more than 10 years. These individuals are termed as long-term non-progressors (LTNP) [152, 153] and

within this group there are those who maintain very low viral loads (<50 copies RNA/ml) and are described as 'elite controllers' [154]. In addition, high-risk individuals have been identified that are routinely exposed to HIV-1 yet remain uninfected are termed HIV-1 exposed persistently seronegative (HESN) [155]. Studies of these groups as well as those with a normal course of infection have revealed in-sights as to which responses are associated with improved clinical outcome and have guided the field in which cell types and functions we should aim to induce through vaccination.

1.4.1 Innate response

The innate immune response is the first line of defence against viral and bacterial infections, occurring before the adaptive response has begun. In HIV-1 infection, interferon-alpha (IFN-α) is a potent inhibitor of viral replication [156, 157] and this cytokine is produced at the highest levels by plasmacytoid dendritic cells (pDC) [158]. Once infected by HIV-1, these cells are triggered to produce IFN-α by recognition of viral RNA through toll-like receptor 7 [159]. However, they do not go on to produce infectious virus as the receptor Langerin induces endocytosis and degradation of HIV-1, in contrast to DC-SIGN [160]. In chronic HIV-1 infection these pDC are depleted but in LTNP these cells are present in high numbers suggesting that they may help to delay disease progression [161, 162].

NK cells are also important sentinels of the innate immune system that continually monitor the 'normal state' of cells and are capable of secreting cytokines and lysing infected or transformed cells [163]. Their response is controlled by the interaction of activating and inhibitory receptors, as well as co-stimulatory molecules expressed on the surface of the NK cells with their cognate ligands expressed on the target cell [164]. There are several NK cell receptor families, outlined in Table 1, that participate in recognition of infection. NK cells can also mediate antibody dependant cellular cytotoxicity (ADCC) through their FCγ receptor

III (CD16) which binds to the Fc fragment of IgG inducing cellular activation and target cell lysis.

Table 1 NK cell main receptor families

Receptor Family	Interacting Molecules	Activating (A) or Inhibitory (I)
Killer-immunoglobulin-like receptor (KIR)	Classical MHC class I (A, B & C)	A & I
NKG2D (Natural-killer, Group-2 member D)	MHC class I-chain-related protein A	A
	MHC class I-chain-related protein B	
	Retinoic acid early transcript 1	
	UL16 Binding protein-1,-2,-3 & -4	
CD94-NKG2 members A/C/E	HLA-E	A & I
Natural cytotoxicity receptors (NCR)	Viral hemagglutinin	A

Adapted from Pegram et al. 2011 [164].

Recently ADCC has been implicated in playing a role in reducing the risk of HIV-1 infection following vaccination in humans [165]. Support of this correlate comes from a mucosal SIV challenge study, in which vaccine-induced Env-specific ADCC correlated with reduced acute viremia [166]. In a separate study investigating the functionality of the first isolated HIV-1 broadly neutralising antibody (bNAb) b12, clearance of virus and virally infected cells was mediated by Fc receptor binding and was most effective when both complement and ADCC functions were present [167].

The influence of NK cells on the course of viral infection has also been examined in a cohort of over 1000 individuals infected with HIV-1, with those bearing the activation receptor KIR3DS1 together with the HLA Bw4 with isoleucine at position 80 (Bw4-80I), showing slower progression to AIDS [168]. This relationship was investigated further and

NK cells bearing the KIR3DS1 receptor were capable of reducing *in vitro* viral replication and lysing HLA Bw4-80I targets [169]. Furthermore, in a cohort of HESN individuals there was an over-representation of persons homozygous for KIR3DS1 when compared to those with primary HIV-1 infection, suggesting that their NK cells are more active and potentially more effective in controlling HIV-1 [170]. Lowering the threshold for NK cell activation has also been implicated in protection from HIV-1 infection, as inhibitory receptors were expressed in the absence of their cognate receptors within a cohort of HESN sex workers [171]. In support of this theory HIV-1 has been shown to harbour mutations which are believed to enhance the engagement of the NK inhibitory receptor KIR2DL2, resulting in reduced HIV-1 suppression by $KIR2DL2^+$ NK cells [172].

1.4.2 T cell response

Although $CD8^+$ T cells are unable to prevent primary infection from occurring, there is a body of evidence supporting their role in the control of viral infection. Studies within acutely infected individuals showed that with the presence of early HIV-1-specific CTL responses and high CTL precursor frequencies, viral control was observed [173, 174]. This data is supported by $CD8^+$ T cell depletion studies performed in the SIV model [175-177], where the rise in viral load was temporally associated with the decrease in $CD8^+$ T cell counts. Moreover, in elite controller macaques viral control was regained by broad $CD4^+$ and subdominant $CD8^+$ T cell populations [177]. In HESN individuals HIV-specific cytotoxic $CD8^+$ T cells are repeatedly found and are believed to control and clear the initial virus infection [178-180]. In addition, HIV-specific $CD4^+$ T cells have also been found within HESPN in the absence of humoral responses and may also aid in a rapid cell-mediated response and protection from low dose infection [181]. Furthermore, in most cases of HIV-1 infection, the progression of disease is hallmarked by the decline in the HIV-1-specific $CD8^+$

T cell response concomitant with an increase in viral load and reduction in $CD4^+$ T cell counts (Figure 6).

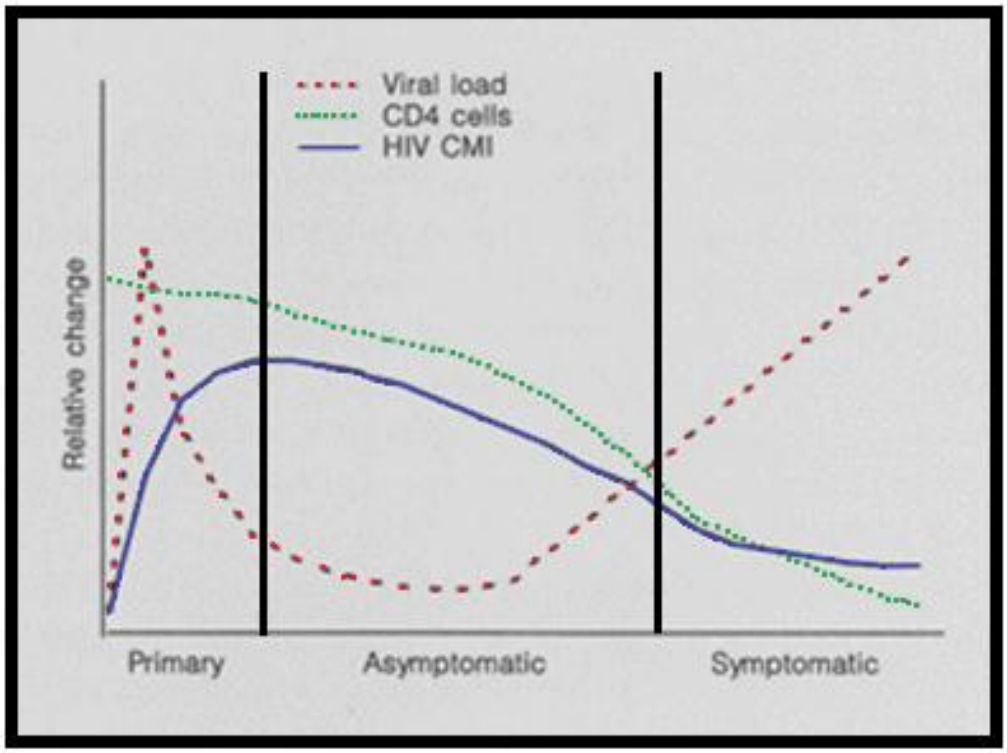


Figure 6 The dynamics of $CD8^+$ and $CD4^+$ T cell counts and viral load during HIV-1 infection. Adapted from Moss et al. 1997 [182]. The cell mediated immune response (CMI) peaks during primary infection and declines steadily with the contraction of viral load, reaching a steady 'set point' that can be used to predict time until onset of AIDS. This asymptomatic phase can last between 8-10 years before a rise in viremia is observed which occurs as $CD4^+$ T cell help is severely diminished resulting in $CD8^+$T cells that are no longer capable of virus control.

Examination of the viral species during acute infection has revealed escape mutations within T-cell epitopes, highlighting viral evolution to subvert recognition by the first responding T cells [118, 183]. These mutations ultimately led to the loss of viral control in the absence of T cell responses to more conserved viral epitopes [118]. CTL recognition of virally infected cells is heavily influenced by HLA type [184, 185] and alleles capable of presenting a breadth of epitopes, particularly from structurally relevant regions of the virus

such as Gag [186, 187] afford a greater advantage to the host. This advantage may potentially be due to a reduction of viral fitness [188] caused by mutations within these regions.

Evidence for the quality of the HIV-1-specific T cell response being of greater importance than its frequency, comes from LTNPs. There are several functional characteristics which set apart CTL from progressors and LTNPs, including preserved proliferative capabilities [189], high levels of cytolytic granules [190] and multi-functionality of effector cells [191]. The enhanced antiviral effect from targeting the Gag protein [192] by high avidity CTL clones [193] was also demonstrated in this population.

1.4.3 B cell response

Ideally a humoral response to HIV-1 would be present at the time of viral infection and result in the binding and clearance of cell-free virions by neutralising antibodies. In HIV-1 infection, antibodies to the envelope protein are detectable in the sera of patients as early as 2 weeks but these antibodies are non-neutralising [194]. A study of acute HIV-1 infection has shown that antibodies can be found complexed with virus ~18 days after transmission, but their protective role is currently unknown [195]. The earliest free plasma antibodies were found to be specific for gp41 and were comprised of IgM, IgG and IgA. Gp120-specific antibodies appeared two weeks later, but none of these early (within the first 40 days of transmission) antibodies had any effect on viral load [195]. This is in part due to the highly promiscuous glycosylation of the viral envelope, which allows for rapid escape and shields vulnerable sites from antibody binding [196]. Neutralising antibodies do develop, but not until months after infection and they are highly specific to the autologous isolate [194, 196, 197].

Encouragingly, bNAbs have been isolated from select chronically infected patients but they represent a very low percentage of their total HIV-1-specific antibody response [198].

Several bNAbs have been well characterised (b12, 2F5, 4E10, 2G12, Z13, 447-52D & 17b) [199] and mapped for binding on the HIV-1 envelope glycoprotein surface. These studies have revealed that the regions targeted by these individual bNAbs include the recessed CD4 binding site [200], the gp41 membrane-proximal external region [201], conserved oligomannose residues [202], the V3 loop of gp120 [203] and CD4 induced epitopes [204, 205], occurring as a result of envelope binding and conformational change. Passive transfer of neutralising antibodies to rhesus macaques gave protection from SIV but only with high levels of antibody [206-208]. The potency of 2G12 was found to be greater and suggested that some antibody specificities may be superior in terms of viral clearance [209]. In 2009, the isolation of two new highly potent bNAbs, PG9 and PG16 [210], re-invigorated the field and since then multiple groups have discovered high potency bNAbs [211-215], through the improvement of envelope design and plasma B cell cloning.

Table 2 Potency and neutralisation breadth of isolated bNAbs

bNAb Generation	Example bNAb	Potency (median IC_{50})	Virus Neutralisation Breadth
1st	b12	2.82 $\mu g/ml^{-1}$	34%
	2G12	2.38 $\mu g/ml^{-1}$	32%
2nd	PG9	0.23 $\mu g/ml^{-1}$	77%
3rd	PG128	0.02 $\mu g/ml^{-1}$	72%
	35O22	0.033 $\mu g/ml^{-1}$	62%

Potency and neutralisation data taken from Walker et al. 2011 [214] and Huang et al. 2014 [215].

Designing the appropriate vaccine immunogen/s capable of inducing these responses however remains a formidable challenge as these antibodies show extensive somatic hypermutation and are no longer representative of the germ line genes [210, 212]. Nevertheless, discovering these antibodies was the first step towards the development of a bNAb vaccine. The field now needs to focus on the design and administration of sequential

Env immunogens to mimic the natural maturation induced by HIV-1 recognition and escape [216] and this will need to be supported by an effective T follicular helper cell response for optimal B cell maturation [217].

1.5 Vaccines against disease

Historically vaccines were developed to train the immune response to control and clear viral or bacterial pathogens; they were not designed to prevent the vaccinee from becoming infected as we would hope to do with an HIV-1 vaccine [218]. Prevention of disease was achieved largely through the induction of both antibodies and/or cytotoxic T cell responses using live-attenuated viruses (e.g. smallpox, measles, mumps, rubella and varicella zoster vaccinations [219]), whole killed organisms (e.g. typhoid, rabies, hepatitis A) or purified proteins (e.g. diphtheria and tetanus toxoids) [220].

For HIV-1, there are no known infected individuals who have cleared HIV-1 from the immune system or recovered from AIDS and as a result the immune correlates of protection remain unknown. However, proven success with live-attenuated vaccines for other diseases led to this strategy being tested for HIV-1, in the rhesus macaque model of SIV infection. Several live-attenuated SIV vaccines were investigated but the results from these studies, although initially encouraging, raised a number of safety concerns. The attenuated Nef mutant viruses used for vaccination were shown to be able to repair over time, and revert to more pathogenic strains that went on to cause disease [221-223]. In light of this data, a triple mutant SIV virus (Vpr, Nef and negative regulatory element deletions) was developed to try and improve vaccine safety [224]. However, when tested within adult and neonate macaques, the adults which showed initial control of viremia went on to develop chronic SIV infection [225] and the neonates failed to show any control of this virus [226], progressed rapidly to AIDS and 6/9 died within 4.5 years [225]. Therefore, even in the absence of high viral loads

attenuated replication competent SIV is capable of adapting to cause disease, which ultimately suggests that this strategy is unsuitable for an HIV-1 vaccine.

To address the aforementioned safety concerns, alternative modalities have been developed and assessed as potentially safer HIV-1 vaccine candidates including inactivated viruses, recombinant glycoproteins, and proteins or epitopes delivered by naked DNA [227, 228] or replication-defective viral vectors [229, 230] and various combinations of these modalities [229, 231, 232]. Inactivated whole SIV and virus infected cells protected macaques against SIV challenge [233-236], but in most cases there was no correlation with SIV-specific antibody levels [237]. Subsequently, these vaccines were found to induce antibody responses to the components of the cells-lines used to produce the virus, and it was levels of these antibodies that related to protection [238, 239]. The results of these studies led the field toward the use of highly purified subunit glycoproteins for the induction of a humoral response [240]. However, the first human trials with monomeric recombinant envelope glycoproteins also proved to be unsuccessful in generating neutralising antibodies which recognised primary isolates of HIV-1 [241] and in vaccinees that went on to acquire HIV-1 there was no evidence of immune pressure placed on to the virus or difference in the clinical course compared to unvaccinated controls [242]. These largely disappointing results shifted the HIV-1 vaccine field toward the induction of T cells, through applications of both DNA and replication-incompetent viral vectors. In animal models these vectors have shown great potential in their ability to induce strong cell-mediated responses, especially when used in prime-boost regimens, and as a result several have progressed through to human clinical trials [243] and are discussed below.

The induction of a broadly neutralising antibody response, as described above, is still deemed essential for the ultimate preventative HIV-1 vaccine [244]. Since the very first trials with monomeric glycoproteins, new ‘truly bNAbs’ have been isolated and characterised from

chronically infected individuals, which has refuelled the idea that a bNAb vaccine is achievable [245]. Many groups are currently working on improved envelope structures, such as gp120 trimers [246, 247], deglycosylated envelopes [248-250] and envelopes engineered to target the germ-line cells of bNAb [251, 252]. Hopefully these new immunogens will be capable of inducing bNAbs of high potency through vaccination.

1.5.1 Current state of the HIV-1 vaccine field

To date, there have been more than 195 HIV-1 clinical trials completed [253], testing a range of HIV-1 immunogens with a variety of delivery vectors; from protein to viruses. However, only 3 candidates have reached completion of large scale efficacy testing (Phase III), and a further 3 reached Phase IIb but were terminated early due to safety concerns [253]. Of these Phase IIb and III vaccines, AIDSVAX, was the first candidate to reach Phase III and focused solely on the induction of antibodies, whilst the Phase IIb (HVTN 502, 503 and 505) vaccines have focused on eliciting T-cell responses. The only trial to have shown any efficacy against HIV-1, RV144, was designed to induce both T- and B-cell responses. These vaccines are described in further detail below, with a summary also provided in Table 3.

Table 3 Summary of HIV-1 vaccine candidates reaching phase IIb and III clinical trials.

Study Reference and Phase	Candidate Vaccine	Sample Size	Study Population	Location	Result
Vax004 (Phase III)	AIDSVAX B/B gp120 in alum	5400	MSM, high risk women	USA	No efficacy
Vax003 (Phase III)	AIDSVAX B/E gp120 in alum	2500	Injection drug users	Thailand	No efficacy

HVTN 502 (Step Study, Phase IIb)	MRK HAdV-5 Gag/Pol/Nef clade B	3000	MSM, high risk heterosexual men and women	North and South America, Australia, Carribean	No efficacy, trial stopped. Trend of increased incidence in vaccinees
HVTN 503 (Phambilli, Phase IIb)	MRK HAdV-5 Gag/Pol/Nef clade B	3000 (planned, with 801 enrolled)	Heterosexual men and women	South Africa	No efficacy, trial stopped. Trend of increased incidence in vaccinees
HVTN 505 (Phase IIb)	DNA (Gag/Pol/Nef B, Env A, B, C) HAdV-5 (Gag/Pol B, Env A, B, C)	2496	Circumcised MSM and transgender MSM HAdV-5 seronegative	USA	Stopped due to futility, no efficacy on HIV-1 acquisition or plasma VL
RV144 (Phase III)	ALVAC-HIV vCP1521 and AIDSVAX gp120 B/E in alum	16, 403	Community risk	Thailand	31.2% efficacy against HIV-1 acquisition, no effect on plasmaVL

ALVAC CP1521 = recombinant canary pox expressing Gag and Protease clade B and CRF01_AE gp120 linked to the transmembrane anchoring portion of gp41; MSM = men who have sex with men; VL = viral load. (Information taken from Excler et al. 2013 [254]).

1.5.2 AIDSVAX - Vax004 and Vax003

Vax004 and Vax003 administered AIDSVAX, a gp120 immunogen in an alum adjuvant, and were clade matched specific to the countries in which the trials were conducted. Vax004 [255] tested a bivalent clade B/B Env protein in a sexual transmission cohort of MSM and women, whereas Vax003 [256] tested a bivalent clade B/E Env protein in a parenteral transmission cohort of injection drug users (IDU). Unfortunately, neither of the vaccine candidates was efficacious. In Vax003 and Vax004, both CD4 blocking antibodies and gp120 neutralising antibodies to the vaccine strains were induced, but these were not effective in reducing the incidence of HIV-1 infection or in delaying time to commence treatment following infection. It was postulated that these antibodies were not broadly

responsive to the diverse isolates in circulation [257]. Despite these results, the AIDSVAX B/E construct was combined with an attenuated canary pox virus (ALVAC) prime in the RV144 trial described below.

1.5.3 HVTN 502-Merck STEP Study and HVTN 503-Phambili trials

The HVTN 502 (STEP) [258] and 503 (Phambili) [259] studies were designed to induce T-cell responses against HIV-1 clade B Gag, Pol and Nef, with the immunogens delivered by replication defective human adenovirus serotype 5 (HAdV-5). Both studies were phase II test-of-concept, designed to explore whether the vaccine could reduce HIV-1 acquisition or decrease viral load. The HVTN 502 study was conducted within a cohort at high risk of sexual transmission, in countries suffering from a clade B epidemic, whereas HVTN 503 was conducted in a lower risk heterosexual cohort from South Africa which is affected mainly by HIV-1 clade C. Both studies were stopped early for futility following interim analyses; there was no efficacy observed and in the post-hoc analysis there was a trend of increased incidence of HIV-1 infection in men who were HAdV-5 seropositive or uncircumcised [258, 259]. Subsequent analyses into breakthrough infections revealed that the vaccine had a sieve effect, which limited which viruses were able to establish infection [260]. There was also evidence for decreased viral load in vaccinees that made more than two Gag-specific T cell responses [261]. More recently, these cohorts have been shown to respond very poorly to previously identified ‘beneficial regions’ of the viral proteome including those in Gag when vaccinated with full length HIV-1 proteins. These data suggest that new immunogens should include only proteome regions that are associated with proven fitness costs to the virus in order to achieve effective virus control [262].

1.5.4 HVTN 505

The HAdV-5 vector was also used in the HVTN 505 study, in a DNA-HAdV-5 prime-boost regimen, to deliver clade B Gag/Pol/Nef and clade A, B, C Env to a cohort of men at

high risk of infection [263]. This study, however, was also halted due to lack of efficacy as there was no reduction in HIV-1 acquisition or effect on set-point viral load post-infection [263].

1.5.5 RV144

More recently, the RV144 vaccine trial, conducted within individuals at community risk of HIV-1 infection in Thailand, showed modest (31.2%) efficacy in the prevention of HIV-1 infection. However, in the vaccinees who became infected there was no reduction in viral load [165]. The protection afforded by this vaccine was suggested to be through the induction of non-neutralising IgG specific for the V1/V2 loops of the envelope (gp120) [264]. Support of this data arose from a study into the breakthrough viruses from vaccine recipients, which showed that vaccine efficacy increased when the infecting isolate was sequence matched at position K169 and mismatched at position I181 in the V2 loop [265]. Furthermore, isolation of four V2-specific monoclonal antibodies from RV144 vaccinees demonstrated that these antibodies were able to induce ADCC but had limited neutralisation capabilities [266]. The failure of the RV144 vaccine to have any effect on set-point viral load, may have been due to the fact that HIV-1 specific $CD8^+$ T cells were not induced through vaccination with the ALVAC [vCP1521] prime and AIDSVAX gp120 B/E boost [264].

1.5.6 Insights gained from HIV-1 vaccine trials conducted to date

Overall these clinical trials demonstrated that an HIV-1 vaccine will need to induce potent broadly neutralising antibodies that could work together with ADCC inducing antibodies to not only prevent infection from the array of circulating HIV-1 isolates but also limit viral dissemination in the event of infection. Support from a broad cytotoxic T-cell response focused toward conserved regions of the virus such as Gag would limit the fitness of the evolving quasispecies potentially allowing HIV-1 to be effectively controlled without the need for antiretroviral treatment.

1.6 Tackling HIV-1 diversity with the HIVconsv T-cell vaccine

1.6.1 Overcoming HIV-1 diversity by immunogen design

The immunogen is one key component of a vaccine and together with the choice of appropriate delivery vector and adjuvants can be tailored to induce humoral, cell-mediated or dual adaptive responses [267]. As highlighted, the great diversity of HIV-1 makes designing a single all-encompassing immunogen a significant challenge. Nevertheless, several strategies have been proposed, including using sequences based on ancestral centre-of-the-tree [268], consensus [269], conserved [270, 271] and more recently mosaic immunogens [272].

Both ancestral and consensus sequences can be derived from phylogenetic trees; ancestral represents the sequence most likely to have given rise to the subtype(s) whereas a consensus sequence is derived from the most common amino acid at each site based on circulating viruses thus making it a 'central sequence'[273]. These two strategies can be used to make a single clade (e.g. subtype C) or multi-clade (M-group) vaccine [273]. Conserved sequences are based on the regions of virus that display the lowest levels of variability [274]; which may be because they are structurally relevant for virus integrity or because they are not under any form of immune pressure. In contrast to conserved immunogens, mosaic immunogens are computer-generated from database HIV-1 sequences and contain multiple 9-mer epitopes that result in the greatest breadth (number of different epitopes) and depth (variants of the same epitope) of coverage [272]. Mosaic vaccines look promising in the rhesus macaque model where they have induced greater breadth and depth of peptide recognition by $CD8^+$ and $CD4^+$ T cells when compared with natural or consensus immunogens [275].

1.6.2 The HIVconsv immunogen

Our group focuses its research on the cell-mediated arm of the adaptive immune response particularly on the induction of both $CD4^+$ and $CD8^+$ HIV-1-specific T cells. We

have therefore designed a chimeric T-cell immunogen, designated HIVconsv (conserved region), which aims to overcome the vast diversity of HIV-1 by including 14 of the most conserved regions from four of the major HIV-1 clades (A, B, C and D). T-cell responses are targeted towards mainly subdominant viral epitopes, which in the event of mutation should significantly reduce viral fitness. The immunogen encompasses 2.5 kbp from the HIV-1 proteome and embedded within these regions are 24% of the $CD8^+$ T cell epitopes, of ≤12 amino acids, published in the Los Alamos National Laboratory HIV Sequence Database in 2007 [270].

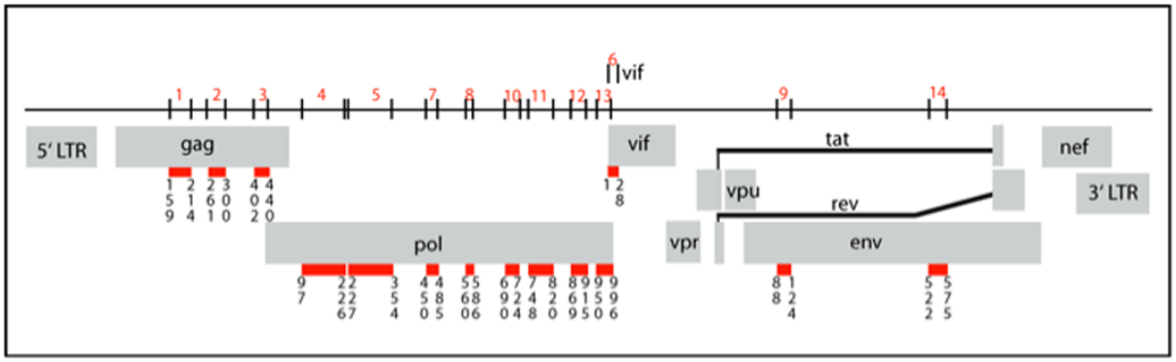


Figure 7 The 14 conserved regions of HIV-1 included in the HIVconsv immunogen. Numbers written above the proteome represent each of the 14 regions included in HIVconsv. The numbers written vertically beneath each protein fragment represent the start and end amino acid based on the HIV-1 HXB2 reference sequence. Figure taken from Letourneau et al. 2007 [270].

The vaccines were delivered using a combination of plasmid DNA (pDNA), replication-incompetent modified vaccinia virus Ankara (MVA) and replication-incompetent chimpanzee adenovirus serotype-63 (ChAdV-63). These were assessed in 3 heterologous prime-boost regimens in healthy HIV-1 uninfected volunteers. The pre-clinical assessment of these vaccines and regimens are discussed in Chapter 3. The choice of vaccine vector for the trial is outlined briefly below.

Plasmid DNA is advantageous as it is non-pathogenic, can be given without generating anti-vector immunity [276], and in animal models is able to induce both humoral and

cell-mediated responses [277]. In humans, pDNA vaccines have been shown to be safe, but when administered alone are weakly immunogenic [278]. However, when delivered in prime-boost regimens with MVA or alternative viral vectors a significantly greater induction of T cells is observed [278-280].

Attenuated MVA was developed through serial passage of the Ankara strain on chicken embryo fibroblasts [281], resulting in multiple genome deletions [282] which prevent replication within human cells [283, 284]. This modification makes the vector a safer candidate than previously utilised Vaccinia strains, and this was demonstrated during the final stages of the small pox eradication programme, where MVA was administered to 120,000 individuals at risk of infection without significant side-effects [285]. Since then it has been used as a viral vector for clinical vaccine candidates, against a range of infections and has shown a good safety profile in healthy and HIV-1 infected vaccinees [286-289]. The MVA vector can incorporate a large vaccine insert of up to 25 kbp and is capable of efficiently boosting both T-cell and B-cell responses dependent upon the immunogen design [290]. It was therefore evaluated for its ability to boost conserved region HIV-1-specific T cells within the HIV-CORE 002 trial.

The non-replicating ChAdV-63 vector was selected for use in the HIV-CORE 002 trial to overcome the high levels of HAdV-5 neutralising antibodies (NAbs) prevalent within populations at risk of HIV-1 infection [291-293]. HAdV-5 NAbs are generated in response to natural adenovirus infection and through passive immunisation from mother to infant [291]. When HAdV-5 vectors were used for vaccine delivery in humans, HAdV-5 NAbs posed a problem as they dampened the insert specific T-cell response [258, 294]. In contrast, the ChAdV-63 vector has been shown to have limited seroprevalence within 193 Caucasian volunteers and was highly immunogenic in animal models, inducing T cells at comparable frequencies to the potent HAdV-6 vector [295]. Thus, the ChAdV63.HIVconsv vaccine was

developed and was evaluated for its ability to prime and boost T-cell responses in human volunteers within the HIV-CORE 002 trial.

1.7 How do we prioritise HIV-1 vaccine candidates?

Currently the HIV-1 field has limited knowledge of which T-cell specificities and functions will result in control of HIV-1 infection, but studies of individuals who are able to control the virus without therapy and HESN have given some indication as to which type of cell-mediated responses may be most beneficial to induce through vaccination. Consequently, in depth characterisation of vaccine-induced responses are commonly performed and typically include the IFN-γ ELISpot assay [294, 296, 297], intracellular cytokine staining (ICS) [296, 298] and cellular cytotoxicity assays [299]. Together, these give an indication of both the quantity and quality of the T cell response.

Both T-cell frequency and specificity can be determined by the IFN-γ ELISpot and functional information on cytokine production and ability to kill peptide-pulsed target cells can be determined through ICS and CTL killing assays. However, these responses are all measured with limited ability to predict control of natural HIV-1 infection. Multiple evasion mechanisms are used by HIV-1 to avoid detection by host immune cells including, mutating viral amino acids important for both CTL recognition and HLA binding, and down-regulating cell surface expression of HLA molecules (reviewed in [300]). These effects on the host cell are not taken in to account when peptides are used as a stimulus in the more commonly applied immunogenicity methods. A novel assay that was shown to be predictive of the clinical state of an individual is the virus inhibition assay (VIA), and several versions of this assay have been described [298, 301-303]. The *ex vivo* VIA assay has not previously been used with human HIV-1 prophylactic vaccine trial samples but has shown promise in predicting the rate of $CD4^+$ T cell decline in HIV-1 infected individuals [304]. Furthermore, this assay could distinguish HIV-1 controllers from progressors suggesting that this function

may help to predict vaccine efficacy [305]. In vaccinated rhesus macaques the results from an *ex vivo* VIA showed that the magnitude of virus inhibition pre-challenge correlated with viral load set-point post SIV challenge [306]. Moreover, this was suggested to be mediated by Gag-specific T cells [306]. Cultured VIA methods have also been described [302] and more recently used in the assessment of vaccine-induced T cell responses [307, 308]; the principal advantage of this method is the ability to assess multiple viral isolates for breadth of virus control.

1.8 Aims of this thesis

The principal aim of this research was to characterise the HIVconsv vaccine-elicited T-cell response in healthy HIV-1/2-negative volunteers from the HIV-CORE 002 clinical trial, using several of the aforementioned methods. This work was undertaken to inform the field on the use of these vectors in novel heterologous prime-boost regimens and to evaluate the specificity and quality of the T cells induced by the novel chimeric HIVconsv immunogen, information that could ultimately help to improve on the next generation of T-cell vaccines against HIV-1.

The key research aims were:

1. To establish the immunogenicity of the candidate HIV-1 vaccines in healthy individuals

2. To establish a virus inhibition assay for use with vaccine trial samples and use this to examine the inhibitory capacity of $CD8^+$ T cells induced through HIVconsv vaccination

3. To investigate which T-cell specificities contribute to control of *in-vitro* HIV-1 infection and assess the mechanism of action of these cells in order to help inform future vaccine design

2 Materials and Methods

2.1 Isolation and Freezing of PBMC

Whole blood (50 ml) from healthy volunteers was diluted with sterile PBS (50 ml, Sigma-Aldrich, St. Louis, MO). 25 ml of blood was layered onto each Leucosep tube (Greiner Bio-One GmbH) containing 15 ml of Ficoll Hypaque solution (Axis-Shield, Dundee, Scotland). Leucosep tubes were centrifuged at 2,000 rpm for 15 minutes with the brake off to allow density gradient separation of the blood components. The centrifuge used throughout was an Allegra X-R12; rotor SX4750 (Beckman Coulter, High Wycombe, UK). PBMC was aspirated using pastettes into clean Falcon tubes and washed twice in PBS by topping up to 50 ml and centrifugation at 1,200 rpm for 10 minutes. PBMC were then re-suspended in 10 ml of R-10 media and counted using a hemocytometer and trypan blue exclusion.

PBMC was frozen by preparation of cryopreservation solution, 10% DMSO (Sigma-Aldrich) in heat-inactivated sterile filtered FBS (Sigma-Aldrich) which was chilled to 4 °C before use. PBMC was centrifuged at 1,200 rpm for 10 minutes to pellet the cells. The cells were then re-suspended in the remaining R-10 media. Based on the cell count, cells were frozen at 10^7/ 1 ml of cryopreservation solution which was added dropwise whilst swirling. PBMC was aliquoted into 2 ml cryopreservation tubes, 0.5 ml per tube. Tubes were immediately transferred to a pre-chilled 2-8 °C Mr Frosty and once full placed at -80 °C overnight. The following day cells were transferred into a LN_2 storage tank.

2.2 *Ex vivo* IFN-γ ELISpot Assay

Freshly isolated PBMC re-suspended in R-10 media from healthy volunteers was used to set up the ELISpot, a total of $6x10^6$ PBMC were required per assay. ELISpot plates, 96 well with PVDF membrane (S5EJ044I10; Merck Millipore, Darmstadt, Germany) were pre wet for 1 minute with 35% Ethanol (Fisher Scientific, Loughborough, UK) in sterile water (Sigma-Aldrich). The plates were washed 4 times with 200 µl per well of sterile PBS and

blotted to tissue. Coating anti-human IFN-γ monoclonal antibody clone 1-D1K (Mabtech, Naka Strand, Sweden) at 10 µg/ml was prepared in sterile PBS and 100 µl per well was added to the plate. The plate was placed at 2 - 4 °C overnight or for up to 3 days in a sealed container containing moistened tissue to maintain hydration. On the day of the ELISpot the pre-coated plate was washed 4 times with 200 µl per well sterile PBS and then blocked with 200 µl per well of R-10 media and placed at 37 °C, 5% CO_2 for a minimum of 1 hour. The plate was then emptied and blotted to tissue and the PBMC were diluted to $4x10^6$/ml in R-10 media. PBMC were added at 50 µl per well in addition 50 µl per well of each stimulant peptide pool or control were added to the plate and each well was mixed several times by pipetting up and down. The loaded plate was placed at 37 °C, 5% CO_2 for 18-24 hours. Secondary biotinylated anti-Human IFN-γ monoclonal antibody clone 7-B6-1 (Mabtech) at 1 µg/ml was prepared in assay diluent (0.5 % FBS in PBS), PBMC was emptied from the plate and the plate was washed 6 times with 200 µl per well of PBS. 100 µl per well of secondary antibody was added and the plate was incubated at 18-24 °C for 2 hours. The streptavidin-alkaline phosphatase conjugate (Mabtech) at 1 µg/ml was prepared in assay diluent and after washing the plate 6 times in PBS, 100 µl per well was added. The plate was incubated at 18-24 °C for 1 hour. $BCIP^{NBT}$ substrate (Mabtech) was brought to room temperature and filtered through a 0.45 µm filter (Millipore). After washing the plate 6 times with 200 µl per well of PBS, 100 µl per well of substrate was added for 5 minutes at 18-24 °C. The plate was then emptied into the sink and washed several times under running water and after removal of the protective plastic backing, washed on the back and left to air dry overnight in the dark.

Positive controls used as part of the assay were the Phytohaemagglutinin (PHA) mitogen (Sigma-Aldrich) at 10 µg/ml and CEF peptides at 1.5 µg/ml (ARP7099; Centre for AIDS reagents- NIBSC, Potters Bar, UK). A natural killer leukemia cell line was also used as

an additional positive control, 50 µl per well at $1x10^4$/ml was added with phorbol-12 myristate 13-acetate (PMA) at 4 µg/ml (Sigma-Aldrich), Ionomycin at 1 µg/ml (Sigma-Aldrich) and IL-2 at 10 IU/ml (Proleukin; Novarits, Camberley, UK). The negative control (mock) was R-10 media with 0.5% DMSO. Plates were read on an AID (Autoimmun Diagnostika GmbH, Germany) plate reader.

2.3 Growth of HIV-1 Virus Stocks

2.3.1 Thawing and Activation of PBMC for Viral Propagation

Healthy PBMC from buffy coat was used to propagate viral stocks based on protocols by Vicenzi et al. 2001 [309] and Van't Wout et al. 2008 [310]. Cells were thawed using Benzonase (Novagen, Darmstadt, Germany) at 50 IU/ml in R-10 which had been pre-warmed. Cells were washed a total of 3 times in 15 ml R-10 to remove any residual DMSO by spinning at 1,500 rpm for 5 minutes. A cell count was performed and cells were diluted to $1x10^6$/ml. For cell activation PHA was added to give a final concentration of 5 µg/ml. Cells were transferred to a 25-cm^2 flask and cultured upright at 37 °C, 5% CO_2 for 72 hours.

After 72 hours activation cells were collected into a 50 ml falcon tube. Residual cells were scraped from the base of the flask and the flask was rinsed with R-10. The cells were washed three times in 50 ml R-10 at 1,500 rpm for 5 minutes. After the final wash cells were re-suspended in R-10 with IL-2 at 20 IU/ml and a cell count was performed, cells were diluted to $1x10^6$/ml.

2.3.2 HIV-1 Infection of Activated PBMC and Set-up of Kinetics Plates

Kinetics staining of percentage infection levels was performed at 6 time points therefore $3.8x10^6$ cells (200,000/well in triplicate per day) were placed into a 15 ml falcon and placed at 37 °C, 5% CO_2 to be plated as uninfected controls and unstained cells. The uninfected controls were plated in round bottomed 96 well plates and topped up with R-10/IL-2 to 150 µl

total volume. To maintain humidity 150 µl of PBS was placed into empty wells. The cells were then placed at 37 °C, 5% CO_2. All remaining cells were used for viral infection. In a Category III laboratory one vial of high titer virus for HIV-1 clade B (BaL) ARP118, HIV-1 clade A (92UG029) ARP177.1-26 and HIV-1 clade C (ES X-1936 C) ARP1073 (Centre for AIDS reagents-NIBSC) were thawed by placing at room temperature and 100 µl per $1x10^6$ PBMC was used for infection. Cells were pelleted at 1,500 rpm for 5 minutes residual supernatant was poured off and the cell pellet was gently re-suspended. The virus was added directly into the cells and vortexed to mix. The cells were then spinoculated at 2,000 rpm, 25 °C, for 2 hours. Following spinoculation 50% of the viral supernatant was removed from the falcon tube. A cell count was performed and cells were diluted to $1x10^6$/ml.

For the Kinetics analysis one row of 6 wells containing 200,000 cells per well was plated. Cells were topped up to 150 µl total volume. All remaining wells were filled with 150 µl of PBS. The plate was placed at 37 °C, 5% CO_2 until staining was performed.

The remaining stock cells were cultured in an appropriate tissue culture flask which was placed at 37 °C, 5% CO_2. Flow cytometry staining of the p24 infection level (section 2.8) was performed from day 3 and used to assess the day for viral harvest. Infection levels of 6-8% by p24 staining were considered suitable and the virus was harvested.

2.4 Harvesting Virus Stock

Cells were harvested by re-suspending the stock flask with a strippette and pipette boy and transferring to a 50 ml falcon tube. The original culture flask was kept. The stock was centrifuged at 1,500 rpm, 5 minutes at room temperature to pellet the cells. One millilitre aliquots were stored at - 80 °C in cryo-vials. Approximately 1 ml of supernatant was left in the falcon tube with the cells to allow for cell free virus propagation. The remaining cells in the falcon tube were re-suspended and topped up to the same starting volume with warm

R-10/IL-2 (20 IU/ml). The stock was then cultured at 37 °C, 5% CO_2 and kinetics staining continued. When viral infection levels remained high a second harvest was performed.

2.5 Titration of HIV-1 Virus Stock

PBMC isolated from buffy coat were thawed and activated for 72 hours, the activated cells were then collected, washed, counted and diluted to $1x10^6$/ml in R-10/IL-2. One vial of high titre virus was thawed at room temperature and a virus dilution plate was prepared. Serial dilutions of 1 in 10 (225 µl of media and 25 µl of virus stock) were made starting with 250 µl of neat virus so that dilutions ranged from 10^{-0} to 10^{-9}. In a round-bottomed plate 100,000 cells per well were plated in quadruplet and to this 50 µl of viral dilution was added to each well. A control plate was also prepared which contained 4 wells with 100,000 cells per well for uninfected samples, a live dead stain and unstained FACS control. To both plates 150 µl of PBS was aliquotted into empty wells and the plates were placed at 37 °C, 5% CO_2. Plates were stained for HIV-1 p24 infection levels (section 2.8) on day 6 post infection with HIV-1 B, day 4 for HIV-1 clade A and day 7 for HIV-1 clade C.

2.6 *Ex vivo* Virus Inhibition Assay

2.6.1 $CD4^+$ Target and $CD8^+$ Effector Isolation and Activation

PBMC from vaccinees and controls were thawed using Benzonase (Novagen) at 50 IU/ml in R-10 which had been pre-warmed. Cells were washed a total of 3 times in 15ml R-10 to remove any residual DMSO by spinning at 1500 rpm for 5 minutes, cells were counted in R-10 media before being transferred to MACS buffer (2 mM EDTA, 0.5% BSA in PBS).

$CD4^+$ targets and $CD8^+$ effectors were isolated using positive selection beads for $CD8^+$ T cells (130-045-201; Miltenyi Biotech, Bisley, UK). For efficient isolation, samples were separated into 10^7 cells per 15 ml falcon tube, MACS buffer was then removed by

centrifugation and the cells were re-suspended in the residual volume before incubation with 20 µl MACS beads per 10^7 cells for 20 minutes at 2-8 °C.

Following the incubation cells were washed once, 1,500 rpm, 18-25 °C for 10 minutes and re-suspended in 500 µl of MACS buffer. MS columns (130-042-201; Miltenyi Biotech) were placed into a Mini MACS magnetic field and washed once with 500 µl of MACS buffer. Magnetically labelled cells were then loaded onto the column and the negative fraction ($CD4^+$) was collected into a 15 ml falcon tube. The column was washed a further three times with 500 µl MACS buffer and all supernatant collected. The $CD8^+$ fraction was then eluted using 1 ml MACS buffer and a plunger into a second falcon. Both fractions were washed and re-suspended in R-10 media at $1x10^6$/ml. The $CD4^+$ fraction was activated by the addition of PHA to give a final concentration 5 µg/ml. $CD4^+$ targets were cultured upright at 37 °C, 5% CO_2 for 72 hours. To determine the purity and percentage recovery of the isolated fractions, several PBMC samples were counted and stained with fluorochromes for CD3 APC-Cy7, CD8 APC and CD4 PerCP (section 2.8 for clones used) for both the $CD8^+$ and $CD4^+$ cell fractions.

$CD8^+$ effector cells were isolated on the day that $CD4^+$ targets were infected with HIV-1 BaL. Positively isolated $CD8^+$ effectors were re-suspended in R-10 and placed to rest for 2 hours minimum at 37 °C, 5% CO_2. Effectors were counted after resting and re-suspended in R-10/IL-2 at $1x10^6$/ml for use in the *ex vivo* VIA.

Negative selection was performed as an alternative method to positive selection for isolation of unlabelled $CD8^+$ T cells. After the transfer of PBMC into a small residual volume of MACS buffer the biotinylated antibody cocktail was added at 10 µl per 10^7 cells for 10 minutes at 2-8 °C, followed by 20 µl MACS Microbead cocktail (130-094-156; Miltenyi Biotech) per 10^7 cells for 15 minutes at 2-8 °C. $CD8^+$ T cells were then separated on MS columns and prepared for the *ex vivo* VIA as described in section 2.7.

2.7 Set-up of *Ex vivo* Virus Inhibition Co-cultures

Activated $CD4^+$ target cells were washed, counted and infected with HIV-1 BaL as described in section 2.3.2 and following spinoculation the infected cells were washed twice in 10 ml R-10. In a round bottomed plate $0.6x10^6$ targets at 50,000 per well were set aside as Uninfected, Unstained and Live/Dead controls. One set of controls (3x uninfected, 2x unstained and 1x Live/Dead) were used on each day of intracellular p24 staining.

$CD4^+$ target cells were re-suspended in R-10/IL-2 at 20 IU/ml and then plated at 50,000 targets per well in triplicate. Depending upon the effector to target ratio required the $CD8^+$ T cells were adjusted accordingly to between 200,000 (4:1) to 50,000 (1:1) per well. All wells were topped up to 200 µl with R-10/IL-2 (20 IU/ml). Two plates were set up, one for day 5 and a second for day 7.

2.8 Quantification of HIV-1 Infection by Flow Cytometry

On the day of staining plates containing uninfected controls and co-cultures were pelleted at 1,800 rpm, 20 °C for 5 minutes. Supernatants (150 µl) were removed to a new round-bottomed plate, sealed with a plate seal and stored at -80 °C until use. PBMC was then washed with the addition of 150 µl of FACS buffer (0.1% BSA, 0.01% NaN_3 (Sigma-Aldrich) and centrifugation at 1,800rpm, 4 °C for 5 minutes. Supernatant was decanted gently to waste and blotted to tissue; all further washes were performed in this way.

Aqua fixable Live/Dead cell stain (Invitrogen, Carlsbad, CA) was prepared 0.5 µl into 99.5 µl PBS (Sigma-Aldrich) per well. Aqua Live/Dead stain was added and plates were wrapped in foil for 20 minutes at 18-24 °C. After incubation a wash was performed as above cells were then fixed with the addition of 220 µl 20 µg/ml Lysolecithin (Sigma-Aldrich) in 4% Paraformaldehyde (Alfa Aesar, Heysham, UK), for 2 minutes at 18-24 °C. Cells were then pelleted after fixation and permeabilised using 50% methanol (Fisher Scientific) in PBS which was stored at -10 to -20°C with 220 µl added per well. The permeabilisation step was

performed for 15 minutes at 2-8 °C followed by centrifugation and supernatant removal. 0.1% Nonidet P-40 (Sigma-Aldrich) in PBS was next added at 220 µl per well and plates were placed at 2-8 °C for 5 minutes. Cells were then washed before the antibody staining cocktail containing 1.5 µl anti-p24 (KC57-FITC; 6604665, Beckman Coulter), 1 µl anti-CD8 APC (clone OKT; 17-0086-42, e-bioscience, Hatfield, UK), 1 µl anti-CD3 APC-Cy7 (clone HIT3a; 300318, Biolegend, SanDiego, CA) and 1 µl anti-CD4 PerCP (clone SK3; 345770, BD Biosciences, San Jose, CA) into 100 µl FACS buffer total was added per well.

One compensation tube per colour was also prepared containing 100 µl FACS buffer, one drop of positive and negative anti-mouse Ig compensation beads (BD Bioscience) and the same volume of antibody per tube as was added per well. The compensation tubes and plates were then wrapped in foil and placed at 18-24 °C for 20 minutes. After staining the plates were washed with 100 µl per well of FACS buffer and the compensation tubes with 1 ml FACS buffer. The plates were then re-suspended in 200 µl FACS buffer per well and the compensation tubes in 400 µl.

Samples from the plates were transferred to cluster tubes with an additional 200 µl FACS buffer for reading on the CyAn ADP flow cytometer (Beckman Coulter). Further data analysis was performed using FlowJo software (Tree Star Inc. Ashland, OR, USA) versions 8.7 and 9.5.

2.9 Cultured Virus Inhibition Assay

Samples were shipped in LN_2 to the IAVI Human Immunology Laboratory at the Chelsea and Westminster Hospital, London. The assay was performed based on the protocol by Spentzou et al. 2010 [307]. Briefly, for each vaccinee autologous $CD4^+$ T cells from a pre-vaccination time point were used as common targets with autologous $CD8^+$ T cell effectors from pre and post vaccination time points. $CD4^+$ and $CD8^+$ T cells were first expanded for 7 days in R-10/IL-2 at 50 IU/ml using CD3/8 and CD3/4 bi-specific antibodies,

respectively at 0.5 µg/ml (Donated by Prof. Wong, Harvard University). $CD4^+$ T cells were washed, counted and infected with 8 different HIV-1 viral isolates. Four were lab strain isolates; IIIB (clade B, CXCR4), U455 (clade A, CXCR4), ELI (clade A, CXCR4) obtained from the NIH AIDS reagent repository and Bal (clade B, CCR5) obtained from the NIBSC centre for AIDS reagents. Three were infectious molecular clones generously donated by Prof. G. Shaw (University of Birmingham, Alabama); CH077 (clade B, CCR5), CH106 (clade B, CCR5) and 247FV2 (clade C, CCR5). One was a primary isolate; ZA97012 (clade C, CCR5). All isolates were used at MOI 0.01 except for Bal which was used at MOI 0.005.

Infection was performed by pelleting the $CD4^+$ T cells, removing the supernatant and directly adding each virus to the cell pellets. Cells were vortexed and placed at 37 °C, 5% CO_2 for 3-4 hours. Following infection, the cells were washed twice in R-10 by centrifugation at 1,500 rpm, 10 minutes, 18-25 °C. Cells were then re-suspended at $1x10^6$/ml in R-10/IL-2 at 100 IU/ml, $0.5x10^6$ cells were plated per well in a 48 well plate (Nunc; Sigma-Aldrich).

$CD8^+$ T cells were also washed, counted and re-suspended in R-10 at $1x10^6$/ml. The $CD8^+$ T cells from each time point tested were added at $0.5x10^6$/ml to the relevant $CD4^+$ target wells. One well of infected $CD4^+$ targets alone was also maintained for each virus, additional R-10 was added to these wells to give a final R-10/IL-2 concentration of 50 IU/ml.

Cultures were fed on days 3, 6, 8 and 10 by the removal and replenishment of 0.5 ml R-10/IL-2 at 50 IU/ml. On day 13 supernatants were collected and stored at -20 °C for p24 ELISA and Luminex analysis.

2.10 Expanded $CD8^+$ T Cell ELISpot Assay

The remaining expanded $CD8^+$ T cells from the cultured VIA, section 2.9 were re-suspended in 2 ml R-10 and placed at 37 °C, 5% CO_2 for 18 hours. ELISpot plates were coated with anti-Human IFN-γ, blocked and developed as described in section 2.2.

After overnight resting $CD8^+$ T cells were counted and re-suspended at $4x10^6$/ml in R-10, ELISpot plates were set up using 200,000 $CD8^+$ T cells per well, in R-10 media. Wells contained either mock (R-10 only), PHA mitogen (Sigma-Aldrich) at 10 µg/ml, or a pool of protein specific peptides prepared from the individual HIVconsv peptides. Four peptide pools were prepared these were Gag, Pol 1, Pol 2, and Env with Vif.

Peptides were added at a final concentration of 1.5 µg/ml, all wells were mixed by pipetting up and down several times and incubated for 16-18 hours at 37 °C, 5% CO_2. Results were calculated by subtracting the average mock value from the peptide stimulated wells. Results for peptide pools Pol 1 and 2 were added together and all values were calculated as SFU/10^6 cells.

2.11 HIV-1 Quantitative p24 ELISA

To determine the total p24 concentration in viral supernatants stored from the *ex vivo* viral suppression assays p24 ELISAs (VPK-108-H5, Cell Biolabs, San Diego, CA) were performed according to the manufacturer's instructions. Frozen virus supernatant was used for all assays, multiple dilutions were run for each sample to ensure that they fell within the standard curve and all dilutions were prepared in R-10 media. Media was also run as a negative control. Plates were analysed immediately after development on a BioTek ELx800 Absorbance Microplate reader with Gen5 software version 1.10.8 (BioTek Instruments Inc, Vermont, USA).

All frozen supernatant samples from the cultured VIAs were analysed using an Alliance p24 ELISA kit (PerkinElmer, Cambridge, UK). Multiple dilutions of each sample were prepared to ensure that they fell within the standard curve. All samples were diluted in R-10 media and the assays were run according to the manufacturer's instructions. Plates were read at 492 nm with a 620 nm reference on a Tecan Sunrise ELISA plate reader with Magellan Clinical software version 4.50.

Data analysis of the standard curve and p24 concentrations were determined in Microsoft Excel 2010 and for all cultured VIAs in GraphPad Prism version 5.04 (GraphPad Software, San Diego, CA).

2.12 Luminex Analysis

Luminex analysis on cryopreserved PBMC from the DDDCM arm was performed based on the protocol by Defawae et al. 2012 [311]. Briefly, cells were thawed and rested overnight in R-10. The following day cells were washed once in R-10 and counted. PBMC were diluted to $5x10^6$/ml and $5x10^5$ cells were added into 96-well round bottom plates (Nunc, Sigma-Aldrich) and stimulated with anti-CD28 and anti-CD49d at a final concentration of 1 µg/ml. In addition cells were cultured with either HIVconsv peptide pool 1-6 (1 µg/ml), an SEB positive control (1 µg/ml), or 0.5% DMSO negative control. Cells were cultured for 48 hours at 37 °C, 5% CO_2 after which plates were centrifuged at 1,500 rpm for 7 minutes to pellet the cells and 150 µl supernatant was collected per well. The supernatant was stored at -80 °C until use in the luminex analysis.

The human Milliplex HCYTOMAG-60K kit (Millipore) was used to determine the presence of 12 analytes from the peptide stimulated supernatant, these were IL-2, IL-4, IL-5, IL-9, IL-10, IL-13, IL-17A, IFN-γ, GM-CSF, TNF-α, TNF-β and MIP-1β. Samples were not diluted before assaying, cytokine standards supplied by the manufacturer were run on each plate and the assay was performed according to the manufacturer's instructions.

Cultured VIA supernatants were analysed using the Bio-Plex Pro Human cytokine group I and II assay (Bio-Rad). A customized panel of 10 analytes; RANTES, MIP-1α, MIP-1β, TNF-α, SDF-1α, MIG (CXCL9), IP-10 (CXCL10), IL-1α, IFN-γ and IL-7 was tested. Samples were diluted in R-10 media to 1 in 2 and 1 in 10 before plating. Standards provided by the manufacturer were run on each plate and all steps were conducted according to the manufacturer's instructions.

All samples were read on a Bio-Plex 100 instrument (Bio-Rad, Hemel Hempstead, UK). 5PL standard curves were generated by the Bio-Plex Manager software version 4.1 and interpolated results were exported to Excel. Sample values were background (DMSO) subtracted and all assay controls passed their respective acceptance criteria.

2.13 Peptide and Epitope Mapping

2.13.1 Preparing a Short Term Cell Line (STCL)

Vaccinee responses to individual peptides covering the HIVconsv immunogen were mapped using cryopreserved PBMC from week 28. The cells were thawed, counted and re-suspended at a concentration of 1 to 3 $x10^6$ cells per ml in R-10 with IL-7 at 1 µl/ml. To each well 900 µl of cells along with 100 µl of 15 µg/ml peptides were plated. Cells and antigen were gently swirled to mix and PBS was added to empty wells to maintain humidity. The plates were incubated at 37 °C, 5% CO_2 for 10 days. On day 3 cells were fed with IL-2 at a final concentration of 100 IU/ml. On day 7, R-10 media and IL-2 were added to the plate to give 100 IU/ml of IL-2 in 2ml. The cells were washed on day 10 by transferring to a 15 ml falcon tube and topping to 12 ml with R-10. The cells were centrifuged for 10 minutes at 1,500 rpm at room temperature with the brake on, supernatant was poured off and the cells were re-suspended. This was repeated for a total of three washes, after which the cells were re-suspended in 1 ml of R-10 and placed with loose lids at 37 °C, 5% CO_2 for 48 hours.

2.13.2 Cultured ELISpots for Peptide Mapping

ELISpot plates were coated in advance with anti-Human IFN-γ, blocked and developed as described in section 2.2. The STCL were washed in R-10 by centrifugation at 1,500 rpm, for 10 minutes at room temperature with the brake on. The cells were then counted by trypan blue dye exclusion and re-suspended at $0.6x10^6$/ml in R-10. 50 µl of cell suspension was added in duplicate along with 50 µl of each individual peptide to give a final concentration of

1.5 µg/ml and wells were mixed by pipetting. The plates were placed at 37 °C, 5% CO_2 for 16-18 hours before development.

2.13.3 ICS for Epitope Mapping

STCLs were prepared from a total of $15x10^6$ PBMC to enable mapping of 5 peptides. The STCLs were stimulated with the parent 15-mer peptide as described in section 2.13.1. On day 12 cells were incubated with a master mix of anti-CD28 and anti-CD49d at 1 µg/ml, Brefeldin A at 10 µg/ml and Golgi Stop at 20 µg/ml. The stimulants were either 1.5 µg/ml truncated peptide, 1 µg/ml SEB (positive control) or R-10 (negative control) all cells were also labelled with anti-CD107a PE-Cy7 (BD Biosciences). Cells were stimulated for a total of 6-8 hours and then placed at 4 °C overnight.

The following day cells were stained in FACS buffer using surface markers anti-CD4 PE (clone RPA-T4; 561844, BD Biosciences), anti-CD8 FITC (clone RPA-T8; 561948, BD Biosciences) and Aqua Live/Dead (Invitrogen). Cells were permeabilized using 100 µl Cytofix/Cytoperm solution (BD Biosciences) for 15 minutes at 4 °C and then washed twice, 1,800 rpm for 5 minutes and supernatant tipped off, before staining with anti-CD3 ECD (A07748; Beckman Coulter), anti-IFN-γ V450 (560371; BD Bioscience) and anti-TNF-α APC (562084; BD Bioscience) in permeabilisation buffer (1:9) buffer to water (BD Biosciences) at 4 °C for 30 minutes. Cells were then washed 3 times in FACS buffer and fixed in 1% paraformaldehyde before being stored at 4 °C until acquisition on the BD LSRII flow cytometer (BD Biosciences). Data analysis was performed using FlowJo software (Tree Star Inc. Ashland, OR, USA) version 9.5.

2.14 Generation of Gag- and Pol-Specific Cell Lines

Gag-specific and Pol-specific peptides that were previously mapped by a short-term cell line and IFN-γ ELISpot were used to make a positive pool for each individual assessed. Vaccinee cells were thawed and placed in to culture as described in section 2.13.1., except

that the final rest was carried out in R-5 media for 48 hours. Cells were then sorted by performing an IFN-γ capture assay, cells were stimulated for 3 hours with the peptide pool (10 µg/ml), SEB (1 µg/ml) or R-5 media. All remaining steps were performed according to the manufacturer's instructions (130-054-202; Miltenyi Biotech). Additional cell surface staining with anti-CD8 APC, anti-CD3 APC-Cy7 and anti-CD4 PerCP was performed to facilitate HIV-1 specific $CD8^+$ T cell isolation.

Feeder cells were prepared on the day of cell sorting by isolating PBMC as described in section 2.1 from 3 healthy donors. Cells from each donor were re-suspended in 10 ml R-10 and placed in 25-cm^2 tissue culture flasks for irradiation at 50 gray per flask. Once irradiated the cells were mixed in a 50 ml falcon tube and washed with 50 ml R-10 at 1,500 rpm for 10 minutes. The feeder cells were subsequently counted and diluted to $2x10^6$/ml in R-10 and PHA was added to give 40 µg/ml. Feeder cells were placed at 37 °C, 5% CO_2 until cells were sorted. Once Gag- and Pol-specific cells were sorted in to 100 µl of R-10, 1 ml of feeder cells was added and the total volume was plated into a single well of a 24 well flat-bottomed tissue culture plate, surrounding wells were filled with PBS and cells were maintained at 37 °C, 5% CO_2. Cell lines were fed with R-10/IL-2 at 200 IU/ml as required, or IL-2 alone if growth was slow.

On day 13 cell lines were re-stimulated using irradiated PBMC prepared as described above. Cell lines were transferred to 15 ml falcon tubes, washed in 10 ml R-10 and counted. Cell lines were then pelleted by centrifugation at 1,500 rpm 10 minutes and feeders were added directly to give a feeder to cell line ratio of 2:1. Cells were then plated in to 12 well plates and fed with R-10/IL-2 at 200 IU/ml as required. On day 14 cell lines were ready for use and a sample was stained for cell purity and antigen specificity. Day 14 cell lines were tested by cultured VIA as described in section 2.9.

2.15 *In vitro* Cell Killing Assay

Gag- and Pol-specific cell lines from day 15 were tested in an *in vitro* cell killing assay based on a protocol published by Hermans, et al. 2004 [312]. Briefly, $CD4^+$ T cells remaining from the cultured VIA were separated into 1x 50 ml falcon tube for pulsed cells, and 2x 15 ml falcon tubes for un-pulsed and unstained cells. Pulsed cells were re-suspended at $2x10^6$/ml in PBS and were stained with 8 nM CFSE (65-0850-84; eBiosciences) by adding an equal volume of CFSE stain to cell suspension for 10 minutes in the dark at 18-24 °C. Un-pulsed and unstained cells were placed in an equal volume of PBS. To quench the reaction 5x volume of FCS was added to all tubes and they were placed on ice for 5 minutes. Cells were washed twice by centrifugation at 1,500 rpm for 10 minutes at 18-24 °C.

All cells were re-suspended in R-10 at $2x10^6$/ml and pulsed cells were stained with cell tracker orange, CMTMR (C2927, Invitrogen) reconstituted to a 10 mM solution and diluted by adding 8 µl into 10 ml R-10 to give a working stock. An equal volume of CMTMR working stock was added to the pulsed cell suspension and the same volume of R-10 was added to all other tubes. Samples were placed, with loose lids at 37 °C, 5% CO_2 for 12 minutes, after which they were centrifuged to remove the stain and re-suspended in R-10 at $2x10^6$/ml before being place back at 37 °C, 5% CO_2 for a further 15 minutes. CMTMR stained cells were then washed 3 times in R-10.

All cells were counted by trypan blue exclusion dye. CFSE stained cells were then split into the relevant number of tubes for pulsing with individual peptides (an un-pulsed CFSE sample was also included as a control). Cells were centrifuged and supernatant removed, peptides were added at 2x concentration (3 µg/ml), directly to the re-suspended cell pellet and all samples were placed with lids loose at 37 °C, 5% CO_2 for 2 hours. Following incubation the CFSE and CMTMR stained cells were washed 3 times by centrifugation in R-10 and re-suspended at $1x10^6$/ml.

Targets were added to give 50,000 pulsed and 50,000 un-pulsed per well. Effector Gag- and Pol-specific cell lines were washed and diluted to $10x10^6$/ml and were added into each well to give a 10:1 effector to target ratio. All wells were made to 200 µl volume and empty wells were filled with PBS. The plate was cultured overnight (18 hours) at 37 °C, 5% CO_2. The next day cells were washed by centrifugation at 1,800 rpm, 5 minutes at 18-24 °C. Supernatant was removed and cells were re-suspended in 200 µl FACS buffer. Staining with Live/Dead Violet (L34955; Invitrogen) and anti-CD8 APC was performed for 20 minutes at 18-24 °C in the dark. Cells were then washed in 200 µl FACS buffer and re-suspended in 200 µl 1% paraformaldehyde before being acquired on the CyAn ADP flow cytometer (Beckman Coulter). Data analysis was performed using FlowJo software (Tree Star Inc. Ashland, OR, USA) version 9.5.

2.16 ICS of Antiviral Factors

Gag- and Pol-specific cell lines from day 16 were tested in an ICS assay which had been adapted to include anti-MIP1α and anti-MIP-1β. Gag and Pol-specific cell lines were stimulated with the master mix and individual peptides comprising each Gag- and Pol-peptide pool for 6 hours as described in section 2.13.3. The following day cells were stained with the surface antibodies anti-CD8 APC-efluor780 (47-0087-42; e-bioscience), anti-CD4 BV570 (300533; Biolegend) and Aqua Live/Dead (Invitrogen) for 30 minutes at 4 °C. Cells were then washed and permeabilised as described in section 2.13.3. Intracellular staining was performed using anti-MIP-1α PerCP-eFluor 710 (46-7539; eBioscience), anti-MIP-1β-Alexa Fluor 700 (561278; BD Biosciences), anti-TNF-α APC (562084; BD Bioscience), anti-IFN-γ V450 (560371; BD Biosciences) and anti-CD3 ECD (A07748; Beckman Coulter) for 30 minutes at 18-24 °C. Cells were then washed twice in FACS buffer and fixed in 1% paraformaldehyde before being acquired on the BD LSRII flow cytometer (BD Biosciences). Data analysis was performed using FlowJo software (Tree Star Inc.) version 9.5.

3 HIV-CORE 002: Investigating the safety and immunogenicity of candidate HIV-1 vaccines in HIV-1/2 negative volunteers

3.1 Introduction

There is consensus in the field that an effective HIV-1 vaccine will require both a humoral and cell mediated response to prevent and clear breakthrough virus infection [313]. The design of a vaccine capable of inducing such a combined immune response is, however, a considerable challenge and therefore one rational strategy is to tackle each arm separately [314]. Our group focuses on the induction of T cells as there is considerable evidence from animal [175, 315, 316] and human [173, 174, 317, 318] studies which suggests that $CD8^+$ T cells are capable of controlling virus replication.

One of the greatest hurdles for any HIV-1 vaccine, is the tremendous genetic diversity of the virus [145], combined with its ability to rapidly escape immune pressure exerted within the host [118, 151, 183]. The HIVconsv immunogen was therefore designed to direct the T-cell response toward the most highly conserved regions of the HIV-1 proteome, to increase the breadth of viral clades and escape mutants likely to be cross-recognised. Moreover, priming the T-cell response to focus immune pressure on protein regions which are essential for viral fitness should slow the rate of replication [188] and subsequently reduce the risk of transmission [128].

The HIV-CORE 002 trial began in April 2011, and was a phase-I block-randomised, double-blind, placebo controlled trial primarily assessing the safety of the HIVconsv (conserved regions) immunogen vectored by plasmid DNA (pSG2.HIVconsv), non-replicating modified vaccinia virus Ankara (MVA.HIVconsv) and non-replicating chimpanzee adenovirus serotype 63 (ChAdV63.HIVconsv), which were delivered in heterologous prime-boost regimens.

The primary endpoint for the trial was to assess that the vaccines were safe for use in human volunteers. This was determined by examination and interview during visits to clinic as well as a diary card kept by each vaccinee. As the simian viral vector and HIVconsv immunogen combination had never been trialed in humans before, the vaccine was first assessed for safety. Two healthy HIV-1/2 negative adult volunteers from Oxford were vaccinated with a low dose of $5x10^9$ virus particles (vp), intra-muscularly (i.m.) before proceeding with the other regular dose vaccine groups. The safety data collected from all volunteers who received the candidate vaccines, showed that the vaccines were safe and well tolerated with no serious adverse events or reactions reported [319].

The secondary endpoint for the trial was an evaluation of the immunogenicity of these candidate vaccines, primarily deduced by IFN-γ enzyme-linked ImmunoSpot (ELISpot) assay. Figure 8A shows the immunogen, with annotations of the 6 peptide pools used to analyse vaccine immunogenicity. Figure 8B shows the vaccination schedule for the 4 regimens tested within the trial and these were administered to low risk, HIV-1/2 negative healthy volunteers in Oxford.

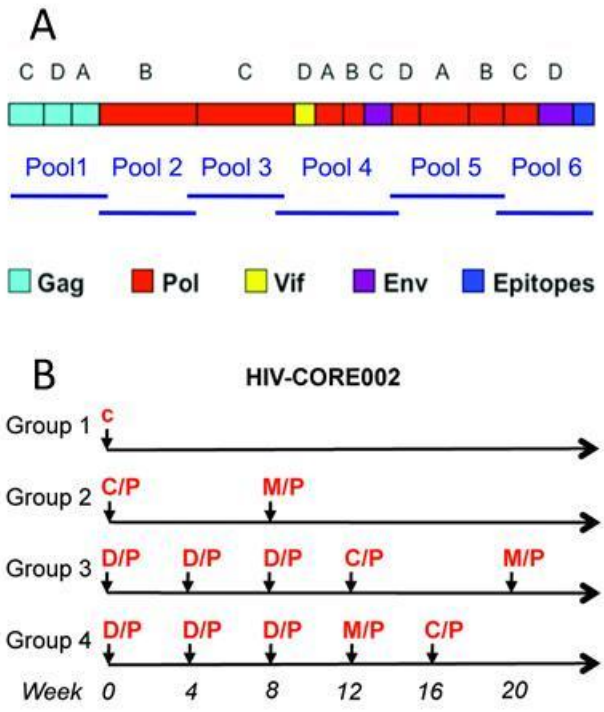


Figure 8 The HIVconsv immunogen and trial design. A schematic representation of the HIVconsv immunogen annotated with clade origin (A, B, C or D) used to derive the consensus sequence. The 6 peptide pools, used for assessment of immunogenicity by IFN-γ ELISpot assay and intracellular cytokine staining (ICS) are also shown. Immunogen regions are colour-coded according to protein origin with navy blue indicating Mamu-A*01 and H-2D^{d}-restricted T-cell epitopes and a mAb Pk tag added to enable protein detection **(A)**. Trial design: The four vaccine regimens administered to healthy volunteers in the HIV-CORE 002 trial are shown. c and C represent low (5x10^{9} vp i.m.) and regular dose (5x10^{10} vp) of ChAdV63.HIVconsv respectively, D is pSG2.HIVconsv DNA (4 mg), M is MVA.HIVconsv (2x10^{8} pfu) and P is placebo. The ratio of vaccinees to placebos was 4:1. Note that for group 4 the interval between M and C was shorter (4 weeks) **(B)**. Figure is taken from Borthwick et al. 2014 [320].

Prior to the HIV-CORE 002 safety trial, these vaccines were assessed pre-clinically. A good safety [321] and immunogenicity profile was demonstrated in BALB/c mice, whereby, T cells recognised multiple peptide pools, produced IL-2 and IFN-γ and showed superior induction through the DNA.HIVconsv, HAdV-5.HIVconsv and MVA.HIVconsv (DAM) regimen [270]. Similarly in rhesus macaques, high frequencies of T cells were induced through DDDAM vaccination [322] and both CD4^{+} and CD8^{+} memory T cells were capable

of proliferating and producing IL-2, IFN-γ or TNF-α [323]. Importantly, within HIV+ patients HIV-1-specific memory T cells were also able to recognise and respond to epitopes encoded within the HIVconsv immunogen [270]; however, these responses were subdominant, likely reflecting the non-protective dominant responses driven by HIV-1 "decoy" epitopes [324, 325].

The IFN-γ ELISpot assay is commonly performed for vaccine candidate evaluation and has been used widely in HIV-1 [258, 259, 297, 326], malaria [327, 328] and tuberculosis [329] vaccine studies. The method accurately quantifies vaccine-induced memory T cells capable of secreting IFN-γ in response to exogenously loaded peptides [330]. In this way, a T cell response to the whole vaccine immunogen can be determined or responses to the complete viral / bacterial genome interrogated. The assay facilitates the assessment of clinical samples as both fresh (*ex vivo*) and frozen PBMC can be used [331] furthermore, the method has been standardised [332] across laboratories providing greater confidence when HIV-1 vaccine candidates are compared.

Several other assays including lymphoproliferation [165], intra cellular cytokine staining (ICS) [298], cellular cytotoxicity [299] and virus inhibition (VIA) [307] have been developed to characterise the T-cell response. These are beginning to be implemented during the evaluation of novel HIV-1 vaccines, as there is growing consensus that assessment of multiple memory T-cell functions, together with cell frequencies, provides a more comprehensive analysis of the cell-mediated response and thus may aid in prioritising vaccines [143]. This chapter therefore describes the use of several of these aforementioned assays including the IFN-γ ELISpot to examine the magnitude, breadth and functional profiles of the HIVconsv vaccine-elicited T cells.

3.2 Aims of chapter 3:

1. Assess the immunogenicity of the low dose HIVconsv immunogen delivered by ChAdV-63 in healthy volunteers by an *ex vivo* IFN-γ ELISpot assay.

2. Determine the proportion of volunteers responding to vaccination using an *ex vivo* IFN-γ ELISpot assay.

3. Assess the breadth of the T-cell response by examining the recognition of individual peptide pools and through peptide mapping of vaccinee responses.

4. Examine the cytokine profile of $CD8^+$ and $CD4^+$ T cells induced by HIVconsv vaccination.

5. Establish if the HIV-1 vaccine induced memory $CD8^+$ and $CD4^+$ T cells are able to proliferate in response to HIVconsv peptides.

3.3 The low dose ChAdV63.HIVconsv vaccine was immunogenic

The first group vaccinated in the HIV-CORE 002 trial received the low dose ($5x10^9$ vp, i.m.) of ChAdV63.HIVconsv. Immunogenicity for all groups was determined using vaccinees' freshly isolated PBMC in *ex vivo* IFN-γ ELISpot assays. All vaccinee samples were assessed for a response to 6 peptide pools encoding 30-32 15/11 mer overlapping peptides spanning the HIVconsv immunogen. An additional pool of immunodominant peptides selected from influenza, Epstein-Barr virus and cytomegalovirus (CEF) were run as a positive control, along with a non-specific phytohaemagglutinin (PHA) stimulus. A negative control of R-10 media with 0.5% DMSO was also included for each sample. *Ex vivo* IFN-γ ELISpot assays were performed with Nicola Borthwick in support of the HIV-CORE 002 trial.

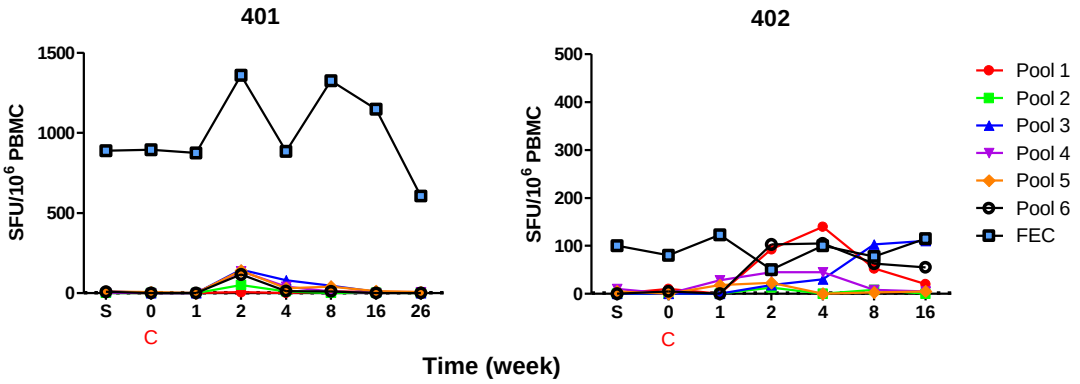


Figure 9 Magnitude and breadth of vaccine-elicited T cells induced by low dose ChAdV63.HIVconsv. *Ex vivo* IFN-γ ELISpot assays were performed on freshly isolated PBMC at each time point. S = screening visit, with the timing of subsequent vaccinations indicated in weeks. Samples were tested against 6 pools of overlapping 15/11 mer peptides spanning the HIVconsv immunogen. A positive control of CEF peptides was also run alongside the negative control (mock) of 0.5% DMSO in R-10 media. All results are displayed as SFU/10^6 PBMC and are background (mock) subtracted. Figure 12A, B and C show the breadth of responses induced by the CM, DDDCM and DDDMC regimens respectively.

Figure 9 indicates the breadth and magnitude of the T cell response to the low dose of ChAdV63.HIVconsv in two healthy volunteers. Peak responses for vaccinees 401 and 402 were detected at 2 weeks and 4 weeks post vaccination, respectively. The group median

frequency of T cells induced at 2 weeks post vaccination was 443 SFU/10^6 PBMC. The breadth of the vaccine response was initially determined by the number of peptide pools recognised per vaccinee. A positive cut-off for each peptide pool was determined from the pre-vaccination (screen and week 0) data for all vaccinees and set at >20 SFU/10^6 PBMC. Vaccinees 401 and 402, showed a positive response to 5/6 and 4/6 peptide pools at 2 and 4 weeks post vaccination respectively.

As, the ChAdV63.HIVconsv vaccine was deemed to be both safe and immunogenic, the remaining groups were sequentially vaccinated with the CM, DDDCM and DDDMC regimens, at the regular dose. Data for the total frequencies of T cells induced by these vaccination regimens are shown in Figure 10.

3.4 HIVconsv vaccines induced high frequencies of HIV-1-specific T cells

The total magnitude of T cells induced by each vaccination regimen was evaluated using the IFN-γ ELISpot assay as described above. The sum of the response to all 6 peptide pools for each vaccinee was determined from the initial screening visit to 28 weeks post primary vaccination. A background cut-off of ≥235 SFU/10^6 PBMC was set based on the mean +2 SD of 6 mock replicates from the pre-vaccination time points for all vaccinees. The group median +2 SD was 70 SFU/10^6 PBMC and the highest value (median +2 SD) for any individual was 235 SFU/10^6 therefore this upper value was used to set a stringent positive cut-off.

Figure 10 shows that for the CM regimen (Figure 10A) a uniformed peak response was detected at 1 week post MVA.HIVconsv boost (week 9) and the group median was 5,150 SFU/10^6 PBMC. The DDDCM (Fig.2B) and DDDMC (Fig.2C) vaccine regimens showed lower total frequencies of T cells with 4,110 and 1,255 SFU/10^6 PBMC determined at 1 week post MVA.HIVconsv boost (week 21) and 1 week post ChAdV63.HIVconsv boost

(week 17), respectively. These vaccination regimens showed a spread of peak responses with DDDCM ranging between 21-28 weeks and DDDMC ranging from 17-24 weeks.

A comparison of the CM (Figure 10A) and DDDCM (Figure 10B) regimens revealed that priming with DNA.HIVconsv resulted in a non-significant increase in the total median frequencies of T cells from 630 at week 4 following C (Figure 10A) to 1,323 SFU/10^6 PBMC at week 14 after DDDC (Figure 10B). However, the peak response time following DDDCM showed a greater spread suggested that the DNA priming may have delayed the recruitment of T cells in some individuals.

The results from the last vaccine regimen DDDMC (Fig.2C) also suggested that the timing of the final ChAdV63.HIVconsv boost may not have been optimal, as at week 13 (DDDM), a sum of 1,330 SFU/10^6 PBMC was determined, however, following the ChAdV63.HIVconsv boost at week 17 the T cell frequency declined to 1,255 SFU/10^6 and did not recover.

The data showed that all vaccine recipients responded to the CM, DDDCM and DDDMC vaccine regimens, with uniquely high T-cell frequencies, and there were no positive responses from those volunteers who received placebo.

When a comparison of median T cell frequencies was made at the peak timepoint for each vaccine regimen (Figure 11), significant differences could be drawn. The CM and DDDCM vaccine regimens showed significantly higher ($P = 0.0037$ and $P = 0.0019$, respectively) T-cell frequencies compared to the DDDMC regimen, suggesting that in terms of magnitude, these two regimens would be most appropriate to progress with in future clinical trials.

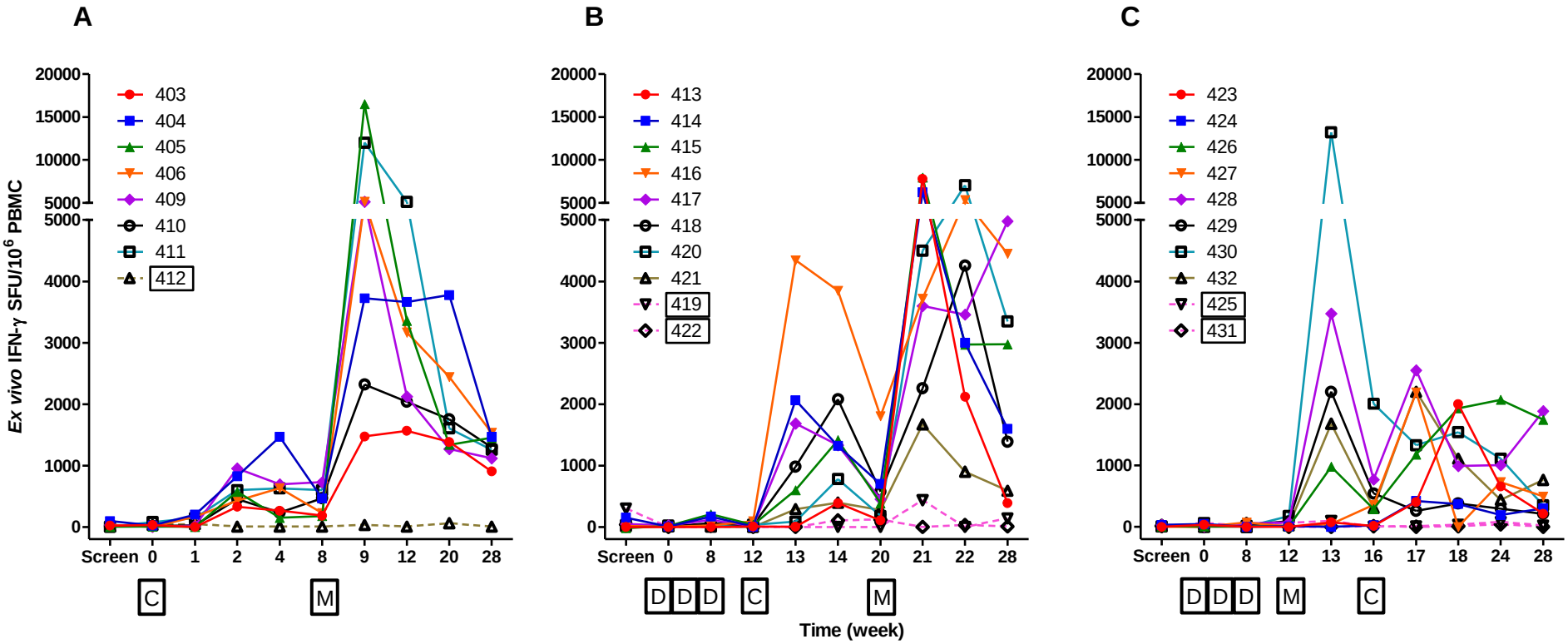


Figure 10 Frequencies of vaccine-elicited T cells recognising conserved regions of HIV-1. The CM regimen **(A)**, DDDCM regimen **(B)** and DDDMC regimens **(C)** were evaluated for immunogenicity. Freshly isolated PBMC were tested in an *ex vivo* IFN-γ ELISpot assay against 6 pools of 15/11 mer overlapping peptides spanning the HIVconsv immunogen. Each vaccinee is colour coded with a rectangular box denoting volunteers receiving placebo. The sums of pools 1-6 are shown for each vaccinee at each time point. Timings for each vaccine administration are indicated below each graph in weeks. The dose administered for each vaccination was D = 4 mg, C = $5x10^{10}$ vp and M = $2x10^{8}$ pfu.

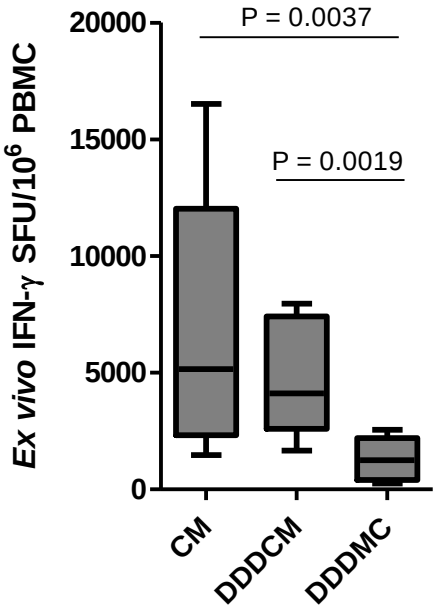


Figure 11 Comparison of vaccination regimens based on summed *ex vivo* IFN-γ ELISpot assay responses. The total response to the six HIVconsv peptide pools was compared for each vaccine regimen, with the box plots representing the mean, 25th and 75th percentile and the whiskers represent the range. Comparisons between median values were determined using the Mann Whitney test, with two-tailed P values of <0.05 considered to be significant.

3.5 A breadth of T-cell specificities were induced by HIVconsv vaccination

The breadth of T-cell responses were initially examined by quantifying the number of peptide pools responded to by each vaccinee. Data from Figure 12A, B and C showed that for the CM and DDDCM vaccine regimens, a breadth of T cell specificities were induced as a total of 7/7 vaccinees at week 9 and 8/8 vaccinees at week 21, responded to all 6 peptide pools. The DDDMC regimen induced a narrower breadth of response with 2/8 vaccinees at week 17 responding to all 6 peptide pools, 5/8 responding to 5 peptide pools and 1/8 responding to 4 peptide pools.

When the frequencies of T cells induced by individual peptide pools were compared in Figure 13A, both the CM and DDDCM regimens showed significantly higher (P = 0.031) median responses to all peptide pools compared with the DDDMC regimen. However, there

was no significant difference between the median frequencies of T cells that were specific for each peptide pool when CM and DDDCM regimens were compared. Interestingly, Figure 13A also showed that the majority of T cells induced by the CM, DDDCM and DDDMC regimens were specific for peptide pool 3 whereas peptide pool 5 induced the lowest frequencies of T cells following vaccination with the CM and DDDCM regimens.

A further analysis of the percentage of responders to each peptide pool irrespective of magnitude (Figure 13B) following each vaccine regimen revealed that the CM and DDDCM regimens also exceeded in the percentage of responders to each pool when compared with the DDDMC regimen. All 6 pools were responded to effectively by the vaccinees that received CM and DDDCM, but pools 1, 2 and 5 were not recognised by all vaccinees from the DDDMC regimen.

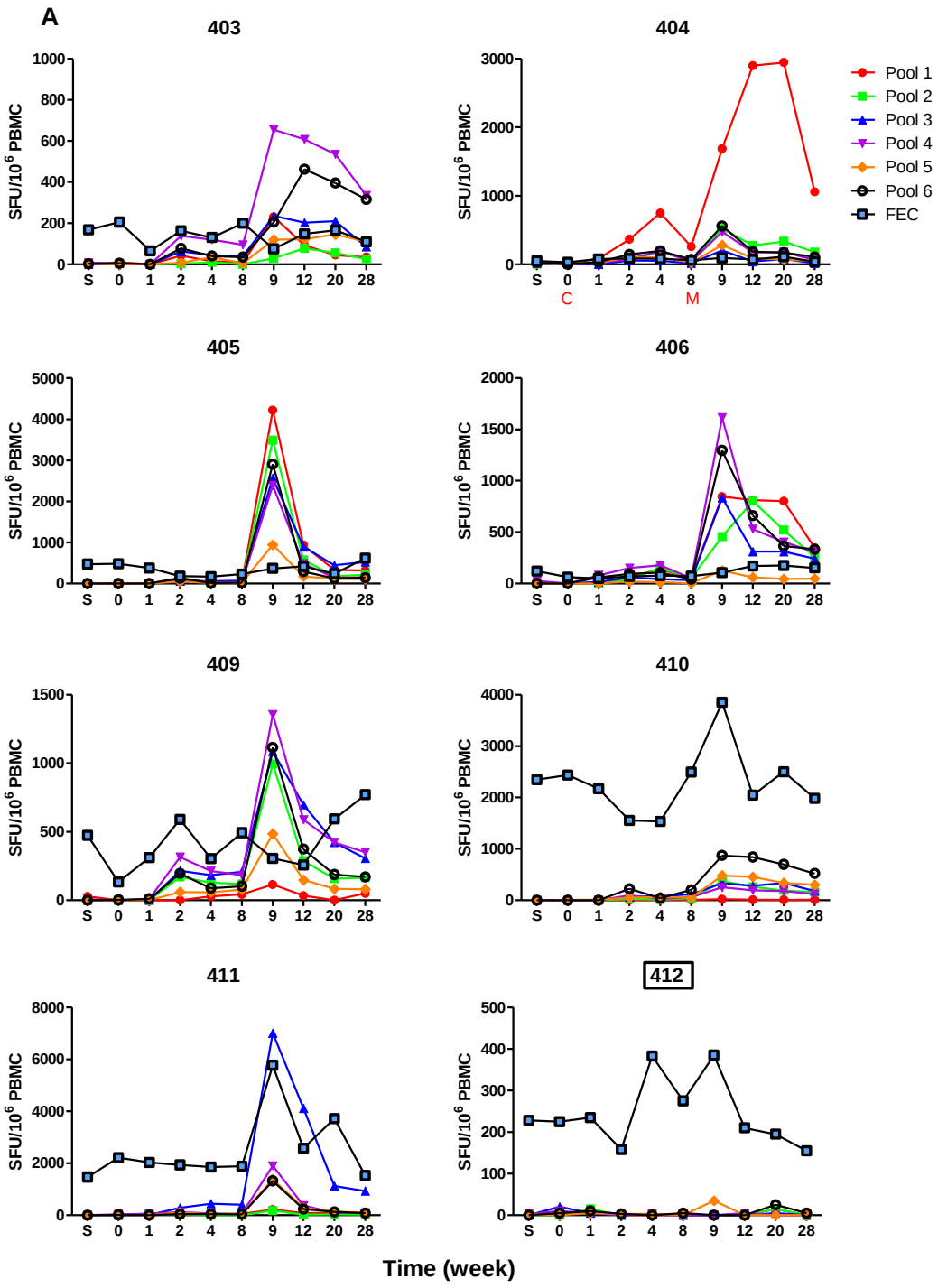
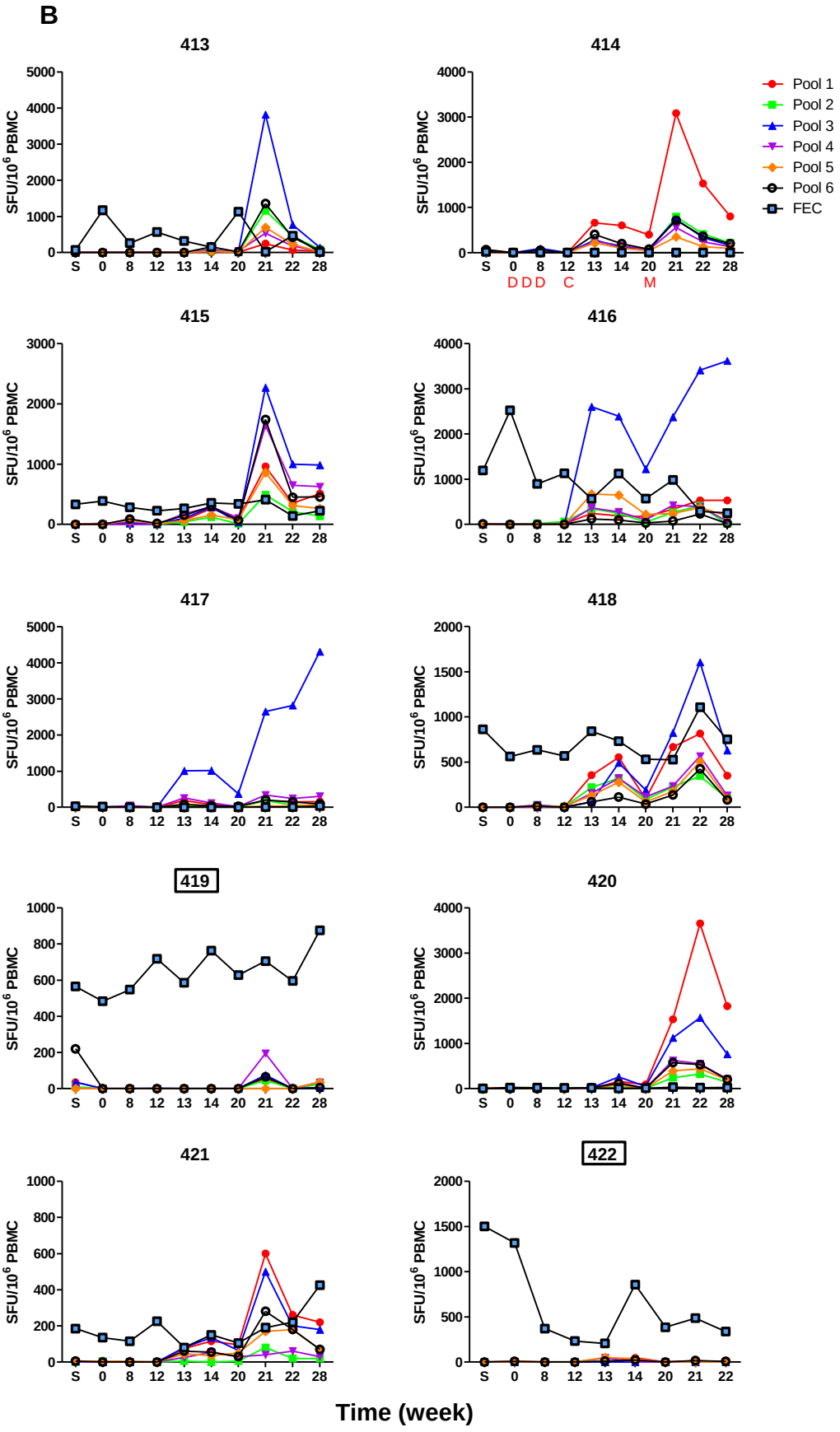
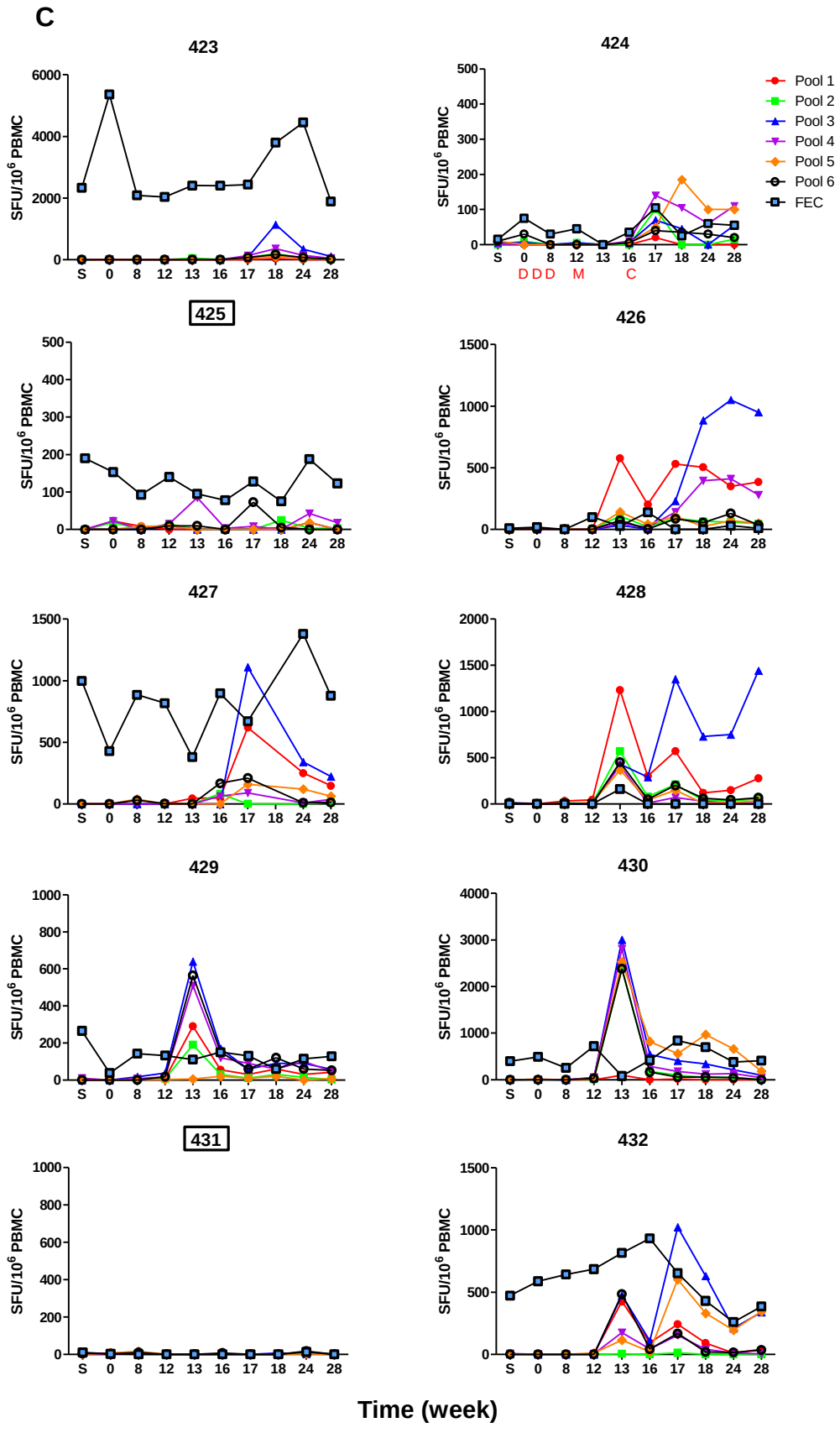


Figure 12 Breadth of T-cell responses induced by the CM, DDDCM and DDDMC regimens. Freshly isolated PBMC were tested in an *ex vivo* IFN-γ ELISpot assay against 6 pools of 15/11 mer overlapping peptides spanning the HIVconsv immunogen. Figure 12 A, B and C show the breadth of responses induced by the regular dose of CM, DDDCM and DDDMC vaccines. C = ChAdV63.HIVconsv, M = MVA.HIVconsv and D = pSG2.HIVconsv. Responses of >20 SFU/10^6 PBMC to a single peptide pool were classed as positive, based on pre-vaccination (S and 0 week) data for all vaccinees. Boxed numbers represent placebo recipients.


B
413
414
415
416
417
418
419
420
421
422
SFU/10^6 PBMC
Time (week)
Pool 1
Pool 2
Pool 3
Pool 4
Pool 5
Pool 6
FEC
S 0 8 12 13 14 20 21 22 28
D D D C M


C
423
424
425
426
427
428
429
430
431
432
SFU/10^6 PBMC
Time (week)
S 0 8 12 13 16 17 18 24 28
D D D M C
Pool 1
Pool 2
Pool 3
Pool 4
Pool 5
Pool 6
FEC

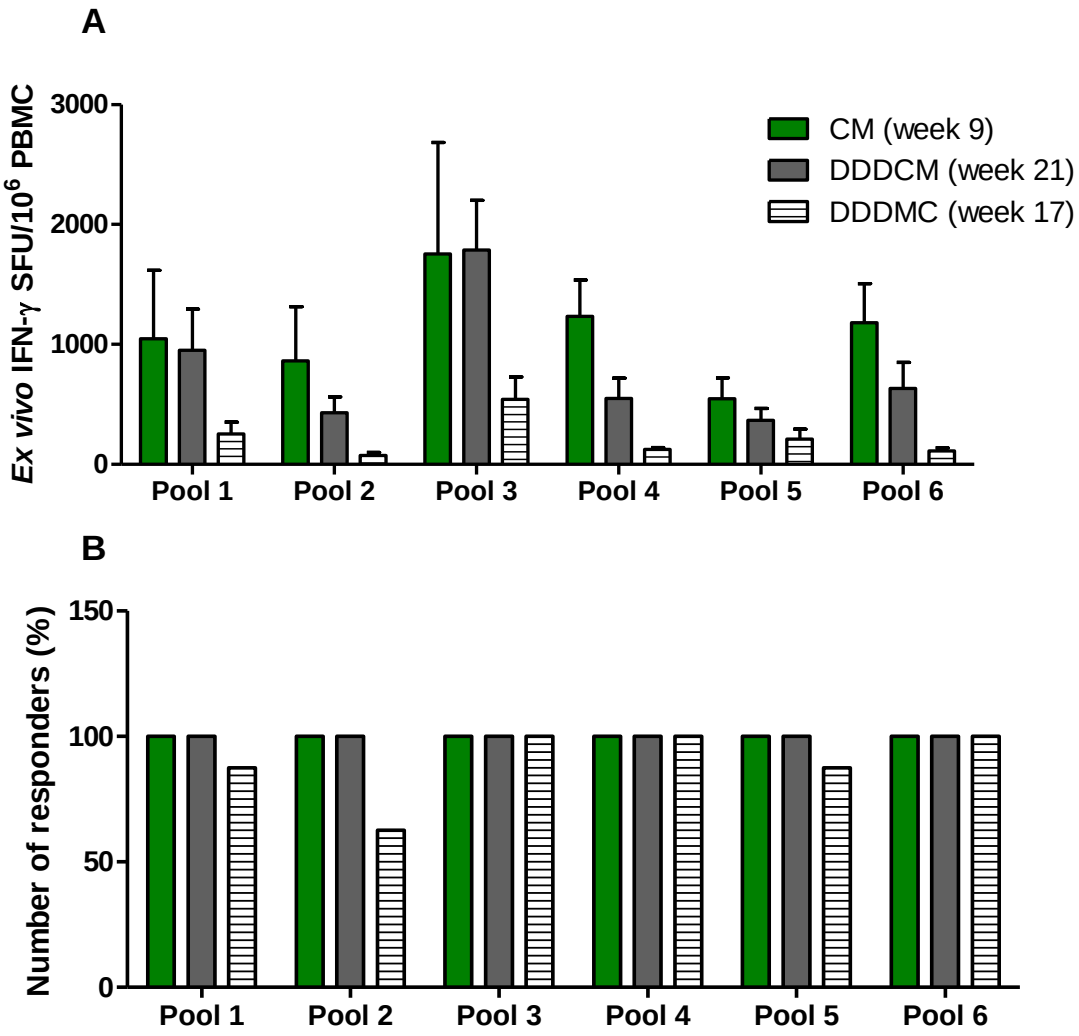


Figure 13 Comparison of magnitude and breadth of T-cell responses induced by CM, DDDCM and DDDMC to individual peptide pools. T cell frequencies were enumerated using an *ex vivo* IFN-γ ELISpot assay with 6 peptide pools comprised of 15/11 mer overlapping peptides covering the HIVconsv immunogen. The group mean frequencies of T cells induced by each vaccine regimen to peptide pools 1-6 are shown with standard error of the mean represented by the error bars **(A)**. The percentage of responders to each peptide pool (1-6) for each vaccine regimen is also shown **(B)**. Vaccine regimens are colour coded.

A more in depth analysis of the breadth of vaccine-induced T-cell responses was performed by peptide mapping PBMC from vaccinees who received CM and DDDCM. All individuals were tested except for vaccinee 405, as they did not have enough cells available. The majority of these vaccinees were mapped by Dr Nicola Borthwick.

Figure 14 shows that each vaccinee recognised on average 13 HIVconsv peptides, equivalent to approximately 10 $CD8^+$ T cell epitopes. Most (60%) of the mapped T-cell responses contained epitopes previously reported within the Los Alamos National Laboratory (LANL) HIV database and matched with the volunteers HLA type, but ~40% had not previously been described. In addition, 20% of T-cell responses were directed to junctional peptides that spanned two adjacent conserved regions, and thus would not contribute to control of HIV-1. Critically, none of the placebo volunteers made T-cell responses to the HIVconsv peptides.

Taken together, these data demonstrated that vaccination with the HIVconsv immunogen induced T cells with broad specificities towards naturally subdominant regions of the HIV-1 proteome. Moreover, these responses were found in all of the vaccinees who received CM and DDDCM, further demonstrating the superiority of these regimens.

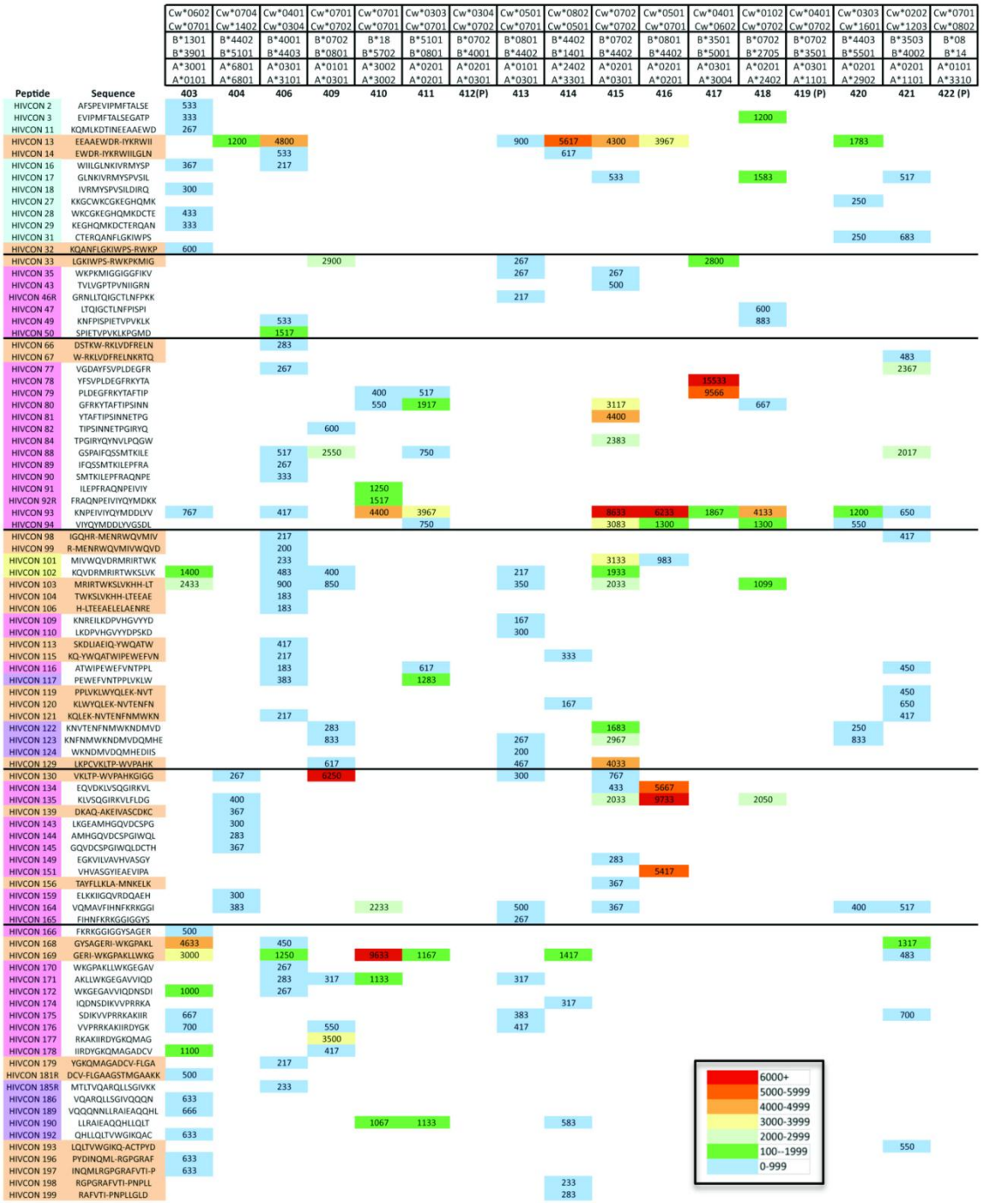


Figure 14 T-cell specificities induced through vaccination with CM and DDDCM regimens. Vaccinee T-cell specificities were mapped using 10 day short-term cell lines, stimulated with peptide pools 1-6. T-cell lines were tested by IFN-γ ELISpot assays with individual peptides covering the HIVconsv immunogen. Boxed numbers represent SFU/10^6 expanded PBMC. At the top of the table HLA types are reported. Individual peptides are colour coded according to their origin: Pink, Pol; Blue, Gag; Yellow, Vif and Purple, Env. Peptides containing a junction, indicated by a hyphen are colour coded orange. Black horizontal lines separate peptide pools 1-6. Figure taken from Borthwick et al. 2014 [320]

3.6 The HIVconsv vaccine elicited CD8$^+$ and CD4$^+$ T cells were polyfunctional

Polychromatic flow cytometry was performed by Dr Beatrice Ondondo to assess the functional profiles of the vaccine-elicited T cells. CD8$^+$ and CD4$^+$ T cell responses to individual peptide pools confirmed that the T cells were of broad specificity as observed for the IFN-γ ELISpot assays (data not shown). In Figure 15, analysis of the group median CD8$^+$ and CD4$^+$ T-cell responses for IFN-γ and TNF-α showed that there were statistically significant differences between the 3 vaccine regimens (P = 0.0012). In addition, pairwise comparisons for CD8$^+$ T cells revealed that IFN-γ producing T-cell frequencies were significantly higher for the CM and DDDCM regimen compared with the controls. Higher frequencies of TNF-α producing T cells were also found for the DDDCM and DDDMC regimens compared to the controls. Examination of the CD4$^+$ T cells showed that the frequencies of both TNF-α and IFN-γ producing T cells were significantly higher for the DDDCM group compared to the controls.

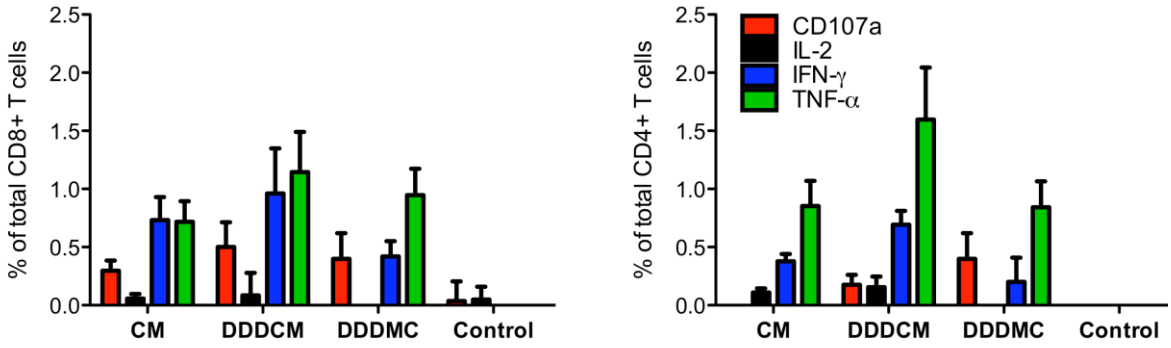


Figure 15 Polychromatic flow cytometry analysis of vaccine-elicited T cells. Frozen PBMC samples from the peak or second highest response timepoint were re-stimulated *in vitro* with 6 HIVconsv-derived peptide pools of 15/11 mer peptides and analysed for their CD3$^+$/CD8$^+$ and CD3$^+$/CD4$^+$ T cells. The total frequencies of each intracellular signalling molecule among individual vaccine regimens and controls are shown. The Kruskal-Wallis test and Dunn's multiple comparison post-test were performed for both the CD8$^+$ and CD4$^+$ T cells. Figure taken from Borthwick et al. 2014 [320].

Further to the examination by an ICS assay, frozen PBMC samples were stimulated for 48 hours with the 6 pools of HIVconsv peptides and supernatants were analysed in a Luminex assay for the presence of 12 different cytokines. Analysis of the CM group was performed by researchers at the Fred Hutchinson Cancer Research Centre and analysis of the DDDMC group was performed in Oxford following the optimised protocol published by Defawe et al. 2012 [311]. The results from this analysis are shown in Figure 16, which demonstrated that T cells from both the CM and DDDCM regimen were able to produce multiple cytokines with IFN-γ, TNF-α, IL-2, MIP-1β, IL-13 and GM-CSF present in all samples. For the CM and DDDCM groups IFN-γ was the dominant cytokine secreted by vaccinees 408, 409, 410, 411, 413, 416, 417 and 420. In contrast, for vaccinees 403, 404 and 406 TNF-α, MIP-1β and IL-2 were present at the highest concentrations, respectively, whereas for vaccinees 418 and 421 IL-13 was most highly secreted. This data supported the ICS analysis and furthermore showed that the vaccine-induced PBMC were capable of producing at least 6 different cytokines from those that were measured here.

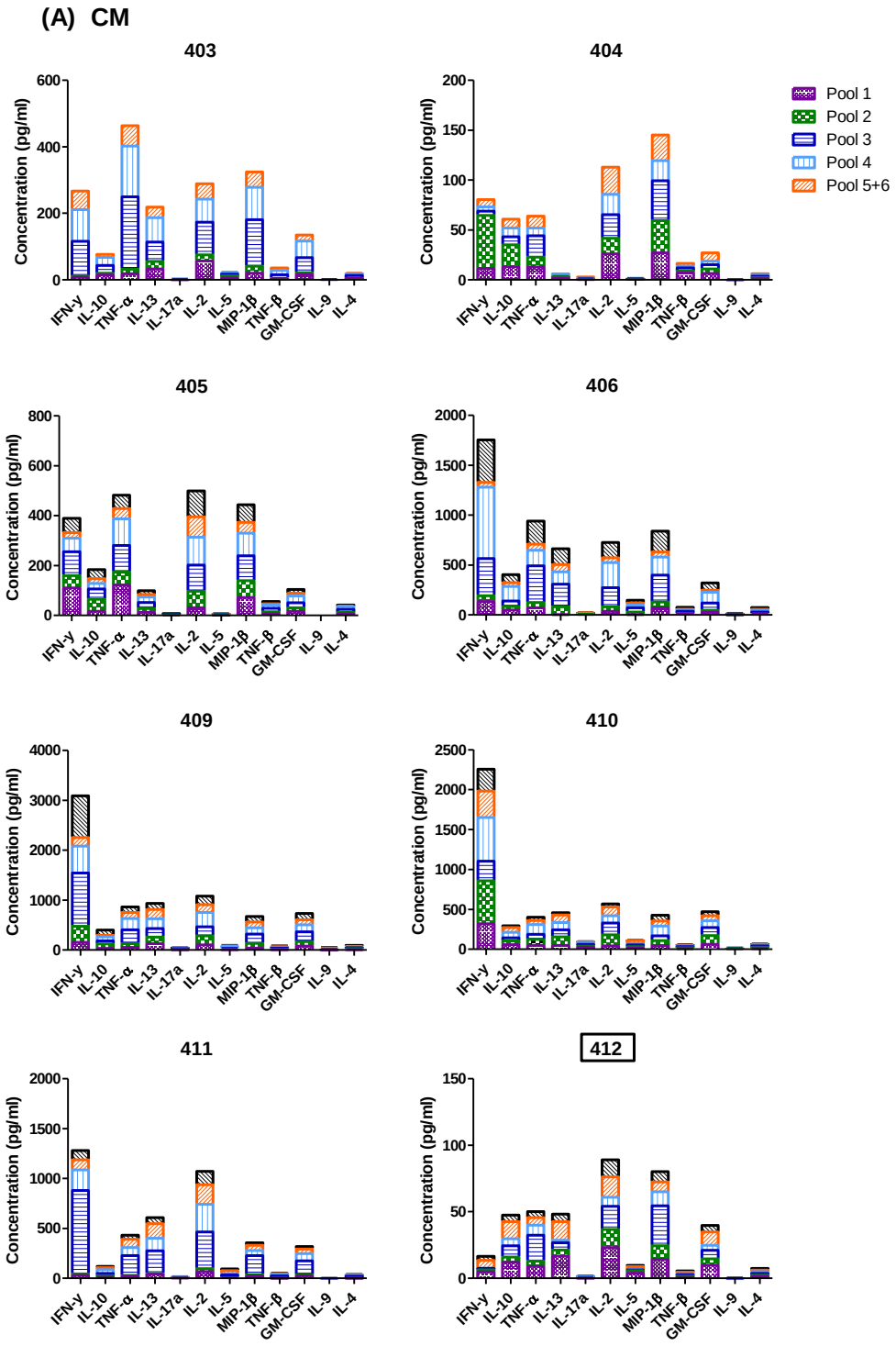
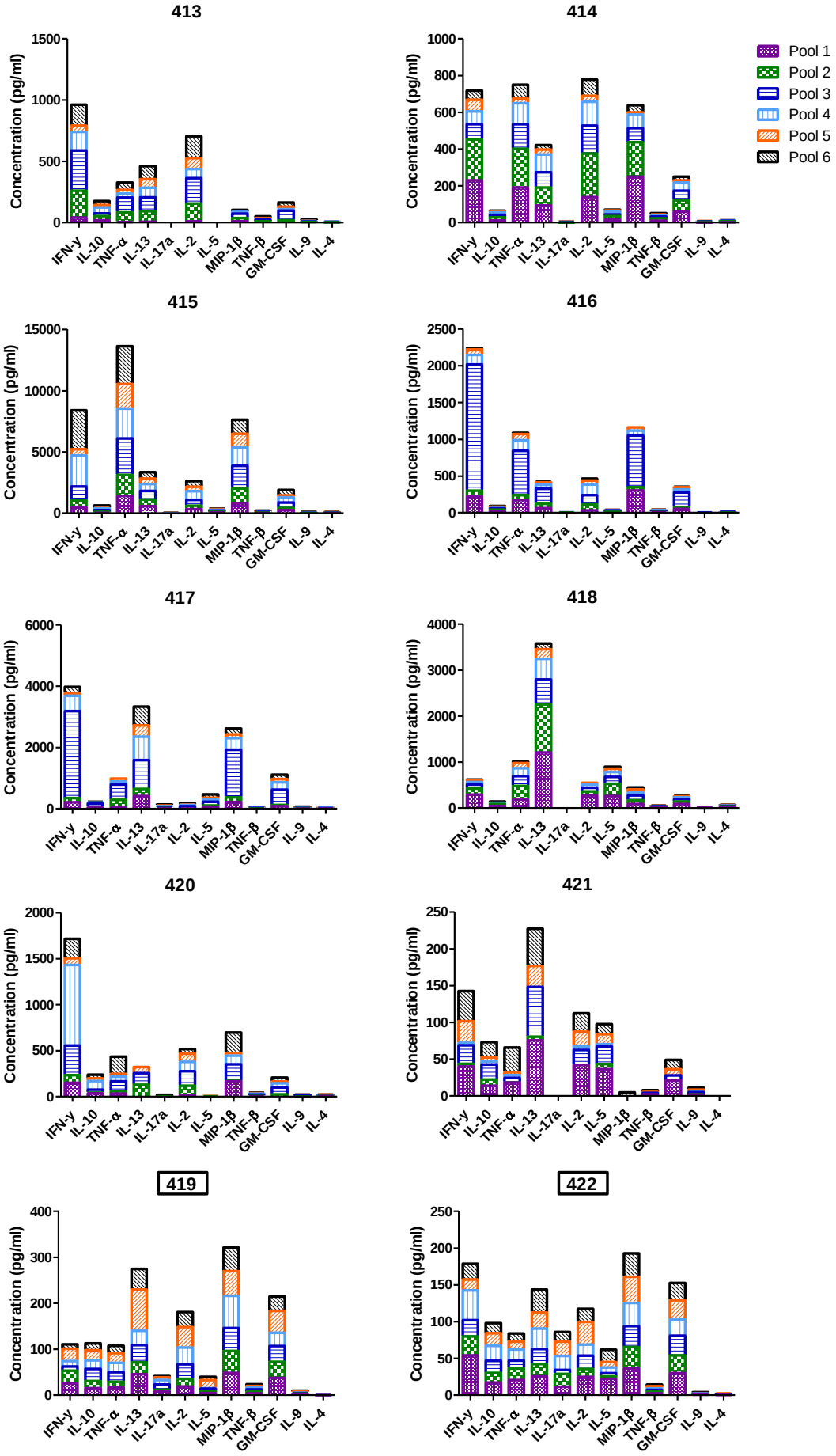


Figure 16 Vaccine-induced cytokine profiles for the CM and DDDCM regimens. The concentrations of 12 cytokines were examined for both the CM (A) and DDDCM (B) vaccine regimens using the Luminex platform and Millipore-Milliplex Map Human high sensitivity kit. Frozen PBMC from CM and DDDCM peak time points of one week post final vaccination (week 9 and 21, respectively), were thawed and stimulated with 6 pools of HIVconsv peptides for 48 hours. Supernatants were collected and frozen at -80 °C until use in the assay. Boxed numbers represent placebo recipients.

(B) DDDCM


413
414
415
416
417
418
420
421
419
422
Concentration (pg/ml)
IFN-γ
IL-10
TNF-α
IL-13
IL-17a
IL-2
IL-5
MIP-1β
TNF-β
GM-CSF
IL-9
IL-4
Pool 1
Pool 2
Pool 3
Pool 4
Pool 5
Pool 6

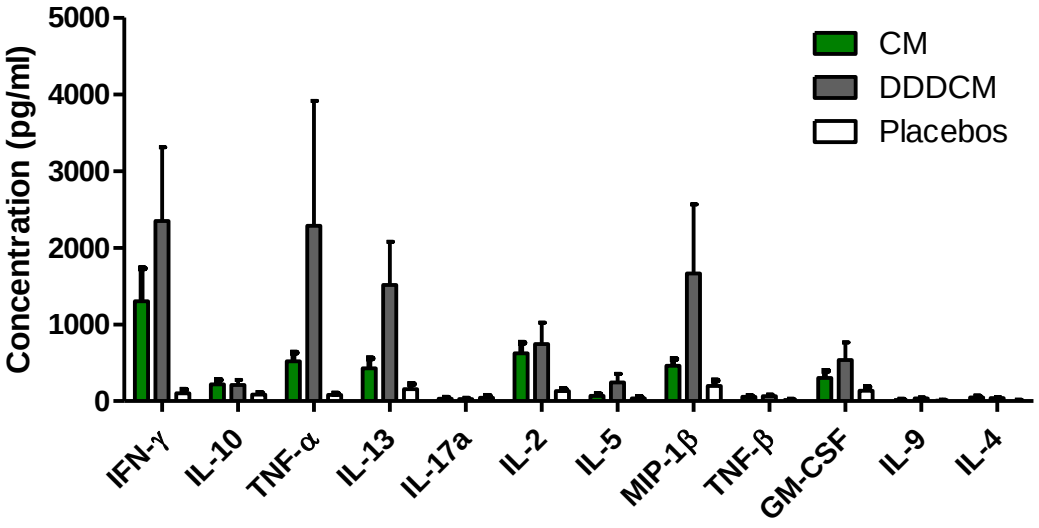


Figure 17 Comparison of vaccine regimen on cytokine induction from peptide stimulated PBMC. The concentrations of 12 cytokines were determined by Luminex analysis of frozen supernatants from peptide stimulated PBMC. Each vaccine regimen is colour coded and the bars represent group mean + standard error of the mean for each cytokine. The Wilcoxon matched-pairs signed rank test was performed on group median values for each cytokine in response to each vaccine regimen and for placebo controls. A value of P = <0.05 was considered significant.

Comparison of the secreted cytokine levels were made between the two vaccine regimens and placebo recipients (Figure 17), which showed that there was no significant difference in the group median cytokine concentration for any cytokine when the CM and DDDCM regimens were compared. In contrast, significantly higher (P = <0.05) concentrations of IFN-γ IL-2, MIP-1β, TNF-α and IL-4 were found for vaccinees receiving CM compared to placebos. Moreover, the greatest cytokine induction was observed in response to DDDCM vaccination, with significantly higher levels of IFN-γ, TNF-α, IL-13, IL-2, MIP-1β, TNF-β, GM-CSF and IL-4 found in comparison to the placebo group.

3.7 Vaccine-induced $CD8^+$ and $CD4^+$ T cells proliferated in response to recall antigen.

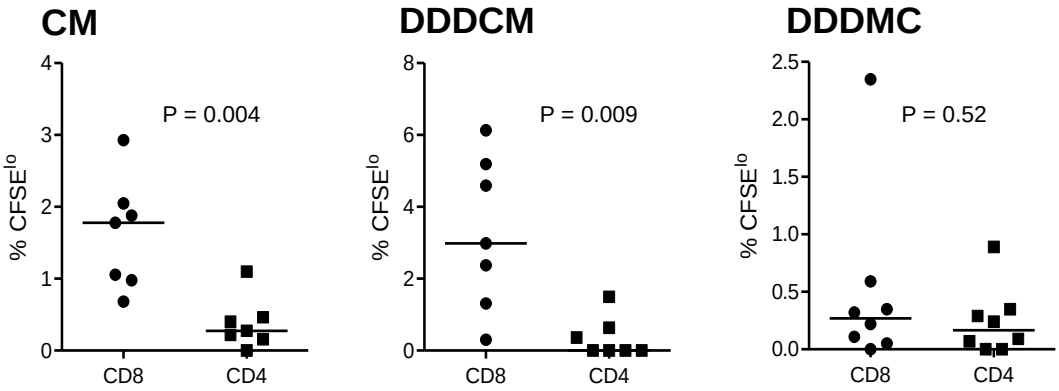


Figure 18 $CD8^+$ and $CD4^+$ T proliferation data for the CM, DDDCM and DDDMC vaccine regimens. CFSE stained PBMC from weeks 0 and 28 were stimulated for 5 days with peptide pools 1-4 covering the HIVconsv immunogen. The background (week 0) subtracted percentages of proliferating $CD8^+$ and $CD4^+$ T cells were determined. For all vaccinees, the summed response to all 4 peptide pools are shown. Figure taken from Borthwick et al. 2014 [320].

An important function of antigen-specific memory T cells, which is maintained in LTNP, is their ability to robustly proliferate in response to recall antigen [189, 190]. Therefore, the proliferative capacity of both $CD4^+$ and $CD8^+$ T cell populations was assessed by Dr Beatrice Ondondo using the carboxyfluorescein succinimidyl ester (CFSE) dilution assay. The results of these analyses revealed that $CD8^+$ T cells from the CM and DDDCM regimens were able to effectively proliferate, with no significant differences found between these two groups. However, there were significantly higher frequencies of T cells ($P = <0.005$) capable of proliferation in the DDDCM group when compared with the DDDMC group.

In contrast, for the CM and DDDCM vaccine regimens fewer $CD4^+$ T cells were able to proliferate in response to peptide stimulation compared with $CD8^+$ T cells with no significant differences found between the levels of $CD4^+$ T cells induced through each vaccine regimen.

Overall the CM and DDDCM regimens elicited T cells with a greater capacity to proliferate in response to antigen re-exposure.

3.8 Chapter 3 Discussion

The HIV-CORE002 trial was performed in order to establish both the safety and immunogenicity of the HIVconsv vaccine candidates in healthy HIV-1/2 negative volunteers. The data collected from all volunteers showed that these vaccines were safe and well tolerated, with mild local and systemic symptoms described following vaccination and no serious adverse events or reactions reported by any volunteers [319].

The HIVconsv immunogen elicited $CD8^+$ and $CD4^+$ T cells that were of high magnitude, wide breadth and of good quality (capable of cytokine secretion, degranulation and proliferation), and in natural HIV-1 infection T cells displaying these characteristics have been associated with a reduction in viral load and slower disease progression [173, 189-191, 333].

The standardised IFN-γ ELISpot assay was used to measure T cell frequencies following administration of three heterologous prime-boost regimens; CM, DDDCM and DDDMC and it revealed that the magnitude of vaccine-elicited T cells and the percentage of responders to the vaccines superseded those previously reported for other prophylactic HIV-1 vaccine candidates when the CM and DDDCM regimens were considered [297, 326, 334].

Encouragingly, these magnitudes were also more than 10-fold greater than those reported for the HVTN 502 STEP study, which failed to prevent infection or reduce early set-point viral load in those vaccinees who became infected [296]. Moreover, the HIV-1-specific T cells induced by both CM and DDDCM showed greater breadth of HIV-1 epitope recognition [261, 335]. T-cell specificity also differed to that elicited by the STEP study; MRK HAdV-5 Gag/Pol/Nef candidate [335], as HIVconsv vaccine-induced T cells were focused on conserved regions of the HIV-1 proteome.

There is increasing evidence to suggest that the quality, including T cell specificity and multiple effector functions, rather than simply the total magnitude of the T cell response, sets apart HIV-1 controllers from progressors [191, 192]. Furthermore, mono-functional IFN-γ secretion has often failed to predict *in vivo* or *in vitro* virus control [258, 298]. Here vaccine-elicited $CD4^+$ and $CD8^+$ T cells demonstrated dual functionality, with most $CD8^+$ T cells (range 0.42 - 0.96%) expressing both IFN-γ and TNF-α. Interestingly, the expression of these two functions has been associated with a more effective cytotoxic response in HIV-1 infected individuals [336]. Degranulation (CD107a positivity), a surrogate marker for cytotoxicity [337] was also evident in $CD8^+$ T cells elicited by all three vaccine regimens, but was only present in $CD4^+$ T cells elicited by DDDCM and DDDMC regimens. ICS analysis also revealed that very few T cells (<0.2%) produced IL-2. Overall, these results show general concordance with the functional profiles [326] but an increase in the total percentages of $CD8^+$ and $CD4^+$ T cells [326, 334, 338] induced by similar vaccine modalities (HAdV-35, HAdV-26) that are currently being explored to overcome the anti-vector immunity shown against HAdV-5 [297].

Perhaps more importantly, the HIV-CORE 002 CM and DDDCM regimens elicited greater T-cell functionality when compared to the HVTN 502 [296], and HVTN 505 [263] studies which both focused on T cell induction but failed to show vaccine efficacy. Furthermore, these two trials alongside a third, HVTN 503 (Phambili study) [259], used the human origin HAdV-5 vector delivered alone or with DNA in a prime-boost regime and saw an unexpected trend of increased HIV-1 infections in vaccinees compared to placebos [258, 263]. The use of an adenovirus of chimpanzee origin may circumvent this effect. However, until the reason/s for the increased incidence is fully determined, alternative vector modalities continue to be explored.

The surprising efficacy trial results from HVTN 502 and 505 have shown that the HIV-1 vaccine field has limited understanding on how to induce the appropriate immune response and what functions and magnitudes will be required for an effective T-cell-mediated vaccine. The development and implementation of novel technologies to better characterise vaccine induced responses is therefore paramount for advancing our knowledge of the immune system. In this chapter a Luminex assay, a relatively new technology, was performed on supernatants collected from peptide stimulated PBMC as it can be used to quantify many more cytokines than flow cytometry within a single sample [311]. This analysis showed that the PBMC elicited through HIVconsv vaccination were capable of producing IL-13, MIP-1β and GM-CSF in addition to the cytokines observed by ICS.

Activated T cells can produce both MIP-1β and IL-13 [339, 340], two cytokines which have been shown to inhibit HIV-1 replication in $CD4^+$ T cells [339, 341] and (bronchoalveolar and monocyte-derived) macrophages [342, 343]. Additional effects of IL-13 include increasing MHC class II expression [340] and antigen uptake by monocytes [344], which has also been shown to enhance the memory $CD4^+$ T cell response that is impaired during chronic HIV-1 infection [344]. The role of GM-CSF on HIV-1 infection is more uncertain as most studies conducted in monocytes have reported an increase in HIV-1 replication in the presence of GM-CSF [345], whereas others have shown inhibition of HIV-1 virion production *in vitro* [346]. This again highlights that further characterisation of the multitude of cell signalling molecules present during viral infection is necessary so that we can learn how to elicit and direct an effective cell-mediated and humoral response against pathogens such as HIV-1.

In this chapter, the HIVconsv vaccine delivered by heterologous prime-boost regimens (CM and DDDCM) was shown to be capable of inducing T cells of high magnitude, surpassing those seen in the HVTN 502 STEP study [258]. Importantly, these responses were

directed toward many highly conserved regions of the HIV-1 proteome, in contrast to what is observed early in natural infection [347, 348]. Furthermore, these memory cells were capable of producing multiple cytokines, including several described to inhibit HIV-1 replication, and of proliferating in response to antigen re-exposure.

More recently we have generated T-cell frequency data from several volunteers who returned for 1.5 year follow on visits, encouragingly these vaccinees still had circulating HIV-1-specific T cells, those who returned from the CM group had a median range of 74 - 203 SFU/10^6 PBMC, and those from the DDDCM group had a range of 30 – 499 SFU/10^6 PBMC. These results show that the HIVconsv vaccines are capable of inducing long-lived memory T cells that could potentially be augmented by booster vaccinations in order to maintain T cells of a higher threshold thus increasing the likelihood for recognition of HIV-1 infected cells.

To investigate whether the T cells induced through vaccination with a synthetic chimeric protein (HIVconsv) could recognise virally presented epitopes and subsequently control HIV-1 replication, an *in vitro* VIA was selected for use with the HIV-CORE 002 trial samples. The optimisation and assessment of this VIA protocol is described in Chapter 4.

3.9 Summary of key findings from Chapter 3

- The low dose ChAdV63.HIVconsv vaccine was immunogenic in the two trial volunteers.

- All (100%) vaccinees made memory T-cell responses to the HIVconsv vaccines, but the highest magnitude of T cells was induced through the CM regimen.

- CM and DDDCM vaccine-induced T-cell specificities were broad recognising on average 6 peptide pools which represented 10 $CD8^+$ T cell epitopes from conserved regions of HIV-1.

- CM and DDDCM vaccine-elicited HIV-1-specific T cells were capable of producing multiple cytokines, including IFN-γ, TNF-α and IL-13.

- All regimens induced $CD8^+$ and $CD4^+$ T cells that proliferated in response to re-call antigen.

4 Optimisation of an *ex vivo* virus inhibition assay for the assessment of vaccine-induced $CD8^+$ T cells

4.1 Introduction

In Chapter 3, the HIVconsv vaccine delivered by viral vectors in CM and DDDCM heterologous prime-boost strategies were shown to induce high frequencies of $CD8^+$ T cells, which were capable of proliferating and producing multiple cytokines. These functions are all key attributes for an effective T cell response. Evidence of these qualities can be found in HIV-1 LTNP, who have remained free of clinical symptoms for over 10 years [189, 191]. However, it remains uncertain whether these responses are present as a result of an initially efficacious antiviral response to HIV-1 or are indeed responsible for the observed viral control.

In order to assess the total $CD8^+$ T cell antiviral response to HIV-1, an *ex vivo* viral inhibition assay (VIA) [303] was selected for optimisation and use with the HIV-CORE 002 vaccine trial samples. The *ex vivo* VIA measures both soluble and cytolytic effector functions of $CD8^+$ T cells, as a response to the infection of autologous $CD4^+$ T cells with a chosen HIV-1 isolate. Importantly, this is without the need for any expansion or stimulation of the selected $CD8^+$ T cell population [301]. An overview of an *ex vivo* VIA is shown in Figure 19.

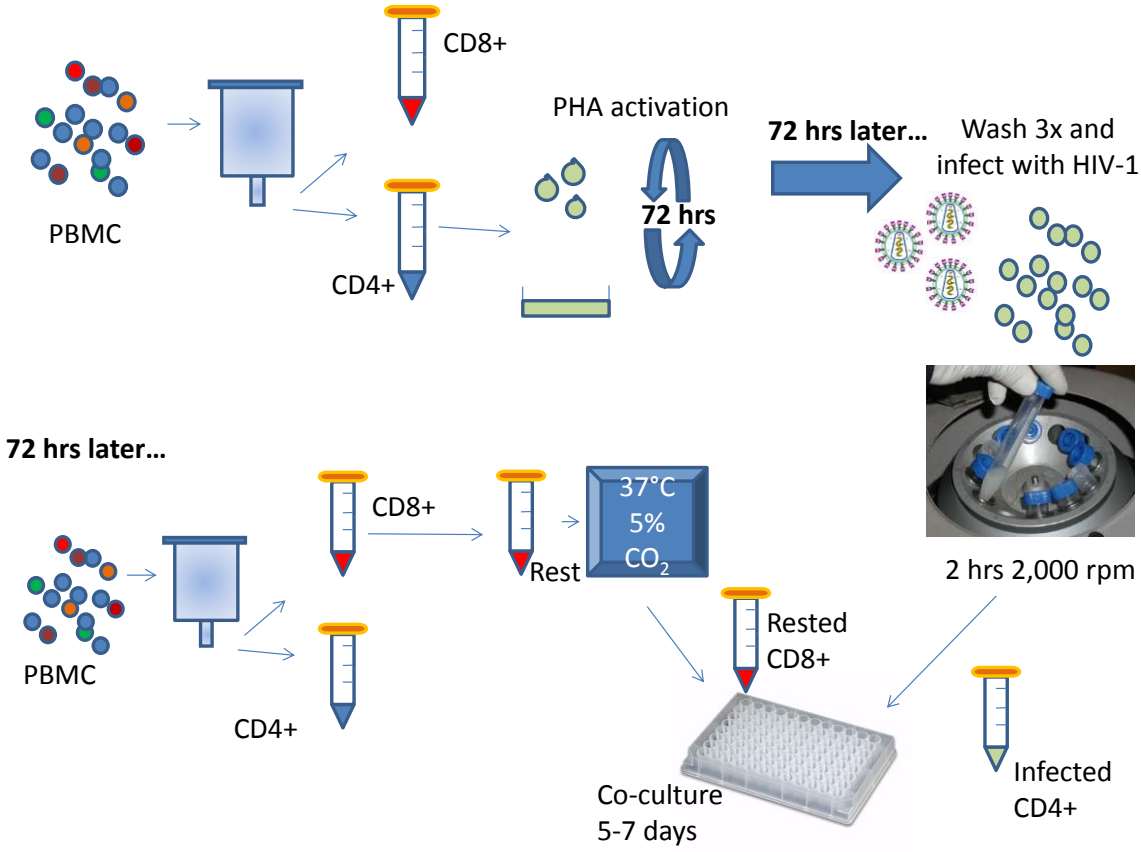


Figure 19 An overview of an *ex vivo* VIA protocol. $CD4^+$ and $CD8^+$ T cells are isolated using magnetic beads. $CD4^+$ T cells are activated with PHA for 72 hrs, after which they are washed and infected with HIV-1 at a selected MOI by a spinoculation methodology. $CD8^+$ T cells are isolated on the day of assay set-up and rested during viral infection. Infected $CD4^+$ T cells are washed following infection and plated with *ex vivo* rested $CD8^+$ T cells at a selected effector to target ratio. Plates are then cultured for 5 to 7 days before being assayed by flow cytometry for intracellular p24 or p24 ELISA of viral supernatants. Adapted from Saez-Cirion et al. 2010 [301].

The observation in 1986 that $CD8^+$ T cells could inhibit autologous viral replication [317] led to an initial examination of the functional capacity of $CD8^+$ T cells from HIV-1-infected individuals to inhibit virus replication of both autologous and lab strain isolates. This initial VIA provided data, which showed that the *ex vivo* inhibitory capacity of $CD8^+$ T cells correlated with the clinical state of the individual [318]. Further support of these results came from analysis by Saez-Cirion in 2007 [305] in work, which demonstrated a clear distinction between the levels of *ex vivo* virus control in HIV controllers, viremic and healthy donors. In this study the HIV-1 controller group showed a reduction in viral p24

levels of >3 log. Furthermore, a recent prospective study of early HIV-1 infection, showed that the suppressive capacity of $CD8^+$ T cells negatively correlated with set-point viral load and strongly predicted the rate of $CD4^+$ T cell decline [304]. The *ex vivo* VIA therefore provides a more composite measure of antiviral activity and insight into vaccine efficacy than can be determined solely by the quantification of HIV-1-specific T cell frequencies or $CD8^+$ T cell multi-functionality in response to select HIV-1-derived peptides.

Furthermore, several studies have highlighted the drawbacks of using peptides as a means of assessing the functionality of T cells. These data suggest that using excess non-physiological concentrations of peptide can overestimate the *in vivo* response to HIV-1-infected cells. Several studies directly comparing $CD8^+$ T cell responses to peptide pulsed and virally infected targets have shown that peptide stimulation results in a greater proportion of responding polyfunctional $CD8^+$ T cells [349]. Moreover, single amino acid changes within a peptide sequence, representative of HIV-1 clade variants [350] and SIV escape variants [351], can lead to the loss of viral control even though killing of targets pulsed with these peptide variants still occurs.

HIV-1 evolution in response to immune pressure can lead to mutations not only within epitopes but also in areas which flank epitopes [352] and these mutations can ultimately result in the loss of epitope presentation. In addition, MHC class I is down-regulated during HIV-1 infection [42], further reducing the amount of peptide presented to T cells. These evasion methods utilised by HIV-1 are not accounted for when exogenous peptides are used for T cell stimulation or target cell sensitisation.

And so, even though T cell responses towards many HIV-1-derived peptides can be measured by IFN-γ ELISpot, ICS and peptide-pulsed killing assays, this does not predict if these T cells will be able to control natural HIV-1 infection. Vaccine-induced T cells will need to recognise both physiological levels of antigen and variants of peptides that are present

in an immunogen, such as HIVconsv, in order to establish and maintain control of HIV-1 replication.

This chapter describes the process of setting up an *ex vivo* VIA and its optimisation for application with HIV-CORE 002 vaccine trial samples.

4.2 Aims of Chapter 4:

1. To grow virus stocks for use in the *ex vivo* VIA, characterise infection kinetics and optimise multiplicity of infection (MOI).

2. Optimise cell isolation methods and examine effector to target ratios.

3. Establish background inhibition levels for this assay by examining a group of healthy controls.

4. Assess if the assay can detect inhibition in HIV^+ individuals.

5. Determine if the $CD8^+$ T cells induced by vaccination with the HIVconsv immunogen are capable of recognising virally infected target cells and controlling viral replication using a clade B HIV-1 isolate Bal.

4.3 Growth of HIV-1 clade A, B and C virus stocks

The majority of HIV-1 heterosexual transmissions occur as a result of infection with a single virion [97], and the primary targets for infection are memory $CD4^+$ T cells expressing the CCR5 co-receptor [98]. Over time, viral tropism broadens to include the use of the CXCR4 co-receptor [353], which is also associated with a more cytopathic phenotype [77]. Despite HIV-1 preferring the use of CCR5 for establishing heterosexual infection [97], there is evidence to suggest that if this co-receptor is not available, for example in CCR5 Δ32 homozygotes, parenteral infection can be initiated by CXCR4 tropic isolates [354, 355].

Therefore, the viral isolates that were selected for assessment within the *ex vivo* VIA were either CCR5 tropic or CXCR4 tropic and from viral clades A, B and C, as the HIVconsv immunogen encoded consensus sequences from HIV-1 clades A, B, C and D [270]. Two primary isolates of Ugandan (92UG029) and Spanish (HIV-1 ES x-1936) origin and one laboratory adapted strain (HIV-1 Bal) were chosen as model HIV strains. The clade A, 92UG029, isolate had been characterised to use predominantly the CXCR4 co-receptor for T cell entry, whereas the clade C HIV-1 ES x-1936 and clade B Bal, isolates were both reported to use the CCR5 co-receptor [356]. The primary isolates are representative of the circulating viruses contributing to the global epidemic. However, the Bal isolate first characterised in 1986 [357], has undergone many rounds of passage within the confines of the laboratory, which may have resulted in its adaptation to this environment as has been shown for CXCR4 tropic viruses [358]. Consequently, the HIV-1 Bal isolate is considered to be less genetically representative of circulating HIV-1 strains. However, as several research groups [301, 304] have used Bal to examine virus inhibition its application does provide a means of comparison with our results.

To establish the percentage of infection for each viral isolate, flow cytometry was performed to determine the number of $CD4^+$ T cells that were positive for the intracellular

p24 capsid protein of HIV-1. The gating strategy used to calculate percentage inhibition by flow cytometry is shown in Figure 20. Each sample was sequentially gated from lymphocytes, to $CD4^+$ T cells represented by the $CD3^+/CD8^-$ population. Virally infected targets were gated as $CD4^+$ T cells which were also $p24^+$ positive. A quadrant was applied as the final gate, as shown in Figure 20, and the percentage of infected cells was calculated using the following formula: (Infected $CD4^+$ T cells (B+D) / Total $CD4^+$ T cells (A+B+D)) x 100.

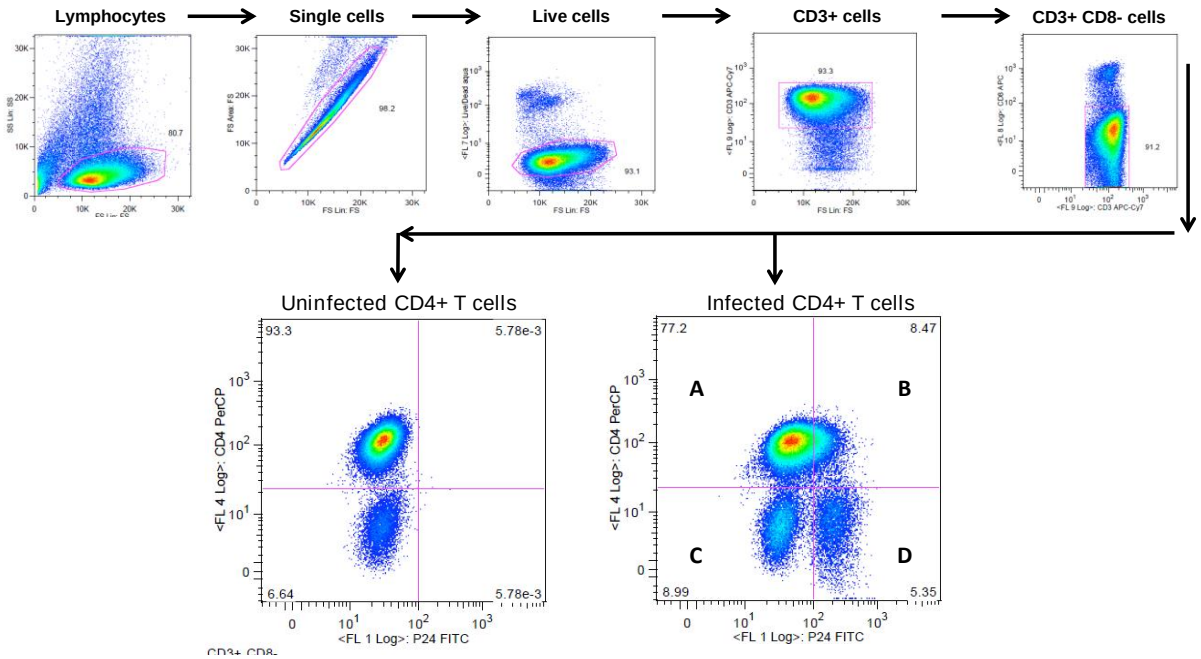


Figure 20 ***Ex vivo*** **VIA gating strategy for the p24 intracellular staining protocol.** HIV-1 infected and uninfected cell culture wells were harvested daily. Cells were stained with Aqua live/dead, $CD3^+$-APC-Cy7, $CD8^+$-APC, $CD4^+$-PerCP and p24-FITC in FACS buffer. Cells were fixed for 2 minutes in 4% Paraformaldehyde with 20 µg/ml lysolecithin and run on a CyAN ADP flow cytometer on the same day. Data was analysed using FlowJo and all calculations were performed in Excel.

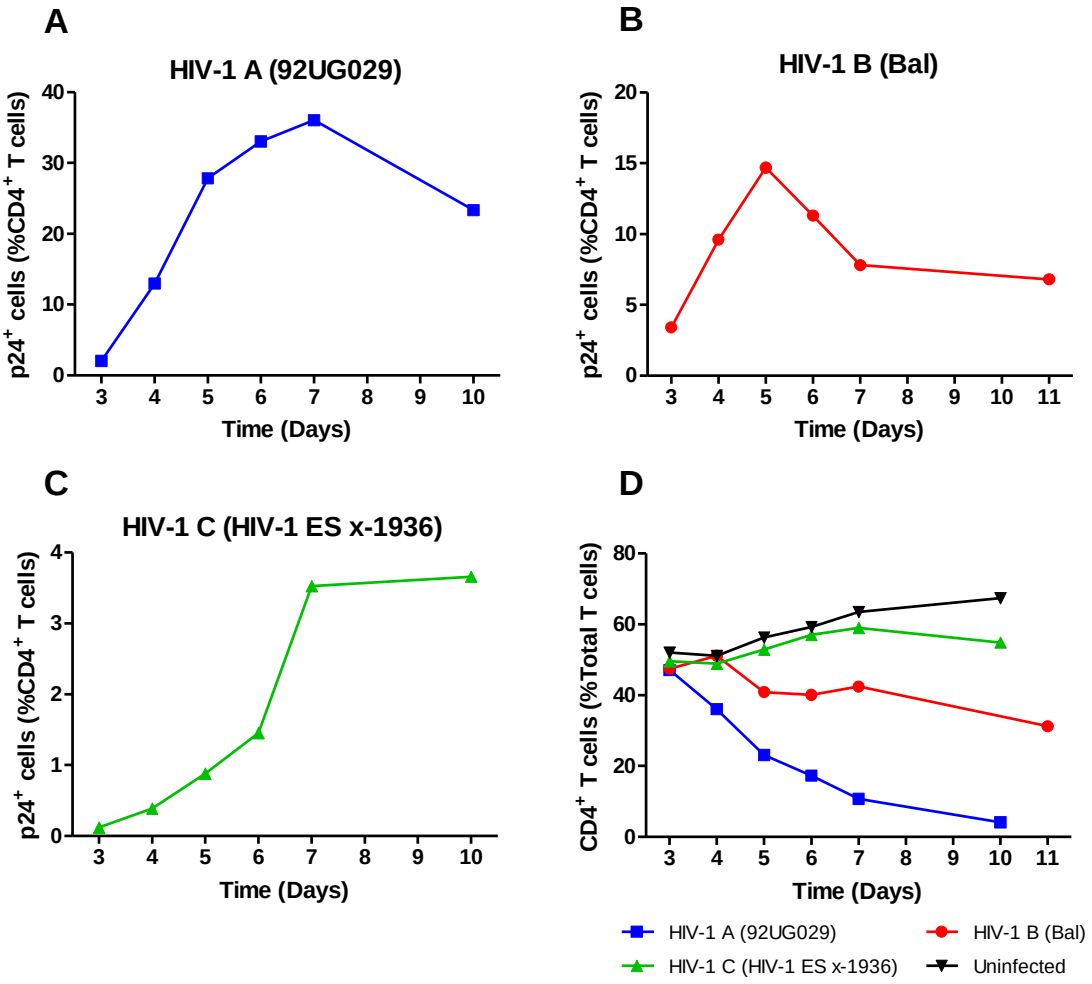


Figure 21 Growth kinetics of HIV-1 virus stocks and CD4$^+$ T cell counts. The daily percentage of infected PBMC was plotted from day 3 to day10 or 11 for HIV-1 viral stock clades A, B and C (A, B and C). The three viral isolates were propagated using PHA activated PBMC from 3 healthy volunteers. Percentage infection was determined using flow cytometry to measure T cells expressing the intracellular HIV-1 capsid protein p24. The CD4$^+$ T cell count from the total T cell count was calculated for each virus at each time point from the growth kinetics experiments (D). Uninfected PBMCs were used as a negative control.

Figure 21 shows the daily expansion levels for clades A, B and C, with each virus stock showing a different pattern of infection kinetics. Infection levels for the clade A virus increased from day 3, peaked at day 7 and then declined up to day 10, whereas the clade B isolate showed an earlier peak at day 5 and gradually declined until day 11. The clade C isolate reached peak titre on day 7 and declined steadily until day 10. The calculated decrease

of $CD4^+$ T cells as infection with each virus stock progresses is shown in Figure 21D. Although initial viral titres were unknown, the same volume of all stock viruses was added to PBMC cultures. The CXCR4- tropic clade A virus infection appeared to result in a more rapid decline in $CD4^+$ T cell survival from 47% on day 3 to 4% on day 10 compared with the clade B and C viruses which maintained $CD4^+$ T cell levels of 31% on day 11 and 55% on day 10 respectively.

4.4 Determining the titre of HIV-1 stocks

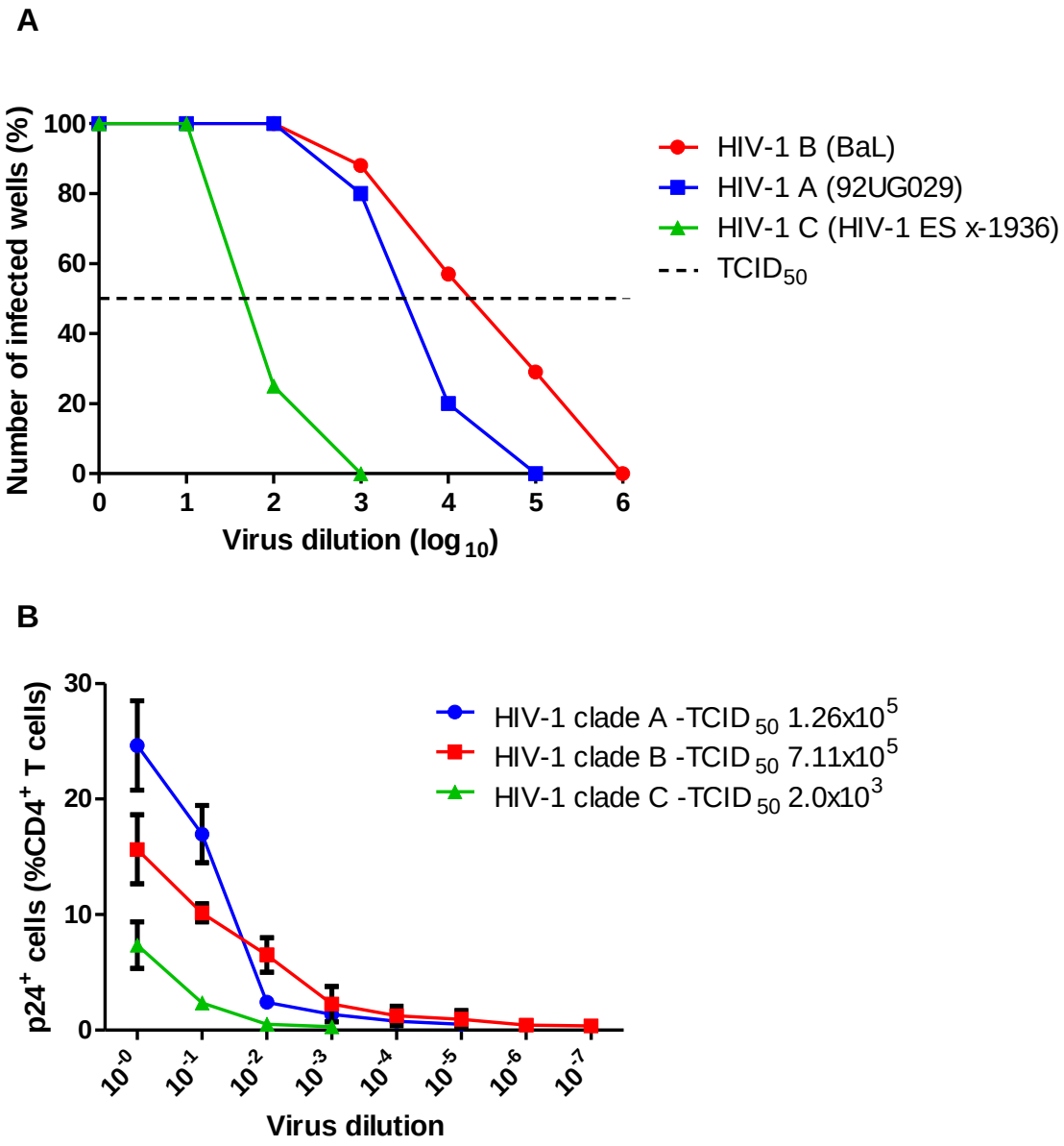


Figure 22 Calculation of $TCID_{50}$ and percentage infection for HIV-1 clade A (92UG029), B (Bal) and C (HIV-1 ES x-1936) viral stocks. Viral stocks were titred on PBMC from the same individual and percentage of infection for each well was determined by flow cytometry analysis of p24 antigen levels on day 5 for HIV-1 clade B, day 4 for HIV-1 clade A and day 7 for HIV-1 clade C. (A) The number of infected wells were calculated and the TCID50 indicated by the dashed line was determined for each virus following the Reed and Muench calculation [359]. (B) The percentage of infection per well was calculated for each virus at each dilution and the results are shown as mean, with error bars representing the standard deviation (SD).

Titration of the three virus stocks, shown in Figure 22, was performed in order to determine the amount of virus to use to infect volunteers' $CD4^+$ T cells, that would result in approximately the same level of viral infection between the clades with an optimum of 10 to 30% on the peak day of infection [301]. Tissue culture infectious dose that results in 50% of infected cultures ($TCID_{50}$) was used to determine the titre of the viral stocks. When the 50% endpoint fell between two viral dilutions, the Reed and Muench calculation [359] was used to more accurately calculate the titre. Figure 22A shows that the clade B stock was of the highest titre followed by clade A and finally clade C with $TCID_{50}$ values of 7.11×10^5, 1.26×10^5 and 2.00×10^3 respectively. The $TCID_{50}$ value was subsequently used to determine the multiplicity of infection (MOI) or number of infectious particles per cell that are added to achieve a desired level of infection. A MOI that falls between 0.1 and 0.001, is commonly used for VIAs [298, 301, 304], and so based on both published values and the percentage infection data for these stock viruses (Figure 22B), clades A and B were assessed at MOI 0.01 whilst the clade C isolate was assessed at MOI 0.001 and 0.0001 in $CD4^+$ T cells from healthy donors.

Figure 23A shows the percentage infection over time in three healthy donors whose $CD4^+$ T cells had been isolated and activated with PHA for 72 hours before being infected at the specified MOI for each HIV-1 isolate. Concurrently, the cell viability during the cell culture period was monitored using an Aqua live/dead fluorescent stain (Figure 22B). The percentage infection data (Figure 23A) showed that the clade A isolate used at MOI 0.01 established 30.7% infection in activated $CD4^+$ T cells on day 3. However, the cell viability in this culture (Figure 23B) was 3.75 fold lower than the uninfected and clade B and C infected cultures on day 3. The very low viability of the cells at the start of the culture prohibited further analysis at any subsequent time points and indicated that a MOI 0.01 was too high for use with the clade A isolate.

In contrast, the clade B isolate used at the same MOI (0.01) resulted in 14.0% infection on day 3, which gradually declined to 3.8% on day 7. The cell viability was also higher compared to the clade A isolate with comparable numbers (56,000) of live cells present in the infected cultures as for the uninfected cultures (60,000) on day 3 and this viability was maintained over the 7 day culture period. The clade C isolate showed the most suitable infection kinetics and cell viability at MOI 0.0001 with 20.9% peak infection detectable on day 4 with equivalent cell viability to the uninfected culture on day 3 and cell viability was also maintained throughout the 7 days of evaluation.

Overall this data demonstrated that the clade A isolate was very cytopathic in comparison with the clade B isolate used at the same MOI and that in order to obtain a similar level of infection between different viral isolates the MOI may need to be adjusted. This variation may also increase when different donors are considered.

The clade A isolate was therefore not continued with for the remaining *ex vivo* VIA optimisation experiments, but could in future be titrated further to find an optimal MOI for its use. Although the clade C isolate showed suitable infection kinetics and cell viability, a large volume of virus was required due to its low titre. Thus, the clade B isolate was initially taken forward for further optimisation within this assay. A good level of infection (14%) was observed on day 3, but the data suggested that the peak timepoint had been missed as a gradual decline was observed from day 3 to 7. Therefore, a further MOI titration experiment was performed in healthy donors (Figure 24).

4.5 HIV-1 infection kinetics and cell viability in CD4$^+$ T cells

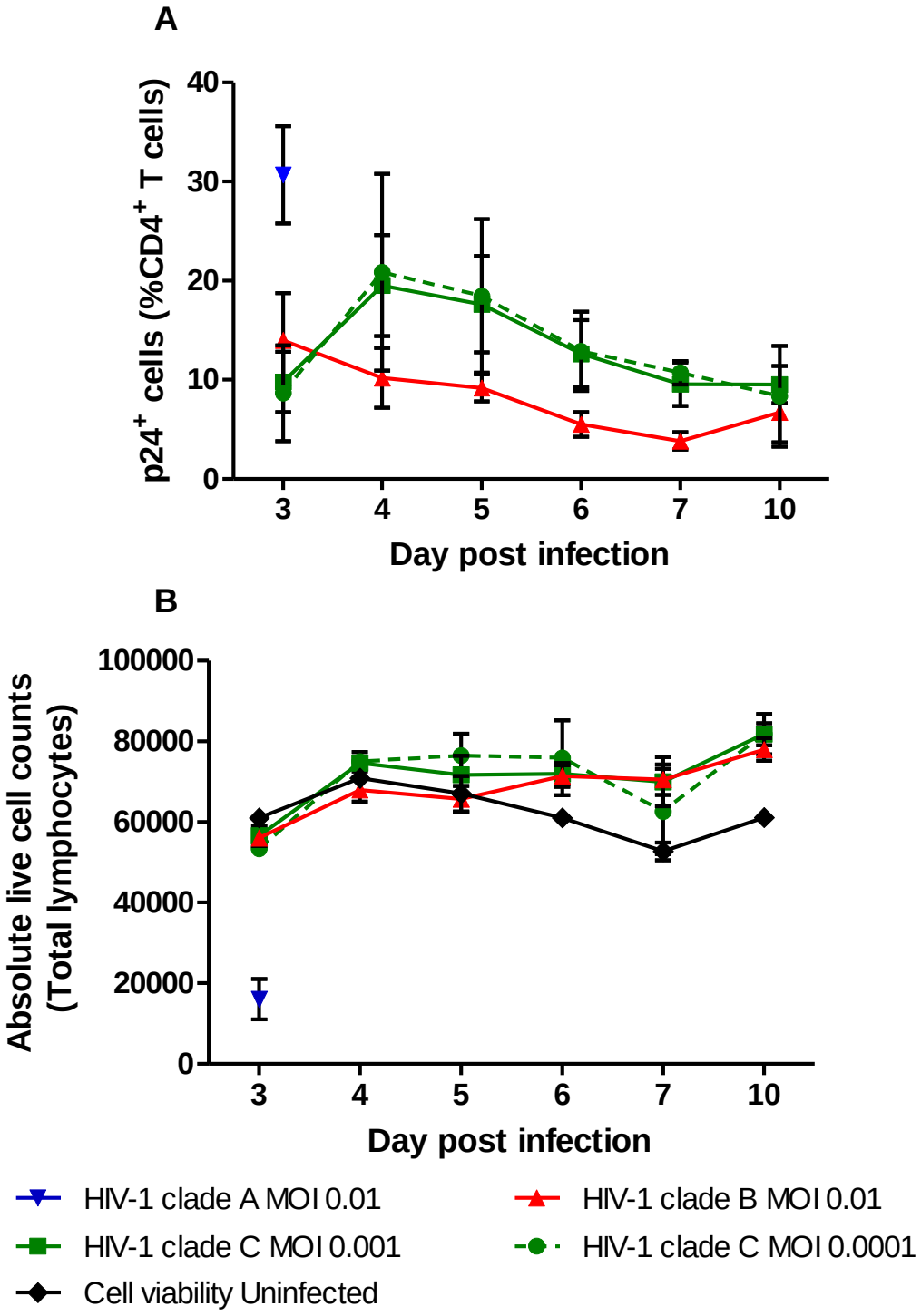


Figure 23 HIV-1 infection kinetics and effect on CD4$^+$ T cell viability. CD4$^+$ T cells from three healthy donors were separated and activated using PHA for 72 hours. The activated cells were infected with each virus stock at the specified MOI. The percentage of infection and cell viability was determined from day 3 to day 10 by flow cytometry. Data are presented as mean ± SD.

4.6 The optimal MOI for HIV-1 Bal isolate is 0.005

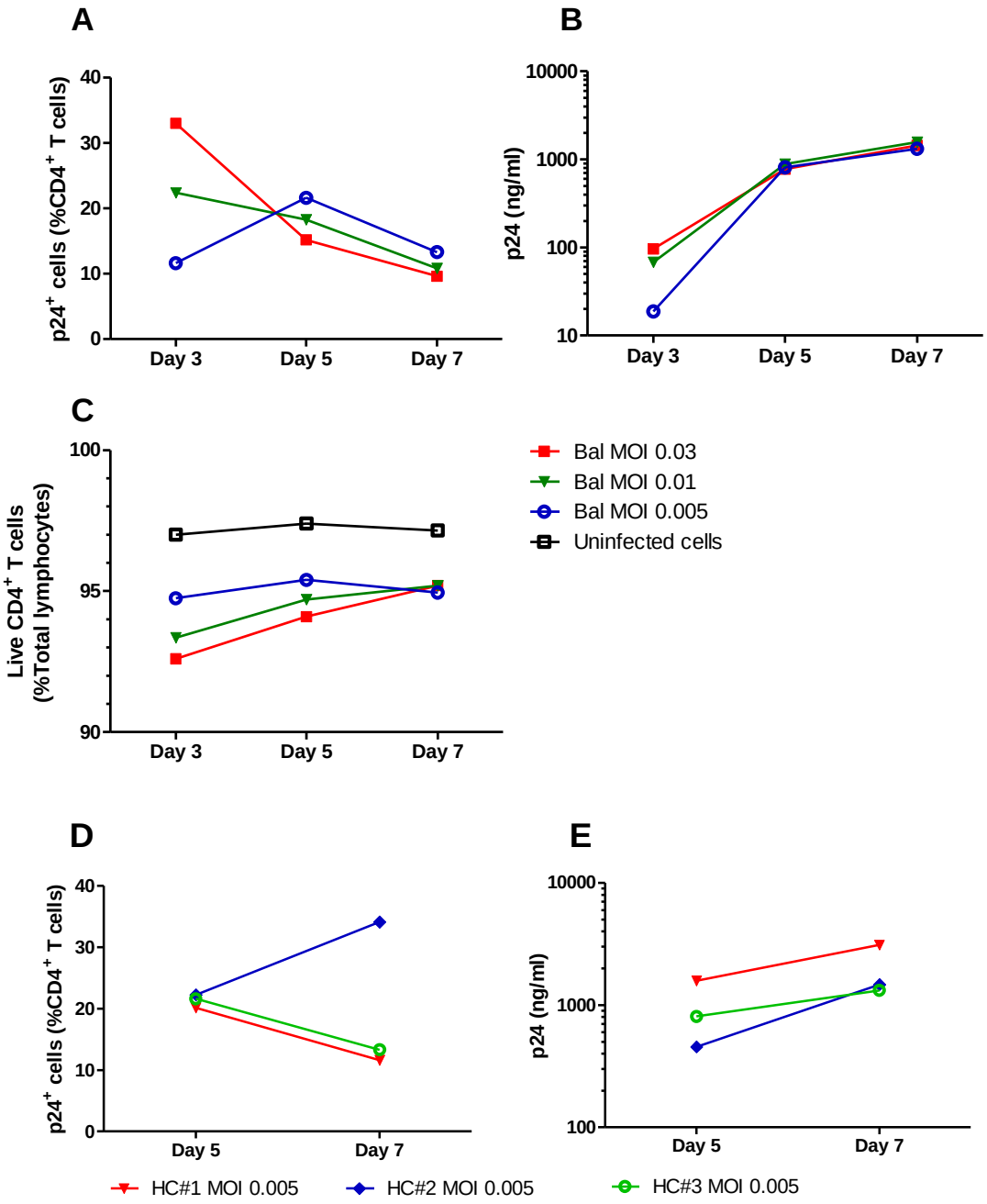


Figure 24 Optimising the MOI for HIV-1 Bal in healthy donors. $CD4^+$ T cells from a healthy donor (HC#1) were isolated and activated using PHA for 72 hours. The HIV-1 Bal isolate was used for infection at a range of MOIs. The percentage of infection was determined on days 3, 5 and 7 by flow cytometry (A) and p24 ELISA (B). Uninfected cells were run as a negative control and subtracted from infection values. Cell viability was also assessed for infected and uninfected cultures using a fixable live dead stain (C). To confirm infection levels two additional healthy controls (HC#2 and HC#3) were tested at MOI 0.005 on days 5 and 7 by flow cytometry (D) and p24 ELISA (E).

To establish the optimal MOI that resulted in approximately 20% infection at the peak timepoint and maintained cell viability levels, several MOIs (0.03, 0.01 and 0.005) were assessed. Activated $CD4^+$ T cells from a healthy donor were infected with HIV-1 Bal at the specified MOIs. Figure 24A showed that MOI 0.005 gave a peak of 21.6% infection on day 5, whereas MOI 0.01 and 0.03 established infection levels of 18.3% and 15.2%, respectively on day 5. The higher MOIs showed a different kinetics pattern with the peak of infection occurring on day 3 and a gradual decline in infection shown up to day 7. Figure 24B demonstrates that the infection level was greater for MOIs 0.03 and 0.01 as 98.4 ng/ml and 68.3 ng/ml of p24 were detected on day 3, compared to 18.8 ng/ml at a MOI 0.005. However, by day 5 all three MOIs showed an average of 824.5 ng/ml p24 which was within the range described to be suitable for detecting differential $CD8^+$ T cell control of HIV-1 infection. The highest cell viability for cultures infected with MOI 0.005 was also observed for days 3 and 5 with 94.8% and 95.4% of $CD4^+$ T cells alive, respectively.

In order to confirm the infection level at MOI 0.005, two additional healthy controls were tested. Figure 24D and E showed that on day 5 the average percentage of infection was 21.3% and the concentration of p24 was 949.3 ng/ml. As a result of these data the MOI 0.005 was selected for use in all further VIA optimisation assays with the HIV-1 Bal isolate.

4.7 Comparable cell purity by negative and positive selection of $CD8^+$ T-cell effectors

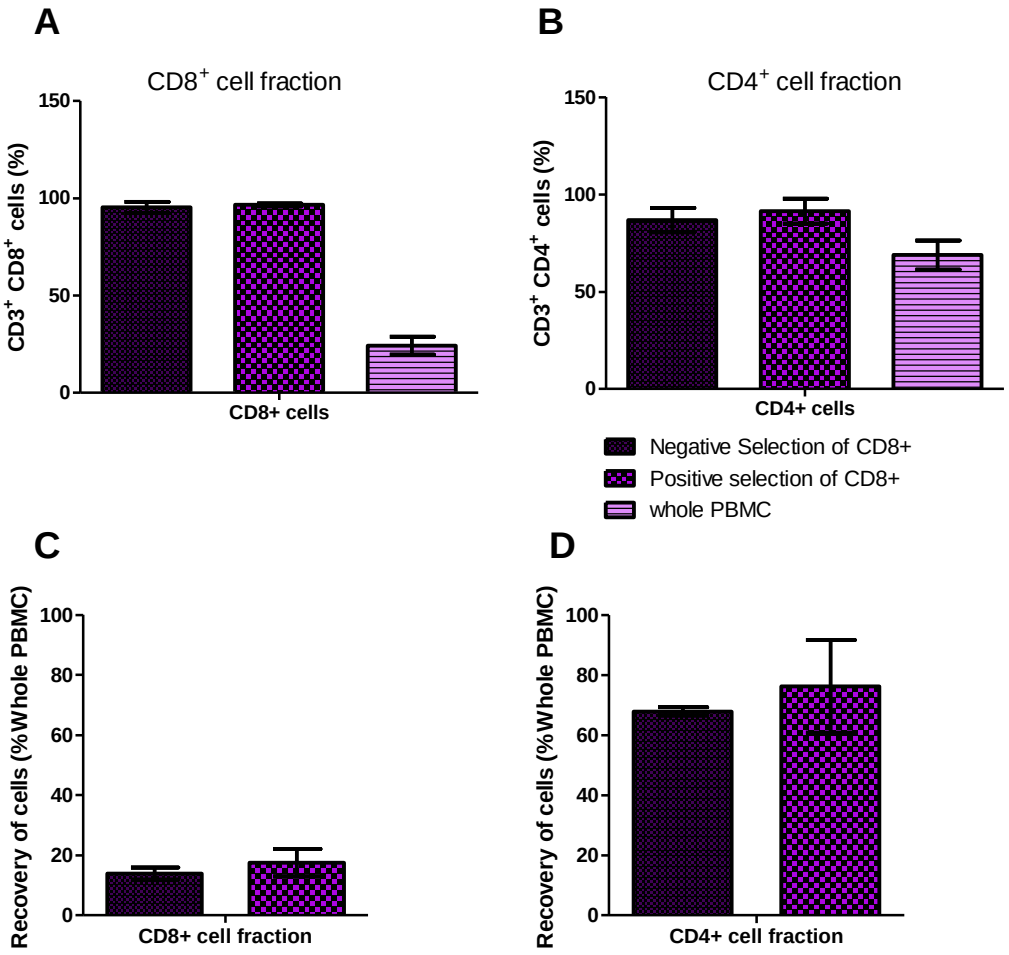


Figure 25 Purity and recovery of $CD8^+$ and $CD4^+$ T cells isolated by negative and positive selection methods. PBMC from three volunteers were separated into $CD8^+$ and $CD4^+$ cell fractions by both positive selection of $CD8^+$ cells and negative selection of $CD8^+$ cells. The resulting cell fractions were counted with a Sceptre Cell Counter to determine percentage recovery (C and D). The cell fractions were also stained with cell surface antibodies for CD3, CD4 and CD8 molecules and run on a flow cytometer on the same day. A sample of unfractionated PBMC was also stained as a control for each of the three volunteers (A and B). The graphs represent the mean ± SD for the three volunteers.

4.8 Negatively selected CD8$^+$ T cells show reduced non-specific virus inhibition

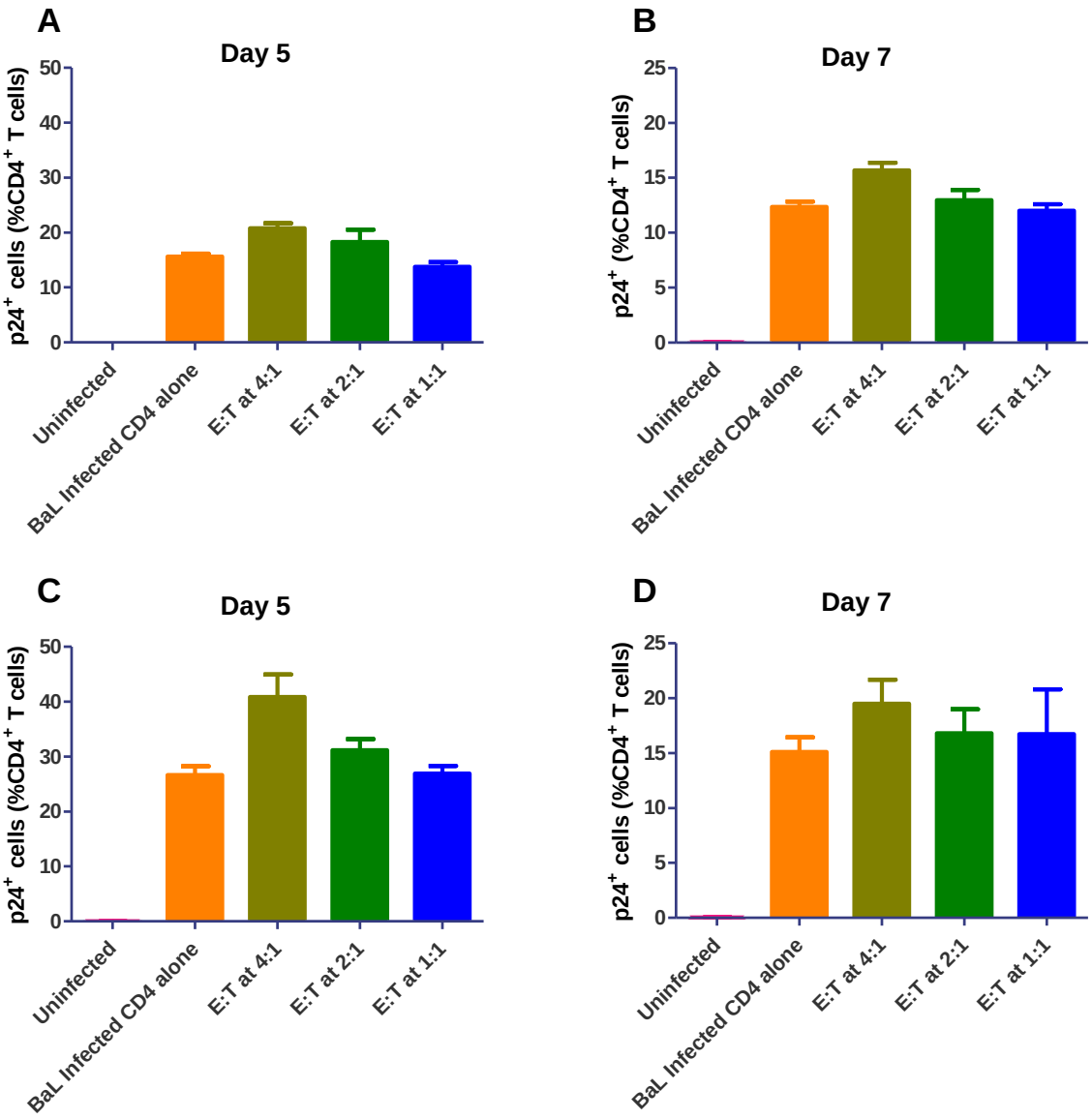


Figure 26 Background HIV-1 Bal inhibition in a healthy donor at three effector to target (E:T) ratios. Healthy control PBMC were separated using MACS beads and the CD4$^+$ cell fraction was stimulated with PHA for 72 hours. CD8$^+$ effectors isolated by positive (A and B) or negative (C and D) MACS bead selection were then cultured at E:T ratios of 4:1, 2:1 or 1:1 and suppression levels were determined by intracellular p24 staining on days 5 and 7 post infection. Controls were infected CD4$^+$ cells alone and uninfected CD4$^+$ cells.

4.9 Establishing the level of non-specific *ex vivo* virus inhibition in healthy controls

The results from Figure 25 and 8 suggested that the optimal method for $CD8^+$ T cell isolation was negative selection with a bead depletion cocktail as this method provided comparable cell purity to positive selection but with reduced background inhibition in healthy controls. The data also showed that the optimal method for isolating $CD4^+$ T cell targets was negative selection with $CD8^+$ beads as this protocol showed both increased cell purity and percentage recovery. Figure 26 also showed that the effector to target cell ratios suitable for use were 4:1, 2:1 and 1:1, when negatively selected effector cells were implemented in the assay. These parameters were therefore used in the *ex vivo* VIA with a panel of PBMC from 11 HIV-1-negative healthy donors to enable the non-specific cut-off for HIV-1 Bal inhibition to be calculated.

The readouts selected for the assay were both flow cytometry of intracellular p24 on day 6 of culture and p24 ELISA of the cell culture supernatants on day 13. The flow cytometry time point was chosen based on the MOI titration data (Figure 24) which showed suitable infection levels between days 5 and 7. The ELISA was chosen to be run in addition to flow cytometry as it has been found to be of greater sensitivity when low levels (less than 1 log) of inhibition are being examined [301]. The ELISA measures the accumulation of viral p24 in the supernatant and therefore a longer culture time of between 7-14 days is typically measured using p24 ELISA readouts [301, 306, 360]. In contrast, intracellular staining of p24 capsid protein can be performed as early as 5 hours post infection [349]. However, the limitation for this early analysis is the number of target cells that are infected, thus a high MOI of 1 is used to ensure sufficient infection levels [349]. This can be partially circumvented when using lower MOIs by waiting until days 3 to 7 to ensure that a significant population of target cells will be infected and subsequent viral suppression can be detected (Figure 24). In order to calculate the percentage inhibition mediated by $CD8^+$ T cells the

following formula was used: ((% infection of target cells alone – % infection of co-culture well) / % infection of target cells alone) x 100.

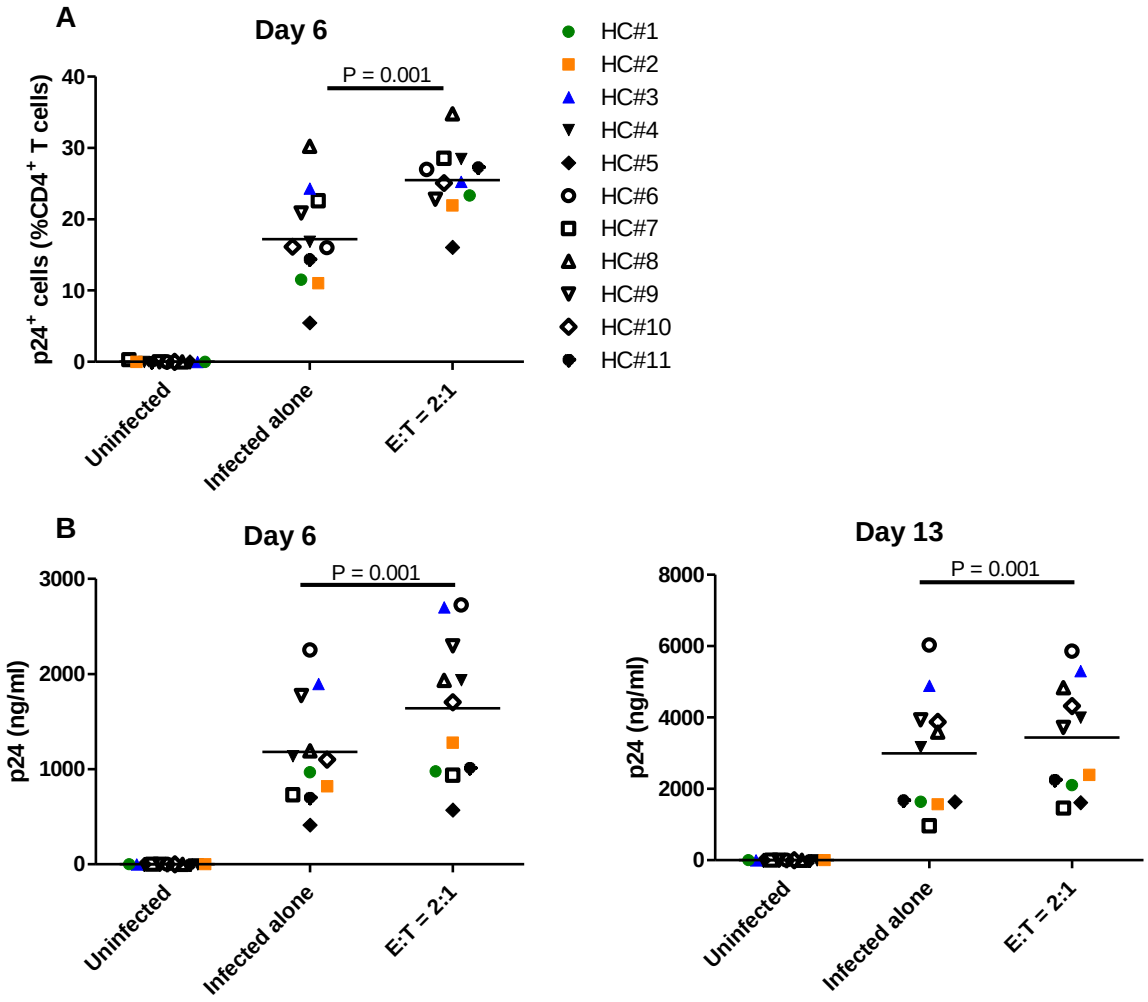


Figure 27 Establishing HIV-1-specific virus inhibition within healthy controls. The percentage of infected cells on day 6 was determined by flow cytometry of intracellular p24, for infected cells alone and at a 2:1 effector to target ratio (E:T), for 11 healthy controls (A). Supernatants from the VIA were stored on days 6 and 13 and a p24 ELISA was used to calculate the concentration of capsid protein for both the infected cells alone and co-culture wells (E:T 2:1) (B). The Wilcoxon matched-pairs signed rank test was performed with (two-tailed) P values <0.05 considered to be significant.

Table 4 Calculation of the e*x vivo* VIA HIV-1 specific cut-off on day 13 by p24 ELISA.

Healthy control	Virus inhibition (ng/ml)	Virus inhibition (log_{10})
HC#1	0.00	0.00
HC#2	0.00	0.00
HC#3	0.00	0.00
HC#4	0.00	0.00
HC#5	25.05	0.01
HC#6	164.83	0.01
HC#7	0.00	0.00
HC#8	0.00	0.00
HC#9	209.12	0.02
HC#10	0.00	0.00
HC#11	0.00	0.00
Mean	**36.27**	**0.00**
STD	**75.54**	**0.01**
Mean + 3xSTD	**262.88**	**0.02**

HC = Healthy control STD = Standard deviation.

The data from Figure 27 and Table 4 showed that healthy donors demonstrated minimal inhibition of HIV-1 Bal at an effector to target ratio of 2:1. Figure 27A & B showed that on day 6, when the percentage of infected cells and p24 ELISA results were considered, there was no detectable virus inhibition from these 11 controls. However, when the p24 ELISA was used for the day 13 supernatants (Figure 27B), three healthy controls (#5, 6 & 9) showed low levels of virus inhibition. Thus, the day 13 p24 ELISA results were used to establish a cut-off of HIV-1 specific inhibition of >262.88 ng/ml or >0.02 log_{10}. Of interest was the overall increase in HIV-1 replication when $CD8^+$ T cells from HIV-1 naïve individuals were present at a 2:1 E:T ratio within the co-culture wells, with this increase was significant at both time points tested and by both methods used for assessment.

4.10 Chronically infected HIV+ patients weakly control HIV-1 Bal when assessed in an *ex vivo* VIA

After establishing the levels of background inhibition in healthy controls the *ex vivo* VIA was used to examine the capacity of $CD8^+$ T cells from chronically infected HIV-1+ patients to control the HIV-1 Bal isolate. Two patients were available for examination; IC202 was on HAART therapy and IC154 was therapy naïve. Patient IC202 had been tested previously within an *ex vivo* VIA against a Bal isolate and had shown 68% suppression on day 6 at a 1:1 E:T ratio. Here the data from Figure 28A shows that inhibition was clearly detectable for patient IC202 on days 6 and 13 by p24 ELISA with 76.2% inhibition observed on day 6 and 65.1% on day 13 by negative selection of $CD8^+$ effectors at an E:T ratio of 2:1. In contrast, by flow cytometry there was no detectable inhibition by positively or negatively selected $CD8^+$ T cells on day 6 (Figure 28C).

In Figure 29, patient IC154 showed the same trend with 55% inhibition of the same Bal isolate (stock 1) on day 6 by p24 ELISA (Figure 29A) but no detectable inhibition by flow cytometry for this stock (Figure 29B). To ensure that the assay was not compromised by the stock chosen, a second Bal stock (stock 2), kindly donated by Dr H. Yang, was also tested for patient IC154. Figure 29C and D showed that Bal stock 2 gave comparable results to stock 1 by each detection method used. This confirmed that the p24 ELISA is a more sensitive method to detect virus inhibition than flow cytometry. Furthermore, the use of positive or negative selection for $CD8^+$ T cell isolation, as shown in Figure 28 and Figure 29, made no significant difference to the inhibition results for either of the patients tested.

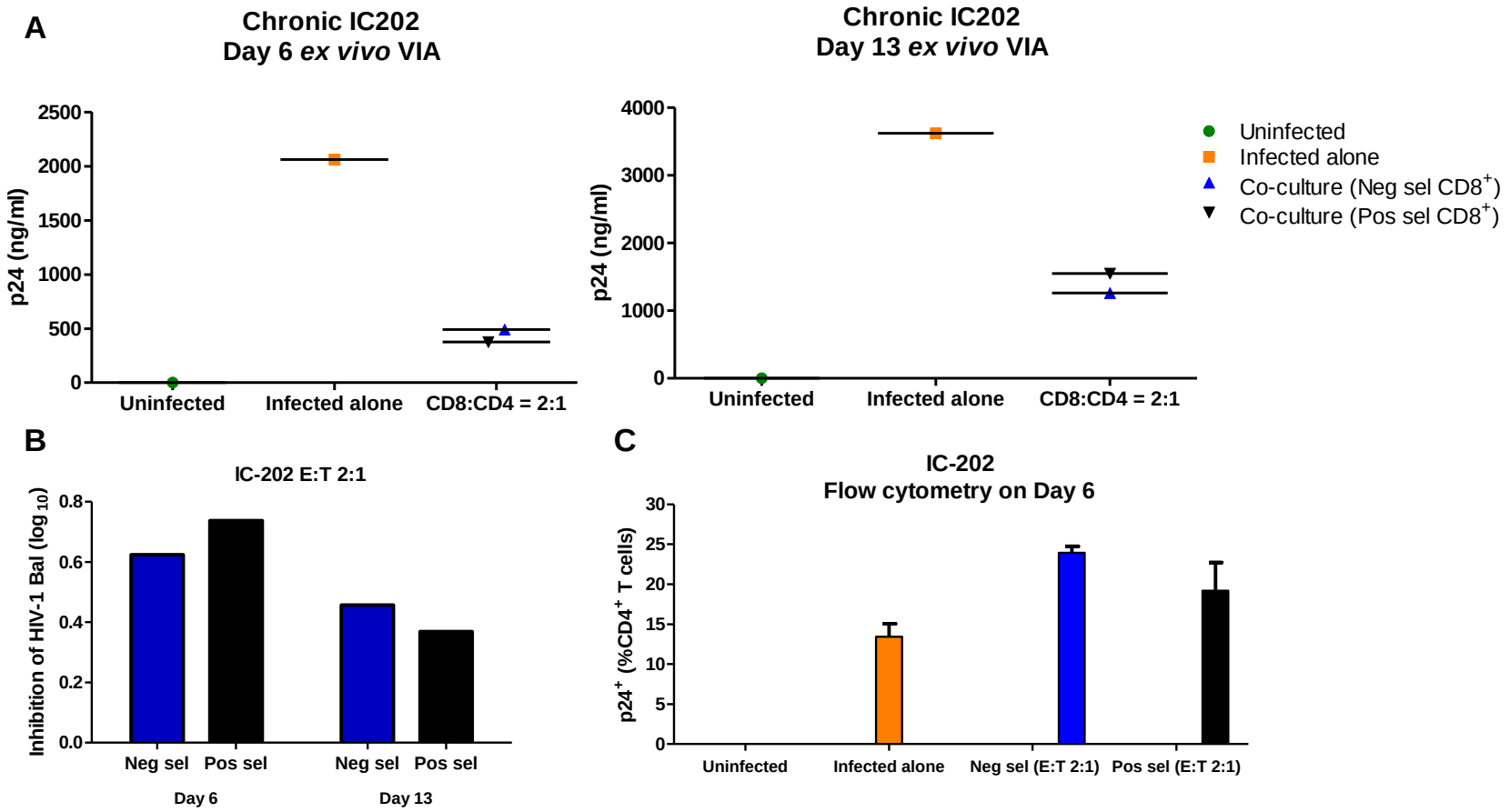


Figure 28 Evaluation of chronic HIV+ patient by *ex vivo* VIA. Chronic HIV+ patient - IC202, was assessed by *ex vivo* VIA for the ability to control HIV-1 Bal. The patient's $CD4^+$ T cells were isolated and activated with PHA for 72 hours before being infected with HIV-1 Bal at MOI 0.005 for 2 hours. On the same day the patient's $CD8^+$ T cells were isolated using either positive or negative selection beads. Infected cells were either plated alone or in co-culture at an E:T ratio of 2:1. Supernatants stored on days 6 and 13 were assayed by p24 ELISA (A and B) and percentage infection was determined by flow cytometry of intracellular p24 on day 6 (C).

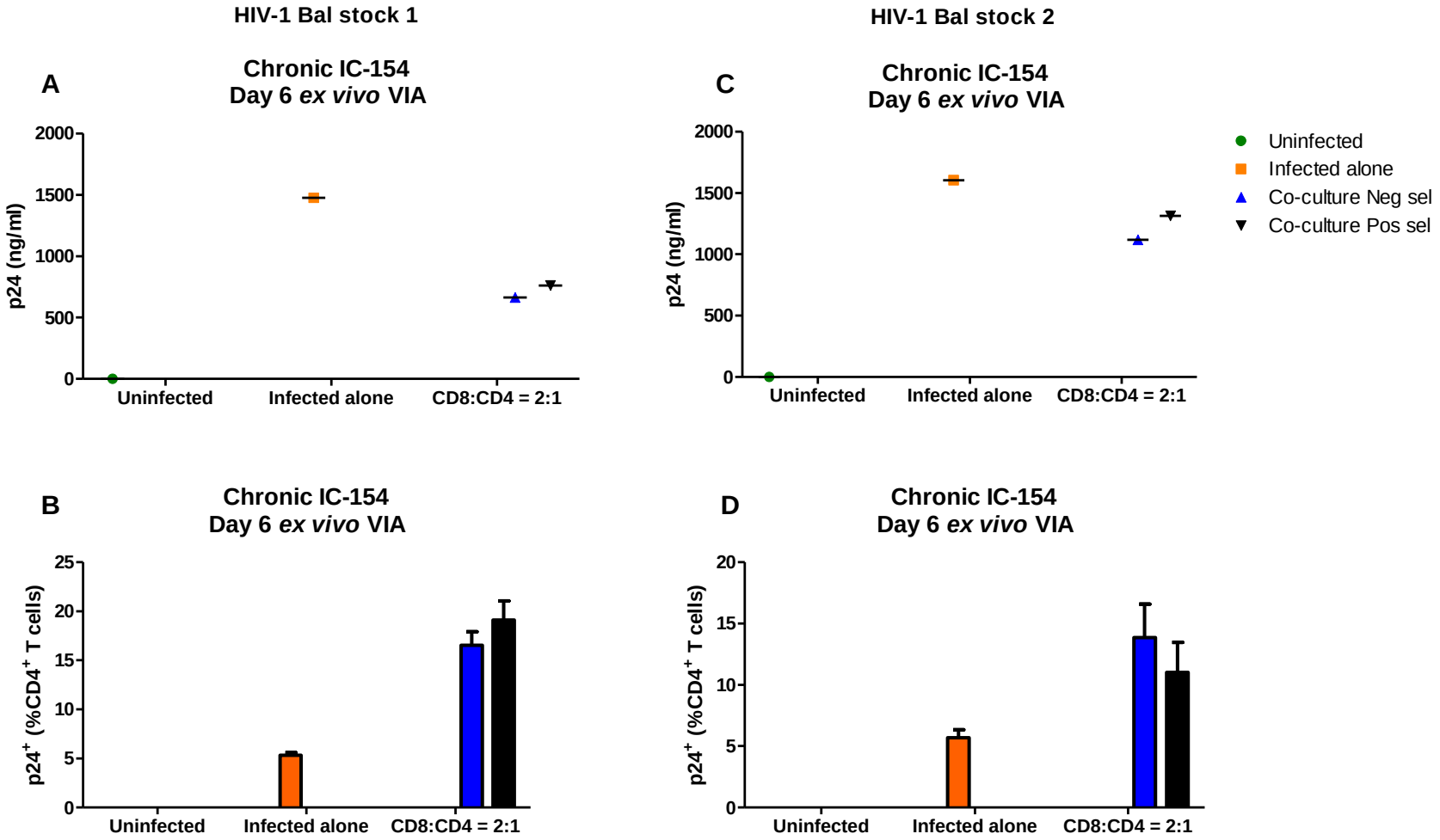


Figure 29 Comparison of HIV-1 Bal stocks in a chronic HIV-1+ patient. Chronic patient IC154 was assessed by *ex vivo* VIA against two HIV-1 Bal isolates. Virus inhibition of Bal stock 1 was assessed by both p24 ELISA (A) and flow cytometry (B) on day 6 post infection. Inhibition of the HIV-1 Bal stock 2 provided by Dr H. Yang, was also assessed in this patient by p24 ELISA (C) and flow cytometry (D) on day 6 post infection.

4.11 Vaccinees show low to undetectable levels of HIV-1 Bal virus control when assessed by an *ex vivo* VIA

Control of HIV-1 Bal viral replication was shown to be limited, but present in chronically infected individuals and was more sensitively detected by p24 ELISA. Therefore, several vaccinees were selected from the CM (404) and DDDCM (418 and 421) vaccine arms to be tested in this assay using both p24 ELISA and flow cytometry readouts. The vaccinees selected showed a range of *ex vivo* IFN-γ ELISpot responses with a sum of 3725, 2260 and 900 SFU/10^6 PBMC respectively at 9, 21 and 22 weeks. In addition, we were kindly provided with two elite controller PBMC samples (8137 and 8267) from Prof. G Shaw. These samples had not been tested against the HIVconsv peptides and so it was unknown as to whether the HIVconsv immunogen sequence was recognised by these elite controllers.

The data shown in Figure 30A and C from the *ex vivo* VIA demonstrated that elite controllers, 8137 and 8267, showed medium to low levels of HIV-1 Bal control on day 6 with levels of 71.7 and 38.0% inhibition detected respectively by flow cytometry, and a 0.560 and 0.525 $\log_{10}$ reduction in p24 respectively detected by ELISA. This inhibitory capacity lowered by day 13 (Figure 30D) with only 0.350 and 0.387 $\log_{10}$ reductions in p24 detected by ELISA for elite controllers 8137 and 8267 respectively.

For the three vaccinees which were examined, only vaccinee 421 was consistently detected by both flow cytometry and p24 ELISA to make a detectable but very low level inhibitory response toward HIV-1 Bal, with a level of 14.4% inhibition observed by flow cytometry and 0.226 $\log_{10}$ inhibition detected by p24 ELISA on day 6.

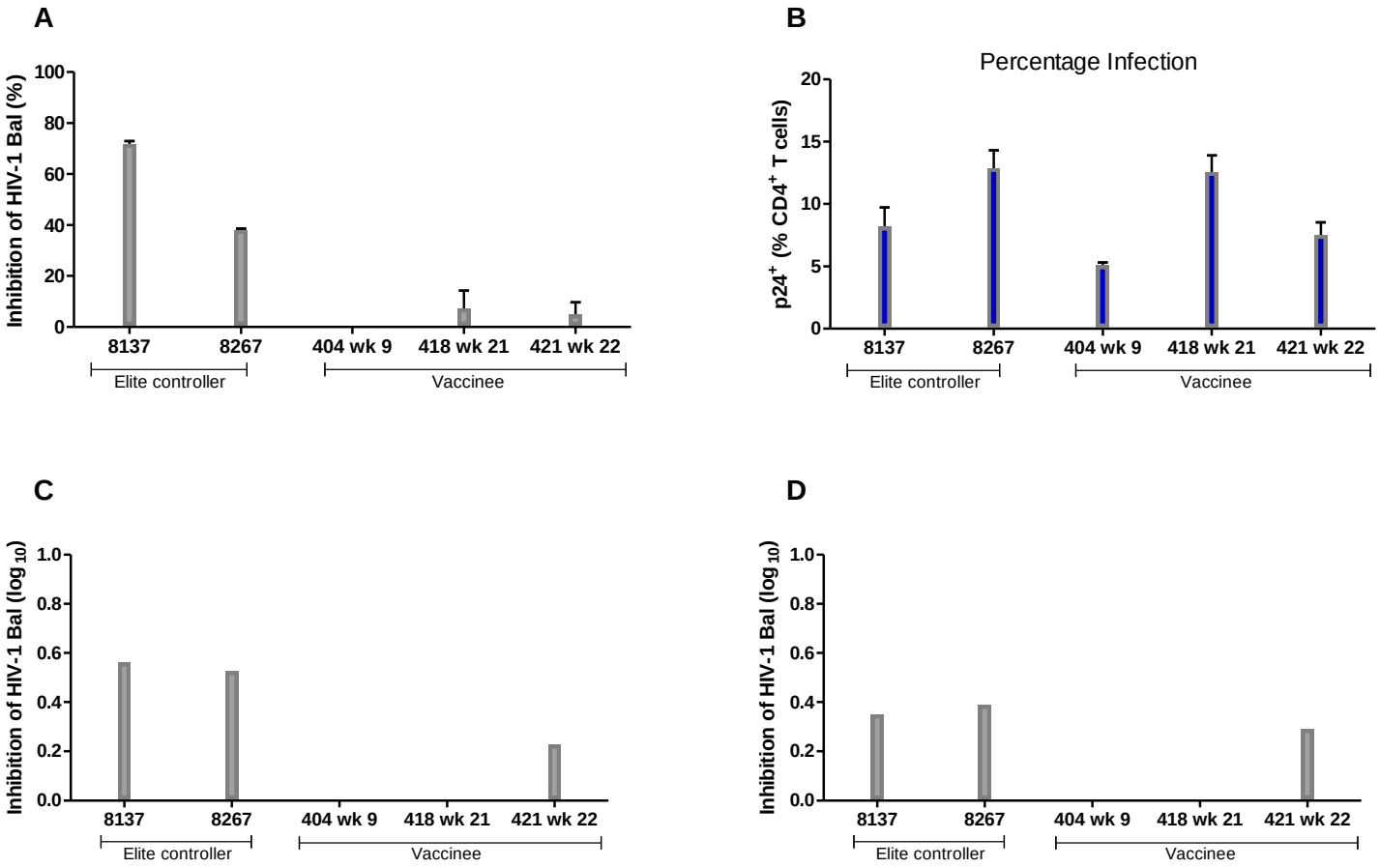


Figure 30 Determining the inhibitory capacity of elite controllers and HIV-CORE 002 vaccinees by an *ex vivo* VIA. Two elite controllers and three vaccinees (404 week 9, 418 week 21 and 421 week 22) were selected for assessment in the *ex vivo* VIA. $CD4^+$ T cells were isolated and activated with PHA for 72 hours and subsequently infected at MOI 0.005 with HIV-1 Bal. Infected $CD4^+$ T cells were cultured alone or together with freshly isolated $CD8^+$ T cells at a 2:1 E:T ratio. Flow cytometry was used to examine percentage inhibition (A) and percentage infection (B) on day 6 and supernatants were stored on days 6 (C) and 13 (D) and tested by p24 ELISA.

4.12 Chapter 4 Discussion

The aim of this chapter was to optimise and establish an *ex vivo* VIA, which could be used to evaluate the HIV-CORE 002 vaccine trial samples for their ability to control HIV-1 infection. Several groups have already described the use of an *ex vivo* VIA to assess HIV+ patient's $CD8^+$ T cell suppressive capacity during various stages of infection [304, 305]. Data from these studies have shown that long term non progressors have an enhanced ability to control virus replication [305] and that in early HIV-1 infection the suppressive capacity of $CD8^+$ T cells was predictive of $CD4^+$ T cell decline [304].

Prior to this work, the HIVconsv vaccine had been assessed by IFN-γ ELISpot assay, to determine frequencies of HIV-1-specific T cells and through proliferation and intracellular cytokine staining assays to determine the functionality and ability to expand in response to HIV-1 peptide stimulation. However, the ability to recognise and respond to naturally presented antigen in the form of HIV-1 infected $CD4^+$ T cells was an important factor for progression of the prophylactic HIVconsv vaccine to further phase III studies, by providing an indication as to whether the $CD8^+$ T cells induced by vaccination could control HIV-1 in the event of infection.

One of the first observations made when working with primary human $CD4^+$ T cells and the three propagated virus stocks was that each isolate varied in both growth kinetics and cytopathic effects. These are important considerations when trying to standardise the assay, as the infection levels must be high enough for inhibition to be evaluated using the chosen method of detection and furthermore the infected $CD4^+$ T cells are required to survive over a 7 day culture period. This data suggested that the clade B and C isolates

may be more suitable for use with this assay than the clade A isolate due to their slower rate of infection and increased cell viability throughout the duration of the assay.

The data also demonstrated that even when the same MOI was used to try and achieve the same percentage of infection between viral clades, comparable levels of infection and cell viability were not obtained. Instead, this highlighted the inherent differences between each of the HIV-1 isolates selected for use. Studies in multiple cohorts have shown that certain viral clades result in a more rapid onset of AIDS, such as infection with clade D viruses in Rakai, Uganda [361], due to the increased depletion of $CD4^+$ T cells [362]. Similarly, within the CASCADE European cohort, significant differences in $CD4^+$ T cell counts were found, with subtype B infections showing the highest rate of $CD4^+$ T cell decline when compared with subtypes A and CRF02 [363].

However, variation in $CD4^+$ T cell counts observed between HIV-1 clades may also be related to the virus co-receptor usage, which was not examined within these cohorts but has been shown to alter the cytopathic effect of HIV-1 [77]. As previously described, the clade A isolate used in these optimisation experiments was CXCR4 tropic and therefore is predicted to have greater cytopathic effect on the target cell population compared with CCR5 tropic isolates. This difference in co-receptor tropism could therefore have accounted for the improved cell viability observed with the CCR5 tropic clade B and C isolates used in these experiments. In HIV-1 infection there is also evidence to show that the greatest cell death is observed not in the infected cell population but in uninfected bystander $CD4^+$ T cells [364], mediated largely by the Env glycoprotein [365] but which is also impacted by the milieu of cytokines induced following infection [366, 367]. Therefore, there may also be differences in the bystander killing induced by different viral clades and by different co-receptor usage which was not directly investigated here.

To achieve the same level of infection between individuals, some laboratories use multiple MOIs [301]. However, this requires additional cells to set up the assay and can therefore become prohibitive due to the limited availability of material from trial samples. Titration of the HIV-1 Bal isolate showed that MOI 0.005 would be suitable for achieving good infection levels of ~20% in multiple individuals saving on the requirement for additional culture wells and enabling additional replicates to be tested for each E:T ratio and additional time points to be set-up.

Cell recovery using different isolation methods was also a consideration as limited numbers of PBMC vials were stored for each vaccinee at each respective time point. Both negative and positive selection of $CD8^+$ T cells yielded >90% recovery and were therefore suitable for use. However, a lower non-specific background level of inhibition was achieved when negative selection was implemented and as a result improved the detection limit for HIV-1-specific virus inhibition.

Despite the ability to detect low levels of virus inhibition with the optimised *ex vivo* VIA assay, only elite controllers and chronic HIV+ patients showed inhibitory responses which were detected most consistently by p24 ELISA rather than through flow cytometry. A comparison conducted by Saez-Cirion et al. (2010) [301] of virus inhibition, assessed both flow cytometry and p24 ELISA methods and highlighted that the p24 ELISA was a more sensitive method for the detection of virus inhibition [301]. Thus, these results suggested that for examination of vaccine samples, the p24 ELISA may be the most suitable method, for detection of low levels of virus inhibition.

Assessment of 3 vaccinees from the HIV-CORE 002 trial demonstrated that *ex vivo* virus inhibition could not be detected for all individuals. For vaccinee 421, who showed

control of virus replication by both detection methods, the level of suppression was very low; <15% by flow cytometry and <0.250 $\log_{10}$ reduction by p24 ELISA. One possible explanation for the low level of HIV-1 Bal inhibition detected for these samples could be that vaccinated healthy individuals have a lower number of circulating HIV-1-specific $CD8^+$ T cells compared with HIV+ patients [368], who are constantly exposed to virus. Evidence in support of this also comes from a recent study conducted in rhesus macaques where increased levels of *ex vivo* virus suppression were found for animals that could spontaneously control a SIV_{MAC251} challenge; analogous to human elite controllers, compared with SIV_{SME543} vaccinated animals [306]. High levels (>2 $\log_{10}$ inhibition) were detected within 'SIV controller' animals, but a mean of 0.6 $\log_{10}$ was the maximum detected for any of the vaccinated animal groups [306]. As a result of this work and observations with animal models, increasing the $CD8^+$ to $CD4^+$ T cell ratio to greater than 2:1 for vaccinees may have been appropriate, as this would have increased the HIV-1-specific $CD8^+$ T-cell frequencies present and subsequently the potential to observe an inhibitory effect.

Another influential factor was the HIV-1 Bal virus chosen for evaluation. This isolate was suppressed to an average of 55% by the two elite controllers, suggesting that this was a challenging virus that was able to evade even strong cellular immune pressure and hence may not have been able to be well controlled in the setting of vaccination. Further work with this assay implementing other HIV-1 isolates would give a greater indication of the capacity for HIVconsv vaccine-elicited T cells to suppress HIV-1.

Taken together the results from Chapter 4 suggested that an *ex vivo* VIA may not be the most suitable method for analysing the total sample set from the HIV-CORE 002 trial, and that further modification such as higher E:T ratios and including additional virus

isolates which can be effectively controlled by elite controllers would need to be implemented before vaccine samples could be assessed.

However, it was decided that rather than continue to optimise this approach, an alternative method; the cultured VIA will be used to increase the frequency of HIV-1-specific T cells in vaccinee samples before making an assessment of their inhibitory capacity. The application of this alternative VIA method to assess the HIV-CORE 002 trial samples is therefore presented in Chapter 5.

4.13 Summary of key findings from Chapter 4

- HIV-1 isolates differ in their kinetics of infection and their pathogenicity. This suggests that a range of representative viral isolates should be used in virus inhibition assays.

- Use of the same MOI between HIV-1 isolates does not ensure that the same percentage of cells will become infected and this must be optimised for each stock.

- The method chosen for $CD8^+$ T cell isolation does not significantly affect the suppressive capacity of the selected population, but does influence the background inhibition levels.

- Healthy controls showed minimal inhibition of HIV-1 Bal and in most cases the addition of an autologous naïve $CD8^+$ T cell population resulted in increased infection rates.

- The p24 ELISA was more sensitive to changes in virus levels than the flow cytometry method used here and is a better choice for assessing low levels of virus inhibition.

- Elite controllers and chronically infected HIV-1 patients demonstrated an *ex vivo* capacity for HIV-1 Bal virus control, while select vaccinees showed limited to no control of this viral isolate. Further optimisation is required to enable the *ex vivo* VIA to be routinely used for the assessment of vaccine efficacy.

5 Assessment of HIVconsv vaccine-elicited $CD8^+$ T cells using an *in vitro* cultured virus inhibition assay

5.1 Introduction

In Chapter 4, an *ex vivo* virus inhibition assay (VIA) was optimised and evaluated for its ability to detect HIV-1 suppressive capacity, mediated by $CD8^+$ T cells induced by HIVconsv vaccination. The data from Chapter 4 demonstrated that the assay could detect virus inhibition in HIV-1 elite controller samples, at a high enough level to be able to compare individuals. However, vaccinee samples tested by the *ex vivo* method displayed very low levels (5 to 12 %) of HIV-1 Bal inhibition by flow cytometry, which in some cases was undetectable by p24 ELISA when compared to the elite controller samples. This was an important factor to consider when testing the complete sample set from the HIV-CORE 002 trial, as not only would it be difficult to compare vaccinee antiviral responses, but potentially many vaccinee responses may have also fallen below the level of detection for this assay. As a result, a published *in vitro* cultured viral inhibition assay (CVIA), originally developed by Fauce et al. in 2007 [302] and subsequently adapted by Spentzou et al. [307], was selected as an alternative approach to test the inhibitory capacity of the HIV-CORE 002 trial samples.

The methodologies used for the CVIA differ from the *ex vivo* VIA described in Chapter 4 due to the inclusion of an initial 7-day antigen-non-specific expansion and enrichment step for the $CD8^+$ T cells [369]. This step results in $CD3^+$ and $CD8^+$ T-cell populations that are >87% pure, with an approximately 5-fold increase in the total cell count by day 7 [307]. Due to the limited cell numbers available for each vaccinee, this expansion enables extra viral isolates to be examined and additional functional analysis to be performed from a single vial of PBMC ($5x10^6$ cells). The sub-population predominantly expanded are reported to be the pre-existing $CD45R0^+$ memory effector

cells [370], whilst maintaining the TCR Vβ profile and specificities present within the whole PBMC sample [370]. This was therefore thought to be a preferable means of amplifying the low inhibition obtained from vaccinee samples by the *ex vivo* VIA. The inclusion of a 7-day- expansion step was also supported by data from Migueles et al. [371], who demonstrated that a 6-day peptide expansion of LTNP PBMC resulted in $CD8^+$ T cells with greater cytotoxic capacity than those expanded from HIV-1 progressors and, more importantly, that at day 0 (pre-expansion), this difference in cytotoxic capacity was un-detectable. Taken together, these studies suggested that expanding the vaccinee PBMC samples before use in the VIA would provide a greater opportunity to firstly detect an inhibitory response, and secondly to allow a comparison between vaccinee inhibitory capacities to be made at an optimal time for measuring any cytotoxic and possibly also soluble effector functions.

The CVIA has been successfully used to assess both HIV+ individuals and vaccinees from the International AIDS Vaccine Initiative (IAVI) V001 trial [372], who received a prime-boost regimen of DNA/HAdV-5-Gag/Pol/Env and Nef. In treatment-naive HIV+ patients with low plasma viral loads (<10,000/ml), the group median inhibition of the IIIB virus was 3.17 (range 1.5 to 4.5) $\log_{10}$ [307]. Encouragingly, the seven V001 vaccinees inhibited the IIIB isolate with a group median of 2.22 $\log_{10}$ [307], but also showed a range of IIIB virus control (1.94 to 3.67 $\log_{10}$). In a more comprehensive analysis, 56 vaccinees who received the adenovirus serotype 35 vectored (HAdV-35) HAdV35-GRIN/ HAdV35-Env immunogens [326] were assessed by CVIA [308]. This analysis also revealed a broad range of inhibition (0.65 to 4.96 $\log_{10}$) for the IIIB virus and this variation in control was also observed for 6 other viral isolates tested. Interestingly, combining the vaccinee CVIA data with epitope mapping information suggested that targeting

immunodominant responses to conserved residues within the viruses led to enhanced *in vitro* virus control [308].

We therefore hypothesised that the highly immunogenic HIVconsv vaccine encoding multiple conserved regions from HIV-1 would induce protective $CD8^+$ T-cell responses towards viral isolates containing these regions.

5.2 Aims of Chapter 5:

1. To assess if $CD8^+$ T cells induced by vaccination with the HIVconsv vaccinees are capable of recognising virally infected target cells and controlling viral replication, using a panel of HIV-1 isolates.

   If possible:

2. Determine the optimal vaccine regimen for induction of antiviral $CD8^+$ T cells.

3. Analyse if host genetics or intrinsic viral characteristics influence viral control.

4. Distinguish which vaccine induced $CD8^+$ T-cell specificities contribute to HIV-1 control.

5. Examine the potential effects of soluble factors on virus inhibition.

5.3 The HIVconsv vaccine-induced $CD8^+$ T cells are capable of controlling HIV-1 clade A and B isolates.

As the HIVconsv immunogen is an artificially designed chimeric protein [270], that encodes regions from the viral genome that are typically subdominant during acute natural infection [347, 373], its ability to induce a CTL response that would result in the recognition and subsequent control of viral replication needed to be proven.

To test the inhibitory capacity of our HIV-CORE 002 vaccine trial samples CVIA analysis was undertaken at the IAVI Human Immunology Laboratory (London), using a panel of viral isolates established by this group [308] and listed in Table 5. The laboratory-adapted isolate HIV-1 Bal, which was used for the *ex vivo* VIA work described in Chapter 4, was also included in the panel.

Table 5 HIV-1 viral isolates selected for CVIA

Virus	Clade	Tropism	Isolate	MOI
IIIB	B	X4	LA	0.01
ELI	A/D	X4	LA	0.01
U455	A	X4	LA	0.01
Bal	B	R5	LA	0.005
ZA97012	C	R5	P	0.01
CH077	B	R5	IMC	0.01
CH106	B	R5	IMC	0.01
247Fv2	C	R5	IMC	0.01
LA = Lab adapted, P = Primary isolate, IMC = Infectious molecular clone				

The viruses selected for assessment of HIV-1 inhibition were from viral clades A, A/D, B and C as these clades were included within the HIVconsv immunogen. In addition, the IAVI group had access to several infectious molecular clones (IMCs), generously donated by Prof. G. Shaw (University of Alabama, Birmingham, AL). These IMCs were selected for assessment as they represent HIV-1 founder viruses that have been isolated and sequenced during acute primary infection [374]. Three laboratory adapted isolates (IIIB, ELI & U455) and one primary isolate (ZA97012) were also chosen for assessment as these viruses have

been shown to replicate efficiently in this assay with HIV-1^+ patient samples [307] and for the IIIB isolate also with vaccinee samples [307, 308, 372].

The IIIB isolate selected for the panel had the Nef gene in the 3' open reading frame of the genome deleted [375]. This was shown to have no effect on the ability of the virus to infect or kill T-cell targets, but does result in reduced rates of viral replication [376]. However, the IIIB virus may also behave differently to other isolates in the panel as Nef has many effects on the host cell, which have been associated with $CD8^+$ T cell immune evasion [377, 378], efficient infection by a single virion [50, 379, 380], enhanced virus infectivity [381, 382] and modulation of apoptosis which results in sustained virus production [49, 383]. Perhaps most relevant is the role in immune evasion which is mediated by Nef's ability to down regulate MHC class I, which is essential for effective CTL recognition of virally infected cells and subsequent cell lysis [42, 384].

Here the 8 different HIV-1 isolates were used to infect expanded autologous $CD4^+$ T cells and these were co-cultured with non-specifically expanded $CD8^+$ T cells from pre-vaccination and 3 post vaccination time points at a 1:1 effector to target ratio. The p24 concentration was measured by a p24 ELISA and inhibition of viral replication was calculated as the $\log_{10}$ reduction of p24 protein when $CD4^+$ T cells were co-cultured with the $CD8^+$ T cells, compared to p24 levels in $CD4^+$ T cells cultured alone. An overview of the CVIA is shown in Figure 31.

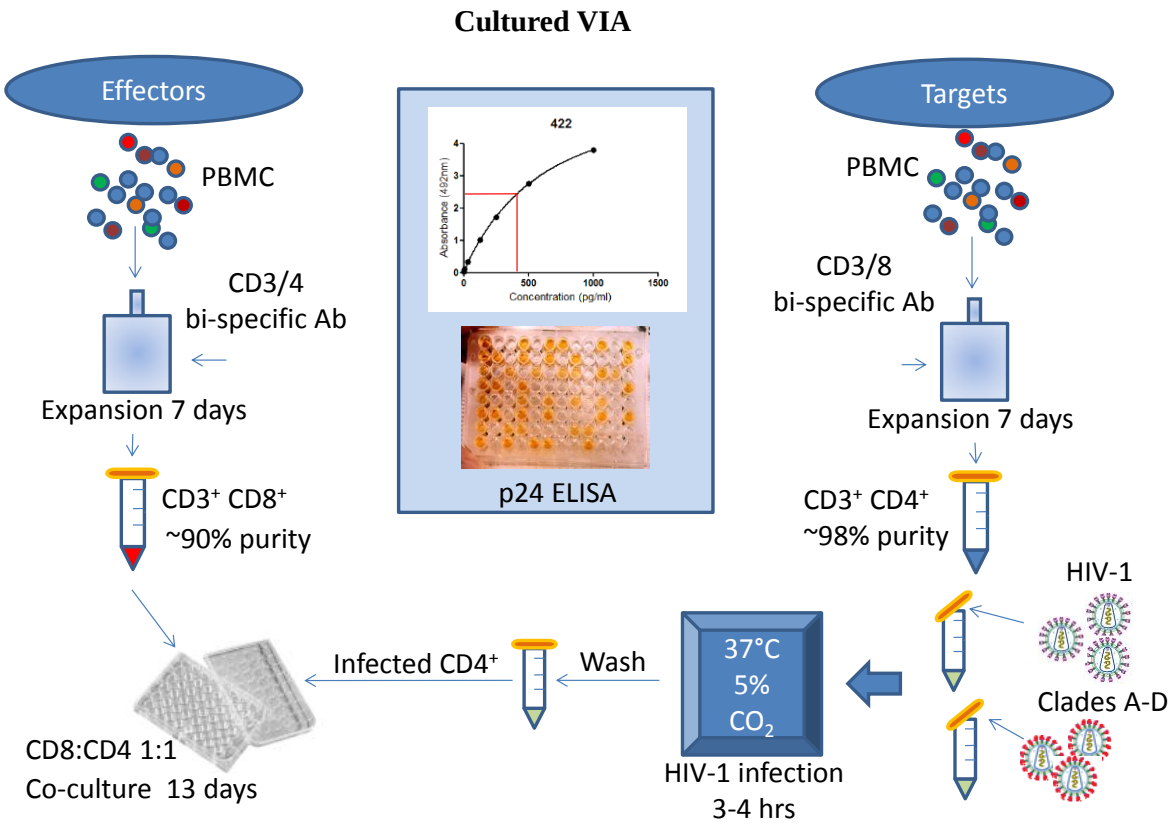


Figure 31 An overview of a cultured viral inhibition assay. $CD8^+$ and $CD4^+$ T cells are non-specifically expanded for 7-days. $CD4^+$ T cells are infected with the HIV-1 isolate of choice and co-cultured with $CD8^+$ T cells at an E:T of 1:1. On days 3, 6, 8 and 10 cells are fed by replenishment of half the media. After 13 days, the supernatants are collected and frozen before being assayed in a p24 ELISA. Diagram is based on the protocol published by Spentzou et al. 2010 [307].

To set criteria for the level of inhibition that was considered to be background, all pre-vaccination samples were used to determine the median inhibition level for each virus, and a stringent 99.9^{th} percentile value was used to determine the background value. When multiple viruses are displayed in the same graph, the highest cut-off value was used to set the background. See Appendix for full results, a summary is provided in Table 6.

Table 6 CVIA assay positivity values based on 99.9th percentile

Virus	Pre-vaccination inhibition values (log_{10})				
	Mean	**Median**	**Min**	**Max**	**99.9th Percentile**
IIIB	0.47	0.45	0.00	1.15	1.14
ELI	0.29	0.27	0.00	0.86	0.85
CH077	0.59	0.58	0.21	1.09	1.09
CH106	0.44	0.43	0.00	1.28	1.27
247Fv2	0.41	0.43	0.00	1.16	1.15
ZA97012	0.28	0.35	0.00	0.59	0.59
U455	0.57	0.51	0.07	1.23	1.23
Bal	0.10	0.00	0.00	0.44	0.44

The breadth of virus inhibition induced by the three vaccine regimens CM, DDDCM and DDDMC when assessed by CVIA are shown in Figure 32A, B and C, respectively.

The CM vaccine regimen, Figure 32A, induced the greatest breadth of virus inhibition with 7/7 (100%) vaccinees demonstrating inhibition of both the U455, clade A and IIIB, clade B HIV-1 isolates. For all of the vaccinees in the CM group, the peak inhibitory response towards most viruses was detectable at 9 weeks post vaccination, equivalent to 1 week post MVA.HIVconsv boost. At this timepoint the viral isolates U455 and IIIB were inhibited in the range of 1.3 - 4 log_{10} for most vaccinees. Despite the non-specific activation of the $CD8^+$ T cell population, the placebo (vaccinee 412) showed no detectable inhibition of any of the viruses employed within the panel.

One vaccinee 411, demonstrated superior breadth of virus control compared to all vaccinees tested by this method. Seven of eight viruses were inhibited by this individual to levels ranging from 2 - 5.8 log_{10}. This individual was one of two within this vaccine group to carry a protective HLA allele B*5101. Importantly, vaccinee 411 showed good control > 3 log_{10} of the transmitted founder isolates CH077 and 247FV2. Two additional vaccinees 403 and 404 also showed recognition of these viruses although suppression levels were notably lower at ~1.3 log_{10}. Although the levels of inhibition shown here were in some cases

minimal, it was encouraging that these founder viruses were recognised by $CD8^+$ T cells induced by vaccination with the HIVconsv immunogen, as this immunogen is based on consensus artificial sequences [270], which may have considerably differed to the circulating transmitted founder virus sequences due to intrinsic viral evolution [72, 81] and host immune pressure [118, 385, 386].

Vaccinees who received the CM regimen also maintained the most durable inhibitory response. Levels of viral inhibition gradually declined over time for all vaccinees after 9 weeks. However, six out of seven vaccinees maintained inhibition above 1.3 $\log_{10}$ for up to 20 weeks post vaccination.

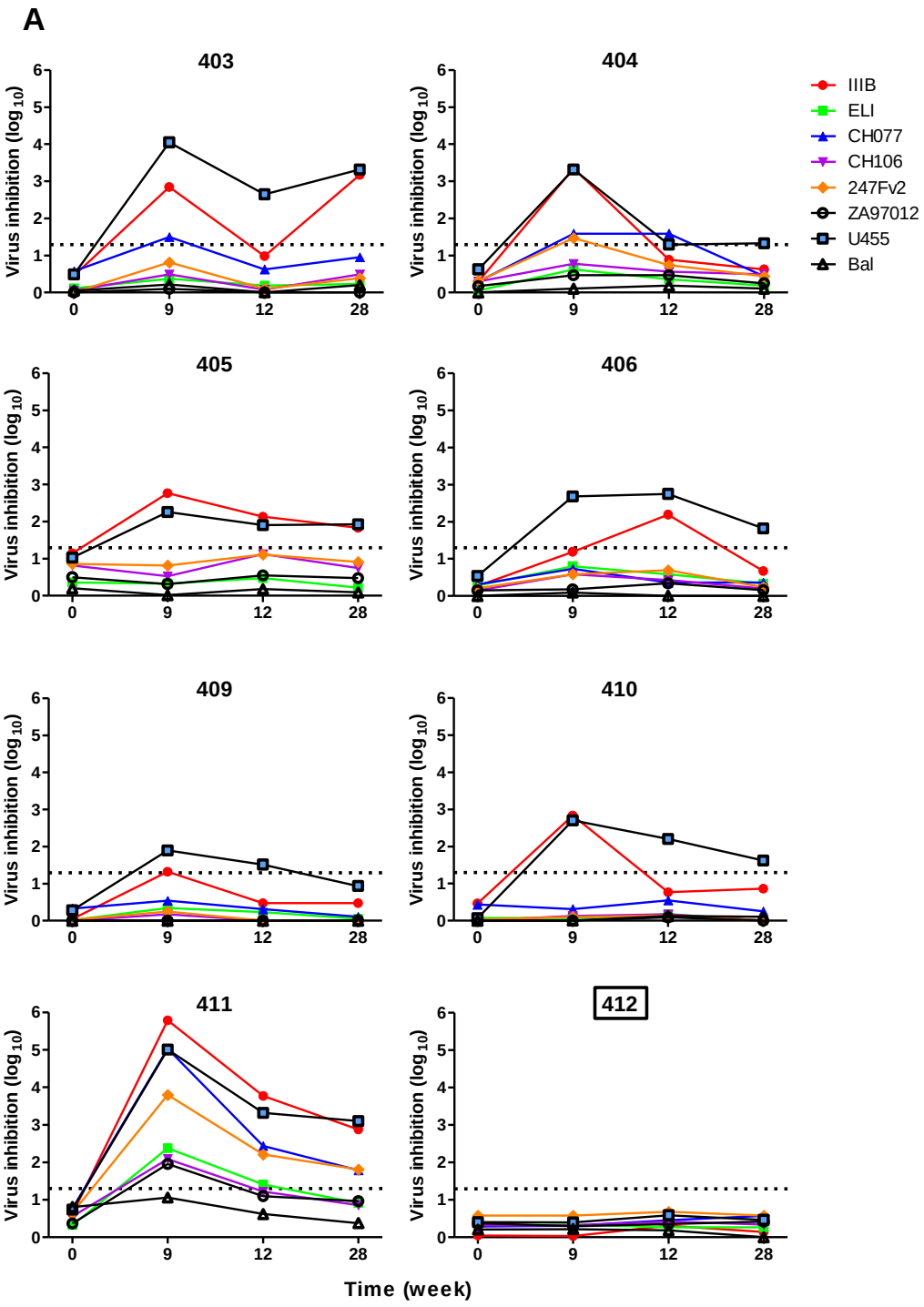
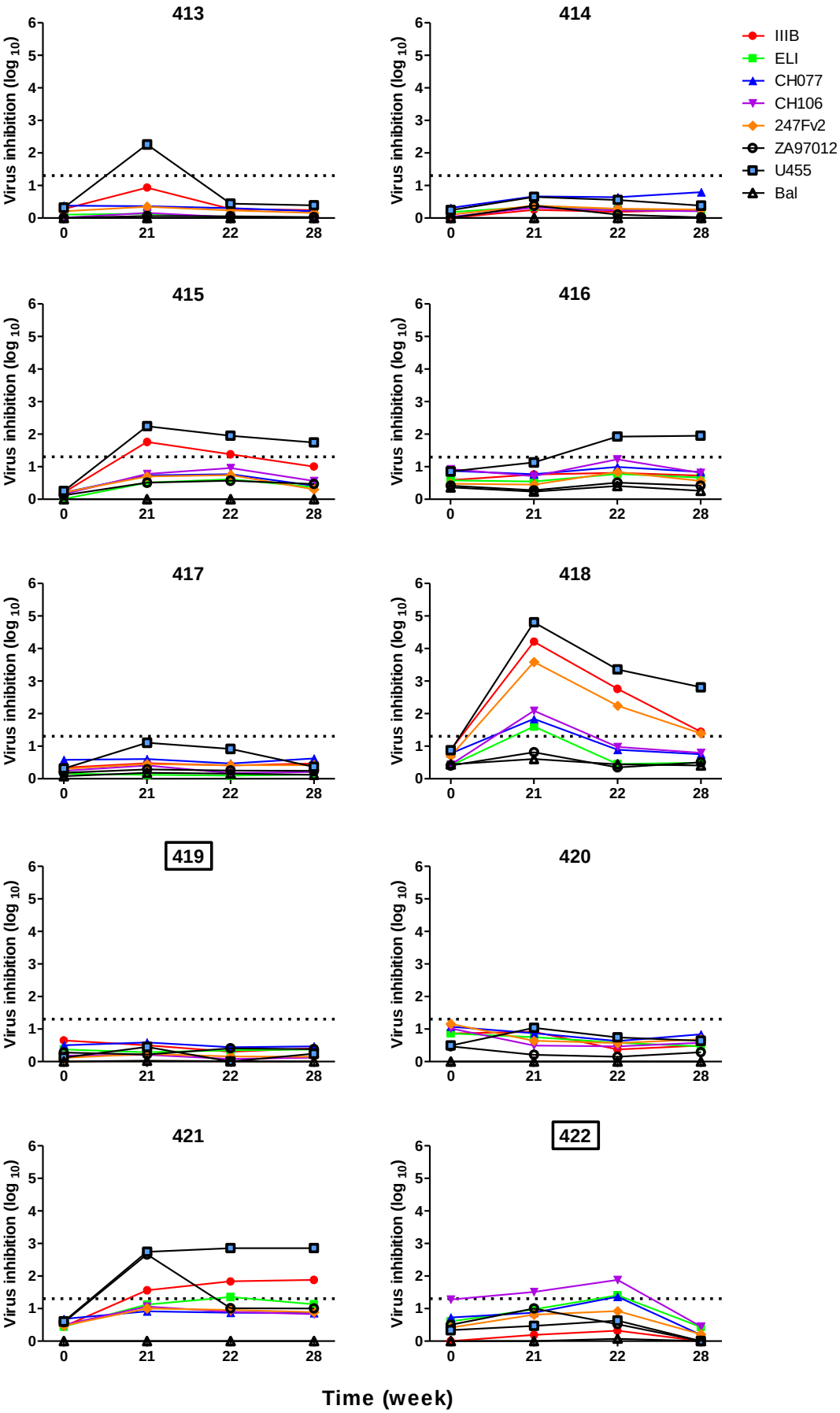
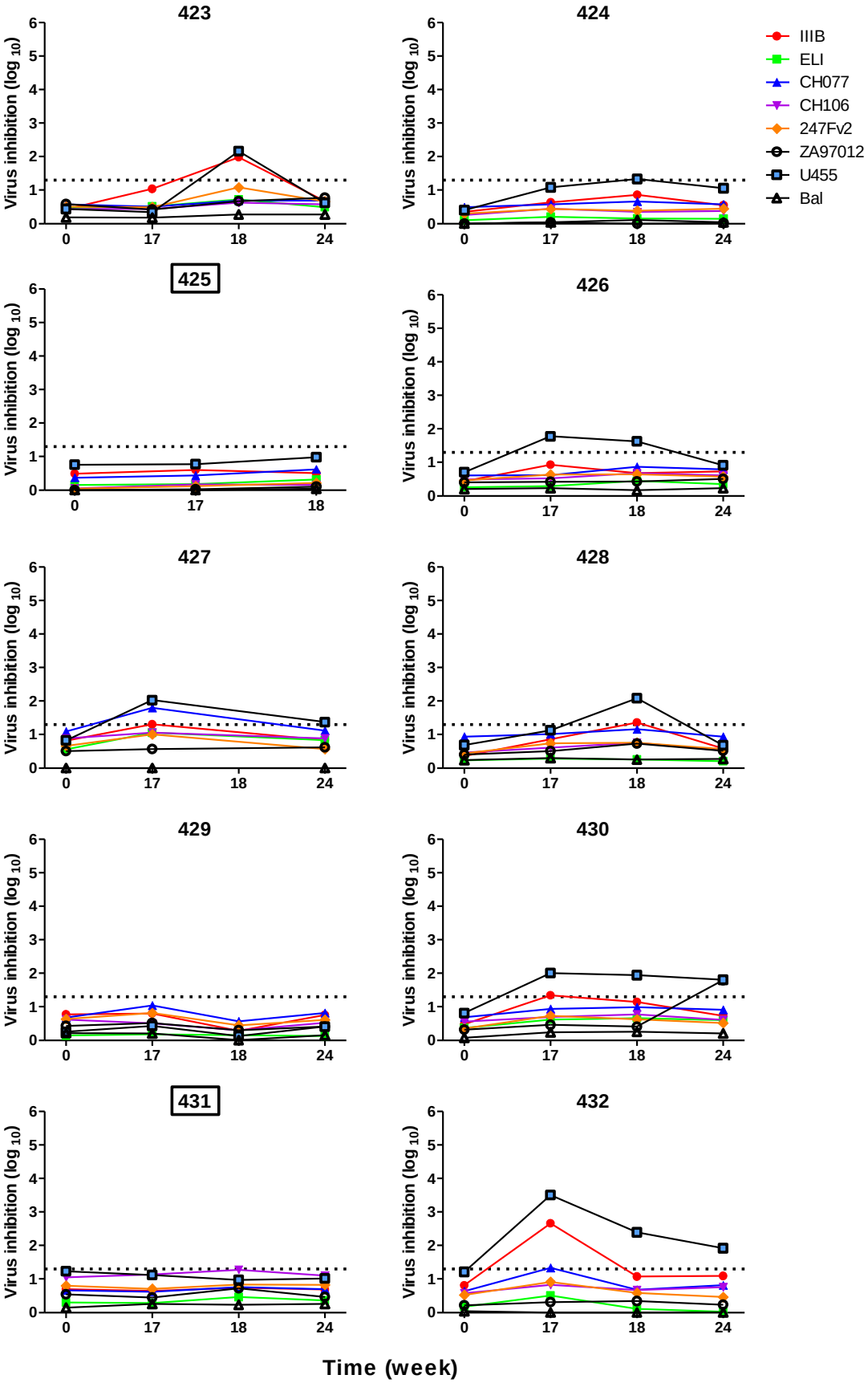


Figure 32A, B and C CVIA data for the CM, DDDCM and DDDMC groups, respectively. Inhibition of HIV-1 replication (log_{10}) data for each vaccine group is shown. The eight HIV-1 isolates tested are listed and colour-coded. Activated and expanded autologous $CD4^+$ T cells were infected and cultured alone or at a 1:1 ratio with activated expanded $CD8^+$ T cells. $CD8^+$ T cells from pre-vaccination (0 weeks) and three time points post vaccination (shown below in weeks) were analysed. The reduction in HIV-1 core protein p24 in co-culture supernatant compared to infected cells alone was determined after 13 days by ELISA. The background cut-off was 1.3 log_{10} (hashed line). Boxed numbers represent placebo recipients.

B


413
414
415
416
417
418
419
420
421
422
Virus inhibition (log 10)
0
1
2
3
4
5
6
0
21
22
28
Time (week)
IIIB
ELI
CH077
CH106
247Fv2
ZA97012
U455
Bal

C


423
424
425
426
427
428
429
430
431
432
Virus inhibition (log 10)
Time (week)
IIIB
ELI
CH077
CH106
247Fv2
ZA97012
U455
Bal

The DDDCM group data depicted in Figure 32B showed that 3/8 vaccinees made an inhibitory response of greater than 1.3 $\log_{10}$ to two or more viruses. In total, 5/8 vaccinees in this group inhibited at least one virus, and as observed for the CM group, the two viruses most commonly controlled were the U455 and IIIB, clade A and B isolates. Individual 421 displayed control of two additional viruses which were ELI and the primary isolate ZA97012, clade A/D and C subtypes, respectively.

Within the DDDCM group there was one broad responder, vaccinee 418, who showed a similar breadth of control to vaccinee 411 in the CM group. Vaccinee 418 made inhibitory responses to 6/8 isolates including the transmitted founder 247FV2, with no control of ZA97012 or Bal at the 21 week timepoint. The magnitude of inhibition for all viruses was also reduced for this vaccinee compared to 411, with the most effectively controlled U455 isolate showing a 4.81 $\log_{10}$ reduction in viral protein at week 21, the peak of the effector response.

The placebo control, 419 showed no detectable inhibition of any isolate. However, minimal inhibition was detectable towards isolates ELI, CH077 & CH106 for placebo 422 with a maximum level of 1.88 $\log_{10}$ inhibition observed for isolate CH106 at week 22.

In contrast to the CM group, a peak inhibition timepoint was not evident for the entire DDDCM group. Peak responses were mainly observed at week 21 corresponding to one week post MVA.HIVconsv boost, but for vaccinees 416 and 421 peak responses were detected at 22 weeks post vaccination suggesting that the memory response may be delayed in certain individuals.

A sustained inhibitory response for up to 28 weeks post vaccination was only detectable for three vaccinees from this group (415, 416 & 421) and two of these were

individuals who had an initially delayed peak response beginning at 22 weeks post vaccination.

The final group examined by CVIA received the DDDMC regimen as shown in Figure 32C. This group showed the lowest magnitude of inhibition out of the three vaccine regimens tested. However, 5 out of 8 vaccinees demonstrated inhibition towards the IIIB and U455 viruses and 2 out of 8 also inhibited the transmitted founder CH077. Broad responders (5 viruses or more) were not observed in this group.

The peak timepoint for virus inhibition showed variation with vaccinees 426, 427, 430 and 432 peaking at 18 weeks, equivalent to 1 week post ChAdv63.HIVconsv boost. For vaccinees 423, 424 and 428 the peak timepoint was at 19 weeks post vaccination.

The placebos 425 and 431, showed no detectable inhibition of any of the isolates tested, at any timepoint. An inhibitory response towards the U455 isolate that was maintained for up to 28 weeks was observed for only two vaccinees 430 and 432.

A clearer distinction between $CD8^+$ T-cell inhibitory capabilities induced by the three vaccine regimens can be detected by comparing the magnitude and durability of the two most efficiently controlled viruses, U455 and IIIB and is therefore depicted in Figure 33.

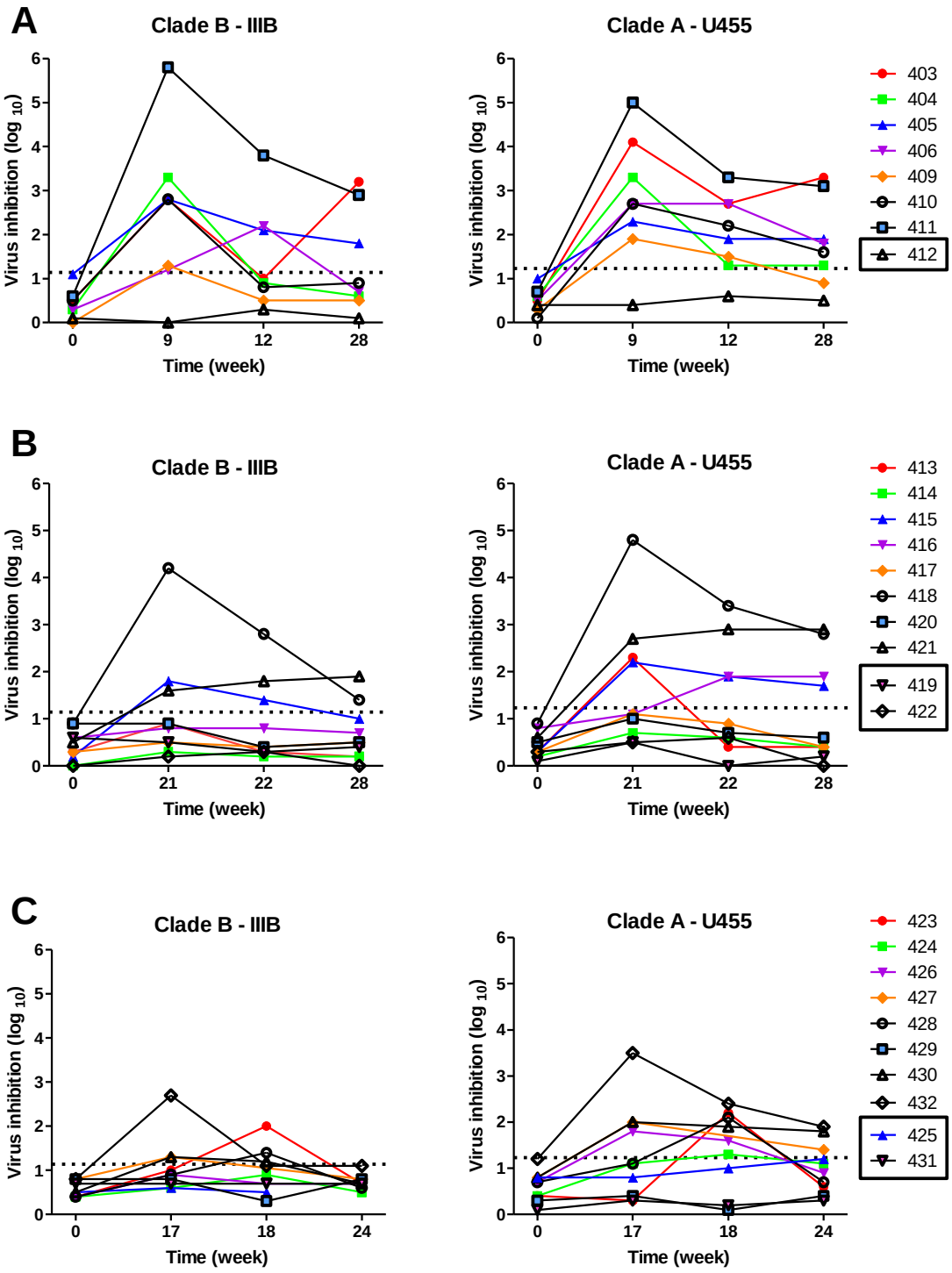


Figure 33 IIIB and U455 CVIA data for each vaccine regimen. **(A)** CM regimen, **(B)** DDDCM regimen and **(C)** DDDMC regimen. Each vaccinee is colour-coded and boxed numbers represent placebo recipients. The background cut-off for IIIB virus inhibition was 1.14 $\log_{10}$ and for virus U455 it was 1.23 $\log_{10}$.

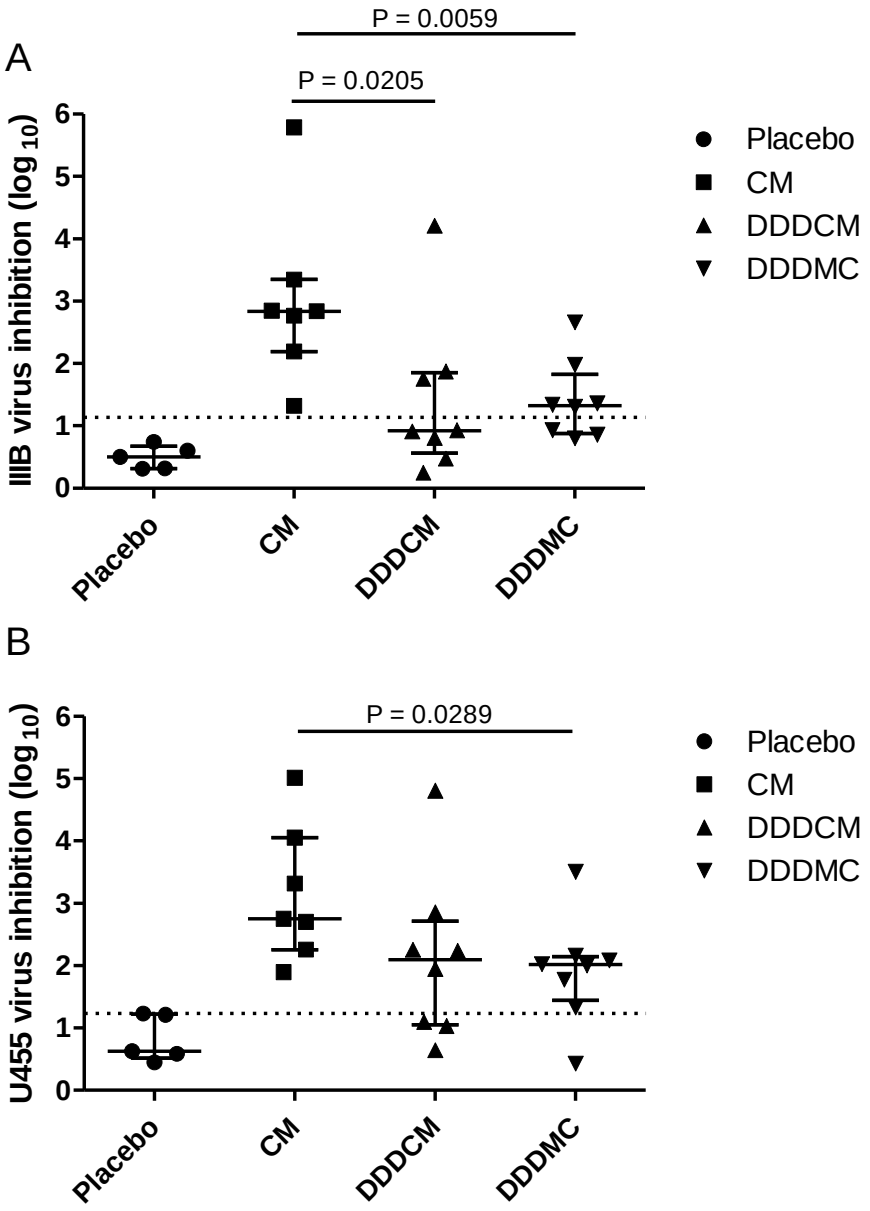


Figure 34 Comparison of vaccine regimens on the induction of viral inhibition. The peak timepoint for each regimen is presented for **(A)** IIIB and **(B)** U455 viruses. For CM, DDDCM and DDDMC this was taken as one week post final vaccination (9, 21 and 17 weeks, respectively). The median value for each group and interquartile range are represented by a bar and whiskers. Significant differences assessed by Mann Whitney test (P = <0.05) between the vaccine regimens are shown.

When a comparison at the peak timepoint for virus inhibition was made between the vaccine regimens for both the IIIB and U455 viruses, the most effective vaccine regimen could be determined. Figure 34A shows that for the IIIB virus, significantly higher median

viral inhibition levels were achieved for both the CM and DDDMC groups (P = 0.0025 & 0.0016) when compared to the placebos. In Figure 34B, when the most frequently controlled U455 isolate was examined a significantly higher median level of inhibition was detected for all three vaccine regimens compared to the placebo group (P = 0.0025, 0.0451 & 0.0295 respectively).

For the IIIB virus, the median inhibition levels were 2.84, 0.92 and 1.33 $\log_{10}$ for CM week 9, DDDCM week 21 and DDDMC week 17, respectively. Whereas for virus U455, the median inhibition was 2.75, 2.10 and 2.02 $\log_{10}$ for CM week 9, DDDCM week 21 and DDDMC week 17, respectively. Comparison of the median viral inhibition levels between the vaccine regimens demonstrated that the CM group had significantly higher virus inhibition when compared to those who received DDDMC for both the IIIB (P = 0.0059) and U455 (P = 0.0289) viruses. In addition, the CM group showed a significantly increased magnitude of IIIB inhibition (P = 0.0205) compared to the DDDCM group, and although not significant this increase was also detectable for the U455 virus.

Overall, data from Figure 32 to Figure 34 demonstrated that the CM vaccine regimen induced a significantly greater magnitude of virus inhibition when the two most efficiently controlled viruses were examined, and furthermore, an increase in both breadth and duration of virus control was also achieved following administration of this regimen.

5.4 Virus replication capacity does not account for differential virus control

There are several confounding factors that can influence the ability of HIV-1 to infect, replicate and propagate comparably in vaccinee $CD4^+$ T cells. In Caucasian populations, a naturally occurring 32-bp deletion in the CCR5 co-receptor gene (*Δ32*) is highly prevalent (~8%) [387] and this mutation results in the failure of CCR5 tropic HIV-1 virus fusion and infection [388]. Furthermore, intrinsic host cell anti-viral factors such as APOBEC3G [52, 389], TRIM5α [390, 391] and tetherin [67] function to impair effective viral DNA production, capsid uncoating, and subsequent virion release from infected T cells. The activation state of the target cell also alters virus production levels [87] and genetic differences among the viral isolates causes variation in both replication efficiency and infection kinetics within healthy donors. The effect of these factors on virus replication, in combination or individually, may translate in to the observed differences in *in vitro* virus control.

Therefore, the replicative capacity of each viral isolate within all vaccinees $CD4^+$ T cells was examined as an indirect measure of both intrinsic host anti-viral effects and genetic variation between viruses. I hypothesised that if these factors had a significant effect upon replication, this could explain the selective control of the U455 clade A isolate displayed by $CD8^+$ T cells in all three vaccine regimens, and furthermore may have played a role in the broad inhibitory responses made by vaccinees 411 and 418. To assess viral replication, the total p24 concentration for each virus on day 13 for all vaccinees was examined.

Figure 35A shows that the median p24 concentration for the U455 virus was 165.2 ng/ml which was the lowest of all the viral isolates tested. In contrast, the IIIB virus which was also well controlled in the CVIA was the most highly replicated isolate by all vaccinees, with a p24 level of 287.3 ng/ml. However, as previously highlighted, this virus had a confounding attribute the deletion of the Nef gene, which results in an increased susceptibility to recognition by HIV-1 specific T cells. The range of replication for all 8

viruses was 41.7 -287.3 ng/ml, and interestingly the Bal isolate, which was the least efficiently controlled isolate by any vaccine group had a median p24 concentration of 165.2 ng/ml which was just above the average, of 161.4 ng/ml, for the panel of 8 isolates. When these replication data were correlated with the viral inhibition results from the peak CVIA timepoint, shown in Figure 35B, there was no observed correlation between the two variables. Therefore, replication capacity had no effect up on $CD8^+$ T-cell inhibition.

It was also clear in Figure 35A that vaccinees 411 and 418 had efficiently replicated all of the viruses from the panel, in most cases to greater than the group median and so potential anti-viral effects within the target cell and poor viral replicative capacity were unlikely to be the reason for the breadth of inhibition observed for these individuals.

Overall, there was no trend between the median level of viral replication and virus control by the vaccinees.

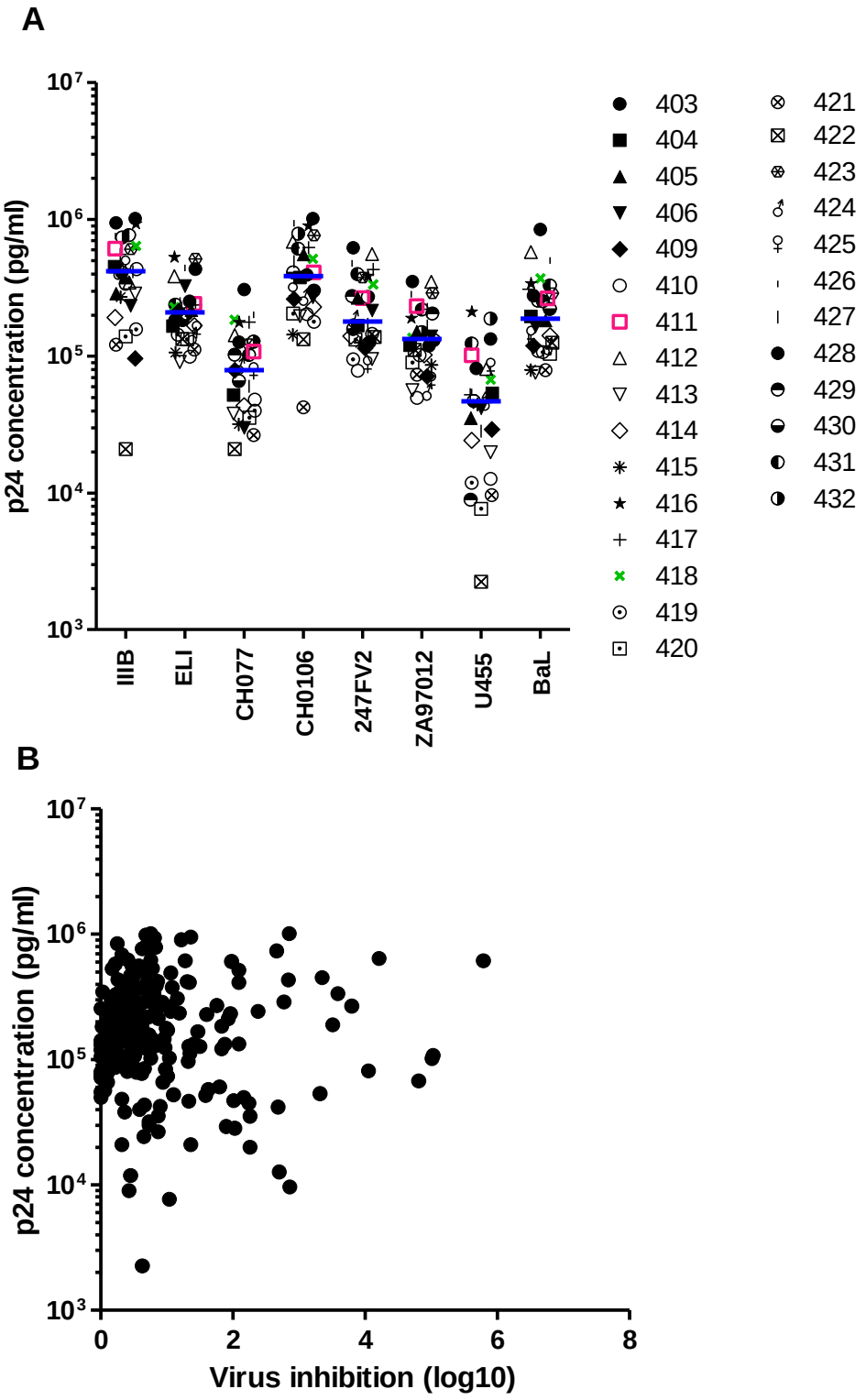


Figure 35 Replicative capacity of HIV-1 viral isolates in vaccinee CD4$^+$ T cells. (A) The p24 concentration in supernatants from infected cells alone for all vaccinees (n=32) on day 13 of culture was determined by p24 ELISA of frozen viral supernatants. The blue bar indicates median values for the individual viral isolate, a pink square and green cross represent vaccinees 411 and 418, respectively, that both showed broad virus inhibition. **(B)** Correlation of p24 concentration on day 13 with virus inhibition data for all vaccinees at the peak CVIA timepoint.

5.5 The influence of HLA on virus control

The HLA genotype of an individual was shown to impact on the time to the onset of AIDS [392, 393]. A delay in disease progression was associated with the presentation of a greater diversity of viral peptides by heterozygous HLA alleles at multiple loci [394, 395] and several HLA alleles were attributed to an increased or decreased risk of clinical progression. In select LTNP cohorts, there appears to be an over-representation of specific 'protective' HLA alleles including B57 [186, 396], B27 [397] and B51 [398]. Conversely, the B*35 [399], B*08 [400, 401] and Cw*04 [394] alleles were associated with a rapid decline in viral control. Variation in HIV-1 progression afforded by numerous HLA alleles was attributed to the amino acids lining the MHC class I binding cleft. Structurally, these residues can facilitate or block viral peptide binding and subsequently effect antigen presentation to cytotoxic $CD8^+$ T cells [402].

Globally, HIV-1 has evolved in response to the immune pressures exerted by HLA and as a result alleles which once were protective, in select populations, now offer no advantage to the host [185]. HIV-1 constantly evolves to avoid host immune detection but maintain fit viral progeny and this interplay contributes to the continual reversion [385, 403] and compensatory mutations [404, 405] that are selected and transmitted.

More recently genetic associations were examined in the context of HIV-1 vaccination with the ALVAC viral vector [406] and replication incompetent HAdV-5 HIV-1 Gag/Pol/Nef used in the Merck STEP study trial [407]. These analyses revealed that the strongest contribution to immunogenicity arose from previously described protective alleles, HLA B*57, B*27 [406] and B*51 [407] and both studies suggested that HLA-C was not influential in the $CD8^+$ T cell vaccine response.

Based on these observations, the effect of HLA genotype on virus control was assessed for all HIVconsv vaccinees. Table 7 provides the full list of HLA genotypes for all

HIV-CORE 002 volunteers with protective HLA alleles and broad virus controllers highlighted.

Table 7 The HLA Genotype of HIV-CORE 002 vaccinees

Vaccine Regimen	Vaccinee ID	HLA Genotype		
		HLA A	**HLA B**	**HLA C**
CM	403	A*3001 / A*0101	B*1301 / B*3901	Cw*0602 / Cw*0701
	404	A*6801 / A*6801	**B*5101** / B*4402	Cw*0704 / Cw*1402
	405	A*0201 / A*0301	B*0702 / B*4402	Cw*0501 / Cw*0702
	406	A*3101 / A*0301	B*4001 / B*4403	Cw*0304 / Cw*0401
	409	A*0101 / A*0301	B*0702 / B*0801	Cw*0702 / Cw*0701
	410	A*3002 / A*3002	**B*5702** / B*18	Cw*0701 / Cw*0701
	411	A*0201 / A*0201	B*0801 / **B*5101**	Cw*0303 / Cw*0701
	412 (P)	A*0301 / A*0201	B*4001 / B*0702	Cw*0702 / Cw*0304
DDDCM	413	A*0101 / A*0301	B*4402 / B*0801	Cw*0501/ Cw*0701
	414	A*2402 / A*3301	B*1401 / B*4402	Cw*0802/ Cw*0501
	415	A*0201 / A*0301	B*4402 / B*0702	Cw*0702 / Cw*0702
	416	A*0201 / A*0201	B*0801 / B*4402	Cw*0701 / Cw*0501
	417	A*3004 / A*0301	B*5001 / B*3501	Cw*0401 / Cw*0602
	418	A*2402 / A*0201	B*0702 / **B*2705**	Cw*0102 / Cw*0702
	419 (P)	A*0301 / A*1101	B*3501 / B*0702	Cw*0401 / Cw*0702
	420	A*2902 / A*0201	B*5501 / B*4403	Cw*0303 / Cw*1601
	421	A*1101 / A*0201	B*4002 / B*3503	Cw*0202 / Cw*1203
	422 (P)	A*0101 / A*3310	**B*14** / B*08	Cw*0701 / Cw*1802
DDDMC	423	A*0101 / A*1101	B*0702 / B*0702	Cw*0702 / Cw*0702
	424	A*0101 / A*0101	**B*5701 / B*5701**	Cw*0602 / Cw*0602
	425 (P)	A*0101 / A*0201	B*1501 / B*4403	Cw*0303 / Cw*1601
	426	A*0301 / A*0201	**B*1402** / B*1401	Cw*0304 / Cw*0802
	427	A*0201 / A*0201	B*0702 / B*4402	Cw*0501 / Cw*0702
	428	A*1101 / A*2402	**B*5101** / B*5501	Cw*0303 / Cw*1502
	429	A*2601 / A*3201	B*3503 / B*4402	Cw*0501 / Cw*1203
	430	A*0201 / A*0201	B*0801 / **B*5701**	Cw*0602 / Cw*0701
	431 (P)	A*0301 / A*2601	B*3501 / B*5601	Cw*0102 / Cw*0401
	432	A*0201 / A*0201	B*18 / **B*5101**	Cw*0202 / Cw*0701

(P) = Placebo. **Bold** alleles represent protective genotypes. **Bold** vaccinee ID represents control of >5 viruses in the CVIA.

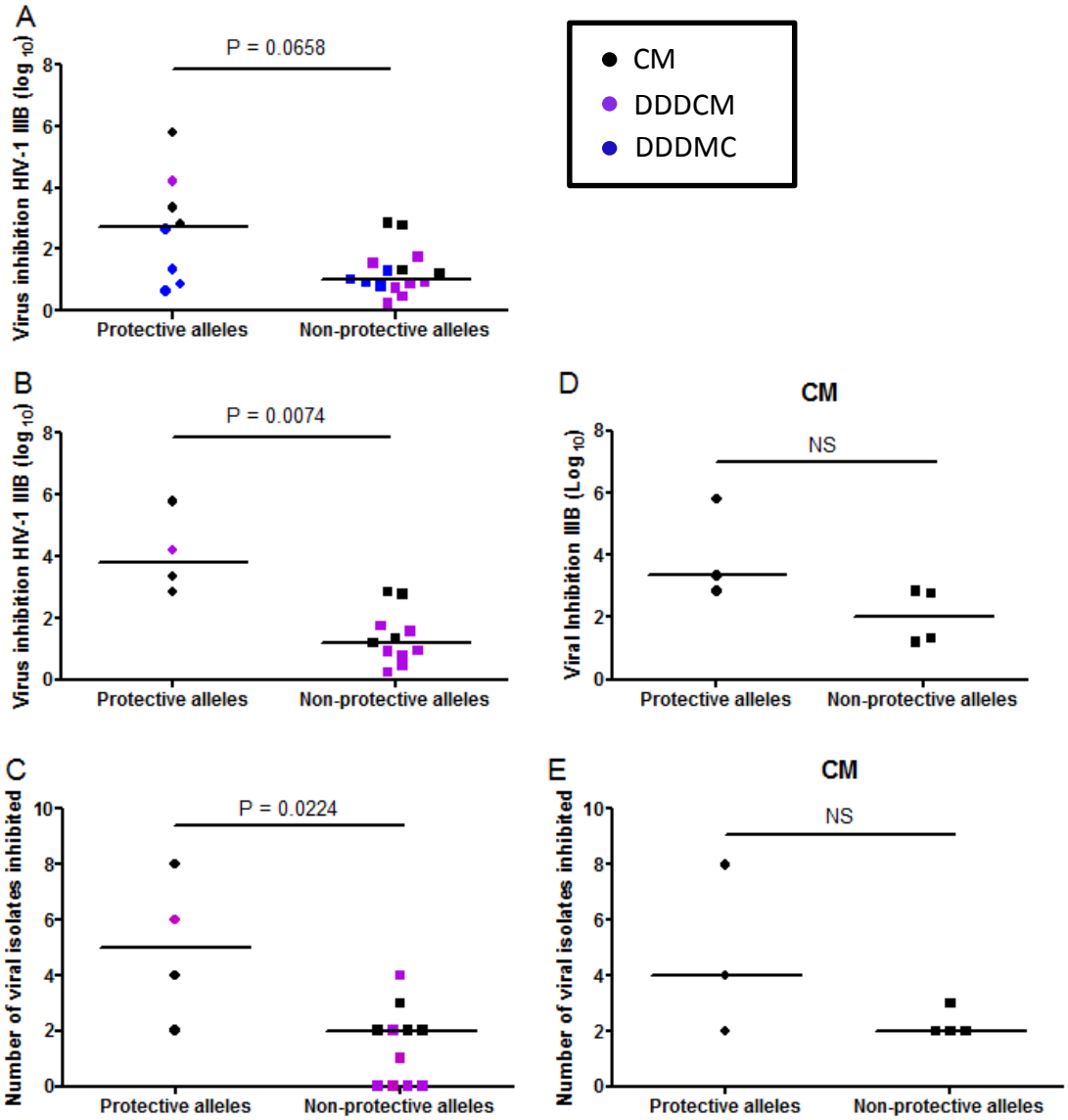


Figure 36 The influence of HLA on virus inhibition. All groups have been stratified by the expression of protective (B*5101, B*5701, B*2705) and non-protective (all other) HLA alleles. **(A)** Inhibition of the IIIB virus by vaccinees from all groups (n=23). **(B)** Inhibition of IIIB virus for CM and DDDCM groups only (n=15). **(C)** Total number of viral isolates inhibited by CM and DDDCM groups only. (D) Inhibition of IIIB virus for the CM group only. (E) Total number of isolates inhibited by the CM group only. The Student's t-test was performed with (two-tailed) P values <0.05 considered significant.

The effect of HLA genotype upon viral suppression was examined by stratifying each vaccine group by those who expressed known protective HLA alleles and those with alleles that have not been described in the literature to be advantageous in delaying time to development of AIDS. The data in Figure 36A demonstrate that when all vaccination regimes are included in the analysis there is no advantage for an individual expressing a protective HLA allele, as the level of viral inhibition, in this case toward the IIIB virus is not significantly higher than for those expressing non-protective alleles. However, if the weakest regimen DDDMC, as assessed by CVIA is removed from the analysis as depicted in Figure 36B, then there is a significant increase ($P = 0.0074$) in the level of viral inhibition that can be achieved when a protective HLA allele is expressed.

Figure 36C suggests that when the number of viral isolates or breadth of inhibition is considered for those regimens that most efficiently induced a CVIA response (CM and DDDCM) there is also a significant advantage in the number of isolates that can be inhibited when a protective HLA allele is present. Although, the spread of the data in the protective HLA group (Figure 36C) indicates that HLA type is not the only factor that is influencing the breadth of the inhibitory response.

When individual vaccine regimens were examined, the CM group showed no differences in magnitude or breadth of viral inhibition between the protective and non-protective allele groups (Figure 36D and E). But, one limitation of this analysis was the low number of vaccinees per group and so further assessment in a greater number of individuals would need to be performed to confirm these results. Currently there are two on-going clinical trials with the HIVconsv vaccines, HIV-CORE 003 and 004, which will be used to further explore these differences.

5.6 Pol- and Gag-specific $CD8^+$ T cells induced by HIVconsv vaccination correlate with virus control

Multiple studies suggested that protective responses against HIV-1 were mostly attributed to targeting of the Gag protein, in LTNP Gag-specific cells were shown to be more potent suppressors of viral replication than T cells specific for other viral proteins, such as Env and Nef [360, 408]. Furthermore, pre-clinical SIV vaccination and challenge studies demonstrated the contribution of Gag-specific, central and effector memory, T cells in control of SIV infection [306, 409]. More recently, data from vaccinees who participated in the Merck STEP study (HAdV-5 Gag/Pol/Nef) suggested that a greater breadth of Gag responses ≥3 was associated with lower viral loads following HIV-1 infection [261].

Pol-specific responses were however, present in HIV-1 controllers [154] where they were shown to recognise virally infected cells [410] and contribute to lower viral loads [333], but in natural infection these responses were often not dominant [347] and therefore were not believed to significantly contribute to viral control.

To address the question of whether Gag- or Pol-specific T cell specificities were responsible for the control of the clade A and B HIV-1 viral isolates, spare expanded $CD8^+$ effector cells were used in expanded IFN-γ ELISpot assays from each time point tested in the CVIA. The HIVconsv peptide pools were re-structured from the six originally used pools in the *ex vivo* ELISpot assays from Chapter 3. Pools of overlapping 15/11 mer HIVconsv peptides were prepared, specific for Gag, Pol, Env and Vif. The Env and Vif peptides were combined together to make one pool (Env & Vif), and due to the large number of Pol-specific peptides covering the immunogen, two Pol pools were used to try to limit potential competition during peptide presentation [411] [412]. The results from the two Pol pools were then combined and all responses were expressed as SFU/10^6 cultured $CD8^+$ T cells, these data are presented in Figure 37.

The $CD8^+$ T cell response to the protein-specific peptide pools shown in Figure 37 revealed that the greatest frequency of effector memory cells were induced by the Pol and Gag protein regions. The Env & Vif regions were particularly weak at inducing T cells when administered by any of the three vaccine regimens. This is likely to be a proportional representation of the overall composition of the HIVconsv immunogen and its subsequent presentation during vaccination, as the sequence encodes 67.3% Pol, 17.4% Gag, 11.7% Env and 3.6% Vif.

Surprisingly, the two broad virus controllers 411 and 418, as measured by CVIA, also showed high frequency, 2436 and 1178 SFU/10^6, $CD8^+$ T cells specific for the Pol protein at 9 and 21 weeks respectively. For the same vaccination time points vaccinees 411 and 418 showed a lower magnitude of Gag-specific $CD8^+$ T cells with 542 and 115 SFU/10^6 quantified, respectively. The ELISpot assay data also highlighted that the strongest virus controller from the DDDMC regimen, vaccinee 432 with >3 $\log_{10}$ reduction in U455 viral protein, had a very high frequency >3500 SFU/10^6 of Pol-specific $CD8^+$ T cells present at the peak timepoint for virus inhibition of 17 weeks.

To determine if there was a relationship between the frequency of protein specific T cells and virus inhibition, a correlation analysis was performed as shown in Figure 38. This examined the frequency of Gag-, Pol- and Env & Vif-specific T cells measured by IFN-γ secretion and levels of clade B (IIIB) and clade A (U455) virus inhibition. For both viruses, significant positive associations were found between the Gag- but more so Pol-specific T-cell frequencies and total magnitude of virus inhibition. The linear regression revealed that 32.7% of the virus inhibition value could be explained by the frequency of Pol-specific T cells and that 4.2% of the virus inhibition level could be explained by the frequency of Gag-specific T cells.

As the Gag- and Pol-specific T-cell frequencies showed a strong association with virus inhibition but had been subjected to 7-days of *in vitro* culture an examination of the *ex vivo* PBMC response was made in relation to virus inhibition. Figure 39 shows the correlation of the *ex vivo* IFN-γ ELISpot assay responses from the CM, DDDCM and DDDMC groups compared to virus inhibition at the peak timepoint for CVIA, and it was encouraging to see that the frequencies of *ex vivo* PBMC also correlated significantly with virus inhibition (U455 P = 0.0097, IIIB P = 0.0053) and explained 12.2% and 21.3% of the virus inhibition level for the U455 and IIIB isolates, respectively.

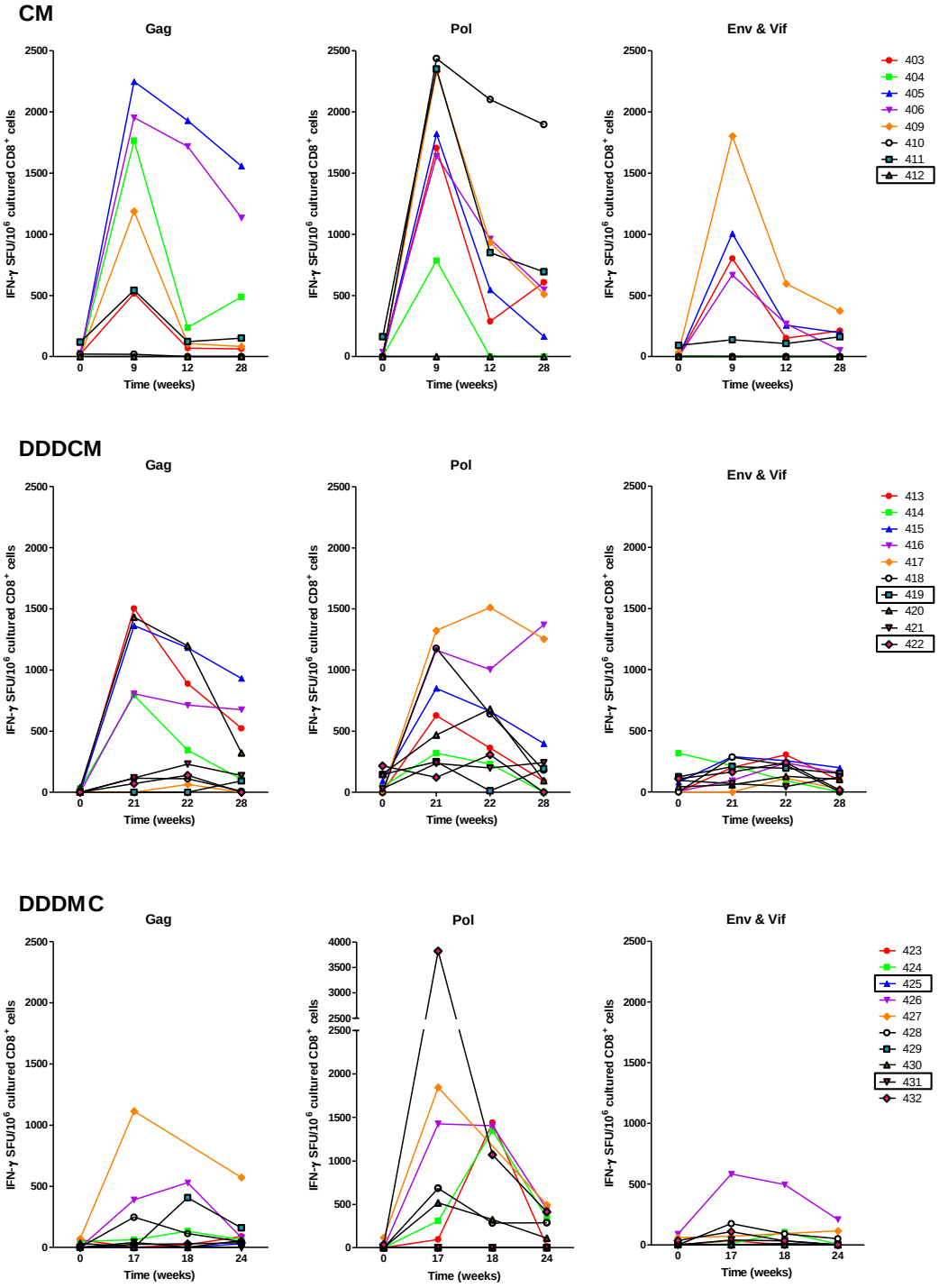


Figure 37 CD8$^+$ T-cell specificity assessed by IFN-γ-ELISpot assay. CD3/4 antibody-expanded CD8$^+$ T cells from vaccinees who received CM, DDDCM and DDDMC were rested overnight before being tested in an IFN-γ ELISpot assay. Four HIVconsv peptide pools were used which comprised of 1xGag, 2xPol (Pol results were summed) and a combined Env & Vif pool. Results were background subtracted and expressed as SFU/10^6 cultured CD8$^+$ T cells. Boxed numbers represent placebo recipients.

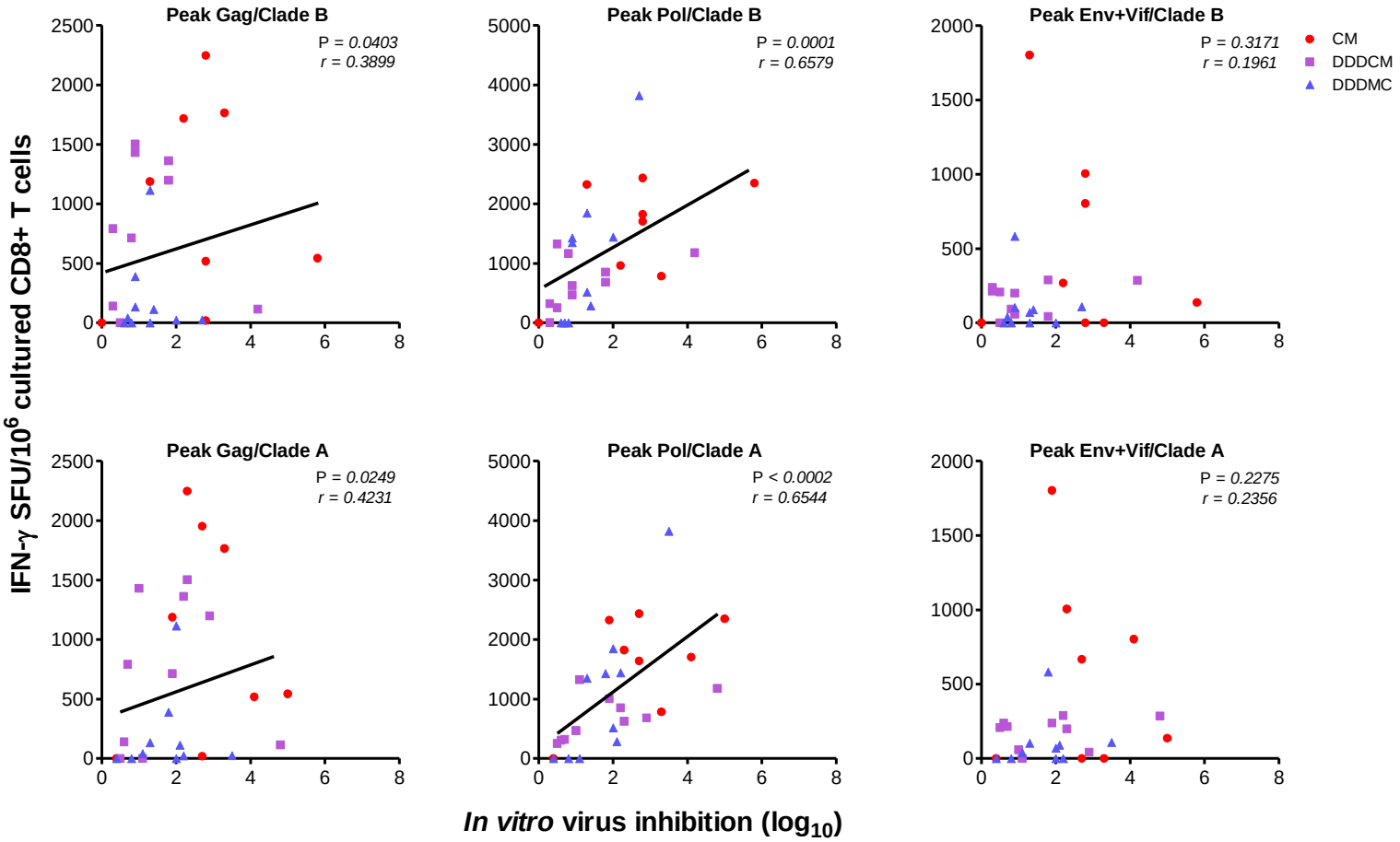


Figure 38 Correlation of frequencies of Gag- and Pol-specific CD8 T cells with virus inhibition. Non-specifically expanded $CD8^+$ T cells from all vaccinees were tested against Gag, Pol Env & Vif peptide pools (Figure 37) and these results were correlated with total virus inhibition from the peak timepoint by CVIA. The two most commonly controlled viruses, clade A (U455) and B (IIIB) used in the analysis are noted above each graph. For each correlation Spearman rank (*r*) and P (two-tailed) values are shown.

5.7 Total frequencies of *ex vivo* PBMC specific for conserved regions of HIV-1 correlate with virus control

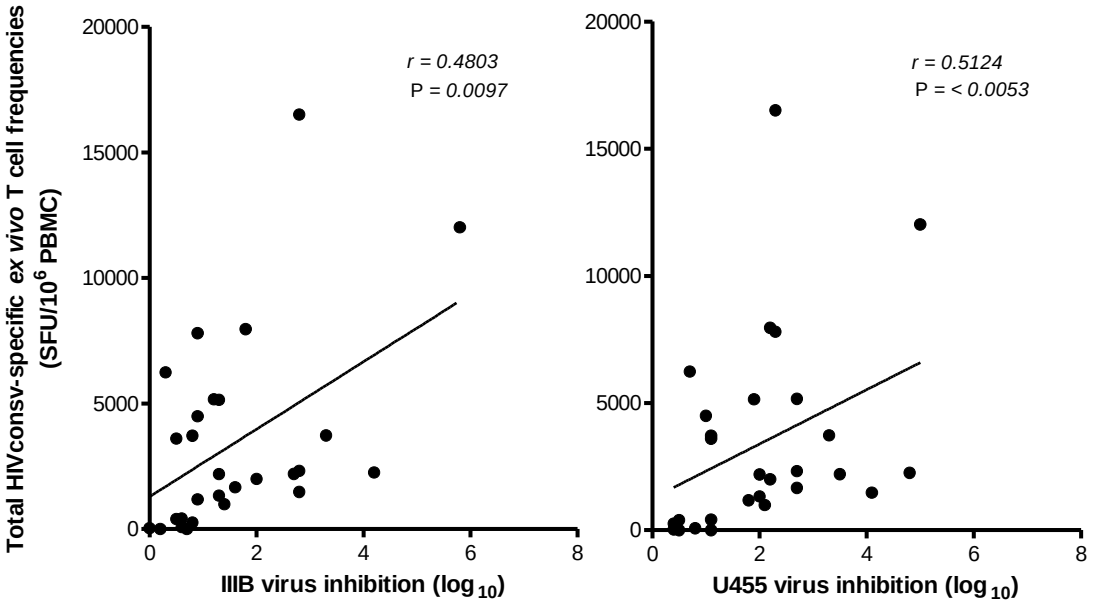


Figure 39 Correlation of total *ex vivo* frequencies of HIVconsv-specific PBMC with virus inhibition. For all vaccinees the summed response to the six HIVconsv peptides pools was correlated with virus inhibition at the peak CVIA timepoint for the clade A (U455) and B (IIIB) viruses. For each correlation Spearman rank (r) and P values (two-tailed) are shown.

5.8 Investigating the role of soluble factors on virus inhibition

Chemokines and cytokines play a role in the spread of viral infection, protective effects such as alerting neighbouring cells of an infection [413, 414], increasing the level and diversity of presented antigens [415-417] and actively blocking HIV-1 co-receptor sites on the surface of target $CD4^+$ T cells can act to limit virus dissemination [339, 418, 419]. Conversely, these small intercellular signalling molecules can act to fuel infection by encouraging an inflammatory environment where $CD4^+$ target cells become activated [420], up-regulate co-receptor expression [421] and become prime targets for HIV-1 infection. Moreover, target cells expressing the appropriate chemokine receptor respond by migrating toward the site of chemokine release [422] and subsequently toward the foci of virus infection.

Therefore, an investigation into the potential role of soluble factors on virus inhibition was performed. A Luminex assay specific for the cytokines IFN-γ, TNF-α, IL-1α, and chemokines MIP-1α, MIP-1β, RANTES, IP-10, MIG and SDF-1α was used to quantify the concentration of these cytokines in CVIA supernatants. These were chosen for examination due to their prominent antiviral roles (TNF-α and IFN-γ) [341, 423], and associated protective (IL-1α, MIP-1α, MIP-1β, RANTES, SDF-1α) or risk (IP-10, MIG) expression profiles in HIV-1 highly exposed persistently sero-negative volunteers (HESN) [424-427], virus controllers [298, 428] and highly suppressive T-cell lines [429].

Luminex was performed on frozen supernatants from the CVIA collected 13 days post infection for vaccinees 403, 411, 418 and 421 for all 8 viruses. For each vaccinee, the cytokine/chemokine levels for co-culture wells ($CD8^+$ T cells with infected $CD4^+$ cells) were examined and compared with infected cells alone. The results for all co-culture samples showed a reduction in overall cytokine and chemokine concentration when compared with infected cells alone but firm conclusions on the $CD8^+$ contribution could not be determined (data not shown). However, the cytokine levels from infected $CD4^+$ cells alone were assessed and the results are shown in Figure 40. The data suggest that increased levels of the chemoattractants MIG and IP-10 correlated with significantly increased HIV-1 virus propagation reflected by the increase in total p24 levels. In contrast to MIG and IP-10 the SDF-1α chemokine correlated significantly with a decrease in total p24 levels.

Overall, the soluble factor data suggest that virus growth was influenced by the cytokine and chemokine profile secreted by activated and infected $CD4^+$ T cells. It will be important to examine the cytokine/chemokine profiles induced by vaccination in the mucosa to determine whether these target cells could be influenced to secrete more protective profiles of these molecules.

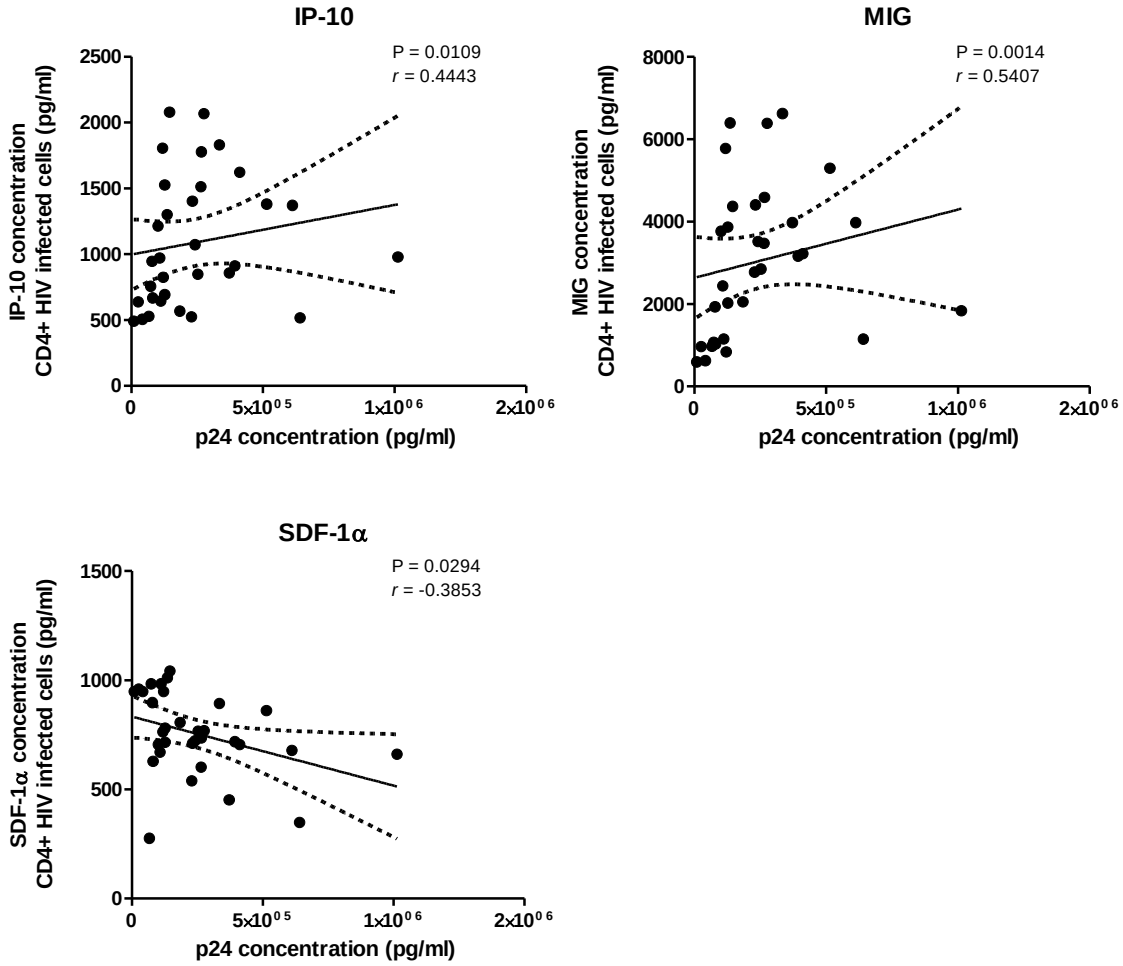


Figure 40 Correlation of p24 concentration with chemokine secretion from virally infected CD4$^+$ target cells on day 13 post infection. For vaccinees 403, 411, 418 and 421 frozen supernatants from the CVIA were analysed by Luminex for the cytokines and chemokines: IFN-γ, MIP-1α, MIP-1β, RANTES, IP-10, MIG and SDF-1α. Correlations between cytokine / chemokine concentration and p24 concentration were performed and significant results are shown. For each correlation Spearman rank (r) and two-tailed p values (P) are given.

5.9 Discussion

In Chapter 5, the ability of conserved region vaccine-elicited $CD8^+$ T cells to control *in vitro* HIV-1 virus replication was examined using a CVIA.

The inhibition results for the CM group were modest in terms of the breadth of virus inhibition detected but were good in terms of the percentage of volunteers making an inhibitory response. Vaccine-induced HIV-1 control has been investigated in a limited number of studies. Vaccinees from the IAVI V001 trial who had received a DNA prime, HAdV-5 boost regime encoding HIV-1 Gag/Pol/Nef (clade B) and Env (clades A, B and C) inhibited 3 isolates in total at the peak of the effector response [307]. More recently, 25 vaccinees who received HAdV-35 Gag, Reverse Transcriptase, Integrase and Nef (Ad35-GRIN) were assessed by CVIA and shown to inhibit up to 4 viruses. However, for the most frequently controlled isolate, U455, 23 of 25 vaccinees showed control and approximately 40% were able to effectively control two or more isolates [308]. A further study evaluated vaccinees from VRC008 and VRC011 who had received three DNA primes encoding Gag/Pol/Nef (clade B) and Env (clades A, B and C), followed by an HAdV-5 boost (encoding all proteins except Nef) and compared them to virus controllers, chronic individuals and healthy donors [298]. This study used 5 envelope pseudotyped NL4-3 HIV-1 viruses and demonstrated that up to 35% of vaccinees failed to inhibit any viral isolate, whereas viral inhibition was observed in 80% of HIV-1 controllers [298]. Therefore, the results from the CM group demonstrate that 100% of vaccinees capable of inhibiting at least two different viral clades is a strong outcome for vaccine-induced T cells. Importantly, the breadth of control displayed by vaccinees 411 and 418 from the CM and DDDCM groups respectively, was markedly above the average range of each group tested here and of similar vaccine modalities encoding some of the same regions from Pol and Gag that are present within the HIVconsv immunogen. An understanding of how this superior breadth of control was achieved by these individuals should aid in future HIV-1 vaccine design.

A further conclusion that could be drawn from the CVIA data is that there may be no need for additional DNA.HIVconsv priming vaccinations to generate an effective antiviral response that is capable of inhibiting viral dissemination. Although the vaccinees in DDDCM received multiple DNA priming injections, this did not increase the magnitude of the inhibitory response or the number of responders within the group when compared to the CM regimen.

A similar result was obtained for the IAVI-V001 prophylactic HIV-1 vaccine trial conducted in Africa comparing HAdV-5 alone with a DNA prime HAdV-5 boost strategy [372], this trial also demonstrated that DNA priming offered no enhancement of viral suppression compared to delivery of HAdV-5 alone. Taken together this data indicates that a short and simple vaccine regimen, such as CM could be used to induce $CD8^+$ T cells capable of suppressing HIV-1. This will become more important in resource limited settings and in rural areas where the cost of multiple vaccines can be prohibitive, and the ability to administer the full vaccine regimen to individuals relies on their returning to clinic for each booster vaccination.

The cell population present in the CM group at the peak time point of one week post MVA.HIVconsv boost demonstrated the greatest capacity for viral control by eliciting a robust and in some cases broad antiviral response. Due to the concomitant peak in IFN-γ ELISpot assay responses seen at this timepoint and described in Chapter 3, it is likely that this population largely represents vaccine induced effector memory $CD8^+$ T cells. Indeed in a small group of B*57 elite suppressors their effector memory (T_{EM}) and terminal effector memory (T_{TEM}) $CD8^+$ T cells showed the earliest and highest levels of virus suppression [430]. Furthermore, their central memory T cells (T_{CM}) also contributed to viral control, but were slower to inhibit peaking two days after T_{EM} responses [430]. In a separate analysis of 10 elite controllers with minimal T_{EM} ELISpot responses and *ex vivo* suppressive

capacity, the presence of a potent but resting $CD8^+$ T_{CM} population was shown. This population could proliferate upon exposure to recall antigen, were highly polyfunctional with up to 64.5% displaying 3 to 5 functions from those examined (IL-2, IFN-γ, TNF-α, MIP-1β & CD107a) and were able to subsequently control virus replication by up to 5 $\log_{10}$ [431].

Further evidence to support the induction of antiviral $CD8^+$ T_{EM} and T_{CM} cells through vaccination comes from SIV challenge studies in rhesus macaques, which showed that pre-challenge virus inhibition levels negatively correlate with viral load set-point following heterologous SIV challenge. Moreover, these responses were strongly correlated with the frequency of Gag-specific T cells [306, 409].

A T cell-mediated response becomes important in the situation of breakthrough infection that can occur despite the presence of HIV-1-specific antibodies [264, 265]. In the RV144 trial which demonstrated 31% efficacy [165], $CD8^+$ T-cell responses were not induced and this lack of CTL response is likely to have contributed to the failure to alter set-point viral load or slow disease progression in those vaccinees who became infected. However, the T cell-mediated response induced by the Merck HAdV-5/ Gag/Pol/Nef vaccine which failed to induce high magnitude, broadly responsive T cells [258], has more recently been shown to have reduced the viral load by 0.5 $\log_{10}$ in vaccinees who made >3 Gag-specific responses and this was more pronounced in those that went on to become infected within 1 year of their final vaccination [261]. The protective effect detected in this sub-population of vaccinees therefore waned over time and a concomitant decrease in $CD8^+$ T cell responses was observed.

These Phase III vaccine trials together with the data from our HIV-CORE 002 trial suggest that the inclusion of a T-cell immunogen is critical and advantageous for priming T-cell responses that can recognise a breadth of conserved virus epitopes, which are key for viral fitness, and without this element breakthrough infections can occur that will go

ultimately unhindered. A heterologous prime-boost regime as effective as CM will certainly be a starting point for the induction of high magnitude, active effector memory populations in the host, but these vectors may not be capable of inducing a T cell population that is maintained over time, demonstrated by the CVIA data where a gradual decrease in the magnitude of virus inhibition occurred after the peak timepoint of 9 weeks.

Novel replicating viral vectors offer an advantage to replication incompetent modalities in the duration of their immune stimulation. One such vector, the rhesus cytomegalovirus (rhCMV) a β-herpesvirus, was successfully used in the vaccination of rhesus macaques against SIV. This study demonstrated that using a replication competent viral vector to prime effector memory T-cell responses, in multiple tissues including the mucosa, resulted in sustained viral control of a SIVmac239 challenge in 50% of the animals [316]. Follow on studies in rhCMV/SIV controller macaques revealed that the duration of control lasted for up to 3 years [432], and that the latent pool of virally infected cells which was established early during natural infection was not detectable at the end of the study suggesting not only sustained viral control but viral clearance [432]. Control was observed in the absence of an Env-specific humoral response but the precise mechanism is still under investigation [316]. $CD8^+$ T cells were induced that showed extended breadth of epitope recognition, by targeting unconventional epitopes presented largely by MHC class II [433]. These MHC class II restricted epitopes revealed a new set of vaccine targets, and increased our knowledge on $CD8^+$ T cell priming through alternative vaccine modalities.

Taken together the evidence suggests that a concerted effort is required for effective viral control, a sustained T_{EM} population appears to be required for rapid viral clearance, which should be supported by T_{CM} $CD8^+$ T cells that are able to proliferate and differentiate in to a virus controlling population. It is therefore of importance to establish the type of memory T-cell populations that are present throughout and following our vaccination regimes, which

can hopefully be addressed in future efforts to characterise the vaccine induced response. Importantly, rhCMV targeting of T_{EM} cells to mucosal sites [316] is also likely to have contributed to the rapid control and limitation of spread of the initial SIV infection. Sampling of mucosal tissues is widely being recognised as a critical step to monitoring the immunogenicity of new vaccines entering clinical trials [434], and elite controller studies suggest that mucosal samples may well provide a more relevant correlate of protection [435]. Novel vaccination strategies such as 'prime and pull' are being designed to target virus-specific effector $CD8^+$ T cell populations to mucosal sites where they become resident memory cells [436]. This occurs whilst only limited numbers of activated effector $CD4^+$ T cells are retained at the mucosa. The strategy also achieves an overall reduction in the inflammatory environment at the portal of virus entry [436], which are all highly desirable effects in the setting of HIV-1 infection.

Soluble factors secreted by many cell types play a role in HIV-1 susceptibility and disease progression and the data presented here suggest that the $CD4^+$ T cell population itself has an effect upon virus infection. The results from the Luminex analysis of activated and HIV-1 infected $CD4^+$ T cells suggested that MIG and IP-10 facilitate HIV-1 replication, this is in agreement with data from highly exposed sex workers from the Benin region which showed significantly increased MIG and higher but non-significant IP-10 concentrations within the cervicovaginal lavage samples in those who went on to contract HIV-1 [427].

In contrast, a protective effect was mediated by SDF-1α secretion, this chemokine possibly acted to limit the spread of infection by directly blocking HIV-1 binding and entry through the CXCR4 co-receptor [437]. Surprisingly, this protective effect mediated by SDF-1α appeared even in target cells infected by CCR5 viruses but there is evidence to suggest an indirect role for SDF-1α, by inducing apoptosis in target cells that receive the signal [438].

These effects may also have occurred in combination in the presence of the CXCR4 tropic isolates.

Unfortunately, some of the soluble molecules previously described to be released by protective $CD8^+$ T cells, such as the β-chemokines specific for CCR5 [339] and the as yet unidentified $CD8^+$ T cell antiviral factor 'CAF' [439] were not able to be addressed using the Luminex platform and supernatant from the CVIA. To further investigate these functions and also enable the examination of the cell activation state and memory phenotypes, ICS could be used for the analysis of the $CD8^+$ T-cell populations [298] [435], in combination with ELISAs or HIV-1-specific $CD8^+$ T cell transcriptome analysis [440] as these methods may be more suitable for evaluating and discovering vaccine-induced cytolytic and non-cytolytic T-cell functions.

HLA type plays a notable role in the control of virus replication during natural HIV-1 infection [396, 398, 399], and the data presented here examining HLA type and vaccine regimens suggest that both factors heavily influence the ability to control viral replication. When all vaccine regimens were included in the HLA analysis, there was no advantage in expressing a protective MHC class I allele. In contrast, the exclusion of the least immunogenic regimen, DDDMC, resulted in a significant increase in both magnitude and breadth of viruses that were controlled. A globally deployable vaccine would aim to be highly immunogenic as seen with the CM regimen and result in the magnitude and breadth of viral inhibition becoming comparable between those expressing protective and non-protective HLA types. The CM regimen data suggested that this was achievable, but the results would need to be confirmed in a larger sample size. Samples obtained from two clinical trials currently in progress, HIV-CORE 003 and 004, could aid with this investigation.

HLA type only offers an advantage in virus control but does not always prevent progression from occurring [441], in vaccinees (CM and DDDCM groups) bearing a

protective HLA allele the wide range in breadth also supported this notion. More recently, Mothe et al. [333] investigated the protective vs non-protective peptide responses in clade B and C HIV-1 infected cohorts. This study found that responding to a greater number of conserved protective peptides was as predictive of viral load as HLA type. Similarly, a study conducted during primary infection in HIV^+ patients carrying protective HLA alleles [442] demonstrated that not all patients made dominant protective responses and that T-cell specificity was more predictive of viral load than simply HLA type alone. Thus, T-cell specificity is a key factor influencing viral control and individuals carrying non-protective HLA alleles can still control infection if the immune response is focused on these protective low entropy epitopes.

T-cell specificity may be one of the differences accounting for the breadth of control demonstrated by vaccinees 411 and 418 and further mapping of the HIV-CORE 002 vaccinee T-cell responses may reveal which epitopes were important for establishing control of HIV-1. The expanded ELISpot assay data suggested that vaccine-induced conserved region Pol-specific T cells may have contributed to a higher degree than conserved region Gag-specific responses to virus control, and these hypotheses can also be explored further by mapping individual peptide responses and determining their effectiveness in a CVIA. Interestingly, although not dominant protective Pol-specific responses were mapped by Mothe et al. [333] and are found during natural HIV-1 infection [347], however, in natural infection they may not be of sufficient quality, quantity, or present early enough to have a significant impact on the course of clinical progression.

A final observation from the CVIA data related to the enhanced control of the clade A and B (U455 and IIIB) viral isolates and very poor control of the clade B Bal isolate that had been used for the *ex vivo* VIA assay optimisation described in Chapter 4. Importantly, there was no association between the replication capacity of the viruses and inhibition levels.

Further knowledge of the T-cell specificity induced by vaccination and comparison with the viral sequence data may reveal an explanation for the observed variation in HIV-1 isolate control.

These results highlight that in an experimental setting the choice of HIV-1 isolate can have a significant effect on whether a vaccine is deemed efficiently immunogenic and capable of HIV-1 control. To help further Phase I vaccine trial assessments, it would be beneficial to have a standardised panel of isolates with known properties [374] including sequence and replication capabilities. Starting with a plasmid stock [443], which could be made available for use across laboratories, analogous to the Tier I, II and III envelopes used to inform antibody neutralisation studies [444, 445] as this would help to reduce the variation associated with continuous propagation of primary stocks in PBMC.

5.10 Summary of key findings from Chapter 5

- The CM regimen induced $CD8^+$ T cells capable of controlling clade A and B viral isolates in 100% of vaccinees, for up to 20 weeks.

- Superior breadth of virus control was observed for vaccinees 411 and 418 from the CM and DDDCM vaccine regimens, respectively.

- Vaccination with the highly immunogenic CM regimen may overcome the effects of HLA genotype on the control of HIV-1.

- High frequencies of conserved region Pol- and Gag-specific T cells correlated with *in vitro* control of HIV-1.

- SDF-1α secreted by infected $CD4^+$ T cells reduced the replication levels of multiple isolates of HIV-1.

6 Characterising vaccine-elicited conserved region Gag- and Pol-specific T cells

6.1 Introduction

In Chapter 5, vaccinee $CD8^+$ T cells were tested by a cultured virus inhibition assay (CVIA) for their ability to control 8 different HIV-1 isolates. Vaccinees 411 and 418 showed enhanced breadth of virus control with 7/8 and 6/8 viruses inhibited respectively, at peak time points. All vaccinees (7/7) from the CM regimen and 3/8 from the DDDCM regimen demonstrated control of two viral isolates, U455; clade A and IIIB; clade B. The non-specifically expanded $CD8^+$ T cells were also tested by IFN-γ ELISpot assay and the correlation analysis suggested that the frequencies of Gag- but more so Pol-specific T cells correlated with *in vitro* virus control.

In the literature most evidence supports the inclusion of the Gag protein within HIV-1 vaccine immunogens, as in chronic HIV-1 infection, individuals who broadly target this protein are able to maintain significantly lower viral loads [446-448]. In addition the recent MRKAd-5 Step Study [258] conducted in high risk HIV-1 negative volunteers suggested that limited T-cell breadth [296], particularly to the Gag protein, was associated with an increased viral load in the event of infection [261].

Moreover, the most highly conserved proteins within HIV-1 are found within the Gag gene [145]. The reason for this conservation is due to structural constraints on the p24 capsid protein, which if mutated result in a replicative fitness cost to the emerging mutant [188]. Thus, reversion [403] and compensatory mutations [405] are often associated with changes in this region. However, there are additional regions of the viral proteome which are highly conserved, including several within the Pol gene [271]. This gene encodes the enzymes Reverse Transcriptase, Integrase and Protease; required for reverse transcription, host cell integration of the viral genome and cleavage of Gag proteins, respectively [449]. Although fewer T-cell responses are made in natural HIV-1 infection to Pol proteins [347], dominant

targeting of these conserved regions by vaccine-induced antiviral T cells could inhibit successful viral propagation.

Due to the rapid replication rate of HIV-1 [72], early recognition and killing of virally infected targets is a desirable attribute for a T-cell mediated HIV-1 vaccine. To this end, studies in to the kinetics of HIV-1 epitope presentation and target cell killing have shown that protective Gag and Pol epitopes are presented early, from incoming infectious virions [349]. Furthermore, $CD8^+$ Gag- and Pol-specific T cells were able to kill virally infected target cells within 6 hours of infection [410, 450, 451]. These studies suggested that clearance of virally infected target cells can be mediated through Gag and Pol T-cell specificities, if these CTL can be induced in high enough frequencies through prophylactic vaccination they could lead to reduced viremia and therefore transmission risk as well as protect the functional adaptive immune system.

To investigate the control of virus replication, by the HIVconsv vaccine induced Gag- and Pol-specific T cells, cell lines were prepared for several vaccinees for examination in the VIA. The CVIA, described in Chapter 5, has been modified by other research groups to use peptide expanded T-cell lines [333] and clonal populations [360, 452] to examine what constitutes an effective antiviral response. The results of these analyses suggested that high avidity $CD8^+$ T cells, targeting low entropy epitopes, found in HIV-1 proteins including Gag, were capable of controlling virus replication. Thus, implying that if the HIVconsv vaccine induced Gag- and Pol-specific T cells of high enough avidity, then these cells would be capable of inhibiting virus replication.

Furthermore, functional analyses of chronically infected individuals have shown that IFN-γ secretion alone does not correlate with cytotoxicity [336, 453]. However, several studies have suggested the importance of polyfunctionality in viral control by T cells. $CD8^+$ T cells from vaccinees and HIV-1 controllers that produce MIP-1β and CD107a have been

associated with increased *in vitro* virus inhibition [298]. In addition, $CD8^+$ T cells capable of producing TNF-α, TNF-β and IFN-γ concomitantly have been shown to have greater HIV-1-specific cytotoxic potential [336, 454] and HIV-1 non progressors, also display highly polyfunctional T-cell profiles [191]. Therefore, an examination of the polyfunctional cytokine secretion profiles of both the Gag- and Pol-specific T-cell lines was also undertaken.

6.2 Aims of Chapter 6

1. Determine whether Gag- and Pol-specific T cells induced by vaccination with HIVconsv can control HIV-1 clades A and B.

2. Examine the cytotoxic and antiviral effector functions of Gag- and Pol-specific T cells in broad virus controllers.

3. Assess individual peptide-specific T-cell lines for their ability to control *in vitro* HIV-1 replication.

4. Map the epitopes which contribute to *in vitro* HIV-1 control in broad virus controllers.

5. Investigate the cross-recognition of HIV-1 achieved by T-cell targeting of the Pol epitope YQYMDDLYV.

6.3 Vaccine-elicited Gag- and Pol-specific T cells can control *in vitro* HIV-1 replication

To determine if conserved region Gag- and Pol-specific T cells induced through HIVconsv vaccination were capable of controlling virus replication, peptide pool expanded Gag and Pol T-cell lines were assessed in the CVIA. The HIVconsv peptides recognised by each vaccinee had been mapped using the IFN-γ ELISpot assay; these peptides were combined into either a Gag or Pol pool and used to generate cell lines for several vaccinees. Table 8 shows the non-junctional peptides that had been mapped for each individual (Chapter 3) and which were combined to generate the $CD8^+$ T-cell lines. Vaccinee 411 displayed no response to Gag peptides by IFN-γ ELISpot mapping assay and as a result only a Pol-specific cell line was generated for this individual.

Figure 41 shows an example of flow cytometry gating that was used to isolate HIV-1-specific $CD8^+$ T cells. An IFN-γ capture assay was employed to isolate cells responding by secretion of IFN-γ to the mapped HIV-1 peptides. Cells were then stained with anti-CD8 APC, anti-CD3 APC-Cy7 and anti-CD4 PerCP mAbs to enable the isolation of pure $CD8^+$ T cells. The sorted cells were cultured for a further 14 days to enable sufficient numbers to be tested by the CVIA.

Vaccinee peptide pool expanded Gag and Pol cell lines were tested against the IIIB, U455 and Bal viruses in the CVIA in the Jenner laboratories, Oxford. Initially 2 elite controllers and 2 placebo volunteers were tested in the CVIA against these isolates to establish that the bi-specific antibody expansions were comparable to those previously reported by IAVI HIL in London, and to determine background virus inhibition levels. The average purity for the $CD4^+$ and $CD8^+$ T cells was 91.7% and 95.2%, respectively. These results were comparable to the published figures [307]. The average background inhibition level for the placebo volunteers was used as the cut-off for each viral isolate and this is represented as the dashed line in Figure 42.

Figure 42 shows that Pol pool cell lines generated from vaccinees 403, 406, 411, 418 and 421 were able to control replication of both the HIV-1 IIIB (clade B) and U455 (clade A) isolates. In contrast, Gag pool cell lines generated from vaccinees 403 and 421 showed control of the IIIB and U455 isolates, but from all other vaccinees were unable to control virus replication. The clade B, Bal virus, was examined as a negative control as in Chapter 5 this isolate was not inhibited by >1.3 $\log_{10}$ by any vaccinee. There was however, low level inhibition between 0.35 and 1 $\log_{10}$ observed for this isolate by vaccinee 421 with both his/her Pol and Gag pool cell lines. Cell lines from all other vaccinees were unable to inhibit this virus.

Table 8 Mapped peptides used for the generation of $CD8^+$ T-cell lines

Protein Region	HIVconsv Peptide Number	HIVconsv Peptide Sequence	Responding Vaccinee
Gag	2	AFSPEVIPMFTALSE	403
	3	EVIPMFTALSEGATP	403, **418**
	11	KQMLKDTINEEAAE	403
	16	WIILGLNKIVRMYSP	403, 406
	17	GLNKIVRMYSPVSIL	**418**, 421
	18	IVRMYSPVSILDIRQ	403
	28	WKCGKEGHQMKDC	403
	29	KEGHQMKDCTERQA	403
	31	CTERQANFLGKIWPS	421
Pol	47	LTQIGCTLNFPISPI	**418**
	49	KNFPISPIETVPVKLK	406, **418**
	50	SPIETVPVKLKPGMD	406
	67	WRKLVDFRELNKRT	421
	77	VGDAYFSVPLDEGFR	406
	78	YFSVPLDEGFRKYTA	421
	79	PLDEGFRKYTAFTIP	**411**
	80	GFRKYTAFTIPSINN	**411, 418**
	88	GSPAIFQSSMTKILE	406, **411**, 421
	89	IFQSSMTKILEPFRA	406
	90	SMTKILEPFRAQNPE	406
	93	KNPEIVIYQYMDDLY	403, 406, **411**, **418**, 421
	94	VIYQYMDDLYVGSD	**411, 418**
	106	HLTEEAELELAENRE	406
	115	KQYWQATWIPEWEF	406
	116	ATWIPEWEFVNTPPL	406, **411**, 421
	117	PEWEFVNTPPLVKLW	406, **411**
	135	KLVSQGIRKVLFLDG	**418**
	164	VQMAVFIHNFKRKG	421
	166	FKRKGGIGGYSAGER	403
	170	WKGPAKLLWKGEGA	406
	171	AKLLWKGEGAVVIQ	406
	172	WKGEGAVVIQDNSDI	403, 406,
	175	SDIKVVPRRKAKIIR	403, 421
	176	VVPRRKAKIIRDYGK	403
	178	IIRDYGKQMAGADC	403

Bold = Vaccinees who demonstrated broad virus control by the CVIA (≥ 5 HIV-1 isolates).

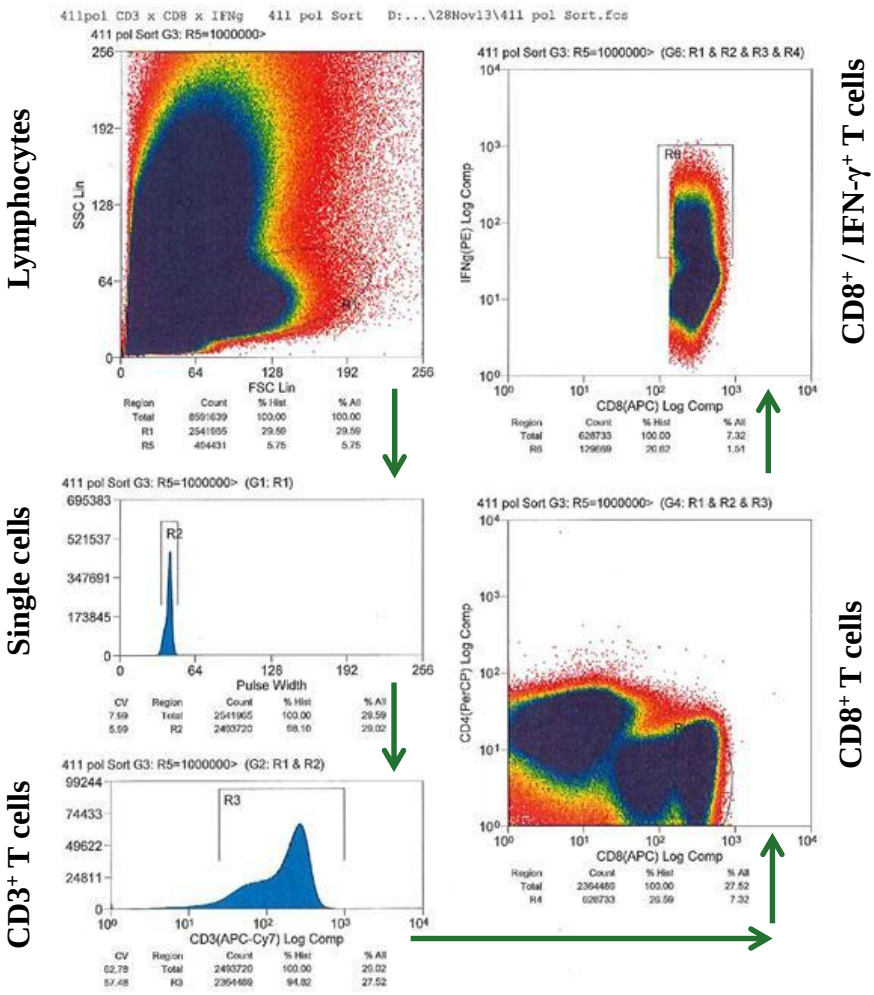


Figure 41 Example flow cytometry gating used to sort a Pol-specific T-cell line. Short-term cell lines were generated from vaccinee PBMC using a pool of peptides mapped by IFN-γ ELISpot assay. On day 10, cells were rested in R5. On day 12, an IFN-γ capture assay was performed followed by cell surface staining with anti-CD8 APC, anti-CD4 PerCP and anti-CD3 APC-Cy7 mAbs. HIV-1-specific $CD8^+$ T cells were sorted in to R10 media based on being lymphocytes, single cells and $CD3^+$, $CD8^+$ and IFN-γ^+.

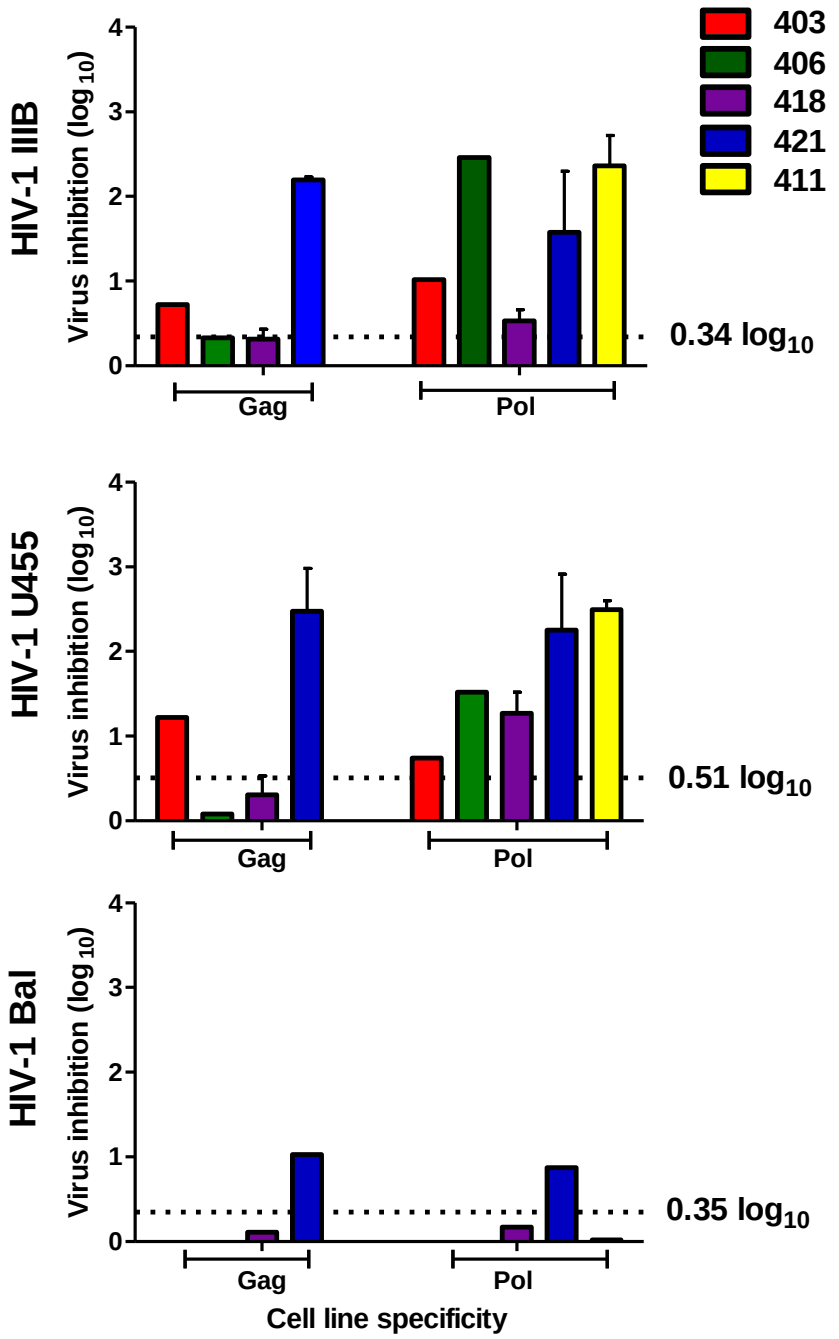


Figure 42 Inhibition of HIV-1 isolates by HIVconsv vaccine-elicited Gag pool- and Pol pool-specific T cells. Gag pool- and Pol pool-specific $CD8^+$ T cell lines were generated for vaccinees 403 (week 9), 406 (week 12), 411 (week 20), 418 (week 21) and 421 (week 22). On day 14, cell lines were placed in to a CVIA against autologous $CD4^+$ T cells infected with HIV-1 IIIB, U455 and Bal at MOIs 0.01, 0.01 and 0.005, respectively. Supernatant from day 13 was stored at -80°C before being assayed by p24 ELISA. Background inhibition levels determined from placebos are indicated by dashed lines. For vaccinees 411, 418 and 421 the cell lines were generated and tested twice by CVIA, the results represent mean ± SD.

6.4 Gag- and Pol-specific T cells from broad virus controllers are cytotoxic and produce soluble antiviral factors

The aim of these experiments was to identify which T-cell specificities were contributing to the observed control of the HIV-1 clade A and B isolates. Currently, it is still un-decided on which epitopes or regions of HIV-1 should be included within a vaccine construct that will ultimately result in virus control in the event of breakthrough infection. To date, sustained control of infection has not been shown by any human clinical trial candidate. Studies in both animal models and HIV+ patients have suggested that Gag is an important viral target for $CD8^+$ T cells [154, 306, 452], and that increased T-cell breadth to conserved regions of the virus is also associated with decreased viremia [333]. Therefore, elucidating the regions of HIV-1 targeted by the broad virus controllers shown in Chapter 5 would help to advance the field in the design of the next generation of vaccine immunogens.

T-cells are able to influence HIV-1 replication and dissemination by their ability to kill virally infected target cells and to secrete multiple cytokines [455]; in the case of HIV-1 these include antiviral MIP-1α, MIP-1β and RANTES [339], and an unknown $CD8^+$ antiviral factor (CAF) [439]. Thus, some of these functions were examined in response to individual peptides to try to determine which T-cell specificities may have been responsible for the reduction in virus replication observed in the CVIA experiments.

An *in vitro* cell killing assay was optimised based on a protocol by Hermans et al. 2004 [312]. This assay allowed for individual T-cell specificities to be evaluated for their cytolytic capacity using autologous $CD4^+$ peptide-pulsed target cells. The gating strategy employed for this assay is shown in Figure 43. Gag peptide pool and Pol peptide pool expanded cell lines for vaccinees 411, 418 and 421 were assessed in the cell killing assay and results are shown in Figure 44.

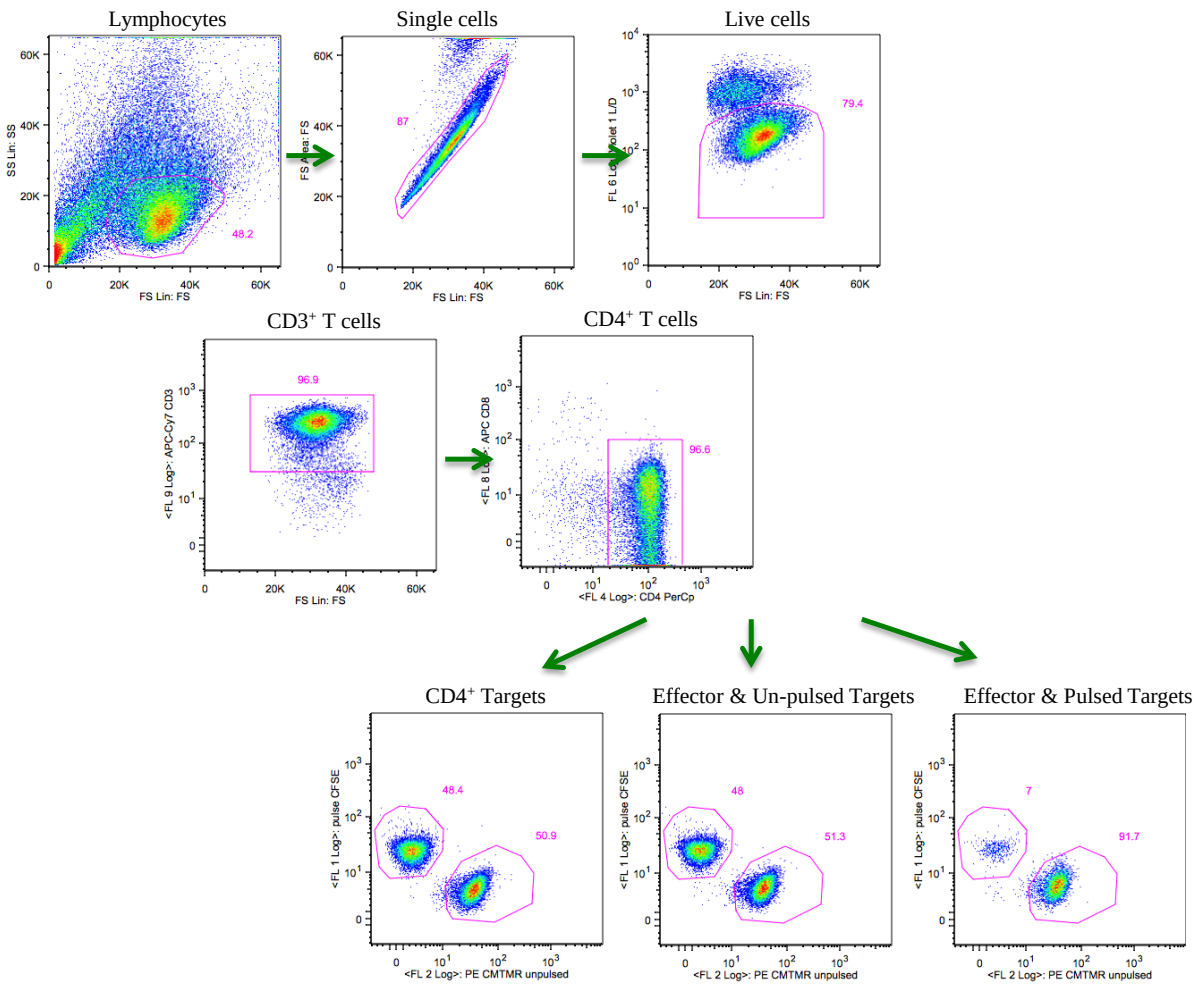


Figure 43 Example flow cytometry gating for the *in vitro* cell killing assay. Pre-vaccination CD4$^+$ T cells were activated and expanded with anti-CD3/4 bi-specific antibody for 7 days. CD4 T cells were then stained with either CMTMR or CFSE. CFSE cells were pulsed with individual peptides and plated at a 1:1 ratio with un-pulsed CMTMR stained cells. Effector Gag pool- and Pol pool- specific T cell lines from day 15 were added in to the culture wells at a 10:1 effector to target ratio. Targets alone and un-pulsed CFSE targets were also set-up as controls. Cells were cultured for 18 hours before being stained with Violet Live/Dead and CD8-APC mAb. Samples were fixed and acquired on the Cyan ADP flow cytometer.

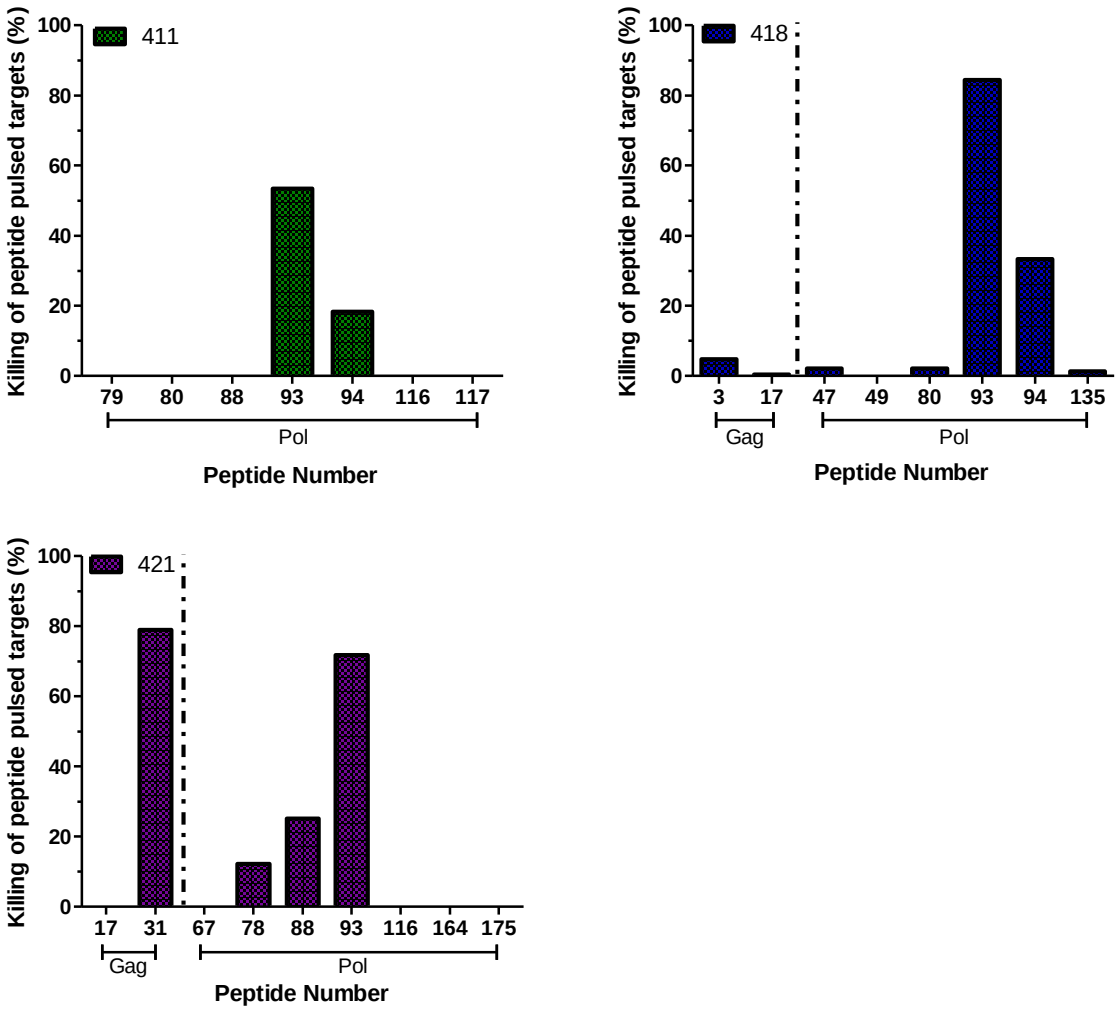


Figure 44 Determining the specificities of vaccine-elicited T cells with cytotoxic effector function. Gag- and Pol peptide pool expanded T-cell lines from vaccinees 411, 418 and 421 were tested in an *in vitro* killing assay. Target $CD4^+$ T cells were pulsed with individual peptides from the pools initially used to generate the T-cell lines. Un-pulsed target cells were used as a negative control and background subtracted values are shown. All co-cultures were setup at an effector ($CD8^+$) to target ($CD4^+$) cell ratio of 10:1. The HIV-1 protein origins of the numbered peptides are indicated beneath each graph. The dashed line separates Gag and Pol responses.

The cell killing assay data, Figure 44, show that for the broad virus controllers, (vaccinees 411 and 418) the majority of the Pol pool-specific T cells induced by HIVconsv vaccination could recognise and kill 53.4% and 83.4% of peptide 93 pulsed target cells, respectively, at an effector to target ratio of 10:1. Peptide 94 also induced a killing response of 18.3% and 33.3% in these two vaccinees, which was lower than for peptide 93. This may have been as a result of an overlapping epitope that was present within both peptides. For

vaccinee 411 there were no other peptides that induced a killing response by their Pol pool-specific T cells. Vaccinee 418, did however, show additional low level killing responses to peptides 47, 80 and 135 of ≤2.1%, suggesting a minimal contribution to the observed Pol pool-specific virus inhibition. For vaccinee 421, who controlled 3/8 virus isolates, the most efficient Pol pool-specific killing response was also induced by peptide 93 as 71.8% of target cells were lysed. In addition, this vaccinee showed a Pol pool-specific killing response to peptides 78 and 88 of 12.2% and 25.1%, respectively.

When the Gag pool-specific T-cell killing responses were evaluated, vaccinee 421 demonstrated the greatest efficiency with 78.9% killing of target cells pulsed with peptide 31. In contrast, vaccinee 418 showed lower cytotoxic capacities with 4.8% and 0.4% killing of targets pulsed with Gag peptides 3 and 17 respectively.

Gag pool- and Pol pool-specific cell lines from virus controllers 411, 418 and 421 were next evaluated for their ability to produce antiviral cytokines and degranulate in response to individual HIVconsv peptides. Frequencies of mono- and polyfunctional T cells exhibiting antiviral effector functions were determined using an antiviral intra-cellular cytokine staining (ICS) panel. The ICS method was adapted from the protocol originally used in Chapter 3. Figure 45 shows the response of Pol pool-specific T cells, from vaccinee 421, to stimulation with peptide 31 and the gating strategy employed for all samples. The mono-functional and polyfunctional T-cell responses to HIVconsv peptides are shown in Figure 46 and Figure 47 respectively.

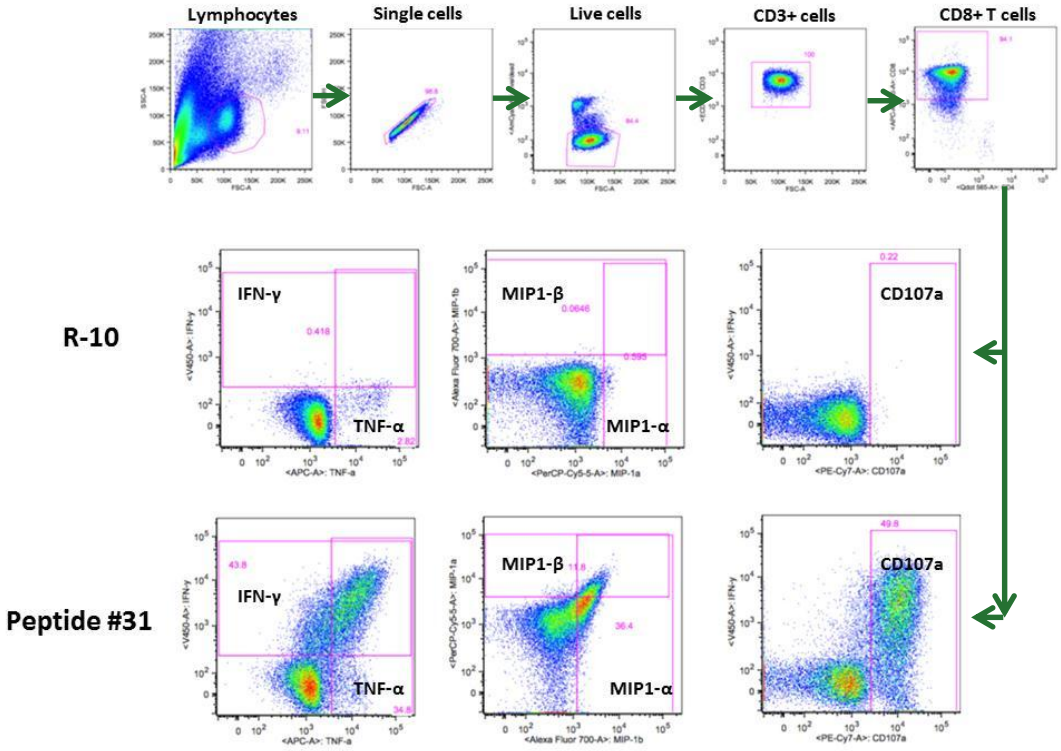


Figure 45 Example flow cytometry gating of mono- and poly-functional antiviral T cells. Gag pool- and Pol pool-specific T-cell lines were stimulated for 6 hours with individual HIVconsv peptides used for cell line generation. The following day cells were stained with anti-CD107a PE-Cy7 mAb and the cell surface markers anti-CD3 ECD anti-CD8 APC-efluor780, anti-CD4 BV570 mAbs and Aqua Live dead. Antiviral functions were assessed by intra-cellular staining with anti-IFN-γ V450, anti-TNF-α APC, anti-MIP-1α PerCP efluor710 and anti-MIP-1β Alxfluor 700 mAbs. Cells were fixed in paraformaldehyde and acquired on a BD LSRII flow cytometer. Cells were sequentially gated from lymphocytes to $CD8^+$ T cells and the R-10 (mock) response was subtracted from the peptide-specific response (peptide#31) to give the reported value.

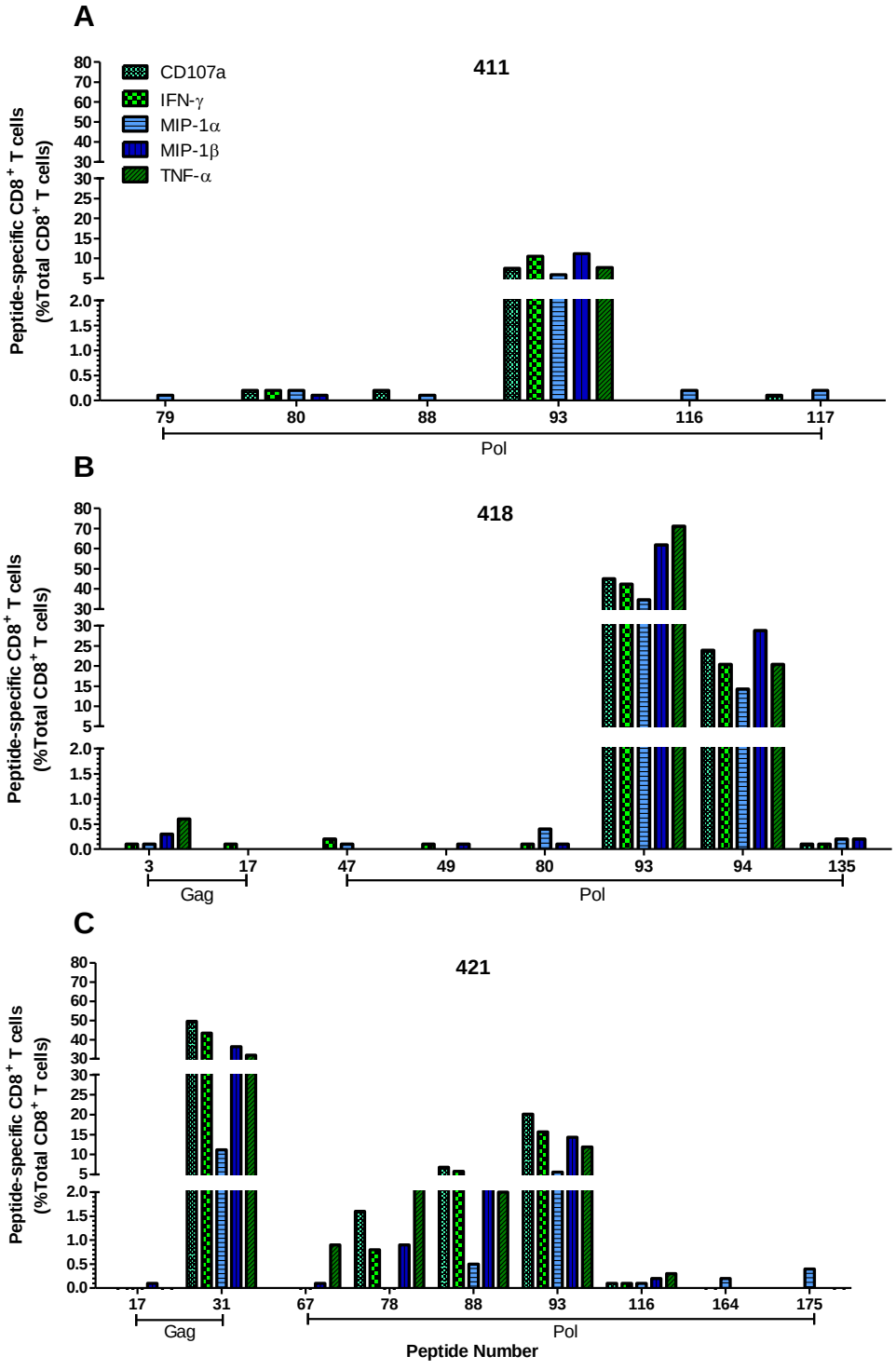


Figure 46 Frequencies of Gag- and Pol-specific T cells with antiviral effector functions. Peptide pool expanded Gag and Pol T-cell lines from vaccinees 411 (A), 418 (B) and 421 (C) were assessed in an ICS assay, for a variety of antiviral effector functions, in response to individual HIVconsv peptides. The HIV-1 protein origin is shown below the peptide number. For each effector function the percentage of $CD8^+$ T cells responding to each peptide is shown.

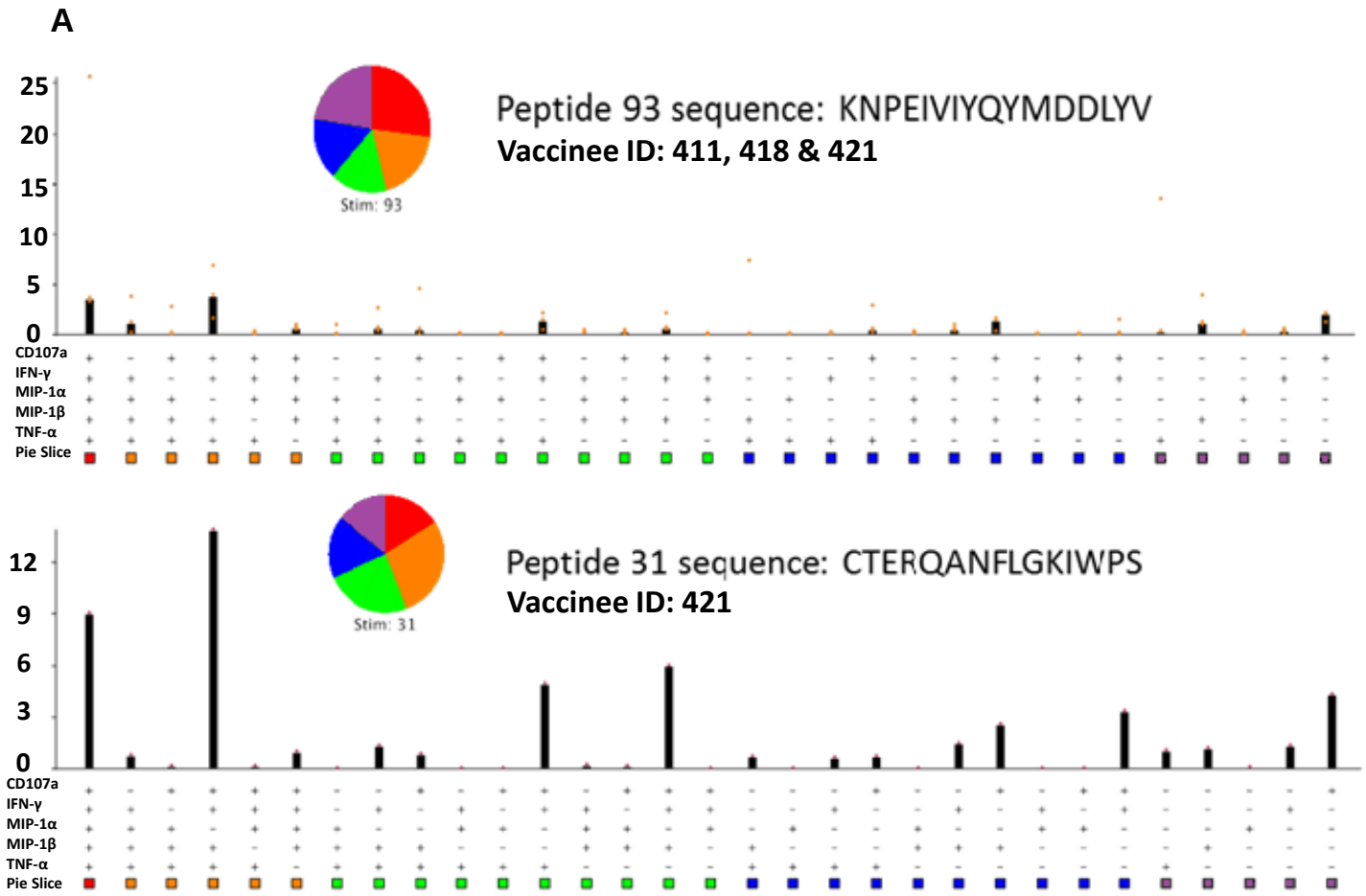


Figure 47A and B Frequencies of polyfunctional peptide pool expanded Gag- and Pol-specific T cells. Polyfunctional responses were determined from the antiviral ICS data. Boolean gating was performed in Flow Jo and results were background corrected in Pestle. The mean frequencies of T cells, with each functional combination, for all vaccinees responding to each peptide are displayed in each SPICE graph. Peptide sequences are shown above each graph. Number of functions; Purple = 1, Blue = 2, Green = 3, Orange = 4 and Red = 5.

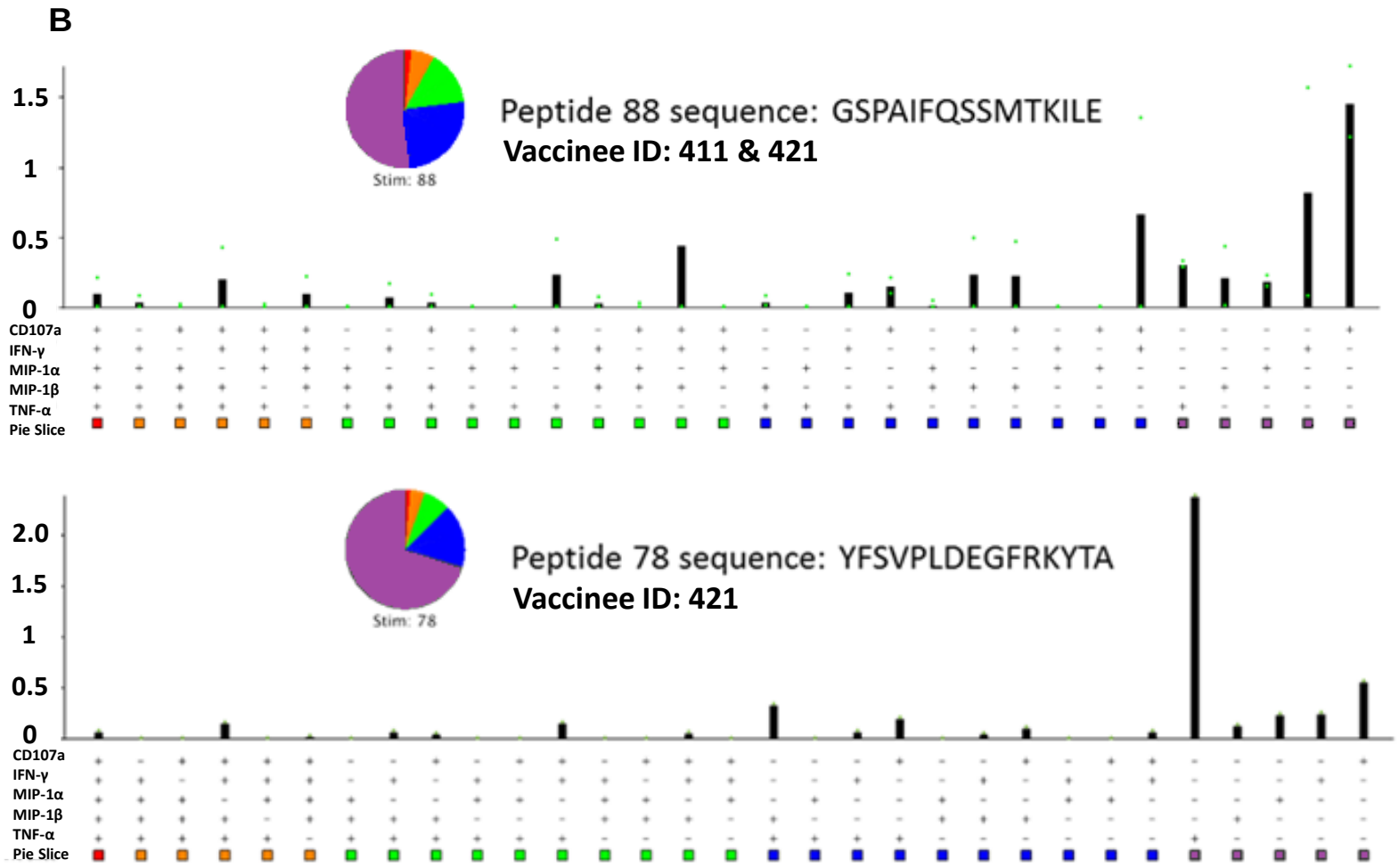

B
1.5
1
0.5
0
Stim: 88
Peptide 88 sequence: GSPAIFQSSMTKILE
Vaccinee ID: 411 & 421
CD107a
IFN-γ
MIP-1α
MIP-1β
TNF-α
Pie Slice
2.0
1.5
1
0.5
0
Stim: 78
Peptide 78 sequence: YFSVPLDEGFRKYTA
Vaccinee ID: 421
CD107a
IFN-γ
MIP-1α
MIP-1β
TNF-α
Pie Slice

Figure 46 showed that in response to peptide 93, $CD8^+$ T cells from all three vaccinees, were able to produce MIP-1α, MIP 1-β , IFN-γ and TNF-α. These cells were also capable of degranulation represented by the staining of CD107a. The percentage of responding T cells for all 3 vaccinees ranged from 7.5 - 45.0% for CD107a, 10.5 - 42.3% for IFN-γ, 5.9 - 34.6% for MIP-1α, 11.2 - 61.8% for MIP-1β and 7.7 – 11.2% for TNF-α. Interestingly, vaccinee 411 showed the lowest frequencies of mono-functional T cells and vaccinee 418 showed the highest frequencies, despite higher levels of virus inhibition detected for vaccinee 411. When the polyfunctional T-cell profiles were examined in response to peptide 93 (Figure 47A) the data showed that most T cells were capable of producing 4-5 effector functions simultaneously, with MIP-1α co-expressed the least.

Vaccinee 421 showed additional response to Pol peptides 88, 78 and 67. Peptides 88 and 78 induced the greatest breadth of mono-functional T cells with CD107a, MIP-1β, IFN-γ and TNF-α producing cells detected. However, lower frequencies of T cells responded to these peptides when compared to peptide 93. Polyfunctionality was also examined in response to peptide 88 for vaccinees 421 and 411, and peptide 78 for vaccinee 421 only (Figure 47B). This analysis revealed that most T cells responding to these peptides had limited polyfunctionality, expressing only 1 – 2 antiviral functions.

Furthermore, when the Gag-specific T-cell response was examined, vaccinee 421 showed a high frequency of T cells (>30%) produced MIP-1β, IFN-γ, TNF-α and degranulated in response to peptide 31. Most T cells that were specific for peptide 31 also showed a polyfunctional effector function (Figure 47A) with 3 - 5 functions co-expressed.

Correlation analyses were performed on these data to assess if the magnitude of the response to each individual peptide was related to the magnitude of the polyfunctional response to the peptide. Magnitude was calculated as the percentage of $CD8^+$ T cells responding to each peptide by any one of the 5 antiviral effector functions. Polyfunctionality

was calculated as the total percentage of T cells expressing 2-5 effector functions in response to each peptide. Figure 48 shows that there were significant positive correlations ($P = <0.05$) between the two variables suggesting that induction of high frequencies of conserved region HIV-1-specific T cells also results in induction of high quality T cell responses. It may however, be better to examine this relationship using tetramers to more accurately determine the frequencies of peptide-specific T cells and combine these results with the polyfunctionality data shown here.

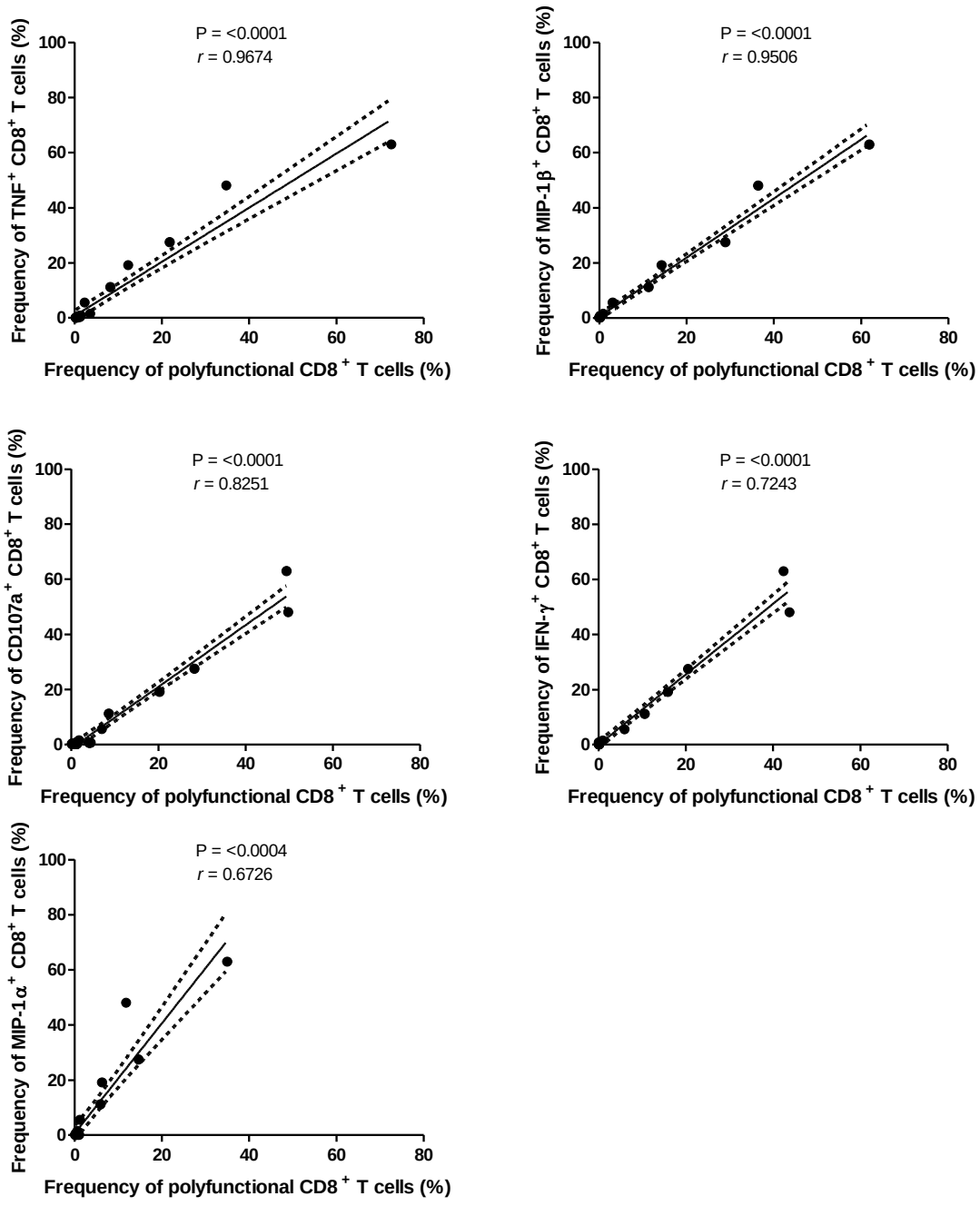


Figure 48 Correlation between the magnitude of peptide pool expanded HIV-1-specific T cells and the magnitude of the polyfunctional T-cell response. The percentage of T cells specific for each HIVconsv peptide were correlated with the total frequencies (%) of polyfunctional T cells (2-5 functions) per peptide. For each correlation Spearman rank (r) and P values (two-tailed) are shown.

6.5 Multiple T-cell specificities can contribute to control of *in vitro* HIV-1 replication

A direct investigation in to which T-cell specificities were able to mediate *in vitro* HIV-1 control was performed by preparing single peptide-specific T-cell lines for vaccinees 411, 418 and 421. The CVIA protocol was adapted to use 10 day short-term cell lines (STCLs) expanded with individual peptides mapped using the IFN-γ ELISpot assay or a pool of the relevant peptides. Non-specific control peptide lines were also prepared from either a pre-vaccination sample stimulated with the relevant HIV-1 peptide pool or a post vaccination sample that was stimulated by a peptide that was not recognised during the IFN-γ ELISpot mapping. These non-specific cell lines were used to set the background virus inhibition levels for each isolate evaluated.

The first vaccinee to be assessed was the broad virus controller 411 who was able to inhibit 7/8 viral isolates when his/her $CD8^+$ T cells were non-specifically expanded and tested in the CVIA (Chapter 5). The individual T-cell lines analysed in the CVIA are displayed in Figure 49A, peptide mapping in this individual revealed that they recognised several Pol peptides, no Gag peptides and a single peptide within Env, as a result the Env peptide was also used to prepare a T-cell line. The results for vaccinee 411 show that all T-cell specificities were able to inhibit IIIB viral replication above the non-specific background level of 0.74 $\log_{10}$. T-cells specific for peptide 80 in Pol showed the greatest capacity for virus control as a 3.56 $\log_{10}$ reduction in p24 was detected. The Env + Pol-pool (E+P-Pool) cell line also showed good control of HIV-1 replication with a reduction in p24 of 3.35 $\log_{10}$ detected. To evaluate the effect of increasing the number of effector cells compared to target cells the CVIA was set-up at increasing E:T ratios of 1:1, 2:1 and 3:1. The data in Figure 49B show that increasing the E:T ratio for the strongest inhibitory T-cell line recognising peptide 80 made no difference to the level of virus inhibition that was achieved, in contrast for the

weakest inhibitory T-cell line specific for peptide 93, doubling the E:T ratio considerably increased the level of virus inhibition by 0.76 $\log_{10}$.

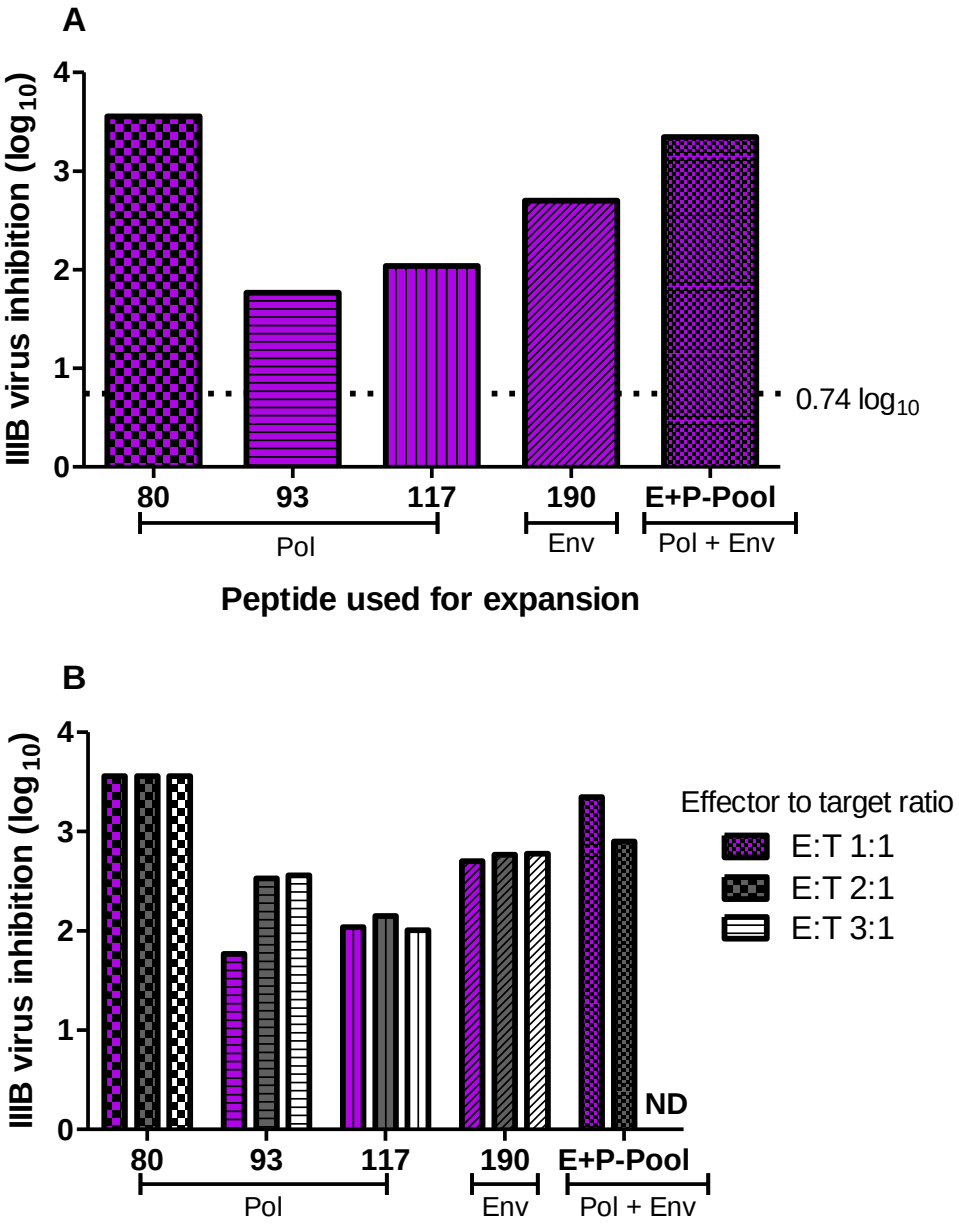


Figure 49 HIV-1 virus inhibition mediated by single peptide-expanded T-cell lines from vaccinee 411. Short-term T-cell lines were generated for vaccinee 411, a broad virus controller, from the peak VIA time point (week 9) and tested in the CVIA against the HIV-1 IIIB isolate. A pre-vaccination T-cell line was also prepared which was stimulated with the same pool of peptides and this was used to set the background inhibition of 0.74 $\log_{10}$ on day 13 of co-culture **(A)**. For each T-cell line several effector to target ratios were assessed in the CVIA, each one is colour-coded; purple = 1:1, grey = 2:1 and white = 3:1. The Env + Pol pool (E+P-Pool) was not assessed (ND) at a 3:1 ratio due to limited cell numbers **(B)**.

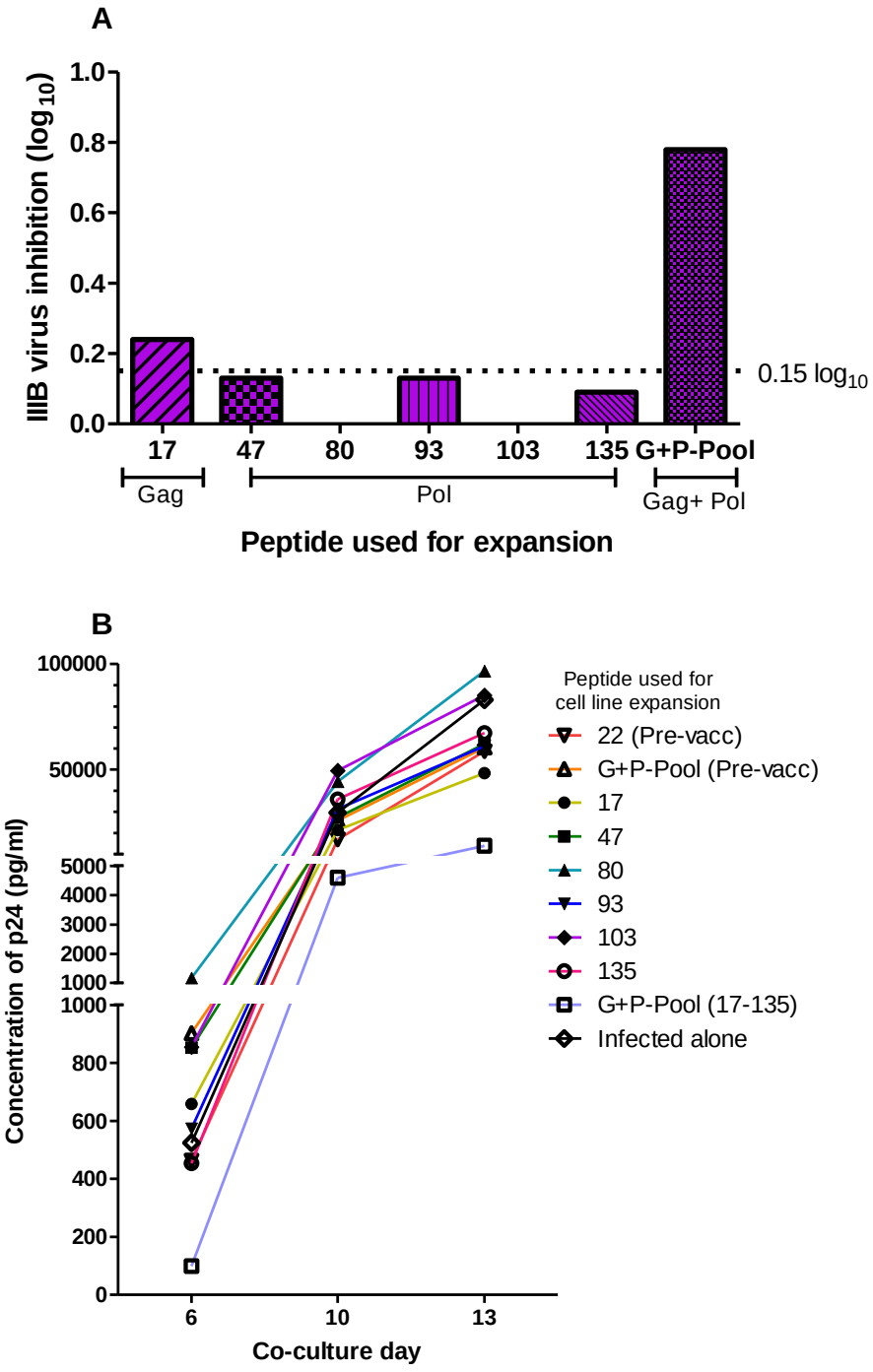


Figure 50 HIV-1 inhibition mediated by single peptide-expanded T-cell lines for vaccinee 418. Short-term cell lines were prepared for vaccinee 418 from IFN-γ ELISpot mapped peptides. These cell lines were tested in a CVIA against the IIIB, clade B, isolate. Supernatants were collected on day 6, 10 and 13 and frozen. A p24 ELISA was performed on the samples and the reduction in p24 concentration was calculated compared to infected cells alone on day 13 **(A)**. Two pre-vaccination cell lines; peptide 22 and a Gag + Pol peptide pool (G+P Pool) were also assessed. Pre-vaccination peptide 22 T-cell line was used to set the background cut-off of

0.15 $\log_{10}$ for the day 13 viral inhibition. The reduction in p24 concentration over time is shown for each T-cell line **(B)**.

Peptide-specific T-cell lines generated for vaccinee 418 were also tested for virus inhibition of the HIV-1 IIIB isolate Figure 50A. The data revealed that these individual cell lines showed very weak control of HIV-1 after 13 days of co-culture and for most T cell specificities (47, 80, 93, 103 and 135) in Pol the level of virus inhibition did not reach above background (0.15 $\log_{10}$). The Gag peptide 17-specific cell line showed minimal control of virus replication, and the greatest inhibition of 0.72 $\log_{10}$ reduction in viral p24, was as a result of the combined Gag and Pol T-cell specificities shown here as the G+P pool response. Early examination of the inhibitory effect for each cell line (Figure 50B) showed that the combined pool of T-cell specificities was able to inhibit the virus after 5 days of co-culture, and that this was maintained over the 13 day analysis. In contrast, the only individual T-cell specificity that made a detectable inhibitory response after 6 days of co-culture was peptide 135 in Pol, and this was minimal. These data also suggest that different T-cell specificities may differ in the time that they mediate control of virus with multiple specificities (G+P Pool cell line) showing an effect earlier than T-cell lines targeting a single peptide.

Vaccinee 421 was the last individual to be assessed using peptide-expanded T-cell lines and CVIA. Figure 51 shows that for vaccinee 421, T cells with the greatest capacity to inhibit HIV-1 IIIB were specific for peptide 31 in Gag and showed a reduction in p24 levels of 2.29 $\log_{10}$. T cells specific for peptides 88 in Pol and 17 in Gag, were also capable of inhibiting virus replication by 1.07 and 1.04 $\log_{10}$, respectively. The Pol pool, represented T cells specific for multiple Pol peptides, and showed higher levels of virus inhibition (1.43 $\log_{10}$ reduction in p24) compared to T cells specific for any individual Pol peptide. In contrast, T cells specific for the Gag pool showed virus inhibition of 1.94 $\log_{10}$, which was 0.35 $\log_{10}$ lower than that detected for peptide 31-specific T cells.

When the clade A U455 isolate was examined T cells specific for individual peptides 67, 88, 93 and 117 were all capable of inhibiting virus replication, by 1.59, 1.91, 1.68 and 2.12 $\log_{10}$, respectively. But, as observed with the IIIB virus, T cells specific for the Pol pool showed increased levels of U455 virus inhibition (2.45 $\log_{10}$ reduction in p24) compared to any individual Pol-specific T-cell line. However, the highest level of virus inhibition was shown for T cells specific for the Gag pool with a reduction in p24 of 3.39 $\log_{10}$. This level of inhibition was slightly higher than shown for peptide 31-specific T cells which showed a 3.16 $\log_{10}$ reduction in viral p24. A two way analysis of variance was performed for these data and revealed that both the specificity of the T cell and the HIV-1 isolate used for infection contributed significantly to the detected levels of virus inhibition. The T-cell specificity and viral isolate accounted for 59.7% ($P<0.0004$) and 34.7% ($P<0.0001$) of the variance, respectively.

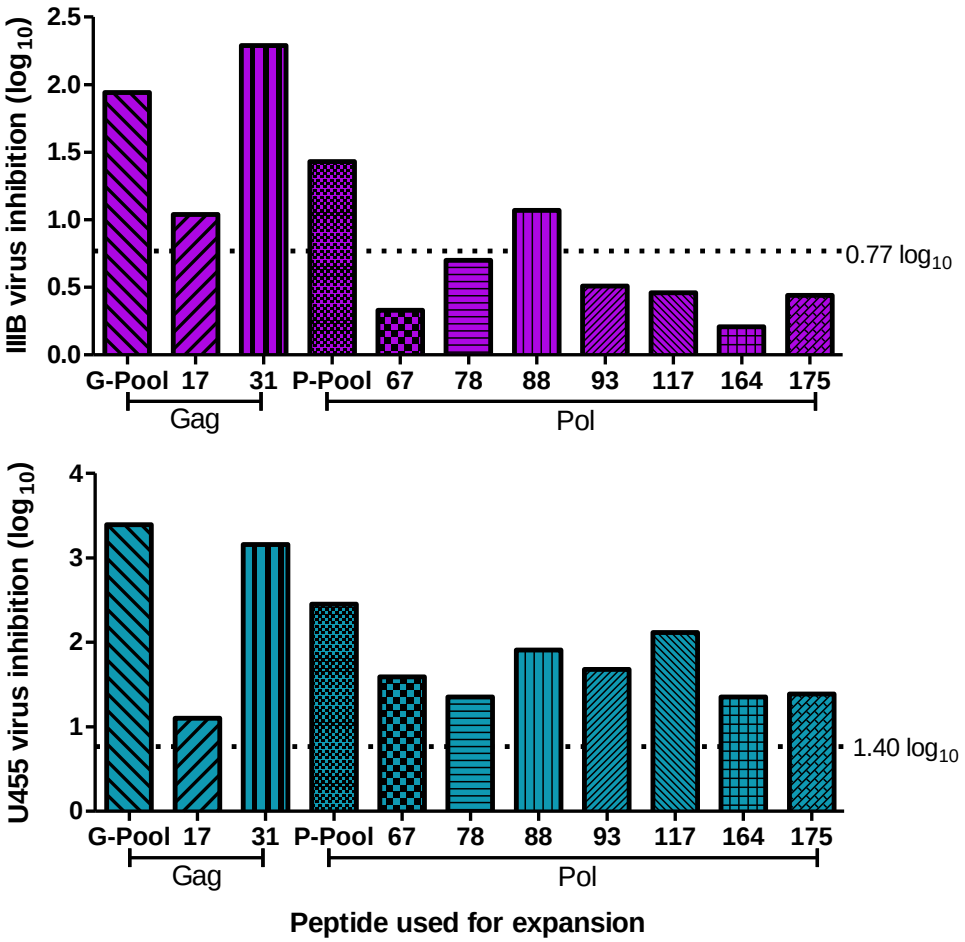


Figure 51 HIV-1 inhibition mediated by single peptide-specific T-cell lines for vaccinee 421. Short-term cell lines were prepared for vaccinee 421 from peptides mapped using the IFN-γ ELISpot assay. These cell lines were tested in a CVIA against the IIIB, clade B, and U455, clade A, viral isolates. Supernatants were collected on day 13 and frozen. A p24 ELISA was performed on the samples and the log reduction in p24 concentration was calculated compared to infected cells alone. An irrelevant cell line (peptide 22) was also assessed and used to set the cut-off of 0.77 $\log_{10}$ and 1.4 $\log_{10}$ for the IIIB and U455 isolates, respectively. G-Pool = Gag peptide pool and P-Pool = Pol peptide pool.

The single peptide-expanded STCLs from all three vaccinees were also evaluated by ICS for IFN-γ, TNF-α, MIP-1β and CD107a production for both the $CD8^+$ and $CD4^+$ T-cell populations. The results, shown in Figure 52, suggest that there were several $CD8^+$ T-cell lines from each vaccinee that were capable of degranulation and production of antiviral effector molecules in response to peptide stimulation. The ICS data also revealed that $CD4^+$ T cells with multiple effector functions were present in the STCL and so may have supported

the $CD8^+$ T cells in the CVIA. However, the ICS data for each $CD8^+$ T-cell line was not predictive of the virus control demonstrated by each STCL in the CVIA. This highlights the importance of evaluation by multiple assays to build up a representative profile of T-cell functionality and also shows that cellular responses to peptide stimulation and HIV-1 infection differ.

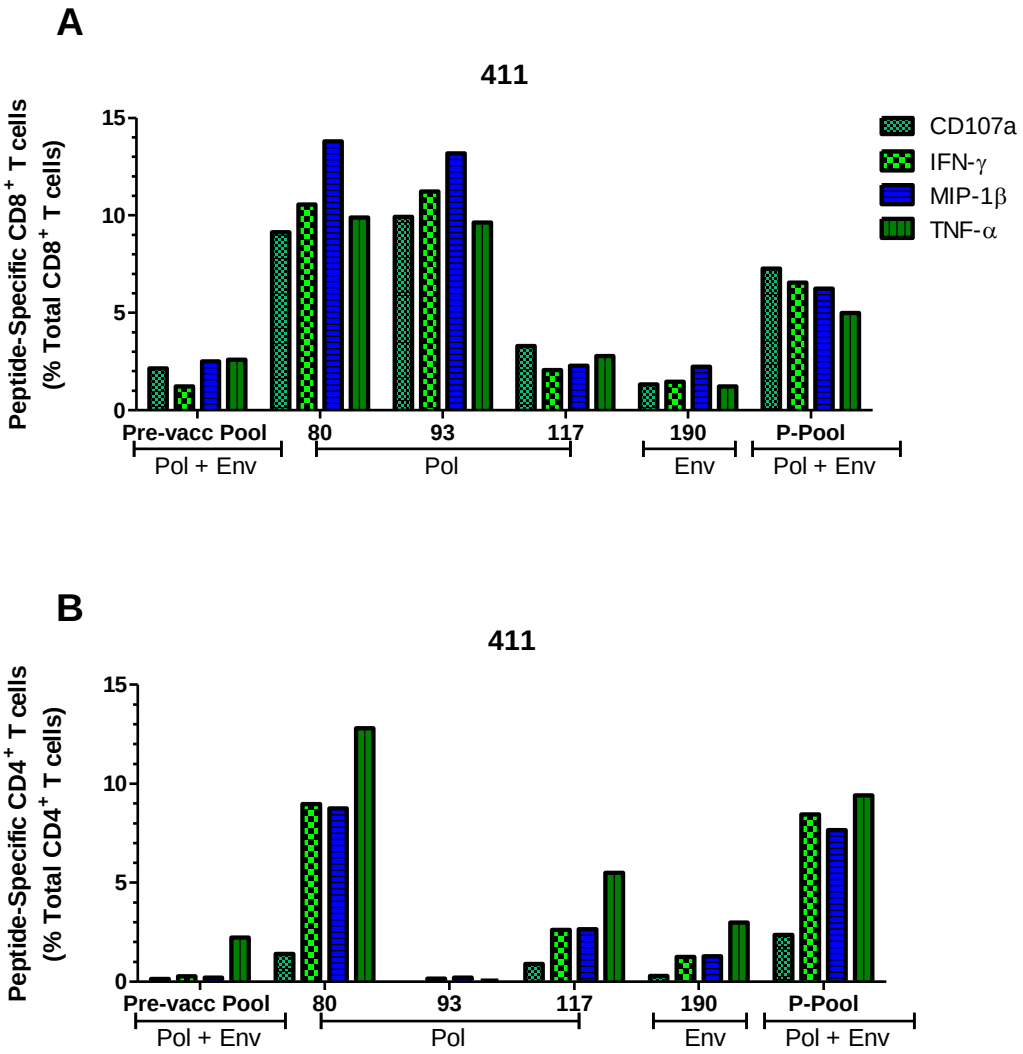
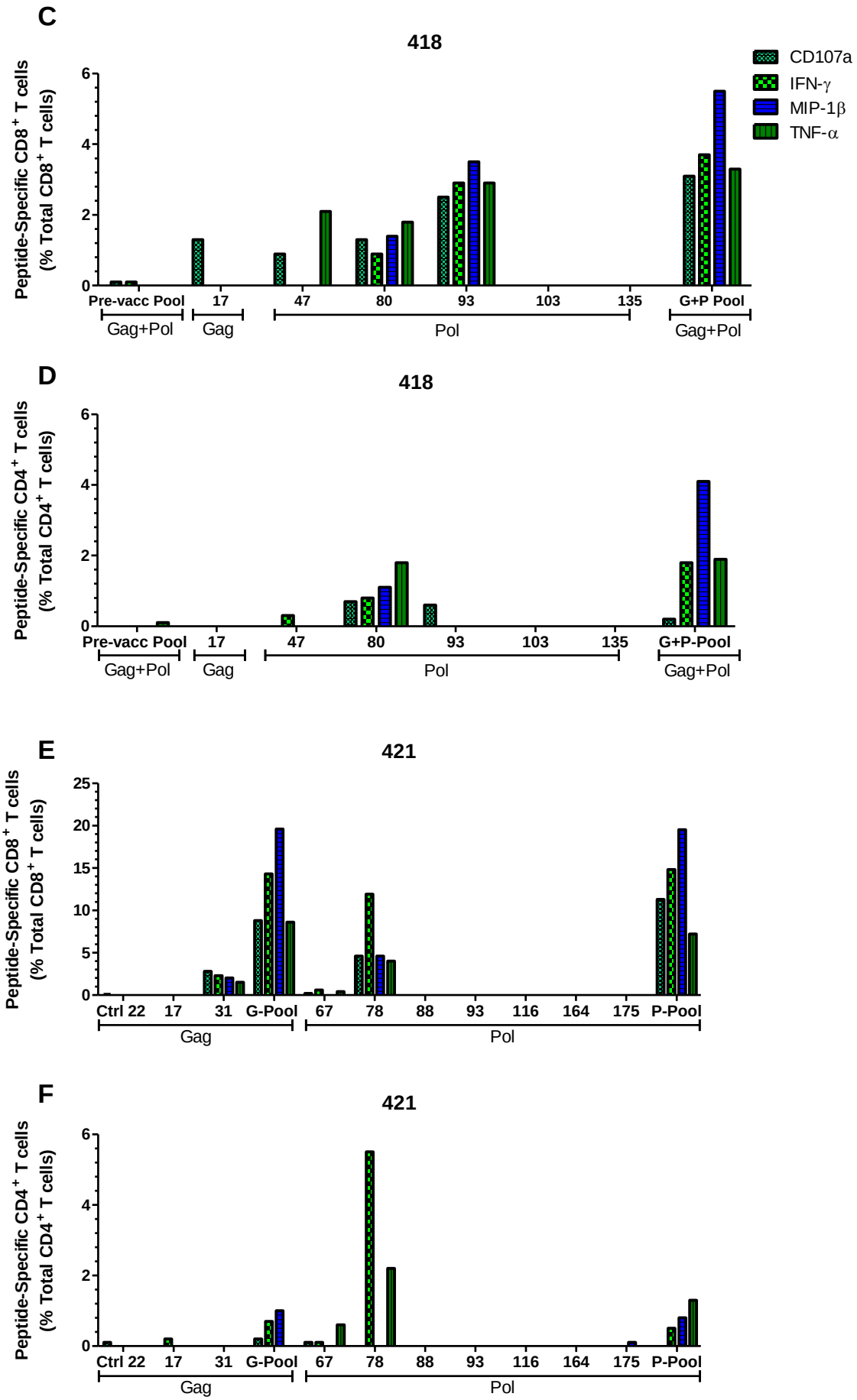


Figure 52 Intracellular cytokine staining of single peptide-expanded T-cell lines from vaccinees 411, 418 and 421. STCLs from all vaccinees were stimulated with the relevant peptide/s for 6 hours before staining for IFN-γ, TNF-α, MIP-1β and CD107a. The background subtracted (nil peptide) percentage of $CD8^+$ (A, C & E) and $CD4^+$ (B, D & F) T cells responding with each function are shown. Below each graph the region of HIV-1 from which each peptide is derived is indicated.


C
418
CD107a
IFN-γ
MIP-1β
TNF-α
Peptide-Specific CD8+ T cells (% Total CD8+ T cells)
Pre-vacc Pool
17
47
80
93
103
135
G+P Pool
Gag+Pol
Gag
Pol
Gag+Pol
D
418
Peptide-Specific CD4+ T cells (% Total CD4+ T cells)
Pre-vacc Pool
17
47
80
93
103
135
G+P-Pool
Gag+Pol
Gag
Pol
Gag+Pol
E
421
Peptide-Specific CD8+ T cells (% Total CD8+ T cells)
Ctrl 22
17
31
G-Pool
67
78
88
93
116
164
175
P-Pool
Gag
Pol
F
421
Peptide-Specific CD4+ T cells (% Total CD4+ T cells)
Ctrl 22
17
31
G-Pool
67
78
88
93
116
164
175
P-Pool
Gag
Pol

Natural killer (NK) cells have also been implicated in control of HIV-1 infection and as a result these cells were quantified in the T-cell lines for vaccinee 418 and were shown to represent <2.7% of the total population following peptide expansion, natural killer T cells (NKT) were also quantified and represented <3.8% of the total lymphocytes. In all cell lines prepared for vaccinee 418, the main cell type present was T cells at >92.6%. Representative FACS plots are shown for T-cell lines specific for the Gag + Pol pool and peptide 17 (Figure 53), cell phenotypes were based on those defined by West et al. 2011 [456]. These results suggest that T cells were the primary contributor to the virus inhibition and cytokine production measured for each STCL, but the small population of NK and NKT cells may have also played a direct or indirect role in these assays.

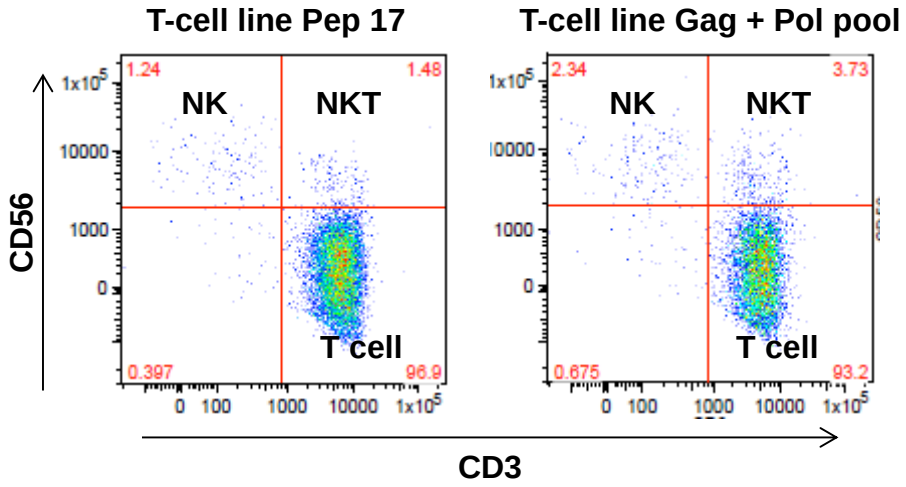


Figure 53 Cell phenotype analyses of peptide-expanded T-cell lines for vaccinee 418. All T-cell lines from vaccinee 418 were stained for NK ($CD3^-$ $CD56^+$), NKT ($CD3^+$ $CD56^+$) and T cells ($CD3^+$ $CD56^-$) to determine the frequencies of each population. The two FACS plots are representative of the phenotypic data generated from this vaccinee.

6.6 Identification of T-cell epitopes contributing to control of *in vitro* HIV-1 infection

$CD8^+$ T cells targeting several Pol and Gag peptides were shown to contribute to control of HIV-1 replication; this was potentially mediated by both cytolysis and secretion of soluble β-chemokines and cytokines. To further define the T-cell epitopes responsible for induction of these functions, and the subsequent reduction in viral replication, epitope mapping was performed. T cells from week 28 were stimulated with the relevant 15-mer parent peptides for 10 days, before being tested for functional responses (IFN-γ, TNF-α and CD107a expression) by ICS to truncated peptide sequences. The loss of the response was representative of the loss of a critical amino acid required for T-cell recognition and function. T-cell responses to multiple peptides were mapped following this protocol for vaccinees 411, 418 and 421.

Figure 54A shows an example of the T-cell response to peptide 93 (parent 15-mer) and to the truncated peptides for vaccinee 411. All three effector functions examined by ICS showed the same pattern of response for each truncated peptide (data not shown). Confirmation of $CD8^+$ and $CD4^+$ T cell phenotype was also made using data from these experiments. Figure 54B shows that for vaccinee 411, peptides 80 and 93 were $CD8^+$ T cell epitopes, and peptide 88 was identified as a $CD4^+$ T cell epitope. Similarly, for vaccinee 418, peptides 93, 103 and 135 were identified as $CD8^+$ T cell epitopes, as were peptides 31, 78, 88 and 93 for vaccinee 421.

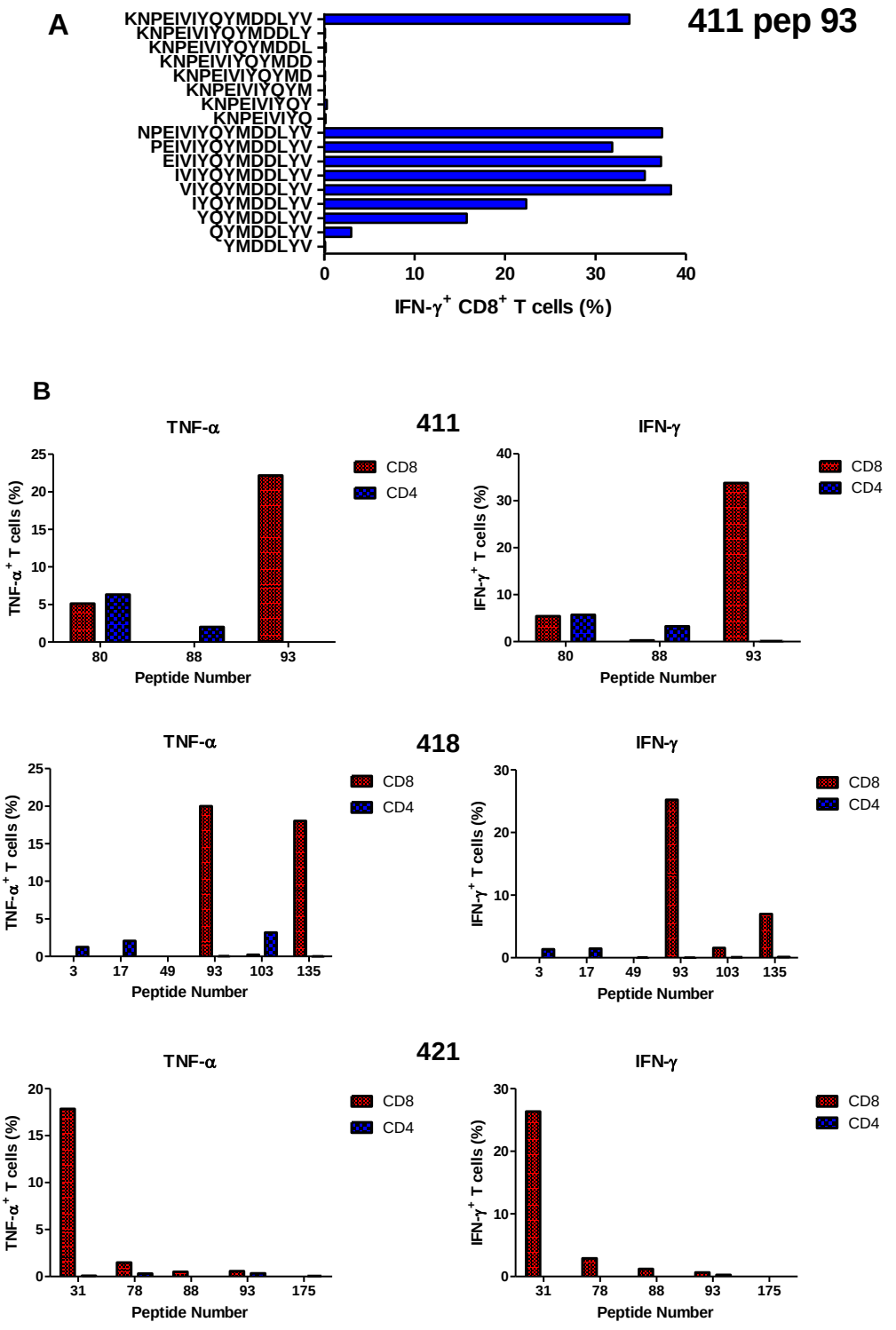


Figure 54 Identification of CD8$^+$ T-cell epitopes contributing to *in vitro* control of HIV-1infection. Epitope mapping was performed for vaccinees 411, 418 and 421. Short-term cell lines were prepared using the parent 15 mer peptide. Cells were rested and then stimulated with truncated peptides for 6 hours. The followed day ICS was performed and cells were acquired on a BD LSRII flow cytometer. Example mapping data for peptide 93 in vaccinee 411 is shown **(A)**. The identification of CD8$^+$ and CD4$^+$ T-cell epitopes was also determined from these data for each vaccinee **(B)**.

Table 9 shows the mapped T-cell epitopes for each vaccinee and the predicted HLA allele that would present this epitope based on the vaccinees HLA type and reported responses in the Los Alamos National Laboratory (LANL) HIV database [457]. The epitope mapping results revealed that for all 3 vaccinees the T-cell epitope in peptide 93 was YQYMDDLYV. In the LANL database this epitope was reported to bind to HLA A*0201. In addition, for vaccinee 421, the epitope present within peptide 31 was mapped to TERQANFL and was reported to be presented by HLA B*4002.

Table 9 Mapped CD8$^+$ T-cell epitopes for vaccinees 411, 418 and 421.

Vaccinee (HLA Type)	Peptide No.	Mapped Epitope	Predicted HLA*
411 (A*0201 / 0201) (B*0801 / 5101) (Cw*0303 / 0701)	80	TAFTIPSI	B*5101
	88	CD4$^+$ epitope	ND
	93	YQYMDDLYV	A*0201
418 (A*2402 / 0201) (B*0702 / 2705) (Cw*0102 / 0702)	93	YQYMDDLYV	A*0201
	103	TWKSLVKH	None
	135	KLVSQGIRKV	None
421 (A*1101 / 0201) (B*4002 / 3503) (Cw*0202 / 1203)	31	TERQANFL	B*4002
	78	SVPLDEGFRK	A*1101
	88	AIFQSSMTK	A*1101
	93	YQYMDDLYV	A*0201

* HLA prediction is based on reported epitope binding in the LANL HIV database [457]. Red indicates a difference in the reported amino acid in the database (S reported). Underlined residues represent HLA anchor residues. ND = Not done.

6.7 Pol-specific T cells recognise multiple escape variants of YQYMDDLYV

A preliminary assessment of the breadth of cross-reactivity by Pol-specific T cells responding to the mapped epitope YQYMDDLYV was performed to provide insight as to whether this epitope may have been responsible for the broad virus control demonstrated by vaccinees 411 and 418. A panel of variant peptides which represented escape variants and antiretroviral drug-induced mutants of this previously reported epitope were tested with the cell lines in an IFN-γ ELISpot assay.

Figure 55 shows that for vaccinee 418 at the highest peptide concentration all 5 peptides were effectively responded to with a range of 172.5 – 214.5 SFU/5x10^4 cells. However, at the lower peptide concentration of 0.002 µg/ml, a greater distinction could be made between T-cell responses to each variant. The most effective induction of T cells was to the mapped peptide sequence of YQYMDDLYV (60.5 SFU/5x10^4 cells), followed by YQY**V**DDLYV (44.5 SFU/5x10^4 cells) and YQYMDDLY**I** (30.5 SFU/5x10^4 cells). The 9-mer peptide that induced the lowest T-cell frequency of 15.5 SFU/5x10^4 cells was **C**QYMDDLYV suggesting an important role for the N-terminal amino acid in T-cell recognition and functional response. However, the C-terminal mutant YQYMDDLY**I** induced a lower frequency of responding T cells compared to the epitope bearing a more central amino acid change of YQY**V**DDLYV suggesting greater plasticity is acceptable in this central region. The 15-mer parent peptide showed a significantly (P = <0.05) lower T cell response (2.5 SFU/5x10^4 cells) compared with the mapped 9-mer epitope YQYMDDLYV at the lowest peptide concentration, however, this 15-mer peptide is likely to have required additional cleavage to the optimal T-cell epitope length of 8-10 amino acids [458, 459]. The data from vaccinee 411 was difficult to interpret due to high background and so is not presented here.

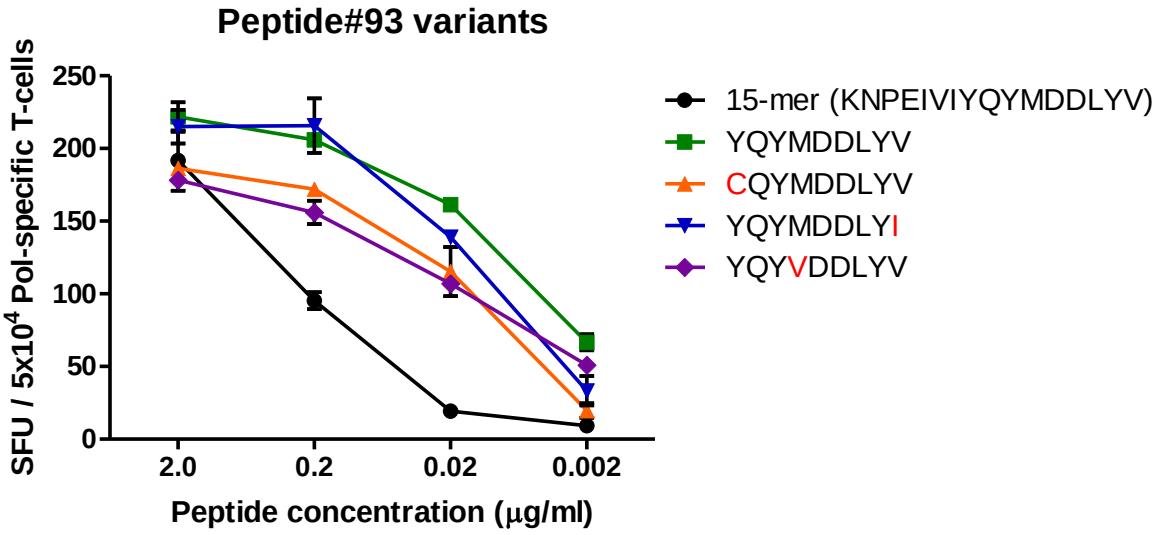


Figure 55 Recognition of multiple variants of YQYMDDLYV by Pol-specific T cells. Pol-specific T cells from vaccinee 418 were tested against peptides representing clade and escape variants of YQYMDDLYV in an IFN-γ ELISpot assay. Peptide variants were serially diluted from 2 µg/ml to 0.002 µg/ml. R-10 was included as a negative control and PHA as a positive control. T cells were plated at $5x10^4$ cells per well, the background subtracted results are shown with error bars representing standard deviation. A 1-way ANOVA was performed at the 0.002 µg/ml peptide concentration with a Dunn's post-test correction.

6.8 Chapter 6 Discussion

The results from this chapter have shown that HIVconsv vaccine-induced Gag- and Pol-specific T cells differed in their ability to control clade A and B HIV-1 replication. Pol-specific T-cell lines from all 5 vaccinees were able to control replication of both the clade A and B virus isolates. However, fewer (2/5) vaccinees Gag-specific T cell lines showed this capability. These results, in contrast to data from animal studies [306] and natural HIV-1 infection [447], suggest that inclusion of conserved regions of Pol within a T-cell vaccine could act to reduce the amount of viral dissemination and slow the rate of progression to AIDS.

In natural infection, there are fewer Pol transcripts produced with an estimated Gag:Pol ratio of 20:1 [460]. This limits the availability of Pol for presentation to T cells and may serve as a reason for reduced T-cell priming by this protein. However, the Pol gene encodes a

number of essential proteins [449] required for the generation of infectious virions [25], and targeting of these conserved proteins by vaccination may offer an advantage to the natural hierarchy of T-cell specificities detected during primary infection [118]. Importantly, shown here, the lower abundance of Pol did not prevent HIV-1 infected T cells from being recognised and inhibited.

After establishing that Pol pool-specific T-cell lines and to a lesser extent Gag pool-specific T-cell lines from all 5 vaccinees could control *in vitro* virus replication, 3 of the vaccinees were examined further for the mechanism of action of these memory T cells. These analyses revealed that both cytotoxic and non-cytotoxic effector functions were induced in response to peptide stimulus. T cells specific for peptides 93 (Pol) and 31 (Gag) could effectively lyse peptide pulsed targets and a large proportion also produced multiple cytokines and β-chemokines (MIP-1α and MIP-1β) which have been shown to impede HIV-1 replication [336, 339].

For vaccinees 411 and 418 T cells specific for peptide 93 in the Pol pool dominated their ICS and cell killing assay responses suggesting that this was the main population contributing to virus control in these individuals. However, for vaccinee 421 their dominant response was driven by T cells specific for peptide 31 from the Gag pool. Vaccinee 421, like the broad virus controllers, also had highly functional T cells specific for peptide 93 in addition to low frequency T cells specific for peptides 88, 78 and 67 from the Pol pool. However, these low frequency T cells showed reduced cytotoxicity and limited polyfunctionality when compared to those specific for peptide 93.

The most compelling data on individual T-cell specificity and control of virus replication came from the single peptide expanded short-term cell lines (STCL) tested in the CVIA against the clade A and B (U455 and IIIB) isolates. Vaccinee 411, the broadest virus controller, was able to inhibit viral replication with all of his/her individual Pol and Env

specific T-cell lines in contrast to the other three vaccinees, but interestingly the peptide 93 cell line was the weakest. The strongest inhibition was detected with the peptide 80 specific cell line and the complete pool (Env + Pol) showed the second highest inhibitory response. In vaccinee 421, T cells specific for peptide 31 showed the greatest ability to control both viral isolates. In contrast, T cells specific for the pool of Pol peptides were able to control more effectively than any single Pol specificity in this individual. This enhanced control of *in vitro* HIV-1 infection by multiple specificities of T cells targeting low entropy Pol epitopes was also observed for vaccinee 418. These single peptide expanded STCL CVIA results were surprising, given the dominant and highly functional response of peptide pool expanded Pol-specific T cells responding to peptide 93 by ICS and *in vitro* cell killing assays for vaccinees 411 and 418, and actually suggest that more effective HIV-1 control comes from a greater breadth of inhibitory T cell responses, data which is supported by studies of HIV-1 infected individuals where greater breadth of T cells specific for conserved epitopes is associated with reduced viral load [333].

When the kinetics of virus inhibition was examined with STCLs from vaccinee 418, the data showed that HIVconsv vaccination can effectively prime multiple Pol- and Gag-specific T cells which when combined show faster control of virus replication than any individual T-cell specificity. STCL CVIA results from all three vaccinees also suggested that certain T-cell specificities such as Gag peptide 31 and Pol peptide 80 can independently control viral replication and these will therefore be important to induce through vaccination.

Identification of the individual epitopes that were targeted by each T-cell line was performed and revealed that for vaccinee 421, the epitope within the dominant Gag peptide 31 was TERQANFL, according to the HLA type expressed by vaccinee 421 this epitope is reported to be presented by HLA B*4002 [457]. Encouragingly, this epitope was found to be broadly recognised by multiple ethnicities [461] as was a region which encompassed this

epitope in clade B viruses [462]. Furthermore, this epitope is largely invariant across viral clades [463] and elicits dual-functional T cells within LTNP [464]. These results imply that T cells of this specificity induced through HIVconsv vaccination could be protective for several populations, against a range of HIV-1 isolates.

In broad virus controller 411, the single peptide expanded STCL specific for peptide 80 exhibited the strongest inhibitory capacity and one of the most dominant responses by ICS analyses. The epitope was mapped to TAFTIPSI which is presented by the B*5101 allele [457] and is commonly targeted in LTNP [398, 465]. This specificity was not shown to be as dominant in the Pol pool cell line which was first prepared for this individual, suggesting that it may have been out-competed by T cells specific for peptide 93. Nevertheless, it may well have contributed to the viral control shown by the Pol pool specific cell line even if T-cell numbers were reduced, and in natural infection the dominant population will be influenced by the presentation of viral peptides which is not accounted for when peptide expanded T-cell lines are prepared.

Epitope mapping within vaccinees 411, 418 and 421 also revealed that within peptide 93, YQYMDDLV was the optimal 9 mer epitope, and it is present within the reverse transcriptase (RT) active site [466]. In the LANL HIV database, this epitope is reported to be presented by HLA A*0201, which is one of the most frequently expressed alleles across ethnicities [462, 467]. The high frequency of A*0201 expression suggests that many people should be able to present this epitope to $CD8^+$ T cells and this was shown for the HIV-CORE 002 volunteers, as all vaccinees expressing this allele responded to this peptide at varying levels. There were additional responses from HIV-CORE 002 volunteers to the 15 mer peptide, mainly in those carrying A*30 alleles and from the Immune Epitope Database and analysis resource (IEDB) these alleles had the greatest predicted binding affinity for VIYQYMDDLYV and so could also present the same region of RT. Site-directed

mutagenesis experiments have shown reduced RT activity when residues with catalytic activity Asp-185 and Asp-186 (D) are targeted, in addition to Tyr-183 (Y) (YQ**Y**M**DD**LYV) [466] suggesting that this is an important epitope for $CD8^+$ T cells to exert immune pressure on.

An assessment of the conservation of these mapped epitopes within the HIV-1 isolates used for the VIA (Appendix) revealed that in general the YV9 epitope was maintained in all but one of the isolates, CH077. Similarly variation within epitope TL8 in Gag was present only in isolate CH106. There were however changes in the flanking amino acids of epitope YV9 which may have had an effect on antigen processing and subsequent presentation. Changes in flanking amino acids were also observed for peptide 80 epitope TI8 and an internal amino acid change was present in the ELI clade A/D isolate.

Despite the generally high conservation seen for the YV9 epitope, variation has been observed within and around the sequence representing escape from both immune pressure [466] and antiretroviral drugs [468]. Here, several escape variants of this epitope were examined for their capacity to be cross-recognised by vaccine-induced $CD8^+$ T cells specific for the wild type sequence. Although the data revealed that these mutations led to diminished T cell responses compared to the wild type, it was encouraging to see that a quarter of the T cells were able to cross-react with the least efficiently recognised N-terminal mutant **C**QYMDDLYV which is present within the transmitted founder virus from patient CH077 [457].

Overall, these data suggest that the dominant T cell populations elicited through vaccination in the broad virus controllers 411 and 418 were targeting epitopes that were likely to cause a reduction in the fitness of viral progeny and moreover that multiple escape variants could be recognised as a proportion of these T cells were cross-reactive.

A recent study by Streeck et al. 2014 has shown that certain T-cell specificities contribute more effectively to the control of HIV-1 infection. Several epitopes within Pol and Gag presented by a range of HLA alleles, rather than only those previously described to be protective, were shown to associate with delayed time to initiation of ART, as was greater breadth of epitope recognition, during acute infection [469]. Overall, our results largely concur with these data as the results for vaccinees 411 and 418 showed the greatest breadth of virus control in Chapter 5 and this was through targeting of multiple Pol and fewer Gag epitopes rather than by one dominant response or targeting of only the Gag protein. Vaccinee 421 also had both broadly specific T cells towards the Pol protein and a dominant response targeting TERQANFL in Gag which was through a 'non-protective' HLA allele but resulted in effective viral control of multiple isolates, the combined specificities were likely to have contributed to the control of the 4 isolates seen in Chapter 5 for this vaccinee.

These data strongly support the inclusion of epitope TERQANFL from Gag within a vaccine immunogen and in maintaining breadth to multiple epitopes with proven fitness costs, including some of those described here in Pol. An increased breadth of response may avoid the loss of control observed in LTNP when virus escapes from a single dominant protective specificity and the remaining T cells fail to exert new pressure on to the virus [470].

These results also show that assessment of vaccine immunogenicity should include the VIA rather than purely peptide based analysis as this provides a more biologically relevant readout and thus can give a greater indication of which vaccine candidates should progress on to larger scale efficacy testing. A systematic approach to define which mutations result in the greatest incapacity of the HIV-1 could be undertaken using a high throughput VIA followed by deep-sequencing of the HIV-1 sequences and used to elucidate key epitopes for inclusion within a prophylactic vaccine.

6.9 Summary of key findings from Chapter 6

- Conserved region Pol- and Gag-specific T cells from multiple vaccinees can control *in vitro* clade A and B HIV-1 replication.

- Pol- and Gag-specific T cells demonstrated both cytolytic and non-cytolytic effector functions which may have contributed to virus control.

- In vaccinee 411 dominant targeting of peptide 80 (TAFTIPSI) resulted in strong inhibition of HIV-1 IIIB, but 3 additional T-cell specificities targeting Pol and Env were also capable of strong inhibition which could explain this vaccinees exceptional breadth of virus control.

- For vaccinee 418 combined Gag- and Pol-specific T cells were more effective in controlling HIV-1 than any individual T-cell specificity, and mediated earlier control of viral replication.

- For vaccinee 421 dominant targeting of peptide 31 (TERQANFL) resulted in control of both HIV-1 clade A and B isolates.

- Cross-recognition of 'YQYMDDLYV' epitope variants was also shown for vaccinee 418, and could therefore have contributed to the breadth of HIV-1 isolates controlled by this individual in the CVIA.

7 Conclusions and recommendations for future work

7.1 Summary of research objectives

The work presented within this thesis focused on investigating a new conserved region immunogen (HIVconsv) designed to elicit T cells that could control HIV-1 replication. The immunogen was delivered by three leading vaccine modalities, in three novel heterologous prime-boost regimens, to healthy volunteers in Oxford. An initial assessment of immunogenicity was made using the gold standard IFN-γ ELISpot assay that is widely used to evaluate clinical vaccine candidates. To investigate HIV-1 control a more recently developed virus inhibition assay (VIA) was selected. Firstly an *ex vivo* VIA method was assessed for use with the vaccine trial samples before moving forward with a cultured VIA. The results from these investigations contributed to two peer reviewed publications (Borthwick et. al 2013 and Naarding et al. 2014). The final research chapter focused on T-cell specificity with an aim to determine if Pol should be included in subsequent vaccine designs, as currently there is still debate over which regions of HIV-1 will induce a protective immune response through vaccination.

7.1.1 Objective 1: To establish the immunogenicity of the candidate HIVconsv vaccines

The first conclusion drawn from Chapter 3 was that the HIVconsv immunogen designed to elicit an HIV-specific T-cell response was highly immunogenic in healthy HIV-1/2 negative adults, resulting in unprecedentedly high frequencies of T cells, when delivered by a heterologous prime-boost regimen of ChAdV63.HIVconsv (C) followed by MVA.HIVconsv (M) and when delivered with the triple DNA priming in regimen DDDCM. Secondly, these vaccine-elicited T cells showed enhanced breadth of HIV-1 epitope recognition, compared with previous T-cell vaccine candidates, with up to 10 different epitopes recognised for vaccinees in both the CM and DDDCM groups. Some discrepancies were noted between

pool responses compared to individual mapped peptides whereby pooled responses were present but individual specificities were unable to be identified. This may have been as a result of stimulation with a high concentration of pooled peptides compared to individual peptides or differences in time points used for the two analyses, suggesting that some specificities may not be persist as long as others. Finally, additional T-cell qualities, such as cell proliferation and chemokine / cytokine secretion, were investigated. The HIVconsv vaccine-elicited T cells were capable of multiple functions, which are often detected in HIV-1 LTNP, and suggested that they may therefore be capable of HIV-1 control.

7.1.2 Objective 2: To establish a virus inhibition assay (VIA) suitable for use with vaccinee samples and assess the HIV-CORE 002 trial sample set

Chapter 4 described the design, optimisation and assessment of the recently described *ex vivo* VIA for use with the HIV-CORE 002 samples. Several primary and lab strain viral isolates were grown and one (HIV-1 Bal) was selected to take forward for optimisation in the assay. After investigating several parameters including; the method of T-cell isolation, effector to target ratios, and choice of readouts (p24 ELISA and flow cytometry) several elite HIV-1 controller and vaccinee samples were tested using the optimised method. The results showed that the HIV-1 Bal isolate was weakly controlled by elite HIV-1 controllers and importantly in the small sample of vaccinees tested most showed very little to no control of HIV-1 Bal. Due to the high cell numbers required for this assay and further optimisation that would be necessary for its use with vaccine trial samples, the cultured VIA was chosen as an alternative method to assess T cell-mediated HIV-1 control.

A cultured VIA, published by Spentzou et al. 2010 [307], was used to analyse the HIVconsv vaccine samples, and allowed for the analysis of eight viral isolates. The data in Chapter 5 showed that the HIVconsv immunogen delivered by the CM regimen induced $CD8^+$ T cells, in all vaccinees, that inhibited *in vitro* HIV-1 replication of a clade A and B isolate.

Two vaccinees, 411 (CM) and 418 (DDDCM), showed superior breadth of virus control with 7/8 and 6/8 isolates inhibited, respectively. It was noted that the HIV-1 Bal isolate used in the *ex vivo* VIA was only controlled by vaccinee 411 and displayed the lowest inhibition of any isolate from the panel. The broad virus controllers both carried a protective HLA allele, prompting an investigation into HLA genotype which suggested that the CM regimen may be capable of overcoming this confounding factor, by increasing the magnitude of inhibition in those that do not carry an advantageous HLA allele. In order to understand which regions of HIV-1 were recognised by the inhibitory $CD8^+$ T cells, spare expanded cells were evaluated using the IFN-γ ELISpot assay and showed that Gag, Pol and Env were targeted by different vaccinees. Furthermore, the frequencies of conserved region Gag- but more so Pol-specific T cells positively correlated with the magnitude of clade A and B virus inhibition. These results strongly support the inclusion of a Pol component in next generation vaccine designs and demonstrate that effective induction of responses through vaccination can alter the natural hierarchy established during infection and subsequently alter clinical outcomes.

Aside from $CD8^+$ T cell-mediated viral inhibition, an examination of the secreted cytokine / chemokine profile of the infected $CD4^+$ T cells was also performed, using a Luminex assay. These analyses revealed that increased levels of the chemoattractants MIG and IP-10 were associated with increased viral replication, whereas increased levels of the CXCR4 binding chemokine SDF-1α was associated with a decrease in HIV-1 replication, regardless of viral co-receptor usage.

7.1.3 Objective 3: To investigate which T-cell specificities mediate control of HIV-1 replication and their mechanism of action

In the final chapter, individual T-cell specificities were investigated for their contribution to viral control in a limited number of vaccinees. The data showed that T cells targeting multiple conserved epitopes within Pol and also Gag could reduce HIV-1 replication

of clade A and B isolates. In most cases, T cells targeting a single conserved peptide achieved lower levels of viral inhibition than T cells targeting multiple peptides. Two T-cell specificities were able to independently decrease virus replication by several orders of magnitude, one within Gag (TERQANFL) and one previously reported within Pol (TAFTIPSI), but importantly in the broad virus controller 411 all T-cell-lines were capable of reducing HIV-1 replication which may have contributed to the greater breadth of control shown by this individual. Cellular cytotoxicity and secretion of antiviral cytokines were examined for these cell-lines and revealed that polyfunctional cytokine secretion was commonly observed for select peptides; however, cell killing of peptide-pulsed target cells was limited. The discrepancy between peptide-based assays and *in vitro* virus control highlighted the need to address the functionality of vaccine-induced T cells in a setting that more closely resembles natural HIV-1 infection, and suggests that a VIA should be standardised for routine use with new vaccine candidates. Preliminary experiments in to cross-recognition of variant HIV-1 epitopes suggested that this may also have contributed to the breadth of virus control shown for vaccinee 418, but this should be explored further with additional epitopes and in a greater number of vaccinees.

7.2 Future work based on this thesis

Often there can be criticism when using cultured cells as a means to examine a cellular response, as the culturing process can lead to changes in functional and phenotypic profiles and select for growth of certain cell populations. It would therefore be advantageous to examine the inhibitory effector profiles of vaccine-elicited T cells in an *ex vivo* VIA. The extent of testing however will be largely limited by the cell numbers available for use.

After analyses of all vaccinees by a cultured VIA shown in chapter 5, there was clear evidence that the HIV-1 Bal isolate that had been used throughout chapter 4 was the most challenging virus to control. A logical alternative would be to assess virus inhibition in

vaccinee samples using the *ex vivo* VIA and an isolate that is known to be suppressed, such as IIIB or U455. In addition, effector to target ratios could be increased as HIV-1 inhibition mediated by vaccine-induced T cells from the HVTN-505 trial was shown at an E:T ratio of 5:1 [471]. If these changes enabled detection of HIV-1 inhibition by vaccine-elicited T cells, then additional viral isolates, representative of circulating strains could be included in the assay. It will also be important, for any method, to include HIV-1 negative, HIV+ viremic patients and elite controller samples to aid in the interpretation of virus inhibition data. The development of the novel *Renilla* luciferase based VIA described by Naarding et al. 2014 [472], is a step in the right direction as this assay is a scale-down version of the cultured VIA, improving on robustness by increasing replicate number and sensitivity by reducing background inhibition levels. This protocol could be further adapted to include *ex vivo* $CD8^+$ T cells as the effector population. The panel of transmitted/founder infectious molecular clones that can be used with this method is also being expanded, which should help to predict which clinical candidate will be most protective in the field.

A clinical correlate of protection still remains elusive for HIV-1, but several research groups have associated select T-cell functional profiles with improved virus control [190, 191, 298]. Here, cytokine secretion profiles were assessed for HIVconsv vaccine-elicited T cells using both flow cytometry and Luminex analysis of cell culture supernatants. Luminex analysis allowed for more cytokines to be investigated and revealed that additional cytokines, to those detected through flow cytometry, were produced from vaccinee PBMC following peptide stimulation. However, this method does not allow for discrimination of individual cell functions without first separating the cells, and currently, flow cytometry panels are limited by how many colours/functions can be accurately assessed due to spectral-overlap [473]. A novel protocol designed to overcome the limitations of flow cytometry panels was described by Lamoreaux et al. 2006 [474] and suggested the use of one fluorochrome to

monitor multiple effector functions. This method has recently been used to examine the effector function profiles of HIV-1 elite controllers, HESPN and non-controllers in response to variant peptides [475] and revealed that cytokine response profiles were significantly different between controllers and HIV-1 infected individuals, and identified several alternative cytokines (IL-13, IL-22 and IL-10) associated with the HESN status [475]. Advancing from flow cytometry, a new technology, mass cytometry (cytometry by time-of-flight, CyTOF) has been used in the examination of up to 26 different markers on a single-cell and these data demonstrated that $CD8^+$ T-cells specific for different viral pathogens exhibit distinct functions and states of differentiation [476]. Application of this technology with vaccine-induced T cells would broaden the range of functions and phenotypes that can be analysed simultaneously and perhaps reveal a signature that consistently correlates with HIV-1 control.

One drawback to much of the analysis performed into T-cell specificities contributing to control of viral replication, by all groups, is that investigations are heavily biased towards the use of IFN-γ for dissecting responses and subsequently isolating HIV-1-specific T cells. However, tetramer [477] and CD107a staining [337] have shown that there are a large percentage of HIV-1-specific T cells that do not produce IFN-γ, and therefore are not being included within these analyses. To try and overcome the bias of IFN-γ selection, T cells could be stimulated with relevant peptide-pulsed target cells and selected based on the up-regulation of the early activation marker CD69 [478] this may broaden the isolated T-cell subsets [479] and provide a greater representation of the functionally heterogeneous T-cell populations induced through vaccination.

In Chapter 6 the ICS assays and STCL CVIA assays revealed that there were differences between vaccinees in both the frequencies of antiviral T cells responding to a particular peptide and virus inhibition mediated by T cells of the same specificity. These

results suggested that simply recognising a specific peptide or maintaining high frequencies of polyfunctional T cells in response to that peptide is not sufficient for virus control. Other factors, such as T cell avidity [193, 480, 481], public / private clonal populations [482] and functional maturation status [483] may vary between vaccinees, even when the same epitope specificity is considered. Indeed, studies into these T-cell properties suggests that T cells which are able to mature in response to antigenic stimulation into those bearing high avidity T-cell receptors (TCRs) preferably derived from public clonotypes will be more effective in the control of virus replication. Unfortunately, these parameters were not investigated here but will be important to characterise in future vaccine studies.

One area that was explored to a limited extent during this work, but which is likely to be essential for optimal vaccine induction of both T- and B-cells is the $CD4^+$ helper T-cell phenotype and function. Evidence from natural infection suggests that a T-cell mediated vaccine will require a strong Th1 type response to effectively prime long-lived memory $CD8^+$ T cells; whereas a B-cell mediated vaccine will require the support of a strong Th2 type response, particularly follicular T cells. However, due to HIV-1 primarily infecting $CD4^+$ T cells it will be important to ensure that there is not significant recruitment to the site of initial viral infection, which has been achieved in a 'prime and pull' vaccine strategy against HSV-2 [436]. Furthermore, vaccines that induce $CD4^+$ T cells capable of directly killing HIV-1 infected cells and secreting antiviral chemokines, such as SDF-1α, may also limit viral replication in the event of infection with HIV-1. The effect of vaccination using the range of different viral vectors and protein subunit vaccines, in various regimens, on the target $CD4^+$ T cell population has not however been extensively investigated.

7.3 The future of HIV-1 vaccines

The key to an effective HIV-1 vaccine will be finding the right immunogen, delivered by the right vector/s, which elicits a sustained cell-mediated and humoral response present in the

relevant location/s. Achieving each of these aims has so far proved to be very challenging, but progress is being made with the development of new technologies, novel vaccine vectors and adjuvants. Analysis of these new vaccines in animal models has allowed researchers to dissect the vaccine-elicited immune response, but most importantly, human clinical trials have provided the greatest insight as to which responses will ultimately be required for protection from and control of HIV-1 infection.

In depth research in to the HIV-1 lifecycle has significantly contributed to the effective design of antiretroviral therapeutics. This knowledge, of key proteins essential for HIV-1 replication, and data on immune responses from large cohorts of HIV-1+ patients [333, 469, 484] is beginning to direct which regions are included in novel HIV-1 immunogens [270, 485]. The development of novel stabilised envelope structures coupled with high-resolution techniques such as X-ray crystallography are being used to characterise the binding sites recognised by broadly neutralising antibodies [246], and the application of peptide-MHC isolation methods together with mass spectrometry [486] are being used to examine the expressed epitopes present on the surface of virally infected cells [487]. Combining this new information with patient clinical data may enable the optimal design of T- and B-cell immunogens and lead to improved vaccine efficacy.

One of the weaknesses of the HIVconsv T cell vaccines, and other Phase I HIV-1 candidates, is limited breadth of HIV-1 control despite broad epitope recognition [308, 320]. Mosaic immunogens are designed to increase the coverage of epitope variants [272] and as our knowledge of which vulnerable epitopes, or regions, are necessary for HIV-1 survival develops, we can use these new mosaic immunogens to increase the depth of epitope recognition. Our group has designed a new set of complimentary mosaic immunogens designed to reduce the number of irrelevant junctional regions elicited through vaccination whilst continuing to focus T cells on conserved protein regions; these are being prepared for

pre-clinical studies to be conducted in 2015. Mosaic immunogens, encoding HIV-1 Gag, Pol and Env have been examined in the rhesus macaque model and shown to induce a protective humoral response, against a chimeric, heterologous clade B, SIV and HIV-1 (SHIV) isolate [488]. In future, mosaic vaccines could be combined to elicit both humoral and cell-mediated antiviral responses, which will hopefully be capable of protecting humans from the diverse HIV-1 isolates in circulation.

The longevity of the immune response is also vital for ensuring that vaccinees remain protected, months to years following vaccination. The data obtained during this thesis suggests that if replication incompetent chimpanzee adenovirus and modified vaccinia virus Ankara vectors are to be used for establishing a T-cell mediated response they are likely to require subsequent booster vaccinations to ensure that a persistent effector T-cell population is present in the event of HIV-1 infection. The development of a replication-competent rhesus CMV vector for vaccination against SIV has been shown to be highly effective in the control and clearance of SIV infection [316, 432]. This vector establishes sustained effector memory, tissue resident $CD8^+$ T cell populations [316], similar to that established using a live-attenuated SIV vaccine which showed effective control of SIVmac239 infection [489]. However, the replication-competent rhesus CMV vector will require considerable work to develop an attenuated, safe vector, suitable for human use. Alternative replication competent viruses are currently being developed for use with HIV-1 immunogens and data from pre-clinical studies are emerging [490].

Improving the range of samples (peripheral blood and mucosal tissues) collected during human clinical trials will also aid in investigations of vaccine-induced T-cell and B-cell homing and HIV-1 control or clearance mediated by tissue resident T- and B-cell populations. Evidence from elite controllers [435] and HESN individuals [491] suggest that mucosal cell populations are more predictive of HIV-1 control compared with systemic samples. The

macaque model has also shown discordance between cell-mediated responses measured in systemic and mucosal compartments [489]. Alternative routes of immunisation also continue to be explored as a means to direct the immune response to mucosal areas where a tissue resident population could be established and maintained [492].

It is hoped that these new avenues of research will culminate in a highly effective prophylactic HIV-1 vaccine which can be deployed globally to significantly reduce the spread of this continuing epidemic. Further pursuit of novel therapeutic strategies aimed at clearing the viral reservoir will also be long awaited for the millions already affected by this devastating virus. Data in this thesis support the overall theoretical approach of using conserved regions for T cell vaccines. The ultimate proof can only come from efficacy studies in humans.

8 References

1. (CDC), C.f.D.C., *Kaposi's sarcoma and Pneumocystis pneumonia among homosexual men--New York City and California.* MMWR Morb Mortal Wkly Rep, 1981. **30**(25): p. 305-8.
2. Jaffe, H.W., D.J. Bregman, and R.M. Selik, *Acquired immune deficiency syndrome in the United States: the first 1,000 cases.* J Infect Dis, 1983. **148**(2): p. 339-45.
3. (CDC), C.f.D.C., *Possible transfusion-associated acquired immune deficiency syndrome (AIDS) - California.* MMWR Morb Mortal Wkly Rep, 1982. **31**(48): p. 652-4.
4. Andreani, T., et al., *Acquired immunodeficiency with intestinal cryptosporidiosis: possible transmission by Haitian whole blood.* Lancet, 1983. **1**(8335): p. 1187-91.
5. Harris, C., et al., *Immunodeficiency in female sexual partners of men with the acquired immunodeficiency syndrome.* N Engl J Med, 1983. **308**(20): p. 1181-4.
6. Barre-Sinoussi, F., et al., *Isolation of a T-lymphotropic retrovirus from a patient at risk for acquired immune deficiency syndrome (AIDS).* Science, 1983. **220**(4599): p. 868-71.
7. Gallo, R.C., et al., *Frequent detection and isolation of cytopathic retroviruses (HTLV-III) from patients with AIDS and at risk for AIDS.* Science, 1984. **224**(4648): p. 500-3.
8. Hahn, B.H., et al., *Molecular cloning and characterization of the HTLV-III virus associated with AIDS.* Nature, 1984. **312**(5990): p. 166-9.
9. Daniel, M.D., et al., *Isolation of T-cell tropic HTLV-III-like retrovirus from macaques.* Science, 1985. **228**(4704): p. 1201-4.
10. Beer, B.E., et al., *Diversity and evolution of primate lentiviruses.* Human retroviruses and AIDS, 1999: p. 460-474.
11. Huet, T., et al., *Genetic organization of a chimpanzee lentivirus related to HIV-1.* Nature, 1990. **345**(6273): p. 356-9.
12. Corbet, S., et al., *env sequences of simian immunodeficiency viruses from chimpanzees in Cameroon are strongly related to those of human immunodeficiency virus group N from the same geographic area.* Journal of Virology, 2000. **74**(1): p. 529-34.
13. Peeters, M., et al., *Isolation and partial characterization of an HIV-related virus occurring naturally in chimpanzees in Gabon.* AIDS, 1989. **3**(10): p. 625-30.
14. Vanden Haesevelde, M.M., et al., *Sequence analysis of a highly divergent HIV-1-related lentivirus isolated from a wild captured chimpanzee.* Virology, 1996. **221**(2): p. 346-50.
15. Gao, F., et al., *Origin of HIV-1 in the chimpanzee Pan troglodytes troglodytes.* Nature, 1999. **397**(6718): p. 436-41.
16. Clavel, F., et al., *Isolation of a new human retrovirus from West African patients with AIDS.* Science, 1986. **233**(4761): p. 343-6.
17. Clavel, F., et al., *Molecular cloning and polymorphism of the human immune deficiency virus type 2.* Nature, 1986. **324**(6098): p. 691-5.
18. Chen, Z., et al., *Genetic characterization of new West African simian immunodeficiency virus SIVsm: geographic clustering of household-derived SIV strains with human immunodeficiency virus type 2 subtypes and genetically diverse viruses from a single feral sooty mangabey troop.* Journal of Virology, 1996. **70**(6): p. 3617-27.
19. Chen, Z., et al., *Human immunodeficiency virus type 2 (HIV-2) seroprevalence and characterization of a distinct HIV-2 genetic subtype from the natural range of simian immunodeficiency virus-infected sooty mangabeys.* Journal of Virology, 1997. **71**(5): p. 3953-60.

20. Whitney, J.B., et al., *Rapid seeding of the viral reservoir prior to SIV viraemia in rhesus monkeys.* Nature, 2014. **512**(7512): p. 74-7.
21. Freed, E.O., *HIV-1 gag proteins: diverse functions in the virus life cycle.* Virology, 1998. **251**(1): p. 1-15.
22. Jacks, T., et al., *Characterization of ribosomal frameshifting in HIV-1 gag-pol expression.* Nature, 1988. **331**(6153): p. 280-3.
23. Louis, J.M., et al., *Kinetics and mechanism of autoprocessing of human immunodeficiency virus type 1 protease from an analog of the Gag-Pol polyprotein.* Proc Natl Acad Sci U S A, 1994. **91**(17): p. 7970-4.
24. Dunn, B.M., et al., *Retroviral proteases.* Genome Biol, 2002. **3**(4): p. REVIEWS3006.
25. Kohl, N.E., et al., *Active human immunodeficiency virus protease is required for viral infectivity.* Proc Natl Acad Sci U S A, 1988. **85**(13): p. 4686-90.
26. Jacobo-Molina, A., et al., *Crystal structure of human immunodeficiency virus type 1 reverse transcriptase complexed with double-stranded DNA at 3.0 A resolution shows bent DNA.* Proc Natl Acad Sci U S A, 1993. **90**(13): p. 6320-4.
27. Larder, B.A., S.D. Kemp, and D.J. Purifoy, *Infectious potential of human immunodeficiency virus type 1 reverse transcriptase mutants with altered inhibitor sensitivity.* Proc Natl Acad Sci U S A, 1989. **86**(13): p. 4803-7.
28. Schultz, S.J. and J.J. Champoux, *RNase H activity: structure, specificity, and function in reverse transcription.* Virus Res, 2008. **134**(1-2): p. 86-103.
29. Van Maele, B. and Z. Debyser, *HIV-1 integration: an interplay between HIV-1 integrase, cellular and viral proteins.* AIDS Rev, 2005. **7**(1): p. 26-43.
30. Allan, J.S., et al., *Major glycoprotein antigens that induce antibodies in AIDS patients are encoded by HTLV-III.* Science, 1985. **228**(4703): p. 1091-4.
31. Hallenberger, S., et al., *Inhibition of furin-mediated cleavage activation of HIV-1 glycoprotein gp160.* Nature, 1992. **360**(6402): p. 358-61.
32. Gelderblom, H.R., et al., *Fine structure of human immunodeficiency virus (HIV) and immunolocalization of structural proteins.* Virology, 1987. **156**(1): p. 171-6.
33. Kornfeld, H., et al., *Lymphocyte activation by HIV-1 envelope glycoprotein.* Nature, 1988. **335**(6189): p. 445-8.
34. Weiss, C.D., J.A. Levy, and J.M. White, *Oligomeric organization of gp120 on infectious human immunodeficiency virus type 1 particles.* Journal of Virology, 1990. **64**(11): p. 5674-7.
35. Leonard, C.K., et al., *Assignment of intrachain disulfide bonds and characterization of potential glycosylation sites of the type 1 recombinant human immunodeficiency virus envelope glycoprotein (gp120) expressed in Chinese hamster ovary cells.* J Biol Chem, 1990. **265**(18): p. 10373-82.
36. Wyatt, R., et al., *The antigenic structure of the HIV gp120 envelope glycoprotein.* Nature, 1998. **393**(6686): p. 705-11.
37. Olshevsky, U., et al., *Identification of individual human immunodeficiency virus type 1 gp120 amino acids important for CD4 receptor binding.* Journal of Virology, 1990. **64**(12): p. 5701-7.
38. Kwong, P.D., et al., *Structure of an HIV gp120 envelope glycoprotein in complex with the CD4 receptor and a neutralizing human antibody.* Nature, 1998. **393**(6686): p. 648-59.
39. Speck, R.F., et al., *Selective employment of chemokine receptors as human immunodeficiency virus type 1 coreceptors determined by individual amino acids within the envelope V3 loop.* Journal of Virology, 1997. **71**(9): p. 7136-9.
40. Gnanakaran, S., et al., *Clade-specific differences between human immunodeficiency virus type 1 clades B and C: diversity and correlations in C3-V4 regions of gp120.* Journal of Virology, 2007. **81**(9): p. 4886-91.

41. Parrish, N.F., et al., *Phenotypic properties of transmitted founder HIV-1.* Proc Natl Acad Sci U S A, 2013. **110**(17): p. 6626-33.
42. Collins, K.L., et al., *HIV-1 Nef protein protects infected primary cells against killing by cytotoxic T lymphocytes.* Nature, 1998. **391**(6665): p. 397-401.
43. Cohen, G.B., et al., *The selective downregulation of class I major histocompatibility complex proteins by HIV-1 protects HIV-infected cells from NK cells.* Immunity, 1999. **10**(6): p. 661-71.
44. Mandelboim, O., et al., *Protection from lysis by natural killer cells of group 1 and 2 specificity is mediated by residue 80 in human histocompatibility leukocyte antigen C alleles and also occurs with empty major histocompatibility complex molecules.* J Exp Med, 1996. **184**(3): p. 913-22.
45. Borrego, F., et al., *Recognition of human histocompatibility leukocyte antigen (HLA)-E complexed with HLA class I signal sequence-derived peptides by CD94/NKG2 confers protection from natural killer cell-mediated lysis.* J Exp Med, 1998. **187**(5): p. 813-8.
46. Fujii, Y., et al., *Soluble Nef antigen of HIV-1 is cytotoxic for human CD4+ T cells.* FEBS Lett, 1996. **393**(1): p. 93-6.
47. Qiao, X., et al., *Human immunodeficiency virus 1 Nef suppresses CD40-dependent immunoglobulin class switching in bystander B cells.* Nat Immunol, 2006. **7**(3): p. 302-10.
48. Swingler, S., et al., *HIV-1 Nef mediates lymphocyte chemotaxis and activation by infected macrophages.* Nat Med, 1999. **5**(9): p. 997-103.
49. Wolf, D., et al., *HIV-1 Nef associated PAK and PI3-kinases stimulate Akt-independent Bad-phosphorylation to induce anti-apoptotic signals.* Nat Med, 2001. **7**(11): p. 1217-24.
50. Aiken, C., et al., *Nef induces CD4 endocytosis: requirement for a critical dileucine motif in the membrane-proximal CD4 cytoplasmic domain.* Cell, 1994. **76**(5): p. 853-64.
51. Harris, R.S., et al., *DNA deamination mediates innate immunity to retroviral infection.* Cell, 2003. **113**(6): p. 803-9.
52. Mangeat, B., et al., *Broad antiretroviral defence by human APOBEC3G through lethal editing of nascent reverse transcripts.* Nature, 2003. **424**(6944): p. 99-103.
53. Bishop, K.N., et al., *APOBEC3G inhibits elongation of HIV-1 reverse transcripts.* PLoS Pathog, 2008. **4**(12): p. e1000231.
54. Iwatani, Y., et al., *Deaminase-independent inhibition of HIV-1 reverse transcription by APOBEC3G.* Nucleic Acids Res, 2007. **35**(21): p. 7096-108.
55. Stopak, K., et al., *HIV-1 Vif blocks the antiviral activity of APOBEC3G by impairing both its translation and intracellular stability.* Mol Cell, 2003. **12**(3): p. 591-601.
56. Sheehy, A.M., N.C. Gaddis, and M.H. Malim, *The antiretroviral enzyme APOBEC3G is degraded by the proteasome in response to HIV-1 Vif.* Nat Med, 2003. **9**(11): p. 1404-7.
57. Marin, M., et al., *HIV-1 Vif protein binds the editing enzyme APOBEC3G and induces its degradation.* Nat Med, 2003. **9**(11): p. 1398-403.
58. Bachand, F., et al., *Incorporation of Vpr into human immunodeficiency virus type 1 requires a direct interaction with the p6 domain of the p55 gag precursor.* J Biol Chem, 1999. **274**(13): p. 9083-91.
59. Bouhamdan, M., et al., *Human immunodeficiency virus type 1 Vpr protein binds to the uracil DNA glycosylase DNA repair enzyme.* Journal of Virology, 1996. **70**(2): p. 697-704.

60. Mansky, L.M., et al., *The interaction of vpr with uracil DNA glycosylase modulates the human immunodeficiency virus type 1 In vivo mutation rate.* Journal of Virology, 2000. **74**(15): p. 7039-47.
61. Heinzinger, N.K., et al., *The Vpr protein of human immunodeficiency virus type 1 influences nuclear localization of viral nucleic acids in nondividing host cells.* Proc Natl Acad Sci U S A, 1994. **91**(15): p. 7311-5.
62. Popov, S., et al., *Viral protein R regulates docking of the HIV-1 preintegration complex to the nuclear pore complex.* J Biol Chem, 1998. **273**(21): p. 13347-52.
63. Rogel, M.E., L.I. Wu, and M. Emerman, *The human immunodeficiency virus type 1 vpr gene prevents cell proliferation during chronic infection.* Journal of Virology, 1995. **69**(2): p. 882-8.
64. Jowett, J.B., et al., *The human immunodeficiency virus type 1 vpr gene arrests infected T cells in the G2 + M phase of the cell cycle.* Journal of Virology, 1995. **69**(10): p. 6304-13.
65. Goh, W.C., et al., *HIV-1 Vpr increases viral expression by manipulation of the cell cycle: a mechanism for selection of Vpr in vivo.* Nat Med, 1998. **4**(1): p. 65-71.
66. He, J., et al., *Human immunodeficiency virus type 1 viral protein R (Vpr) arrests cells in the G2 phase of the cell cycle by inhibiting p34cdc2 activity.* Journal of Virology, 1995. **69**(11): p. 6705-11.
67. Neil, S.J., T. Zang, and P.D. Bieniasz, *Tetherin inhibits retrovirus release and is antagonized by HIV-1 Vpu.* Nature, 2008. **451**(7177): p. 425-30.
68. Rollason, R., et al., *Clathrin-mediated endocytosis of a lipid-raft-associated protein is mediated through a dual tyrosine motif.* J Cell Sci, 2007. **120**(Pt 21): p. 3850-8.
69. Klimkait, T., et al., *The human immunodeficiency virus type 1-specific protein vpu is required for efficient virus maturation and release.* Journal of Virology, 1990. **64**(2): p. 621-9.
70. Willey, R.L., et al., *Human immunodeficiency virus type 1 Vpu protein induces rapid degradation of CD4.* Journal of Virology, 1992. **66**(12): p. 7193-200.
71. Willey, R.L., et al., *Human immunodeficiency virus type 1 Vpu protein regulates the formation of intracellular gp160-CD4 complexes.* Journal of Virology, 1992. **66**(1): p. 226-34.
72. Perelson, A.S., et al., *HIV-1 Dynamics in Vivo: Virion Clearance Rate, Infected Cell Life-Span, and Viral Generation Time.* Science, 1996. **271**(5255): p. 1582-1586.
73. Ho, D.D., et al., *Rapid turnover of plasma virions and CD4 lymphocytes in HIV-1 infection.* Nature, 1995. **373**(6510): p. 123-6.
74. Klatzmann, D., et al., *T-lymphocyte T4 molecule behaves as the receptor for human retrovirus LAV.* Nature, 1984. **312**(5996): p. 767-8.
75. Zhang, L., et al., *HIV-1 subtype and second-receptor use.* Nature, 1996. **383**(6603): p. 768.
76. Scarlatti, G., et al., *In vivo evolution of HIV-1 co-receptor usage and sensitivity to chemokine-mediated suppression.* Nat Med, 1997. **3**(11): p. 1259-65.
77. Connor, R.I., et al., *Change in coreceptor use correlates with disease progression in HIV-1--infected individuals.* J Exp Med, 1997. **185**(4): p. 621-8.
78. Weissenhorn, W., et al., *Atomic structure of the ectodomain from HIV-1 gp41.* Nature, 1997. **387**(6631): p. 426-30.
79. Clapham, P.R. and A. McKnight, *Cell surface receptors, virus entry and tropism of primate lentiviruses.* J Gen Virol, 2002. **83**(Pt 8): p. 1809-29.
80. Harrich, D. and B. Hooker, *Mechanistic aspects of HIV-1 reverse transcription initiation.* Rev Med Virol, 2002. **12**(1): p. 31-45.
81. Preston, B.D., B.J. Poiesz, and L.A. Loeb, *Fidelity of HIV-1 reverse transcriptase.* Science, 1988. **242**(4882): p. 1168-71.

82. Hu, W.S. and H.M. Temin, *Genetic consequences of packaging two RNA genomes in one retroviral particle: pseudodiploidy and high rate of genetic recombination.* Proc Natl Acad Sci U S A, 1990. **87**(4): p. 1556-60.
83. Lauring, A.S. and R. Andino, *Quasispecies theory and the behavior of RNA viruses.* PLoS Pathog, 2010. **6**(7): p. e1001005.
84. Schroder, A.R., et al., *HIV-1 integration in the human genome favors active genes and local hotspots.* Cell, 2002. **110**(4): p. 521-9.
85. Cujec, T.P., et al., *The human immunodeficiency virus transactivator Tat interacts with the RNA polymerase II holoenzyme.* Mol Cell Biol, 1997. **17**(4): p. 1817-23.
86. Nabel, G. and D. Baltimore, *An inducible transcription factor activates expression of human immunodeficiency virus in T cells.* Nature, 1987. **326**(6114): p. 711-3.
87. Oswald-Richter, K., et al., *HIV infection of primary human T cells is determined by tunable thresholds of T cell activation.* Eur J Immunol, 2004. **34**(6): p. 1705-14.
88. Stevenson, M., *HIV-1 pathogenesis.* Nat Med, 2003. **9**(7): p. 853-60.
89. Stauber, R.H. and G.N. Pavlakis, *Intracellular trafficking and interactions of the HIV-1 Tat protein.* Virology, 1998. **252**(1): p. 126-36.
90. Laspia, M.F., A.P. Rice, and M.B. Mathews, *HIV-1 Tat protein increases transcriptional initiation and stabilizes elongation.* Cell, 1989. **59**(2): p. 283-92.
91. Malim, M.H., et al., *The HIV-1 rev trans-activator acts through a structured target sequence to activate nuclear export of unspliced viral mRNA.* Nature, 1989. **338**(6212): p. 254-7.
92. Meng, X., et al., *Protease cleavage leads to formation of mature trimer interface in HIV-1 capsid.* PLoS Pathog, 2012. **8**(8): p. e1002886.
93. De Clercq, E., *The design of drugs for HIV and HCV.* Nat Rev Drug Discov, 2007. **6**(12): p. 1001-18.
94. Lee, B., et al., *Quantification of CD4, CCR5, and CXCR4 levels on lymphocyte subsets, dendritic cells, and differentially conditioned monocyte-derived macrophages.* Proc Natl Acad Sci U S A, 1999. **96**(9): p. 5215-20.
95. Kawamura, T., et al., *R5 HIV productively infects Langerhans cells, and infection levels are regulated by compound CCR5 polymorphisms.* Proc Natl Acad Sci U S A, 2003. **100**(14): p. 8401-6.
96. He, J., et al., *CCR3 and CCR5 are co-receptors for HIV-1 infection of microglia.* Nature, 1997. **385**(6617): p. 645-9.
97. Keele, B.F., et al., *Identification and characterization of transmitted and early founder virus envelopes in primary HIV-1 infection.* Proc Natl Acad Sci U S A, 2008. **105**(21): p. 7552-7.
98. Schnittman, S.M., et al., *Preferential infection of CD4+ memory T cells by human immunodeficiency virus type 1: evidence for a role in the selective T-cell functional defects observed in infected individuals.* Proc Natl Acad Sci U S A, 1990. **87**(16): p. 6058-62.
99. Douek, D.C., et al., *HIV preferentially infects HIV-specific CD4+ T cells.* Nature, 2002. **417**(6884): p. 95-98.
100. Elrefaei, M., et al., *Central memory CD4+ T cell responses in chronic HIV infection are not restored by antiretroviral therapy.* J Immunol, 2004. **173**(3): p. 2184-9.
101. Blaak, H., et al., *In vivo HIV-1 infection of CD45RA(+)CD4(+) T cells is established primarily by syncytium-inducing variants and correlates with the rate of CD4(+) T cell decline.* Proc Natl Acad Sci U S A, 2000. **97**(3): p. 1269-74.
102. Geijtenbeek, T.B., et al., *DC-SIGN, a dendritic cell-specific HIV-1-binding protein that enhances trans-infection of T cells.* Cell, 2000. **100**(5): p. 587-97.
103. Kwon, D.S., et al., *DC-SIGN-mediated internalization of HIV is required for trans-enhancement of T cell infection.* Immunity, 2002. **16**(1): p. 135-44.

104. Hu, J., M.B. Gardner, and C.J. Miller, *Simian immunodeficiency virus rapidly penetrates the cervicovaginal mucosa after intravaginal inoculation and infects intraepithelial dendritic cells.* Journal of Virology, 2000. **74**(13): p. 6087-95.
105. Brenchley, J.M., et al., *CD4+ T cell depletion during all stages of HIV disease occurs predominantly in the gastrointestinal tract.* J Exp Med, 2004. **200**(6): p. 749-59.
106. Guadalupe, M., et al., *Severe CD4+ T-cell depletion in gut lymphoid tissue during primary human immunodeficiency virus type 1 infection and substantial delay in restoration following highly active antiretroviral therapy.* Journal of Virology, 2003. **77**(21): p. 11708-17.
107. Mehandru, S., et al., *Mechanisms of gastrointestinal CD4+ T-cell depletion during acute and early human immunodeficiency virus type 1 infection.* Journal of Virology, 2007. **81**(2): p. 599-612.
108. Mehandru, S., et al., *Primary HIV-1 infection is associated with preferential depletion of CD4+ T lymphocytes from effector sites in the gastrointestinal tract.* J Exp Med, 2004. **200**(6): p. 761-70.
109. Brenchley, J.M., et al., *Microbial translocation is a cause of systemic immune activation in chronic HIV infection.* Nat Med, 2006. **12**(12): p. 1365-71.
110. Estes, J.D., A.T. Haase, and T.W. Schacker, *The role of collagen deposition in depleting CD4+ T cells and limiting reconstitution in HIV-1 and SIV infections through damage to the secondary lymphoid organ niche.* Semin Immunol, 2008. **20**(3): p. 181-6.
111. Levesque, M.C., et al., *Polyclonal B cell differentiation and loss of gastrointestinal tract germinal centers in the earliest stages of HIV-1 infection.* PLoS Med, 2009. **6**(7): p. e1000107.
112. Chun, T.W., et al., *Quantification of latent tissue reservoirs and total body viral load in HIV-1 infection.* Nature, 1997. **387**(6629): p. 183-8.
113. Finzi, D., et al., *Latent infection of CD4+ T cells provides a mechanism for lifelong persistence of HIV-1, even in patients on effective combination therapy.* Nat Med, 1999. **5**(5): p. 512-7.
114. UNAIDS. *UNAIDS report on the global AIDS epidemic 2013*. [PDF] 2013; Available from: http://www.unaids.org/en/media/unaids/contentassets/documents/epidemiology/2013/gr2013/UNAIDS_Global_Report_2013_en.pdf.
115. Miller, C.J., et al., *Genital mucosal transmission of simian immunodeficiency virus: animal model for heterosexual transmission of human immunodeficiency virus.* Journal of Virology, 1989. **63**(10): p. 4277-84.
116. Keele, B.F., et al., *Low-dose rectal inoculation of rhesus macaques by SIVsmE660 or SIVmac251 recapitulates human mucosal infection by HIV-1*. J Exp Med, 2009. **206**(5): p. 1117-34.
117. Haaland, R.E., et al., *Inflammatory genital infections mitigate a severe genetic bottleneck in heterosexual transmission of subtype A and C HIV-1*. PLoS Pathog, 2009. **5**(1): p. e1000274.
118. Goonetilleke, N., et al., *The first T cell response to transmitted/founder virus contributes to the control of acute viremia in HIV-1 infection.* J Exp Med, 2009. **206**(6): p. 1253-72.
119. McMichael, A.J., et al., *The immune response during acute HIV-1 infection: clues for vaccine development.* Nat Rev Immunol, 2010. **10**(1): p. 11-23.
120. Haase, A.T., *Targeting early infection to prevent HIV-1 mucosal transmission.* Nature, 2010. **464**(7286): p. 217-23.
121. Popovic, M., et al., *Isolation and transmission of human retrovirus (human t-cell leukemia virus).* Science, 1983. **219**(4586): p. 856-9.

122. WHO, *Consolidated guidelines on HIV prevention, diagnosis, treatment and care for key populations*. 2014.
123. WHO, *Consolidated guidelines on the use of Antiretroviral drugs for treating and preventing HIV infection - recommendations for a public health approach* 2013, WHO. p. 1-272.
124. Fischl, M.A., et al., *The efficacy of azidothymidine (AZT) in the treatment of patients with AIDS and AIDS-related complex. A double-blind, placebo-controlled trial.* N Engl J Med, 1987. **317**(4): p. 185-91.
125. Yusa, K., et al., *HIV-1 acquires resistance to two classes of antiviral drugs through homologous recombination.* Antiviral Res, 1997. **36**(3): p. 179-89.
126. Hammer, S.M., et al., *A controlled trial of two nucleoside analogues plus indinavir in persons with human immunodeficiency virus infection and CD4 cell counts of 200 per cubic millimeter or less. AIDS Clinical Trials Group 320 Study Team.* N Engl J Med, 1997. **337**(11): p. 725-33.
127. Connor, E.M., et al., *Reduction of maternal-infant transmission of human immunodeficiency virus type 1 with zidovudine treatment. Pediatric AIDS Clinical Trials Group Protocol 076 Study Group.* N Engl J Med, 1994. **331**(18): p. 1173-80.
128. Quinn, T.C., et al., *Viral load and heterosexual transmission of human immunodeficiency virus type 1. Rakai Project Study Group.* N Engl J Med, 2000. **342**(13): p. 921-9.
129. Castilla, J., et al., *Effectiveness of highly active antiretroviral therapy in reducing heterosexual transmission of HIV.* J Acquir Immune Defic Syndr, 2005. **40**(1): p. 96-101.
130. Porco, T.C., et al., *Decline in HIV infectivity following the introduction of highly active antiretroviral therapy.* AIDS, 2004. **18**(1): p. 81-8.
131. de Vincenzi, I., *Triple antiretroviral compared with zidovudine and single-dose nevirapine prophylaxis during pregnancy and breastfeeding for prevention of mother-to-child transmission of HIV-1 (Kesho Bora study): a randomised controlled trial.* Lancet Infect Dis, 2011. **11**(3): p. 171-80.
132. Grant, R.M., et al., *Preexposure chemoprophylaxis for HIV prevention in men who have sex with men.* N Engl J Med, 2010. **363**(27): p. 2587-99.
133. Cohen, M.S., et al., *Prevention of HIV-1 infection with early antiretroviral therapy.* N Engl J Med, 2011. **365**(6): p. 493-505.
134. Basavapathruni, A., C.M. Bailey, and K.S. Anderson, *Defining a molecular mechanism of synergy between nucleoside and nonnucleoside AIDS drugs.* J Biol Chem, 2004. **279**(8): p. 6221-4.
135. Radzio, J. and N. Sluis-Cremer, *Efavirenz accelerates HIV-1 reverse transcriptase ribonuclease H cleavage, leading to diminished zidovudine excision.* Mol Pharmacol, 2008. **73**(2): p. 601-6.
136. FDA. *Antiretroviral drugs used in the treatment of HIV infection*. 2014 Sep 2014]; Current antiretrovials approved for use against HIV-1 infection]. Available from: http://www.fda.gov/ForConsumers/byAudience/ForPatientAdvocates/HIVandAIDSActivities/ucm118915.htm.
137. Crawford, K.W., et al., *Optimising the manufacture, formulation, and dose of antiretroviral drugs for more cost-efficient delivery in resource-limited settings: a consensus statement.* Lancet Infect Dis, 2012. **12**(7): p. 550-560.
138. Holmes, C.B., et al., *Use of generic antiretroviral agents and cost savings in PEPFAR treatment programs.* JAMA, 2010. **304**(3): p. 313-20.
139. Hetherington, S., et al., *Hypersensitivity reactions during therapy with the nucleoside reverse transcriptase inhibitor abacavir.* Clin Ther, 2001. **23**(10): p. 1603-14.

140. Richman, D.D., et al., *The toxicity of azidothymidine (AZT) in the treatment of patients with AIDS and AIDS-related complex. A double-blind, placebo-controlled trial.* N Engl J Med, 1987. **317**(4): p. 192-7.
141. Cornelissen, M., et al., *pol gene diversity of five human immunodeficiency virus type 1 subtypes: evidence for naturally occurring mutations that contribute to drug resistance, limited recombination patterns, and common ancestry for subtypes B and D.* Journal of Virology, 1997. **71**(9): p. 6348-58.
142. Auvert, B., et al., *Randomized, controlled intervention trial of male circumcision for reduction of HIV infection risk: the ANRS 1265 Trial.* PLoS Med, 2005. **2**(11): p. e298.
143. Kim, J.H., et al., *HIV vaccines: lessons learned and the way forward.* Curr Opin HIV AIDS, 2010. **5**(5): p. 428-34.
144. UNAIDS, *UNAIDS report on the global AIDS epidemic 2010.* 2010.
145. Korber, B., et al., *Evolutionary and immunological implications of contemporary HIV-1 variation.* Br Med Bull, 2001. **58**: p. 19-42.
146. Thomson, M.M. and R. Najera, *Molecular epidemiology of HIV-1 variants in the global AIDS pandemic: an update.* AIDS Rev, 2005. **7**(4): p. 210-24.
147. Kandathil, A.J., et al., *Molecular epidemiology of HIV.* Indian J Med Res, 2005. **121**(4): p. 333-44.
148. Hemelaar, J., et al., *Global trends in molecular epidemiology of HIV-1 during 2000-2007.* AIDS, 2011. **25**(5): p. 679-89.
149. Carr, J.K., et al., *Full-length sequence and mosaic structure of a human immunodeficiency virus type 1 isolate from Thailand.* Journal of Virology, 1996. **70**(9): p. 5935-43.
150. McCutchan, F.E., et al., *Genetic variants of HIV-1 in Thailand.* AIDS Res Hum Retroviruses, 1992. **8**(11): p. 1887-95.
151. Goulder, P.J., et al., *Evolution and transmission of stable CTL escape mutations in HIV infection.* Nature, 2001. **412**(6844): p. 334-8.
152. Cao, Y., et al., *Virologic and immunologic characterization of long-term survivors of human immunodeficiency virus type 1 infection.* N Engl J Med, 1995. **332**(4): p. 201-8.
153. Munoz, A., et al., *Long-term survivors with HIV-1 infection: incubation period and longitudinal patterns of CD4+ lymphocytes.* J Acquir Immune Defic Syndr Hum Retrovirol, 1995. **8**(5): p. 496-505.
154. Pereyra, F., et al., *Genetic and immunologic heterogeneity among persons who control HIV infection in the absence of therapy.* J Infect Dis, 2008. **197**(4): p. 563-71.
155. Miyazawa, M., et al., *The 'immunologic advantage' of HIV-exposed seronegative individuals.* AIDS, 2009. **23**(2): p. 161-75.
156. Yamamoto, J.K., et al., *Human alpha- and beta-interferon but not gamma- suppress the in vitro replication of LAV, HTLV-III, and ARV-2.* J Interferon Res, 1986. **6**(2): p. 143-52.
157. Hartshorn, K.L., et al., *Activity of interferons alpha, beta, and gamma against human immunodeficiency virus replication in vitro.* AIDS Res Hum Retroviruses, 1987. **3**(2): p. 125-33.
158. Siegal, F.P., et al., *The nature of the principal type 1 interferon-producing cells in human blood.* Science, 1999. **284**(5421): p. 1835-7.
159. Beignon, A.S., et al., *Endocytosis of HIV-1 activates plasmacytoid dendritic cells via Toll-like receptor-viral RNA interactions.* J Clin Invest, 2005. **115**(11): p. 3265-75.
160. van der Vlist, M. and T.B. Geijtenbeek, *Langerin functions as an antiviral receptor on Langerhans cells.* Immunol Cell Biol, 2010. **88**(4): p. 410-5.
161. Soumelis, V., et al., *Depletion of circulating natural type 1 interferon-producing cells in HIV-infected AIDS patients.* Blood, 2001. **98**(4): p. 906-12.

162. Schmidt, B., et al., *Variations in plasmacytoid dendritic cell (PDC) and myeloid dendritic cell (MDC) levels in HIV-infected subjects on and off antiretroviral therapy.* J Clin Immunol, 2006. **26**(1): p. 55-64.
163. Cooper, M.A., T.A. Fehniger, and M.A. Caligiuri, *The biology of human natural killer-cell subsets.* Trends Immunol, 2001. **22**(11): p. 633-40.
164. Pegram, H.J., et al., *Activating and inhibitory receptors of natural killer cells.* Immunol Cell Biol, 2011. **89**(2): p. 216-24.
165. Rerks-Ngarm, S., et al., *Vaccination with ALVAC and AIDSVAX to prevent HIV-1 infection in Thailand.* N Engl J Med, 2009. **361**(23): p. 2209-20.
166. Gomez-Roman, V.R., et al., *Vaccine-elicited antibodies mediate antibody-dependent cellular cytotoxicity correlated with significantly reduced acute viremia in rhesus macaques challenged with SIVmac251.* J Immunol, 2005. **174**(4): p. 2185-9.
167. Hessell, A.J., et al., *Fc receptor but not complement binding is important in antibody protection against HIV.* Nature, 2007. **449**(7158): p. 101-4.
168. Martin, M.P., et al., *Epistatic interaction between KIR3DS1 and HLA-B delays the progression to AIDS.* Nat Genet, 2002. **31**(4): p. 429-34.
169. Alter, G., et al., *Differential natural killer cell-mediated inhibition of HIV-1 replication based on distinct KIR/HLA subtypes.* J Exp Med, 2007. **204**(12): p. 3027-36.
170. Boulet, S., et al., *Increased proportion of KIR3DS1 homozygotes in HIV-exposed uninfected individuals.* AIDS, 2008. **22**(5): p. 595-9.
171. Jennes, W., et al., *Cutting edge: resistance to HIV-1 infection among African female sex workers is associated with inhibitory KIR in the absence of their HLA ligands.* J Immunol, 2006. **177**(10): p. 6588-92.
172. Alter, G., et al., *HIV-1 adaptation to NK-cell-mediated immune pressure.* Nature, 2011. **476**(7358): p. 96-100.
173. Borrow, P., et al., *Virus-specific CD8+ cytotoxic T-lymphocyte activity associated with control of viremia in primary human immunodeficiency virus type 1 infection.* Journal of Virology, 1994. **68**(9): p. 6103-10.
174. Koup, R.A., et al., *Temporal association of cellular immune responses with the initial control of viremia in primary human immunodeficiency virus type 1 syndrome.* Journal of Virology, 1994. **68**(7): p. 4650-5.
175. Schmitz, J.E., et al., *Control of viremia in simian immunodeficiency virus infection by CD8+ lymphocytes.* Science, 1999. **283**(5403): p. 857-60.
176. Jin, X., et al., *Dramatic rise in plasma viremia after CD8(+) T cell depletion in simian immunodeficiency virus-infected macaques.* J Exp Med, 1999. **189**(6): p. 991-8.
177. Friedrich, T.C., et al., *Subdominant CD8+ T-cell responses are involved in durable control of AIDS virus replication.* Journal of Virology, 2007. **81**(7): p. 3465-76.
178. Rowland-Jones, S.L., et al., *HIV-specific cytotoxic T-cell activity in an HIV-exposed but uninfected infant.* Lancet, 1993. **341**(8849): p. 860-1.
179. Rowland-Jones, S., et al., *HIV-specific cytotoxic T-cells in HIV-exposed but uninfected Gambian women.* Nat Med, 1995. **1**(1): p. 59-64.
180. Langlade-Demoyen, P., et al., *Human immunodeficiency virus (HIV) nef-specific cytotoxic T lymphocytes in noninfected heterosexual contact of HIV-infected patients.* J Clin Invest, 1994. **93**(3): p. 1293-7.
181. Clerici, M., et al., *Cell-mediated immune response to human immunodeficiency virus (HIV) type 1 in seronegative homosexual men with recent sexual exposure to HIV-1.* J Infect Dis, 1992. **165**(6): p. 1012-9.
182. Moss, R.B., et al., *HIV-1-Specific Functional Immune Measurements as Markers of Disease Progression.* J Biomed Sci, 1997. **4**(4): p. 127-131.

183. Borrow, P., et al., *Antiviral pressure exerted by HIV-1-specific cytotoxic T lymphocytes (CTLs) during primary infection demonstrated by rapid selection of CTL escape virus.* Nat Med, 1997. **3**(2): p. 205-11.
184. Carrington, M. and S.J. O'Brien, *The influence of HLA genotype on AIDS.* Annu Rev Med, 2003. **54**: p. 535-51.
185. Kawashima, Y., et al., *Adaptation of HIV-1 to human leukocyte antigen class I.* Nature, 2009. **458**(7238): p. 641-5.
186. Altfeld, M., et al., *Influence of HLA-B57 on clinical presentation and viral control during acute HIV-1 infection.* AIDS, 2003. **17**(18): p. 2581-91.
187. Brennan, C.A., et al., *Early HLA-B*57-Restricted CD8+ T Lymphocyte Responses Predict HIV-1 Disease Progression.* Journal of Virology, 2012.
188. Martinez-Picado, J., et al., *Fitness cost of escape mutations in p24 Gag in association with control of human immunodeficiency virus type 1.* Journal of Virology, 2006. **80**(7): p. 3617-23.
189. Horton, H., et al., *Preservation of T cell proliferation restricted by protective HLA alleles is critical for immune control of HIV-1 infection.* J Immunol, 2006. **177**(10): p. 7406-15.
190. Migueles, S.A., et al., *HIV-specific CD8+ T cell proliferation is coupled to perforin expression and is maintained in nonprogressors.* Nat Immunol, 2002. **3**(11): p. 1061-8.
191. Betts, M.R., et al., *HIV nonprogressors preferentially maintain highly functional HIV-specific CD8+ T cells.* Blood, 2006. **107**(12): p. 4781-4789.
192. Julg, B., et al., *Enhanced anti-HIV functional activity associated with Gag-specific CD8 T-cell responses.* Journal of Virology, 2010. **84**(11): p. 5540-9.
193. Almeida, J.R., et al., *Antigen sensitivity is a major determinant of CD8+ T-cell polyfunctionality and HIV-suppressive activity.* Blood, 2009. **113**(25): p. 6351-60.
194. Moore, J.P., et al., *Development of the anti-gp120 antibody response during seroconversion to human immunodeficiency virus type 1.* Journal of Virology, 1994. **68**(8): p. 5142-55.
195. Tomaras, G.D., et al., *Initial B-cell responses to transmitted human immunodeficiency virus type 1: virion-binding immunoglobulin M (IgM) and IgG antibodies followed by plasma anti-gp41 antibodies with ineffective control of initial viremia.* Journal of Virology, 2008. **82**(24): p. 12449-63.
196. Wei, X.P., et al., *Antibody neutralization and escape by HIV-1.* Nature, 2003. **422**(6929): p. 307-312.
197. Richman, D.D., et al., *Rapid evolution of the neutralizing antibody response to HIV type 1 infection.* Proc Natl Acad Sci U S A, 2003. **100**(7): p. 4144-9.
198. Montefiori, D.C., et al., *Neutralizing and other antiviral antibodies in HIV-1 infection and vaccination.* Curr Opin HIV AIDS, 2007. **2**(3): p. 169-76.
199. Sheppard, N. and Q. Sattentau, *The prospects for vaccines against HIV-1: more than a field of long-term nonprogression?* Expert Rev Mol Med, 2005. **7**(2): p. 1-21.
200. Li, Y., et al., *Broad HIV-1 neutralization mediated by CD4-binding site antibodies.* Nat Med, 2007. **13**(9): p. 1032-4.
201. Montero, M., et al., *The membrane-proximal external region of the human immunodeficiency virus type 1 envelope: dominant site of antibody neutralization and target for vaccine design.* Microbiol Mol Biol Rev, 2008. **72**(1): p. 54-84, table of contents.
202. Scanlan, C.N., et al., *The broadly neutralizing anti-human immunodeficiency virus type 1 antibody 2G12 recognizes a cluster of alpha1--->2 mannose residues on the outer face of gp120.* Journal of Virology, 2002. **76**(14): p. 7306-21.

203. Stanfield, R.L., et al., *Structural rationale for the broad neutralization of HIV-1 by human monoclonal antibody 447-52D.* Structure, 2004. **12**(2): p. 193-204.
204. Kang, C.Y., et al., *Identification of a new neutralizing epitope conformationally affected by the attachment of CD4 to gp120.* J Immunol, 1993. **151**(1): p. 449-57.
205. Thali, M., et al., *Characterization of conserved human immunodeficiency virus type 1 gp120 neutralization epitopes exposed upon gp120-CD4 binding.* Journal of Virology, 1993. **67**(7): p. 3978-88.
206. Shibata, R., et al., *Neutralizing antibody directed against the HIV-1 envelope glycoprotein can completely block HIV-1/SIV chimeric virus infections of macaque monkeys.* Nat Med, 1999. **5**(2): p. 204-10.
207. Hessell, A.J., et al., *Broadly neutralizing monoclonal antibodies 2F5 and 4E10 directed against the human immunodeficiency virus type 1 gp41 membrane-proximal external region protect against mucosal challenge by simian-human immunodeficiency virus SHIVBa-L.* Journal of Virology, 2010. **84**(3): p. 1302-13.
208. Parren, P.W., et al., *Antibody protects macaques against vaginal challenge with a pathogenic R5 simian/human immunodeficiency virus at serum levels giving complete neutralization in vitro.* Journal of Virology, 2001. **75**(17): p. 8340-7.
209. Hessell, A.J., et al., *Broadly neutralizing human anti-HIV antibody 2G12 is effective in protection against mucosal SHIV challenge even at low serum neutralizing titers.* PLoS Pathog, 2009. **5**(5): p. e1000433.
210. Walker, L.M., et al., *Broad and potent neutralizing antibodies from an African donor reveal a new HIV-1 vaccine target.* Science, 2009. **326**(5950): p. 285-9.
211. Wu, X., et al., *Rational design of envelope identifies broadly neutralizing human monoclonal antibodies to HIV-1.* Science, 2010. **329**(5993): p. 856-61.
212. Scheid, J.F., et al., *Sequence and structural convergence of broad and potent HIV antibodies that mimic CD4 binding.* Science, 2011. **333**(6049): p. 1633-7.
213. Huang, J., et al., *Broad and potent neutralization of HIV-1 by a gp41-specific human antibody.* Nature, 2012. **491**(7424): p. 406-12.
214. Walker, L.M., et al., *Broad neutralization coverage of HIV by multiple highly potent antibodies.* Nature, 2011. **477**(7365): p. 466-70.
215. Huang, J., et al., *Broad and potent HIV-1 neutralization by a human antibody that binds the gp41-gp120 interface.* Nature, 2014. **515**(7525): p. 138-42.
216. Ahlers, J.D., *All eyes on the next generation of HIV vaccines: Strategies for inducing a broadly neutralizing antibody response* Discovery Medicine, 2014. **17**(094): p. 187-199.
217. Pissani, F. and H. Streeck, *Emerging concepts on T follicular helper cell dynamics in HIV infection.* Trends Immunol, 2014. **35**(6): p. 278-86.
218. Fauci, A.S., *An HIV vaccine: breaking the paradigms.* Proc Assoc Am Physicians, 1996. **108**(1): p. 6-13.
219. Pantaleo, G. and R.A. Koup, *Correlates of immune protection in HIV-1 infection: what we know, what we don't know, what we should know.* Nat Med, 2004. **10**(8): p. 806-10.
220. Plotkin, S., *History of vaccination.* Proc Natl Acad Sci U S A, 2014. **111**(34): p. 12283-7.
221. Dittmer, U., et al., *Cellular immune response of rhesus monkeys infected with a partially attenuated nef deletion mutant of the simian immunodeficiency virus.* Virology, 1995. **212**(2): p. 392-7.
222. Whatmore, A.M., et al., *Repair and evolution of nef in vivo modulates simian immunodeficiency virus virulence.* Journal of Virology, 1995. **69**(8): p. 5117-23.

223. Stahl-Hennig, C., et al., *Attenuated SIV imparts immunity to challenge with pathogenic spleen-derived SIV but cannot prevent repair of the nef deletion.* Immunol Lett, 1996. **51**(1-2): p. 129-35.
224. Gibbs, J.S., D.A. Regier, and R.C. Desrosiers, *Construction and in vitro properties of SIVmac mutants with deletions in "nonessential" genes.* AIDS Res Hum Retroviruses, 1994. **10**(5): p. 607-16.
225. Baba, T.W., et al., *Live attenuated, multiply deleted simian immunodeficiency virus causes AIDS in infant and adult macaques.* Nat Med, 1999. **5**(2): p. 194-203.
226. Baba, T.W., et al., *Pathogenicity of live, attenuated SIV after mucosal infection of neonatal macaques.* Science, 1995. **267**(5205): p. 1820-5.
227. Boyer, J.D., et al., *Protection of chimpanzees from high-dose heterologous HIV-1 challenge by DNA vaccination.* Nat Med, 1997. **3**(5): p. 526-32.
228. Egan, M.A., et al., *Simian immunodeficiency virus (SIV) gag DNA-vaccinated rhesus monkeys develop secondary cytotoxic T-lymphocyte responses and control viral replication after pathogenic SIV infection.* Journal of Virology, 2000. **74**(16): p. 7485-95.
229. Shiver, J.W., et al., *Replication-incompetent adenoviral vaccine vector elicits effective anti-immunodeficiency-virus immunity.* Nature, 2002. **415**(6869): p. 331-5.
230. Team, A.V.E.G.P., *Cellular and humoral immune responses to a canarypox vaccine containing human immunodeficiency virus type 1 Env, Gag, and Pro in combination with rgp120.* J Infect Dis, 2001. **183**(4): p. 563-70.
231. Letvin, N.L., et al., *Potent, protective anti-HIV immune responses generated by bimodal HIV envelope DNA plus protein vaccination.* Proc Natl Acad Sci U S A, 1997. **94**(17): p. 9378-83.
232. Amara, R.R., et al., *Control of a mucosal challenge and prevention of AIDS by a multiprotein DNA/MVA vaccine.* Science, 2001. **292**(5514): p. 69-74.
233. Desrosiers, R.C., et al., *Vaccine protection against simian immunodeficiency virus infection.* Proc Natl Acad Sci U S A, 1989. **86**(16): p. 6353-7.
234. Murphey-Corb, M., et al., *A formalin-inactivated whole SIV vaccine confers protection in macaques.* Science, 1989. **246**(4935): p. 1293-7.
235. Carlson, J.R., et al., *Vaccine protection of rhesus macaques against simian immunodeficiency virus infection.* AIDS Res Hum Retroviruses, 1990. **6**(11): p. 1239-46.
236. Stott, E.J., et al., *Preliminary report: protection of cynomolgus macaques against simian immunodeficiency virus by fixed infected-cell vaccine.* Lancet, 1990. **336**(8730): p. 1538-41.
237. Moore, J.P. and R.A. Weiss, *AIDS. Passive primate protection.* Nature, 1991. **352**(6334): p. 376-7.
238. Stott, E.J., *Anti-cell antibody in macaques.* Nature, 1991. **353**(6343): p. 393.
239. Le Grand, R., et al., *AIDS vaccine developments.* Nature, 1992. **355**(6362): p. 684.
240. Hu, S.L., et al., *Protection of macaques against SIV infection by subunit vaccines of SIV envelope glycoprotein gp160.* Science, 1992. **255**(5043): p. 456-9.
241. Mascola, J.R., et al., *Immunization with Envelope Subunit Vaccine Products Elicits Neutralizing Antibodies against Laboratory-Adapted but Not Primary Isolates of Human Immunodeficiency Virus Type 1.* Journal of Infectious Diseases, 1996. **173**(2): p. 340-348.
242. Connor, R.I., et al., *Immunological and virological analyses of persons infected by human immunodeficiency virus type 1 while participating in trials of recombinant gp120 subunit vaccines.* Journal of Virology, 1998. **72**(2): p. 1552-76.
243. Johnson, J.A., D.H. Barouch, and L.R. Baden, *Nonreplicating vectors in HIV vaccines.* Curr Opin HIV AIDS, 2013. **8**(5): p. 412-20.

244. Haynes, B.F. and M.J. McElrath, *Progress in HIV-1 vaccine development.* Curr Opin HIV AIDS, 2013. **8**(4): p. 326-32.
245. McCoy, L.E. and R.A. Weiss, *Neutralizing antibodies to HIV-1 induced by immunization.* J Exp Med, 2013. **210**(2): p. 209-23.
246. Julien, J.P., et al., *Crystal structure of a soluble cleaved HIV-1 envelope trimer.* Science, 2013. **342**(6165): p. 1477-83.
247. Khayat, R., et al., *Structural characterization of cleaved, soluble HIV-1 envelope glycoprotein trimers.* Journal of Virology, 2013. **87**(17): p. 9865-72.
248. Crooks, E.T., et al., *Enzyme digests eliminate nonfunctional Env from HIV-1 particle surfaces, leaving native Env trimers intact and viral infectivity unaffected.* Journal of Virology, 2011. **85**(12): p. 5825-39.
249. Tong, T., et al., *HIV-1 virus-like particles bearing pure env trimers expose neutralizing epitopes but occlude nonneutralizing epitopes.* Journal of Virology, 2012. **86**(7): p. 3574-87.
250. Depetris, R.S., et al., *Partial enzymatic deglycosylation preserves the structure of cleaved recombinant HIV-1 envelope glycoprotein trimers.* J Biol Chem, 2012. **287**(29): p. 24239-54.
251. McGuire, A.T., et al., *Engineering HIV envelope protein to activate germline B cell receptors of broadly neutralizing anti-CD4 binding site antibodies.* J Exp Med, 2013. **210**(4): p. 655-63.
252. Jardine, J., et al., *Rational HIV immunogen design to target specific germline B cell receptors.* Science, 2013. **340**(6133): p. 711-6.
253. IAVI, *The International AIDS Vaccine Initiative (IAVI) Clinical trials database*. 2014, IAVI.
254. Excler, J.L., G.D. Tomaras, and N.D. Russell, *Novel directions in HIV-1 vaccines revealed from clinical trials.* Curr Opin HIV AIDS, 2013. **8**(5): p. 421-31.
255. Flynn, N.M., et al., *Placebo-controlled phase 3 trial of a recombinant glycoprotein 120 vaccine to prevent HIV-1 infection.* J Infect Dis, 2005. **191**(5): p. 654-65.
256. Pitisuttithum, P., et al., *Randomized, double-blind, placebo-controlled efficacy trial of a bivalent recombinant glycoprotein 120 HIV-1 vaccine among injection drug users in Bangkok, Thailand.* J Infect Dis, 2006. **194**(12): p. 1661-71.
257. Gilbert, P.B., et al., *Correlation between immunologic responses to a recombinant glycoprotein 120 vaccine and incidence of HIV-1 infection in a phase 3 HIV-1 preventive vaccine trial.* J Infect Dis, 2005. **191**(5): p. 666-77.
258. Buchbinder, S.P., et al., *Efficacy assessment of a cell-mediated immunity HIV-1 vaccine (the Step Study): a double-blind, randomised, placebo-controlled, test-of-concept trial.* Lancet, 2008. **372**(9653): p. 1881-93.
259. Gray, G.E., et al., *Safety and efficacy of the HVTN 503/Phambili study of a clade-B-based HIV-1 vaccine in South Africa: a double-blind, randomised, placebo-controlled test-of-concept phase 2b study.* Lancet Infect Dis, 2011. **11**(7): p. 507-15.
260. Rolland, M., et al., *Genetic impact of vaccination on breakthrough HIV-1 sequences from the STEP trial.* Nat Med, 2011. **17**(3): p. 366-71.
261. Janes, H., et al., *Vaccine-induced gag-specific T cells are associated with reduced viremia after HIV-1 infection.* J Infect Dis, 2013. **208**(8): p. 1231-9.
262. Hancock, G., et al., *Identification of Effective Subdominant Anti-HIV-1 CD8+ T Cells Within Entire Post-infection and Post-vaccination Immune Responses.* PLoS Pathog, 2015. **11**(2): p. e1004658.
263. Hammer, S.M., et al., *Efficacy trial of a DNA/rAd5 HIV-1 preventive vaccine.* N Engl J Med, 2013. **369**(22): p. 2083-92.
264. Haynes, B.F., et al., *Immune-correlates analysis of an HIV-1 vaccine efficacy trial.* N Engl J Med, 2012. **366**(14): p. 1275-86.

265. Rolland, M., et al., *Increased HIV-1 vaccine efficacy against viruses with genetic signatures in Env V2.* Nature, 2012. **490**(7420): p. 417-20.
266. Liao, H.X., et al., *Vaccine induction of antibodies against a structurally heterogeneous site of immune pressure within HIV-1 envelope protein variable regions 1 and 2.* Immunity, 2013. **38**(1): p. 176-86.
267. Hanke, T., *Conserved immunogens in prime-boost strategies for the next-generation HIV-1 vaccines.* Expert Opin Biol Ther, 2014. **14**(5): p. 601-16.
268. Rolland, M., et al., *Reconstruction and function of ancestral center-of-tree human immunodeficiency virus type 1 proteins.* Journal of Virology, 2007. **81**(16): p. 8507-14.
269. Novitsky, V., et al., *Human immunodeficiency virus type 1 subtype C molecular phylogeny: consensus sequence for an AIDS vaccine design?* Journal of Virology, 2002. **76**(11): p. 5435-51.
270. Letourneau, S., et al., *Design and pre-clinical evaluation of a universal HIV-1 vaccine.* PLoS One, 2007. **2**(10): p. e984.
271. Rolland, M., D.C. Nickle, and J.I. Mullins, *HIV-1 group M conserved elements vaccine.* PLoS Pathog, 2007. **3**(11): p. e157.
272. Fischer, W., et al., *Polyvalent vaccines for optimal coverage of potential T-cell epitopes in global HIV-1 variants.* Nat Med, 2007. **13**(1): p. 100-6.
273. Gaschen, B., et al., *Diversity considerations in HIV-1 vaccine selection.* Science, 2002. **296**(5577): p. 2354-60.
274. Hanke, T. and A.J. McMichael, *HIV-1: from escapism to conservatism.* Eur J Immunol, 2011. **41**(12): p. 3390-3.
275. Barouch, D.H., et al., *Mosaic HIV-1 vaccines expand the breadth and depth of cellular immune responses in rhesus monkeys.* Nat Med, 2010. **16**(3): p. 319-23.
276. MacGregor, R.R., et al., *First human trial of a DNA-based vaccine for treatment of human immunodeficiency virus type 1 infection: safety and host response.* J Infect Dis, 1998. **178**(1): p. 92-100.
277. Wang, B., et al., *Gene inoculation generates immune responses against human immunodeficiency virus type 1.* Proc Natl Acad Sci U S A, 1993. **90**(9): p. 4156-60.
278. McConkey, S.J., et al., *Enhanced T-cell immunogenicity of plasmid DNA vaccines boosted by recombinant modified vaccinia virus Ankara in humans.* Nat Med, 2003. **9**(6): p. 729-35.
279. Hanke, T., A.J. McMichael, and L. Dorrell, *Clinical experience with plasmid DNA- and modified vaccinia virus Ankara-vectored human immunodeficiency virus type 1 clade A vaccine focusing on T-cell induction.* J Gen Virol, 2007. **88**(1): p. 1-12.
280. Vuola, J.M., et al., *Differential immunogenicity of various heterologous prime-boost vaccine regimens using DNA and viral vectors in healthy volunteers.* J Immunol, 2005. **174**(1): p. 449-55.
281. Mayr, A., V. Hochstein-Mintzel, and H. Stickl, *Abstammung, Eigenschaften und Verwendung des attenuierten Vaccinia-Stammes MVA.* Infection, 1975. **3**(1): p. 6-14.
282. Meyer, H., G. Sutter, and A. Mayr, *Mapping of deletions in the genome of the highly attenuated vaccinia virus MVA and their influence on virulence.* J Gen Virol, 1991. **72 (Pt 5)**: p. 1031-8.
283. Carroll, M.W. and B. Moss, *Host range and cytopathogenicity of the highly attenuated MVA strain of vaccinia virus: propagation and generation of recombinant viruses in a nonhuman mammalian cell line.* Virology, 1997. **238**(2): p. 198-211.
284. Drexler, I., et al., *Highly attenuated modified vaccinia virus Ankara replicates in baby hamster kidney cells, a potential host for virus propagation, but not in various human transformed and primary cells.* J Gen Virol, 1998. **79 (Pt 2)**: p. 347-52.

285. Mayr, A., et al., *The smallpox vaccination strain MVA: Marker, genetic structure, experience gained with the parenteral vaccination and behavior in organisms with a debilitated defence mechanism.* Zentralblatt fur Bakteriologie. Hygiene. Krankenhaushygiene Betriebshygiene Praventive Medizin - Abt. 1 Orig. B, 1978. **167**(5-6): p. 375-390.
286. Cebere, I., et al., *Phase I clinical trial safety of DNA- and modified virus Ankara-vectored human immunodeficiency virus type 1 (HIV-1) vaccines administered alone and in a prime-boost regime to healthy HIV-1-uninfected volunteers.* Vaccine, 2006. **24**(4): p. 417-25.
287. Moorthy, V.S., et al., *Safety and immunogenicity of DNA/modified vaccinia virus ankara malaria vaccination in African adults.* J Infect Dis, 2003. **188**(8): p. 1239-44.
288. McShane, H., et al., *Recombinant modified vaccinia virus Ankara expressing antigen 85A boosts BCG-primed and naturally acquired antimycobacterial immunity in humans.* Nat Med, 2004. **10**(11): p. 1240-4.
289. Cosma, A., et al., *Therapeutic vaccination with MVA-HIV-1 nef elicits Nef-specific T-helper cell responses in chronically HIV-1 infected individuals.* Vaccine, 2003. **22**(1): p. 21-9.
290. Draper, S.J. and J.L. Heeney, *Viruses as vaccine vectors for infectious diseases and cancer.* Nat Rev Microbiol, 2010. **8**(1): p. 62-73.
291. Thorner, A.R., et al., *Age dependence of adenovirus-specific neutralizing antibody titers in individuals from sub-Saharan Africa.* J Clin Microbiol, 2006. **44**(10): p. 3781-3.
292. Mast T C, e.a. (2005) *International epidemiology of human pre-existing anti-adenovirus Type-5 (Ad5) neutralising antibodies in areas representative of poteintial HIV vaccine trial sites. Poster Exhibition: The XV International AIDS Conference: Abstract no. ThPeC7432*.
293. Appaiahgari, M.B., R.M. Pandey, and S. Vrati, *Seroprevalence of neutralizing antibodies to adenovirus type 5 among children in India: implications for recombinant adenovirus-based vaccines.* Clin Vaccine Immunol, 2007. **14**(8): p. 1053-5.
294. Priddy, F.H., et al., *Safety and immunogenicity of a replication-incompetent adenovirus type 5 HIV-1 clade B gag/pol/nef vaccine in healthy adults.* Clin Infect Dis, 2008. **46**(11): p. 1769-81.
295. Colloca, S., et al., *Vaccine vectors derived from a large collection of simian adenoviruses induce potent cellular immunity across multiple species.* Sci Transl Med, 2012. **4**(115): p. 115ra2.
296. McElrath, M.J., et al., *HIV-1 vaccine-induced immunity in the test-of-concept Step Study: a case-cohort analysis.* Lancet, 2008. **372**(9653): p. 1894-905.
297. Churchyard, G.J., et al., *A phase IIA randomized clinical trial of a multiclade HIV-1 DNA prime followed by a multiclade rAd5 HIV-1 vaccine boost in healthy adults (HVTN204).* PLoS One, 2011. **6**(8): p. e21225.
298. Freel, S.A., et al., *Phenotypic and functional profile of HIV-inhibitory CD8 T cells elicited by natural infection and heterologous prime/boost vaccination.* Journal of Virology, 2010. **84**(10): p. 4998-5006.
299. Nitayaphan, S., et al., *Safety and immunogenicity of an HIV subtype B and E prime-boost vaccine combination in HIV-negative Thai adults.* J Infect Dis, 2004. **190**(4): p. 702-6.
300. McMichael, A.J. and R.E. Phillips, *Escape of human immunodeficiency virus from immune control.* Annu Rev Immunol, 1997. **15**: p. 271-96.
301. Saez-Cirion, A., et al., *Ex vivo T cell-based HIV suppression assay to evaluate HIV-specific CD8+ T-cell responses.* Nat. Protocols, 2010. **5**(6): p. 1033-1041.

302. Fauce, S.R., O.O. Yang, and R.B. Effros, *Autologous CD4/CD8 co-culture assay: a physiologically-relevant composite measure of CD8+ T lymphocyte function in HIV-infected persons.* J Immunol Methods, 2007. **327**(1-2): p. 75-81.
303. Yang, H., et al., *Improved quantification of HIV-1-infected CD4+ T cells using an optimised method of intracellular HIV-1 gag p24 antigen detection.* J Immunol Methods, 2013. **391**(1-2): p. 174-8.
304. Yang, H., et al., *The antiviral inhibitory capacity of CD8+ T cells predicts the rate of CD4+ cell decline in HIV-1 infection.* J Infect Dis, 2012.
305. Saez-Cirion, A., et al., *HIV controllers exhibit potent CD8 T cell capacity to suppress HIV infection ex vivo and peculiar cytotoxic T lymphocyte activation phenotype.* Proc Natl Acad Sci U S A, 2007. **104**(16): p. 6776-81.
306. Stephenson, K.E., et al., *Gag-specific cellular immunity determines in vitro viral inhibition and in vivo virologic control following simian immunodeficiency virus challenges of vaccinated rhesus monkeys.* Journal of Virology, 2012. **86**(18): p. 9583-9.
307. Spentzou, A., et al., *Viral Inhibition Assay: A CD8 T Cell Neutralization Assay for Use in Clinical Trials of HIV-1 Vaccine Candidates.* The Journal of Infectious Diseases, 2010. **201**(5): p. 720-729.
308. Kopycinski, J., et al., *Broad HIV epitope specificity and viral inhibition induced by multigenic HIV-1 adenovirus subtype 35 vector vaccine in healthy uninfected adults.* PLoS One, 2014. **9**(3): p. e90378.
309. Vicenzi, E. and G. Poli, *Infection of CD4+ Primary T Cells and Cell Lines, Generation of Chronically Infected Cell Lines, and Induction of HIV Expression*. Current Protocols in Immunology. 2001: John Wiley & Sons, Inc.
310. van 't Wout, A.B., H. Schuitemaker, and N.A. Kootstra, *Isolation and propagation of HIV-1 on peripheral blood mononuclear cells.* Nat. Protocols, 2008. **3**(3): p. 363-370.
311. Defawe, O.D., et al., *Optimization and qualification of a multiplex bead array to assess cytokine and chemokine production by vaccine-specific cells.* J Immunol Methods, 2012. **382**(1-2): p. 117-28.
312. Hermans, I.F., et al., *The VITAL assay: a versatile fluorometric technique for assessing CTL- and NKT-mediated cytotoxicity against multiple targets in vitro and in vivo.* J Immunol Methods, 2004. **285**(1): p. 25-40.
313. Walker, B.D., R. Ahmed, and S. Plotkin, *Moving ahead an HIV vaccine: use both arms to beat HIV.* Nat Med, 2011. **17**(10): p. 1194-5.
314. Walker, B.D. and D.R. Burton, *Toward an AIDS vaccine.* Science, 2008. **320**(5877): p. 760-4.
315. Jin, X., et al., *Dramatic Rise in Plasma Viremia after CD8+ T Cell Depletion in Simian Immunodeficiency Virus–infected Macaques.* The Journal of Experimental Medicine, 1999. **189**(6): p. 991-998.
316. Hansen, S.G., et al., *Profound early control of highly pathogenic SIV by an effector memory T-cell vaccine.* Nature, 2011. **473**(7348): p. 523-527.
317. Walker, C.M., et al., *CD8+ lymphocytes can control HIV infection in vitro by suppressing virus replication.* Science, 1986. **234**(4783): p. 1563-6.
318. Mackewicz, C.E., H.W. Ortega, and J.A. Levy, *CD8+ cell anti-HIV activity correlates with the clinical state of the infected individual.* J Clin Invest, 1991. **87**(4): p. 1462-6.
319. Hayton, E.J., et al., *Safety and tolerability of conserved region vaccines vectored by plasmid DNA, simian adenovirus and modified vaccinia virus ankara administered to human immunodeficiency virus type 1-uninfected adults in a randomized, single-blind phase I trial.* PLoS One, 2014. **9**(7): p. e101591.
320. Borthwick, N., et al., *Vaccine-elicited human T cells recognizing conserved protein regions inhibit HIV-1.* Mol Ther, 2014. **22**(2): p. 464-75.

321. Ondondo, B., et al., *Absence of systemic toxicity changes following intramuscular administration of novel pSG2.HIVconsv DNA, ChAdV63.HIVconsv and MVA.HIVconsv vaccines to BALB/c mice.* Vaccine, 2013. **31**(47): p. 5594-601.
322. Rosario, M., et al., *Long peptides induce polyfunctional T cells against conserved regions of HIV-1 with superior breadth to single-gene vaccines in macaques.* Eur J Immunol, 2010. **40**(7): p. 1973-84.
323. Rosario, M., et al., *Prime-boost regimens with adjuvanted synthetic long peptides elicit T cells and antibodies to conserved regions of HIV-1 in macaques.* AIDS, 2012. **26**(3): p. 275-84.
324. Lichterfeld, M., et al., *HIV-1 Nef is preferentially recognized by CD8 T cells in primary HIV-1 infection despite a relatively high degree of genetic diversity.* AIDS, 2004. **18**(10): p. 1383-92.
325. Liu, Y., et al., *Conserved HIV-1 epitopes continuously elicit subdominant cytotoxic T-lymphocyte responses.* J Infect Dis, 2009. **200**(12): p. 1825-33.
326. Keefer, M.C., et al., *A phase I double blind, placebo-controlled, randomized study of a multigenic HIV-1 adenovirus subtype 35 vector vaccine in healthy uninfected adults.* PLoS One, 2012. **7**(8): p. e41936.
327. Kimani, D., et al., *Translating the Immunogenicity of Prime-boost Immunization With ChAd63 and MVA ME-TRAP From Malaria Naive to Malaria-endemic Populations.* Mol Ther, 2014.
328. Sun, P., et al., *Protective immunity induced with malaria vaccine, RTS,S, is linked to Plasmodium falciparum circumsporozoite protein-specific CD4+ and CD8+ T cells producing IFN-gamma.* J Immunol, 2003. **171**(12): p. 6961-7.
329. Tameris, M.D., et al., *Safety and efficacy of MVA85A, a new tuberculosis vaccine, in infants previously vaccinated with BCG: a randomised, placebo-controlled phase 2b trial.* Lancet, 2013. **381**(9871): p. 1021-8.
330. Schmittel, A., U. Keilholz, and C. Scheibenbogen, *Evaluation of the interferon-gamma ELISPOT-assay for quantification of peptide specific T lymphocytes from peripheral blood.* J Immunol Methods, 1997. **210**(2): p. 167-74.
331. Streeck, H., N. Frahm, and B.D. Walker, *The role of IFN-gamma Elispot assay in HIV vaccine research.* Nat Protoc, 2009. **4**(4): p. 461-9.
332. Cox, J.H., et al., *Results of an ELISPOT proficiency panel conducted in 11 laboratories participating in international human immunodeficiency virus type 1 vaccine trials.* AIDS Res Hum Retroviruses, 2005. **21**(1): p. 68-81.
333. Mothe, B., et al., *Definition of the viral targets of protective HIV-1-specific T cell responses.* J Transl Med, 2011. **9**: p. 208.
334. Baden, L.R., et al., *First-in-human evaluation of the safety and immunogenicity of a recombinant adenovirus serotype 26 HIV-1 Env vaccine (IPCAVD 001).* J Infect Dis, 2013. **207**(2): p. 240-7.
335. Li, F., et al., *Mapping HIV-1 vaccine induced T-cell responses: bias towards less-conserved regions and potential impact on vaccine efficacy in the Step study.* PLoS One, 2011. **6**(6): p. e20479.
336. Lichterfeld, M., et al., *HIV-1-specific cytotoxicity is preferentially mediated by a subset of CD8(+) T cells producing both interferon-gamma and tumor necrosis factor-alpha.* Blood, 2004. **104**(2): p. 487-94.
337. Betts, M.R., et al., *Sensitive and viable identification of antigen-specific CD8+ T cells by a flow cytometric assay for degranulation.* Journal of Immunological Methods, 2003. **281**(1-2): p. 65-78.
338. Barouch, D.H., et al., *Characterization of humoral and cellular immune responses elicited by a recombinant adenovirus serotype 26 HIV-1 Env vaccine in healthy adults (IPCAVD 001).* J Infect Dis, 2013. **207**(2): p. 248-56.

339. Cocchi, F., et al., *Identification of RANTES, MIP-1 alpha, and MIP-1 beta as the major HIV-suppressive factors produced by CD8+ T cells.* Science, 1995. **270**(5243): p. 1811-5.
340. McKenzie, A.N., et al., *Interleukin 13, a T-cell-derived cytokine that regulates human monocyte and B-cell function.* Proc Natl Acad Sci U S A, 1993. **90**(8): p. 3735-9.
341. Annunziato, F., et al., *Limited expression of R5-tropic HIV-1 in CCR5-positive type 1-polarized T cells explained by their ability to produce RANTES, MIP-1alpha, and MIP-1beta.* Blood, 2000. **95**(4): p. 1167-74.
342. Denis, M. and E. Ghadirian, *Interleukin 13 and interleukin 4 protect bronchoalveolar macrophages from productive infection with human immunodeficiency virus type 1.* AIDS Res Hum Retroviruses, 1994. **10**(7): p. 795-802.
343. Montaner, L.J., R.T. Bailer, and S. Gordon, *IL-13 acts on macrophages to block the completion of reverse transcription, inhibit virus production, and reduce virus infectivity.* J Leukoc Biol, 1997. **62**(1): p. 126-32.
344. Papasavvas, E., et al., *IL-13 acutely augments HIV-specific and recall responses from HIV-1-infected subjects in vitro by modulating monocytes.* J Immunol, 2005. **175**(8): p. 5532-40.
345. Crowe, S.M. and A. Lopez, *GM-CSF and its effects on replication of HIV-1 in cells of macrophage lineage.* J Leukoc Biol, 1997. **62**(1): p. 41-8.
346. Matsuda, S., et al., *Suppression of HIV replication in human monocyte-derived macrophages induced by granulocyte/macrophage colony-stimulating factor.* AIDS Res Hum Retroviruses, 1995. **11**(9): p. 1031-8.
347. Liu, M.K., et al., *Vertical T cell immunodominance and epitope entropy determine HIV-1 escape.* J Clin Invest, 2013. **123**(1): p. 380-93.
348. Bansal, A., et al., *CD8 T-cell responses in early HIV-1 infection are skewed towards high entropy peptides.* AIDS, 2005. **19**(3): p. 241-50.
349. Kloverpris, H.N., et al., *Early antigen presentation of protective HIV-1 KF11Gag and KK10Gag epitopes from incoming viral particles facilitates rapid recognition of infected cells by specific CD8+ T cells.* Journal of Virology, 2013. **87**(5): p. 2628-38.
350. Bennett, M.S., et al., *Cross-clade detection of HIV-1-specific cytotoxic T lymphocytes does not reflect cross-clade antiviral activity.* J Infect Dis, 2008. **197**(3): p. 390-7.
351. Valentine, L.E., et al., *Recognition of escape variants in ELISPOT does not always predict CD8+ T-cell recognition of simian immunodeficiency virus-infected cells expressing the same variant sequences.* Journal of Virology, 2008. **82**(1): p. 575-81.
352. Ranasinghe, S.R., et al., *The antiviral efficacy of HIV-specific CD8 T-cells to a conserved epitope is heavily dependent on the infecting HIV-1 isolate.* PLoS Pathog, 2011. **7**(5): p. e1001341.
353. Bjorndal, A., et al., *Coreceptor usage of primary human immunodeficiency virus type 1 isolates varies according to biological phenotype.* Journal of Virology, 1997. **71**(10): p. 7478-87.
354. O'Brien, T.R., et al., *HIV-1 infection in a man homozygous for CCR5 delta 32.* Lancet, 1997. **349**(9060): p. 1219.
355. Michael, N.L., et al., *Exclusive and persistent use of the entry coreceptor CXCR4 by human immunodeficiency virus type 1 from a subject homozygous for CCR5 delta32.* Journal of Virology, 1998. **72**(7): p. 6040-7.
356. NIBSC. *(National Institute for Biological Standards and Control) Centre for AIDS Reagents*. 1989 [cited 2014 05 August]; List of all viruses held by CFAR which can be requested for research.]. Available from: http://www.nibsc.org/spotlight/centre_for_aids_reagents/reagent_listings.aspx.
357. Gartner, S., et al., *The role of mononuclear phagocytes in HTLV-III/LAV infection.* Science, 1986. **233**(4760): p. 215-9.

358. Platt, E.J., S.L. Kozak, and D. Kabat, *Critical role of enhanced CD4 affinity in laboratory adaptation of human immunodeficiency virus type 1.* AIDS Res Hum Retroviruses, 2000. **16**(9): p. 871-82.
359. Koup, R.A., et al., *Isolation and Quantitation of HIV in Peripheral Blood*. Current Protocols in Immunology. 2001: John Wiley & Sons, Inc.
360. Chen, H., et al., *Differential neutralization of human immunodeficiency virus (HIV) replication in autologous CD4 T cells by HIV-specific cytotoxic T lymphocytes.* Journal of Virology, 2009. **83**(7): p. 3138-49.
361. Kiwanuka, N., et al., *Effect of human immunodeficiency virus Type 1 (HIV-1) subtype on disease progression in persons from Rakai, Uganda, with incident HIV-1 infection.* J Infect Dis, 2008. **197**(5): p. 707-13.
362. Kiwanuka, N., et al., *HIV-1 viral subtype differences in the rate of CD4+ T-cell decline among HIV seroincident antiretroviral naive persons in Rakai district, Uganda.* J Acquir Immune Defic Syndr, 2010. **54**(2): p. 180-4.
363. Touloumi, G., et al., *Impact of HIV-1 subtype on CD4 count at HIV seroconversion, rate of decline, and viral load set point in European seroconverter cohorts.* Clin Infect Dis, 2013. **56**(6): p. 888-97.
364. Finkel, T.H., et al., *Apoptosis occurs predominantly in bystander cells and not in productively infected cells of HIV- and SIV-infected lymph nodes.* Nat Med, 1995. **1**(2): p. 129-34.
365. Garg, H., J. Mohl, and A. Joshi, *HIV-1 induced bystander apoptosis.* Viruses, 2012. **4**(11): p. 3020-43.
366. Miura, Y., et al., *Critical contribution of tumor necrosis factor-related apoptosis-inducing ligand (TRAIL) to apoptosis of human CD4+ T cells in HIV-1-infected hu-PBL-NOD-SCID mice.* J Exp Med, 2001. **193**(5): p. 651-60.
367. Zhang, M., et al., *Identification of a potential HIV-induced source of bystander-mediated apoptosis in T cells: upregulation of trail in primary human macrophages by HIV-1 tat.* J Biomed Sci, 2001. **8**(3): p. 290-6.
368. Betts, M.R., et al., *Analysis of total human immunodeficiency virus (HIV)-specific CD4(+) and CD8(+) T-cell responses: relationship to viral load in untreated HIV infection.* Journal of Virology, 2001. **75**(24): p. 11983-91.
369. Wong, J.T. and R.B. Colvin, *Selective reduction and proliferation of the CD4+ and CD8+ T cell subsets with bispecific monoclonal antibodies: evidence for inter-T cell-mediated cytolysis.* Clin Immunol Immunopathol, 1991. **58**(2): p. 236-50.
370. Jones, N., et al., *Evaluation of antigen-specific responses using in vitro enriched T cells.* J Immunol Methods, 2003. **274**(1-2): p. 139-47.
371. Migueles, S.A., et al., *Lytic granule loading of CD8+ T cells is required for HIV-infected cell elimination associated with immune control.* Immunity, 2008. **29**(6): p. 1009-21.
372. Jaoko, W., et al., *Safety and Immunogenicity Study of Multiclade HIV-1 Adenoviral Vector Vaccine Alone or as Boost following a Multiclade HIV-1 DNA Vaccine in Africa.* PLoS One, 2010. **5**(9): p. e12873.
373. Yu, X.G., et al., *Consistent patterns in the development and immunodominance of human immunodeficiency virus type 1 (HIV-1)-specific CD8+ T-cell responses following acute HIV-1 infection.* Journal of Virology, 2002. **76**(17): p. 8690-701.
374. Salazar-Gonzalez, J.F., et al., *Genetic identity, biological phenotype, and evolutionary pathways of transmitted/founder viruses in acute and early HIV-1 infection.* J Exp Med, 2009. **206**(6): p. 1273-89.
375. Fisher, A.G., et al., *Infectious mutants of HTLV-III with changes in the 3' region and markedly reduced cytopathic effects.* Science, 1986. **233**(4764): p. 655-9.

376. Terwilliger, E., et al., *Effects of mutations within the 3' orf open reading frame region of human T-cell lymphotropic virus type III (HTLV-III/LAV) on replication and cytopathogenicity.* Journal of Virology, 1986. **60**(2): p. 754-760.
377. Schwartz, O., et al., *Endocytosis of major histocompatibility complex class I molecules is induced by the HIV-1 Nef protein.* Nat Med, 1996. **2**(3): p. 338-42.
378. Greenberg, M.E., A.J. Iafrate, and J. Skowronski, *The SH3 domain-binding surface and an acidic motif in HIV-1 Nef regulate trafficking of class I MHC complexes.* EMBO J, 1998. **17**(10): p. 2777-89.
379. Wildum, S., et al., *Contribution of Vpu, Env, and Nef to CD4 down-modulation and resistance of human immunodeficiency virus type 1-infected T cells to superinfection.* Journal of Virology, 2006. **80**(16): p. 8047-59.
380. Craig, H.M., M.W. Pandori, and J.C. Guatelli, *Interaction of HIV-1 Nef with the cellular dileucine-based sorting pathway is required for CD4 down-regulation and optimal viral infectivity.* Proc Natl Acad Sci U S A, 1998. **95**(19): p. 11229-34.
381. Aiken, C. and D. Trono, *Nef stimulates human immunodeficiency virus type 1 proviral DNA synthesis.* Journal of Virology, 1995. **69**(8): p. 5048-56.
382. Qi, M. and C. Aiken, *Nef enhances HIV-1 infectivity via association with the virus assembly complex.* Virology, 2008. **373**(2): p. 287-97.
383. Geleziunas, R., et al., *HIV-1 Nef inhibits ASK1-dependent death signalling providing a potential mechanism for protecting the infected host cell.* Nature, 2001. **410**(6830): p. 834-8.
384. Yang, O.O., et al., *Nef-mediated resistance of human immunodeficiency virus type 1 to antiviral cytotoxic T lymphocytes.* Journal of Virology, 2002. **76**(4): p. 1626-31.
385. Allen, T.M., et al., *Selective Escape from CD8+ T-Cell Responses Represents a Major Driving Force of Human Immunodeficiency Virus Type 1 (HIV-1) Sequence Diversity and Reveals Constraints on HIV-1 Evolution.* Journal of Virology, 2005. **79**(21): p. 13239-13249.
386. Wood, N., et al., *HIV evolution in early infection: selection pressures, patterns of insertion and deletion, and the impact of APOBEC.* PLoS Pathog, 2009. **5**(5): p. e1000414.
387. Lucotte, G., *Frequencies of 32 base pair deletion of the (Delta 32) allele of the CCR5 HIV-1 co-receptor gene in Caucasians: a comparative analysis.* Infect Genet Evol, 2002. **1**(3): p. 201-5.
388. Samson, M., et al., *Resistance to HIV-1 infection in caucasian individuals bearing mutant alleles of the CCR-5 chemokine receptor gene.* Nature, 1996. **382**(6593): p. 722-5.
389. Luo, K., et al., *Cytidine deaminases APOBEC3G and APOBEC3F interact with human immunodeficiency virus type 1 integrase and inhibit proviral DNA formation.* Journal of Virology, 2007. **81**(13): p. 7238-48.
390. Stremlau, M., et al., *The cytoplasmic body component TRIM5alpha restricts HIV-1 infection in Old World monkeys.* Nature, 2004. **427**(6977): p. 848-53.
391. Stremlau, M., et al., *Specific recognition and accelerated uncoating of retroviral capsids by the TRIM5alpha restriction factor.* Proc Natl Acad Sci U S A, 2006. **103**(14): p. 5514-9.
392. Kaslow, R.A., et al., *Influence of combinations of human major histocompatibility complex genes on the course of HIV-1 infection.* Nat Med, 1996. **2**(4): p. 405-11.
393. Keet, I.P., et al., *Consistent associations of HLA class I and II and transporter gene products with progression of human immunodeficiency virus type 1 infection in homosexual men.* J Infect Dis, 1999. **180**(2): p. 299-309.
394. Carrington, M., et al., *HLA and HIV-1: heterozygote advantage and B*35-Cw*04 disadvantage.* Science, 1999. **283**(5408): p. 1748-52.

395. Tang, J., et al., *HLA class I homozygosity accelerates disease progression in human immunodeficiency virus type 1 infection.* AIDS Res Hum Retroviruses, 1999. **15**(4): p. 317-24.
396. Migueles, S.A., et al., *HLA B*5701 is highly associated with restriction of virus replication in a subgroup of HIV-infected long term nonprogressors.* Proc Natl Acad Sci U S A, 2000. **97**(6): p. 2709-14.
397. Magierowska, M., et al., *Combined genotypes of CCR5, CCR2, SDF1, and HLA genes can predict the long-term nonprogressor status in human immunodeficiency virus-1-infected individuals.* Blood, 1999. **93**(3): p. 936-41.
398. Kawashima, Y., et al., *Long-term control of HIV-1 in hemophiliacs carrying slow-progressing allele HLA-B*5101.* Journal of Virology, 2010. **84**(14): p. 7151-60.
399. Itescu, S., et al., *HLA-B35 is associated with accelerated progression to AIDS.* J Acquir Immune Defic Syndr, 1992. **5**(1): p. 37-45.
400. McNeil, A.J., et al., *Association of HLA types A1-B8-DR3 and B27 with rapid and slow progression of HIV disease.* QJM, 1996. **89**(3): p. 177-85.
401. Steel, C.M., et al., *HLA haplotype A1 B8 DR3 as a risk factor for HIV-related disease.* Lancet, 1988. **1**(8596): p. 1185-8.
402. null, et al., *The major genetic determinants of HIV-1 control affect HLA class I peptide presentation.* Science (New York, N.Y.), 2010. **330**(6010): p. 1551-1557.
403. Leslie, A.J., et al., *HIV evolution: CTL escape mutation and reversion after transmission.* Nat Med, 2004. **10**(3): p. 282-9.
404. Schneidewind, A., et al., *Escape from the dominant HLA-B27-restricted cytotoxic T-lymphocyte response in Gag is associated with a dramatic reduction in human immunodeficiency virus type 1 replication.* Journal of Virology, 2007. **81**(22): p. 12382-93.
405. Brockman, M.A., et al., *Escape and compensation from early HLA-B57-mediated cytotoxic T-lymphocyte pressure on human immunodeficiency virus type 1 Gag alter capsid interactions with cyclophilin A.* Journal of Virology, 2007. **81**(22): p. 12608-18.
406. Kaslow, R.A., et al., *Polymorphisms in HLA class I genes associated with both favorable prognosis of human immunodeficiency virus (HIV) type 1 infection and positive cytotoxic T-lymphocyte responses to ALVAC-HIV recombinant canarypox vaccines.* Journal of Virology, 2001. **75**(18): p. 8681-9.
407. Fellay, J., et al., *Host Genetic Determinants of T Cell Responses to the MRKAd5 HIV-1 gag/pol/nef Vaccine in the Step Trial.* Journal of Infectious Diseases, 2011. **203**(6): p. 773-779.
408. Saez-Cirion, A., et al., *Heterogeneity in HIV suppression by CD8 T cells from HIV controllers: association with Gag-specific CD8 T cell responses.* J Immunol, 2009. **182**(12): p. 7828-37.
409. Yamamoto, T., et al., *Virus inhibition activity of effector memory CD8(+) T cells determines simian immunodeficiency virus load in vaccinated monkeys after vaccine breakthrough infection.* Journal of Virology, 2012. **86**(10): p. 5877-84.
410. Payne, R.P., et al., *Efficacious early antiviral activity of HIV Gag- and Pol-specific HLA-B 2705-restricted CD8+ T cells.* Journal of Virology, 2010. **84**(20): p. 10543-57.
411. Adorini, L., et al., *In vivo competition between self peptides and foreign antigens in T-cell activation.* Nature, 1988. **334**(6183): p. 623-5.
412. Babbitt, B.P., et al., *Antigenic competition at the level of peptide-Ia binding.* Proc Natl Acad Sci U S A, 1986. **83**(12): p. 4509-13.
413. Salazar-Mather, T.P., T.A. Hamilton, and C.A. Biron, *A chemokine-to-cytokine-to-chemokine cascade critical in antiviral defense.* J Clin Invest, 2000. **105**(7): p. 985-93.

414. Frucht, D.M., et al., *IFN-gamma production by antigen-presenting cells: mechanisms emerge.* Trends Immunol, 2001. **22**(10): p. 556-60.
415. Shirayoshi, Y., et al., *Interferon-induced transcription of a major histocompatibility class I gene accompanies binding of inducible nuclear factors to the interferon consensus sequence.* Proc Natl Acad Sci U S A, 1988. **85**(16): p. 5884-8.
416. Wallach, D., M. Fellous, and M. Revel, *Preferential effect of gamma interferon on the synthesis of HLA antigens and their mRNAs in human cells.* Nature, 1982. **299**(5886): p. 833-6.
417. Groettrup, M., et al., *Interferon-gamma inducible exchanges of 20S proteasome active site subunits: why?* Biochimie, 2001. **83**(3-4): p. 367-72.
418. Bleul, C.C., et al., *The lymphocyte chemoattractant SDF-1 is a ligand for LESTR/fusin and blocks HIV-1 entry.* Nature, 1996. **382**(6594): p. 829-33.
419. Oberlin, E., et al., *The CXC chemokine SDF-1 is the ligand for LESTR/fusin and prevents infection by T-cell-line-adapted HIV-1.* Nature, 1996. **382**(6594): p. 833-5.
420. Seder, R.A., *Acquisition of lymphokine-producing phenotype by CD4+ T cells.* J Allergy Clin Immunol, 1994. **94**(6 Pt 2): p. 1195-202.
421. Patterson, B.K., et al., *Regulation of CCR5 and CXCR4 expression by type 1 and type 2 cytokines: CCR5 expression is downregulated by IL-10 in CD4-positive lymphocytes.* Clin Immunol, 1999. **91**(3): p. 254-62.
422. Loetscher, M., et al., *Chemokine receptor specific for IP10 and mig: structure, function, and expression in activated T-lymphocytes.* J Exp Med, 1996. **184**(3): p. 963-9.
423. Wong, G.H. and D.V. Goeddel, *Tumour necrosis factors alpha and beta inhibit virus replication and synergize with interferons.* Nature, 1986. **323**(6091): p. 819-22.
424. Lajoie, J., et al., *A distinct cytokine and chemokine profile at the genital mucosa is associated with HIV-1 protection among HIV-exposed seronegative commercial sex workers.* Mucosal Immunol, 2012. **5**(3): p. 277-87.
425. Iqbal, S.M., et al., *Elevated T cell counts and RANTES expression in the genital mucosa of HIV-1-resistant Kenyan commercial sex workers.* J Infect Dis, 2005. **192**(5): p. 728-38.
426. Hirbod, T., et al., *Upregulation of interferon-alpha and RANTES in the cervix of HIV-1-seronegative women with high-risk behavior.* J Acquir Immune Defic Syndr, 2006. **43**(2): p. 137-43.
427. Lajoie, J., et al., *Chemokine expression patterns in the systemic and genital tract compartments are associated with HIV-1 infection in women from Benin.* J Clin Immunol, 2010. **30**(1): p. 90-8.
428. Freel, S.A., et al., *Initial HIV-1 antigen-specific CD8+ T cells in acute HIV-1 infection inhibit transmitted/founder virus replication.* Journal of Virology, 2012. **86**(12): p. 6835-46.
429. Wilkinson, J., et al., *Characterization of the phenotypic and lymphokine profile associated with strong CD8+ anti-HIV-1 suppressor activity (CASA).* Clin Exp Immunol, 2002. **127**(1): p. 145-50.
430. Buckheit, R.W., 3rd, et al., *Inhibitory potential of subpopulations of CD8+ T cells in HIV-1-infected elite suppressors.* Journal of Virology, 2012. **86**(24): p. 13679-88.
431. Ndhlovu, Z.M., et al., *Elite controllers with low to absent effector CD8+ T cell responses maintain highly functional, broadly directed central memory responses.* Journal of Virology, 2012. **86**(12): p. 6959-69.
432. Hansen, S.G., et al., *Immune clearance of highly pathogenic SIV infection.* Nature, 2013. **502**(7469): p. 100-4.
433. Hansen, S.G., et al., *Cytomegalovirus vectors violate CD8+ T cell epitope recognition paradigms.* Science, 2013. **340**(6135): p. 1237874.

434. Sibeko, S. and S. Makvandi-Nejad, *From the laboratory to clinical trials and back again: lessons learned from HIV prevention trials.* Am J Reprod Immunol, 2013. **69 Suppl 1**: p. 106-15.
435. Ferre, A.L., et al., *Mucosal immune responses to HIV-1 in elite controllers: a potential correlate of immune control.* Blood, 2009. **113**(17): p. 3978-89.
436. Shin, H. and A. Iwasaki, *A vaccine strategy that protects against genital herpes by establishing local memory T cells.* Nature, 2012. **491**(7424): p. 463-7.
437. Feng, Y., et al., *HIV-1 entry cofactor: functional cDNA cloning of a seven-transmembrane, G protein-coupled receptor.* Science, 1996. **272**(5263): p. 872-7.
438. Colamussi, M.L., et al., *Stromal derived factor-1 alpha (SDF-1 alpha) induces CD4+ T cell apoptosis via the functional up-regulation of the Fas (CD95)/Fas ligand (CD95L) pathway.* J Leukoc Biol, 2001. **69**(2): p. 263-70.
439. Levy, J.A., C.E. Mackewicz, and E. Barker, *Controlling HIV pathogenesis: the role of the noncytotoxic anti-HIV response of CD8+ T cells.* Immunol Today, 1996. **17**(5): p. 217-24.
440. Nakaya, H.I. and B. Pulendran, *Systems vaccinology: its promise and challenge for HIV vaccine development.* Curr Opin HIV AIDS, 2012. **7**(1): p. 24-31.
441. Braibant, M., et al., *Disease progression due to dual infection in an HLA-B57-positive asymptomatic long-term nonprogressor infected with a nef-defective HIV-1 strain.* Virology, 2010. **405**(1): p. 81-92.
442. Dinges, W.L., et al., *Virus-specific CD8+ T-cell responses better define HIV disease progression than HLA genotype.* Journal of Virology, 2010. **84**(9): p. 4461-8.
443. Ochsenbauer, C., et al., *Generation of transmitted/founder HIV-1 infectious molecular clones and characterization of their replication capacity in CD4 T lymphocytes and monocyte-derived macrophages.* Journal of Virology, 2012. **86**(5): p. 2715-28.
444. Mascola, J.R., et al., *Recommendations for the design and use of standard virus panels to assess neutralizing antibody responses elicited by candidate human immunodeficiency virus type 1 vaccines.* Journal of Virology, 2005. **79**(16): p. 10103-7.
445. Seaman, M.S., et al., *Tiered categorization of a diverse panel of HIV-1 Env pseudoviruses for assessment of neutralizing antibodies.* Journal of Virology, 2010. **84**(3): p. 1439-52.
446. Kiepiela, P., et al., *CD8+ T-cell responses to different HIV proteins have discordant associations with viral load.* Nat Med, 2007. **13**(1): p. 46-53.
447. Edwards, B.H., et al., *Magnitude of functional CD8+ T-cell responses to the gag protein of human immunodeficiency virus type 1 correlates inversely with viral load in plasma.* Journal of Virology, 2002. **76**(5): p. 2298-305.
448. Geldmacher, C., et al., *CD8 T-cell recognition of multiple epitopes within specific Gag regions is associated with maintenance of a low steady-state viremia in human immunodeficiency virus type 1-seropositive patients.* Journal of Virology, 2007. **81**(5): p. 2440-8.
449. Lever, A.M.L., *HIV: the virus.* Medicine. **37**(7): p. 313-316.
450. Sacha, J.B., et al., *Gag-specific CD8+ T lymphocytes recognize infected cells before AIDS-virus integration and viral protein expression.* J Immunol, 2007. **178**(5): p. 2746-54.
451. Sacha, J.B., et al., *Pol-specific CD8+ T cells recognize simian immunodeficiency virus-infected cells prior to Nef-mediated major histocompatibility complex class I downregulation.* Journal of Virology, 2007. **81**(21): p. 11703-12.
452. Yang, O.O., et al., *Suppression of human immunodeficiency virus type 1 replication by CD8+ cells: evidence for HLA class I-restricted triggering of cytolytic and noncytolytic mechanisms.* Journal of Virology, 1997. **71**(4): p. 3120-8.

453. Varadarajan, N., et al., *A high-throughput single-cell analysis of human CD8(+) T cell functions reveals discordance for cytokine secretion and cytolysis.* J Clin Invest, 2011. **121**(11): p. 4322-31.
454. Jassoy, C., et al., *Human immunodeficiency virus type 1-specific cytotoxic T lymphocytes release gamma interferon, tumor necrosis factor alpha (TNF-alpha), and TNF-beta when they encounter their target antigens.* Journal of Virology, 1993. **67**(5): p. 2844-52.
455. Price, D.A., et al., *Antigen-specific release of beta-chemokines by anti-HIV-1 cytotoxic T lymphocytes.* Curr Biol, 1998. **8**(6): p. 355-8.
456. West, E.J., et al., *Immune activation by combination human lymphokine-activated killer and dendritic cell therapy.* Br J Cancer, 2011. **105**(6): p. 787-95.
457. LANL, *Los Alamos National Laboratory (LANL) HIV Molecular Immunology Database*. 2010, NIAID & Dept. of Energy.
458. Van Bleek, G.M. and S.G. Nathenson, *Isolation of an endogenously processed immunodominant viral peptide from the class I H-2Kb molecule.* Nature, 1990. **348**(6298): p. 213-6.
459. Rotzschke, O., et al., *Isolation and analysis of naturally processed viral peptides as recognized by cytotoxic T cells.* Nature, 1990. **348**(6298): p. 252-4.
460. Briggs, J.A., et al., *The stoichiometry of Gag protein in HIV-1.* Nat Struct Mol Biol, 2004. **11**(7): p. 672-5.
461. Sabbaj, S., et al., *Cross-reactive CD8+ T cell epitopes identified in US adolescent minorities.* J Acquir Immune Defic Syndr, 2003. **33**(4): p. 426-38.
462. Frahm, N., et al., *Consistent cytotoxic-T-lymphocyte targeting of immunodominant regions in human immunodeficiency virus across multiple ethnicities.* Journal of Virology, 2004. **78**(5): p. 2187-200.
463. Malhotra, U., et al., *Comprehensive epitope analysis of cross-clade Gag-specific T-cell responses in individuals with early HIV-1 infection in the US epidemic.* Vaccine, 2007. **25**(2): p. 381-90.
464. Peretz, Y., et al., *Relative contribution of HIV-specific functional lymphocyte subsets restricted by protective and non-protective HLA alleles.* Viral Immunol, 2011. **24**(3): p. 189-98.
465. Zhang, Y., et al., *Multilayered defense in HLA-B51-associated HIV viral control.* J Immunol, 2011. **187**(2): p. 684-91.
466. Menendez-Arias, L., A. Mas, and E. Domingo, *Cytotoxic T-lymphocyte responses to HIV-1 reverse transcriptase (review).* Viral Immunol, 1998. **11**(4): p. 167-81.
467. Fernandez-Vina, M.A., et al., *DNA typing for HLA class I alleles: I. Subsets of HLA-A2 and of -A28.* Hum Immunol, 1992. **33**(3): p. 163-73.
468. Vollbrecht, T., et al., *Control of M184V HIV-1 mutants by CD8 T-cell responses.* Med Microbiol Immunol, 2012. **201**(2): p. 201-11.
469. Streeck, H., et al., *Emergence of individual HIV-specific CD8 T cell responses during primary HIV-1 infection can determine long-term disease outcome.* Journal of Virology, 2014.
470. Goulder, P.J., et al., *Late escape from an immunodominant cytotoxic T-lymphocyte response associated with progression to AIDS.* Nat Med, 1997. **3**(2): p. 212-7.
471. Frahm, N., et al., *CD8(+) T-cell Mediated HIV Inhibition after Vaccination with a DNA/Recombinant Ad5 (rAd5) HIV Vaccine Is Similar to that Seen in Treated HIV Infection.* AIDS Res Hum Retroviruses, 2014. **30 Suppl 1**: p. A84.
472. Naarding, M.A., et al., *Development of a luciferase based viral inhibition assay to evaluate vaccine induced CD8 T-cell responses.* J Immunol Methods, 2014. **409**: p. 161-73.

473. Bendall, S.C., et al., *A deep profiler's guide to cytometry*. Trends Immunol, 2012. **33**(7): p. 323-32.
474. Lamoreaux, L., M. Roederer, and R. Koup, *Intracellular cytokine optimization and standard operating procedure.* Nat Protoc, 2006. **1**(3): p. 1507-16.
475. Ruiz-Riol, M., et al., *Alternative Effector-Function Profiling Identifies Broad HIV-Specific T-Cell Responses in Highly HIV-Exposed Individuals Who Remain Uninfected.* J Infect Dis, 2014.
476. Newell, E.W., et al., *Cytometry by time-of-flight shows combinatorial cytokine expression and virus-specific cell niches within a continuum of CD8+ T cell phenotypes.* Immunity, 2012. **36**(1): p. 142-52.
477. Sun, Y., et al., *A systematic comparison of methods to measure HIV-1 specific CD8 T cells.* J Immunol Methods, 2003. **272**(1-2): p. 23-34.
478. Lopez-Cabrera, M., et al., *Molecular cloning, expression, and chromosomal localization of the human earliest lymphocyte activation antigen AIM/CD69, a new member of the C-type animal lectin superfamily of signal-transmitting receptors.* J Exp Med, 1993. **178**(2): p. 537-47.
479. Rutella, S., et al., *Induction of CD69 antigen on normal CD4+ and CD8+ lymphocyte subsets and its relationship with the phenotype of responding T-cells.* Cytometry, 1999. **38**(3): p. 95-101.
480. Almeida, J.R., et al., *Superior control of HIV-1 replication by CD8+ T cells is reflected by their avidity, polyfunctionality, and clonal turnover.* J Exp Med, 2007. **204**(10): p. 2473-85.
481. Mothe, B., et al., *CTL responses of high functional avidity and broad variant cross-reactivity are associated with HIV control.* PLoS One, 2012. **7**(1): p. e29717.
482. Price, D.A., et al., *Public clonotype usage identifies protective Gag-specific CD8+ T cell responses in SIV infection.* J Exp Med, 2009. **206**(4): p. 923-36.
483. Slifka, M.K. and J.L. Whitton, *Functional avidity maturation of CD8(+) T cells without selection of higher affinity TCR.* Nat Immunol, 2001. **2**(8): p. 711-7.
484. Streeck, H., et al., *Human Immunodeficiency Virus Type 1-Specific CD8+ T-Cell Responses during Primary Infection Are Major Determinants of the Viral Set Point and Loss of CD4+ T Cells.* Journal of Virology, 2009. **83**(15): p. 7641-7648.
485. Kulkarni, V., et al., *Altered response hierarchy and increased T-cell breadth upon HIV-1 conserved element DNA vaccination in macaques.* PLoS One, 2014. **9**(1): p. e86254.
486. Purcell, A.W. and J.J. Gorman, *Immunoproteomics: Mass spectrometry-based methods to study the targets of the immune response.* Mol Cell Proteomics, 2004. **3**(3): p. 193-208.
487. Ternette, N., et al., *The First Glance at the HLA Class I-Associated Immunopeptidome from HIV-1 Infected Cells* In Press, 2014.
488. Barouch, D.H., et al., *Protective efficacy of a global HIV-1 mosaic vaccine against heterologous SHIV challenges in rhesus monkeys.* Cell, 2013. **155**(3): p. 531-9.
489. Fukazawa, Y., et al., *Lymph node T cell responses predict the efficacy of live attenuated SIV vaccines.* Nat Med, 2012. **18**(11): p. 1673-81.
490. Parks, C.L., L.J. Picker, and C.R. King, *Development of replication-competent viral vectors for HIV vaccine delivery.* Curr Opin HIV AIDS, 2013. **8**(5): p. 402-11.
491. Kaul, R., et al., *HIV-1-specific mucosal IgA in a cohort of HIV-1-resistant Kenyan sex workers.* AIDS, 1999. **13**(1): p. 23-9.
492. Belyakov, I.M. and J.D. Ahlers, *What role does the route of immunization play in the generation of protective immunity against mucosal pathogens?* J Immunol, 2009. **183**(11): p. 6883-92.

9 Appendix

HIV-CORE 002 pre-vaccination samples analysed in the cultured virus inhibition assay against 8 HIV-1 isolates.

These values were used to set background inhibition levels for each individual isolate and for the complete panel.

Virus	Vaccinee ID							
	403	**404**	**405**	**406**	**409**	**410**	**411**	**412**
IIIB	0.5	0.3	1.1	0.3	0.0	0.5	0.6	0.1
ELI	0.1	0.1	0.4	0.3	0.0	0.1	0.3	0.3
CH077	0.6	0.3	ND	0.3	0.3	0.4	0.8	0.3
CH106	0.1	0.3	0.8	0.1	0.0	0.0	0.6	0.3
247Fv2	0.0	0.3	0.9	0.2	0.0	0.0	0.7	0.6
ZA97012	0.0	0.2	0.5	0.1	0.0	0.0	0.4	0.4
U455	0.5	0.6	1.0	0.5	0.3	0.1	0.7	0.4
BaL	0.1	0.0	0.2	0.0	0.0	0.0	0.3	0.2

Virus	Vaccinee ID									
	413	**414**	**415**	**416**	**417**	**418**	**419**	**420**	**421**	**422**
IIIB	0.3	0.0	0.2	0.6	0.3	0.9	0.6	0.9	0.5	0.0
ELI	0.1	0.2	0.0	0.6	0.2	0.4	0.4	0.9	0.5	0.6
CH077	0.4	0.3	0.2	0.9	0.6	0.8	0.5	1.1	0.7	0.7
CH106	0.0	0.0	0.2	0.9	0.2	0.4	0.2	1.0	0.5	1.3
247Fv2	0.2	0.1	0.2	0.5	0.3	0.7	0.1	1.2	0.5	0.4
ZA97012	0.0	0.0	0.1	0.4	0.2	0.4	0.3	0.5	0.6	0.5
U455	0.3	0.2	0.3	0.8	0.3	0.9	0.1	0.5	0.6	0.3
BaL	0.0	0.0	0.0	0.4	0.1	0.4	0.0	0.0	0.0	0.0

Virus	Vaccinee ID									
	423	424	425	426	427	428	429	430	431	432
IIIB	0.4	0.4	0.5	0.4	0.8	0.4	0.8	0.5	0.7	0.8
ELI	0.5	0.1	0.2	0.3	0.6	0.2	0.1	0.4	0.3	0.2
CH077	0.6	0.5	0.4	0.6	1.1	0.9	0.7	0.7	0.7	0.6
CH106	0.4	0.3	0.0	0.5	0.9	0.5	0.6	0.6	1.0	0.6
247Fv2	0.5	0.3	0.0	0.5	0.7	0.4	0.6	0.3	0.8	0.5
ZA97012	0.6	0.0	0.0	0.4	0.5	0.4	0.4	0.3	0.5	0.2
U455	0.4	0.4	0.8	0.7	0.8	0.7	0.3	0.8	1.2	1.2
BaL	0.2	0.0	0.0	0.2	0.0	0.2	0.2	0.1	0.1	0.0

Table of HIVconsv peptide sequences found within the HIV-1 isolates used in the cultured VIAs.

	Peptide No.	HIVconsv Peptide Sequence	Mapped Epitope	Peptide Sequence of HIV-1 isolates:							
				IIIB	U455	ZA97012	CH077	ELI	247FV2	CH106	Bal
Gag	31	CTERQANFLGKIWPS	TERQANFL	CTERQANFLGKIWPS	CTERQANFLGKIWPS	CTERQANFLGRIWPS	CTERQANFLGKIWPS	CTERQANFLGRIWPS	CTERQANFLGKIWPS	CIERQANFLGKIWPS	CTERQANFLGKIWPS
Pol	79	PLDEGFRKYTAFTIP	TAFTIPSI	PLDEDFRKYTAFTIP	PLDESFRKYTAFTIP	PLDESFRKYTAFTIP	PLHEDFRKYTAFTIP	PLDEDFRKYTAFTIS	PLDEDFRKYTAFTIP	PLDKDFRKYTAFTIP	PLDKEFRKYTAFTIP
	80	GFRKYTAFTIPSINN	TAFTIPSI	DFRKYTAFTIPSINN	SFRKYTAFTIPSINN	SFRKYTAFTIPSINN	DFRKYTAFTIPSINN	DFRKYTAFTISSINN	DFRKYTAFTIPSINN	DFRKYTAFTIPSINN	EFRKYTAFTIPSINN
	93	KNPEIVIYQYMDDLYV	YQYMDDLYV	QNPDIVIYQYMDDLYV	QHPDIVIYQYMDDLYV	KNPEIVIYQYMDDLYV	QNPEIHICQYMDDLYV	QNPEMVIYQYMDDLYV	QNPEIVIYQYMDDLYV	QNPDIVIYQYMDDLYV	QNPEIVIYQYMDDLYV
	94	VIYQYMDDLYVGSDL	YQYMDDLYV	VIYQYMDDLYVGSDL	VIYQYMDDLYVGSDL	VIYQYMDDLYVGSDL	HICQYMDDLYVSSDL	VIYQYMDDLYVGSDL	VIYQYMDDLYVGSDL	VIYQYMDDLYVGSDL	VIYQYMDDLYVGSDL

Red amino acid indicates changes from the HIVconsv sequence used for vaccination.